2-18-2020

Assessment of Soil Protein and Refractory Soil Organic Matter Across Two Chronosequences of Newly Developing Marshes in Coastal Louisiana, USA

Stuart Alexander McClellan
Louisiana State University and Agricultural and Mechanical College

ASSESSMENT OF SOIL PROTEIN AND REFRACTORY SOIL ORGANIC MATTER ACROSS TWO CHRONOSEQUENCES OF NEWLY DEVELOPING MARSHES IN COASTAL LOUISIANA, USA

A Dissertation

Submitted to the Graduate Faculty of the
Louisiana State University and
Agricultural and Mechanical College
in partial fulfillment of the
requirements for the degree of
Doctor of Philosophy

in

The Department of Environmental Sciences

by
Stuart Alexander McClellan
B.S., The University of Texas at Austin, 2008
May 2020

for

Sydney

Acknowledgements

This dissertation research would have certainly not been possible without the help, guidance, and expertise of many people, who I sincerely thank. Firstly, I thank my major advisor and mentor, Dr. Ed Laws, for giving me the valuable opportunity to branch out and pursue my own study—yet he was always there to discuss and help troubleshoot any aspect of my research whenever challenges arose, and I have learned a great deal as a student under his guidance. My committee also greatly supported me throughout my long journey of study, providing key advice throughout all stages of this research, as well as providing equipment and lab space. Dr. Tracy Quirk played an integral role in helping me shape my research interests into a coherent and feasible study, and she also taught me many of the field techniques that I used here. I thank Kate Abbott, Alexandra Christensen, and Andy Muench for fieldwork support; and Tommy Blanchard, Grace Cagle, Virginia Johnson, and Megan Kelsall for laboratory and methodology assistance. I also thank Dr. Siyuan Ye and the Qingdao Institute of Marine Geology for giving me the opportunity to perform my preliminary research in the Liaohe Delta of northeastern China (and to experience the culture along the way).

Finally, I would not have been able to endure the challenges of graduate school without the caring support of my parents, sister, friends, and colleagues, including Anika Aarons, Kate Abbott, Tom Aepelbacher, Linda Beltran, Heng Cai, Steve Carbajal, Alexandra Christensen, Kelly Connelly, Rachel Correll, Donnie Day, Megan Kelsall, Chris Kunz, Morgan McKee, Ian Minich, Andy Muench, Jeff Obelcz, Nichole Ohlinger, Nick Olsen, Jaya Srivastava, Lisa Tremmel, Kendall Valentine, Baoling Wang, Jiaze Wang, and Sara Wang.

This research was supported by a Program Development grant from Louisiana Sea Grant. A DNA extraction kit was awarded by QIAGEN.

Advisory committee:
Edward A. Laws, PhD (chair)
Ronald D. DeLaune, PhD (minor advisor)
Tracy Elsey-Quirk, PhD
Aixin Hou, PhD
Ralph J. Portier, PhD

Table of Contents

List of Acronyms

AAA	amino acid analysis
AAE	autoclaved alkaline-extractable
AAES	autoclaved alkaline-extractable solids
AMF	arbuscular mycorrhizal fungi
ANCOVA	analysis of covariance
ANOVA	analysis of variance
BR-AAE	Bradford-reactive autoclaved alkaline-extractable
BRSP	Bradford-reactive soil protein
BSA	bovine serum albumin
C	carbon
CHN	carbon-hydrogen-nitrogen
DI	deionized
DNA	deoxyribonucleic acid
GRSP	glomalin-related soil protein
HA	humic acids
HSD	honestly significant differences
HUN	hydrolysable unknown nitrogen
i.d.	internal diameter
kb	kilo base-pairs
kDa	kilodaltons
LN	labile nitrogen
LOC	labile organic carbon
Max-AAE	maximum estimated autoclaved alkaline-extractable
Min-AAE	minimum estimated autoclaved alkaline-extractable
MSA	methanesulfonic acid
MW	molecular weight
N	nitrogen
NAVD88	North American vertical datum of 1988 (relative to)
NMR	nuclear magnetic resonance
OC:N	organic-carbon-to-nitrogen ratio (weight per weight)
PAGE	polyacrylamide gel electrophoresis
PCR	polymerase chain reaction
RN	refractory nitrogen
ROC	refractory organic carbon
SD	standard deviation
SE	standard error
SLR	sea level rise
SOM	soil organic matter
SON	soil organic nitrogen
TAE	tris acetate EDTA (ethylenediaminetetraacetic acid)
TN	total nitrogen (of soil)
TOC	total organic carbon (of soil)
WLD	Wax Lake Delta

Abstract

The impacts of sea-level rise and hydrologic manipulation are threatening the stability of coastal marshes throughout the world, thereby increasing the potential for re-mineralization of soil organic matter (SOM) in these systems. Such threats have prompted marsh restoration efforts, particularly in coastal Louisiana, yet it is unclear how the slowly decomposing (refractory) and quickly decomposing (labile) fractions of SOM may be differentially affected by different approaches to marsh restoration. Additionally, otherwise labile compounds may accumulate in the soil via a range of protective mechanisms, including rapid burial and association with organic compounds that are thought to enhance soil aggregation, such as autoclaved alkaline-extractable protein (AAEP)—a.k.a. glomalin-related soil protein. Here, I examined the upper 30 cm of soil across two chronosequences of coastal marshes—located in Sabine National Wildlife Refuge (Sabine) and in Wax Lake Delta (WLD)—representing the two principal approaches to coastal wetland restoration in Louisiana (dredge-spoil infilling and sediment diversion, respectively). By estimating the amounts of refractory organic carbon and nitrogen (ROC and RN), labile organic carbon and nitrogen (LOC and LN), and AAEP, I aimed to compare how these fractions accumulate within these two distinct systems and contribute to the total organic carbon and nitrogen (TOC and TN). Because methodological limitations have confounded previous efforts to accurately quantify the AAEP fraction, I applied a novel approach for estimating the quantity of AAEP in the studied soils based on amino acid analysis. Each fraction was highly positively correlated with TOC. Overall, the contributions of the fractions to TOC and TN were similar between the chronosequences and tended to increase with marsh age. AAEP was primarily co-purified with ROC, and was negatively correlated with LOC/TOC ratios, suggesting that it may not be involved in LOC preservation. Although a greater proportion of the new carbon accumulation in Sabine was refractory relative to WLD, the WLD marshes appeared to accumulate ROC more quickly—a paradox explainable by the characteristically faster accretion rates in WLD. The overall correlation between ROC and TOC did not differ between the two chronosequences and was remarkably similar to those previously observed elsewhere in coastal Louisiana.

Chapter 1.
An Introduction

This dissertation research initially began on the basis of investigating potential links between soil fungi and soil carbon (C) storage in wetland systems. I began my initial project with the aim of measuring the soil C contribution of a recently defined fraction of soil organic matter (SOM) that has often been attributed to a particular class of soil fungi. However, my initial observations led me to think more carefully about the chemistry of this and other fractions of SOM, and how these various components can be related. This ultimately led to the research presented here, which addresses questions in the realms of analytical chemistry, biochemistry, and soil biogeochemistry—all within the context of wetland soil development. Although the primary focus of this research is on autoclaved alkaline-extractable soil protein, it also includes an investigation into the overall stability of SOM. Indeed, the overall theme of SOM stability and preservation is what provided the initial motivation for the investigation of the soil protein fraction, and it is the theme that unites all parts of this dissertation. Furthermore, whereas the studies presented here were conducted in coastal wetlands of Louisiana, USA, it is expected that many of the overall findings will be applicable to coastal wetlands elsewhere in the US and the world.

In this chapter, I give a brief review of the background information that will help provide context for the subsequent chapters—further and more detailed background information is provided at the beginning of each chapter—followed by an overview of these subsequent chapters. Lastly, because all of the studies described in this dissertation made use of samples collected from the same set of study sites, I provide all of the basic descriptions and soil sample characteristics together at the end of this chapter.

1.1. Background

Among the numerous ecosystem services that vegetated coastal wetlands provide is C sequestration and subsequent long-term C storage. Coastal saline wetlands alone bury an estimated 84–234 Tg of C per year globally (McLeod et al., 2011) despite occupying <1% of the total land area (Spencer et al., 2016). The three factors to which this disproportionately high C burial per unit area is primarily attributed are high rates of primary production, fast rates of accretion, and the characteristically slow decomposition rates of organic matter in anoxic soils (Reddy and DeLaune, 2008). This SOM heavily influences the chemical and physical properties of soil; it contributes to the water retention capacity of soil, and it plays a key role in the biological cycling of elements such as C and N. In addition to providing a substantial sink for atmospheric C, this store of SOM can improve the stability of the soil matrix through its involvement in soil aggregation (Tisdall and Oades, 1982; Barthès and Roose, 2002), which is particularly important for coastal wetlands. Climate change–induced sea level rise (SLR) combined with increased population growth and manipulation of watersheds in coastal regions has threatened the global extent of coastal wetlands by impeding their ability to acclimate to changing environmental stressors and thus their ability to remain subaerial (Kirwan and Megonigal, 2013). The issue of land loss in coastal Louisiana, USA is one example of this. An

estimated 490,000 hectares of Louisiana's coastal wetlands have been lost since the 1930s and an additional ~132,000 hectares are projected to be lost by 2050 under a no-restoration scenario (Barras et al., 2003; DeLaune and White, 2012; Couvillion et al., 2017). In this region, decreased sediment and freshwater supply to much of the coastal wetland area has made these wetlands more susceptible to SLR and storm surges (Wilson and Allison, 2008; DeLaune and White, 2012), therefore threatening their store of C. Upon exposure to the aerobic conditions of the ocean, this C may have a much greater potential to be re-mineralized to CO_2, negating the effect of high primary production, and potentially contributing to hypoxic bottom water along the adjacent coastal shelf (Bianchi et al., 2010; Steinmuller and Chambers, 2019; Steinmuller et al., 2019).

Such potential for re-mineralization can also depend, however, on the relative resistance to degradation (or stability) of this organic C. SOM contains a conglomerate of innumerable organic C and nitrogen (N) compounds, each of which has varying degrees of stability that depend on both intrinsic and extrinsic factors. Here, I will define the organic matter that exhibits a relatively high intrinsic stability as being *refractory* and the converse being *labile*. Intrinsic stability relates to the chemical stability of a given compound in terms of thermodynamics and without regard to the environment in which the compound exists; whereas, extrinsic stability necessarily derives from this environment. Therefore, factors that can contribute to the extrinsic stability of a compound are numerous and can include the intermolecular associations with other organic compounds, metals, and mineral surfaces (Knicker and Hatcher, 1997; Kleber et al., 2015), as well as physicochemical factors such as the degree to which a given compound is physically protected from enzymes by encapsulation within soil aggregates (Jastrow et al., 2007). Hence, depending on all of these factors, some components of SOM may quickly decompose whereas others may be slower to decompose. In the case of wetland soils, the generally lower availability of efficient electron acceptors, such as oxygen, means that the decomposition of intrinsically labile compounds may be slowed to the extent that a substantial amount might accumulate in the surficial soil (Reddy and DeLaune, 2008). Furthermore, if these labile compounds are stabilized by association with other compounds or through physical protection in soil aggregates, then they may, nevertheless, persist and contribute to long term C burial. On the other hand, if the soil structure is disrupted and these compounds become exposed to oxidative environments, they are more liable to degrade and ultimately contribute to emission of CO_2 (Steinmuller et al., 2019). It is therefore important to consider the relative amounts of refractory versus labile SOM in coastal wetland soils. Yet, compared to upland soils, there have been relatively few studies that have distinguished between the refractory and labile SOM fractions in coastal wetland soils, and even fewer that have evaluated the relative accumulation of these fractions across the stages of new wetland development. One of the aims of this dissertation research was to investigate the relative partitioning of the total SOM between the refractory and labile fractions at multiple stages of coastal marsh soil development.

In addition to the accumulation of refractory SOM, the preservation of otherwise labile SOM through its association with other organic compounds might also be an important mechanism by which this C can survive aerobic conditions (Lützow et al., 2006). For instance, in a scenario where the wetland soil is eroded and transported to more oxygenated environments, the labile SOM that is entrapped within soil aggregates may be more likely to be

preserved than the SOM that is not (Fig. 1.1). One fraction of SOM that is thought to be involved in soil aggregation and preservation of labile SOM is the originally termed glomalin-related soil protein (GRSP) fraction (Rillig, 2004; Rillig and Mummey, 2006; Zhang et al., 2017). GRSP is an operationally defined pool of proteinaceous SOM that has appeared in some of the more recent discussions of soil C storage and soil aggregation (King, 2011; Treseder and Holden, 2013; Poirier et al., 2018). However, there has been ongoing debate regarding its composition and potential sources (Whiffen et al., 2007; Gillespie et al., 2011; Hurisso et al., 2018; Moragues-Saitua et al., 2019).

The definition of GRSP is based on the glomalin protein, which was originally identified by the immunoreactivity of soil extracts and aggregates towards an antibody raised against spores of *Glomus intraradices* (Wright et al., 1996; Wright and Upadhyaya, 1998)—one of numerous taxa of arbuscular mycorrhizal fungi (AMF), which form mutualistic associations with the majority of vascular plant roots (Smith and Read, 2008). This is the basis of claims that GRSP is primarily representative of proteins originating from AMF (Lovelock et al., 2004; Nichols and Wright, 2004). Yet, since its original description by Wright and Upadhyaya (1996), glomalin as a concept and glomalin as a measurable entity have diverged considerably, in part because of the paucity of information regarding its amino acid sequence and the observed lack of specificity of the glomalin antibody (MAb32B11) in environmental samples (Rosier et al., 2006). Nonetheless, the terms GRSP or Bradford-reactive soil protein have most commonly been used to represent an operationally defined proxy of glomalin that invariably involves extraction from soil in an alkaline buffer at high temperature (121°C). This assay therefore selects for proteins that are relatively heat stable, inherently or otherwise. The method of quantification most frequently involves the use of the inexpensive and convenient Bradford dye-binding protein assay (Bradford (1976) or modification thereof) to quantify total protein in the extracts—an assay that is generally insensitive to peptides with fewer than approximately 7–25 residues (Sedmak and Grossberg, 1977; Mayer et al., 1986). It is this general definition on which studies of GRSP have been most commonly based, and several such studies have concluded that GRSP is positively correlated with soil C storage (Rillig et al., 2001a; Lovelock et al., 2004), soil aggregation (Rillig et al., 2001b; Rillig, 2004; Bedini et al., 2009; Spohn and Giani, 2010; Dai et al., 2015), and AMF colonization (Bedini et al., 2009; Wilson et al., 2009; Bedini et al., 2010). Thus, glomalin as a putative gene product of AMF morphed into an operationally defined pool of soil protein that, as yet, cannot be directly linked to AMF but that may potentially represent a fraction of slowly decomposing organic C and N in soils and a potential contributor to the preservation of labile SOM.

Given that a direct causal link between AMF and this proteinaceous fraction has not been established, the term autoclaved citrate-extractable protein has recently been proposed as a replacement for GRSP (Hurisso et al., 2018) and has appeared in a few studies since (Frost et al., 2019; Geisseler et al., 2019; Mann et al., 2019). However, the original operational definition was not specific to a citrate-based extractant, and Wright et al. (2006) have suggested that other alkaline buffers can be more efficient extractants than citrate. Thus, I will use the more general term autoclaved alkaline-extractable (AAE) protein henceforth when referring to this operationally defined pool of soil protein. Furthermore, I will take the position that AAE protein constitutes the total proteinaceous component of the extracts yielded by the extraction method, whereas the term AAE solids will refer to the total extracted solids.

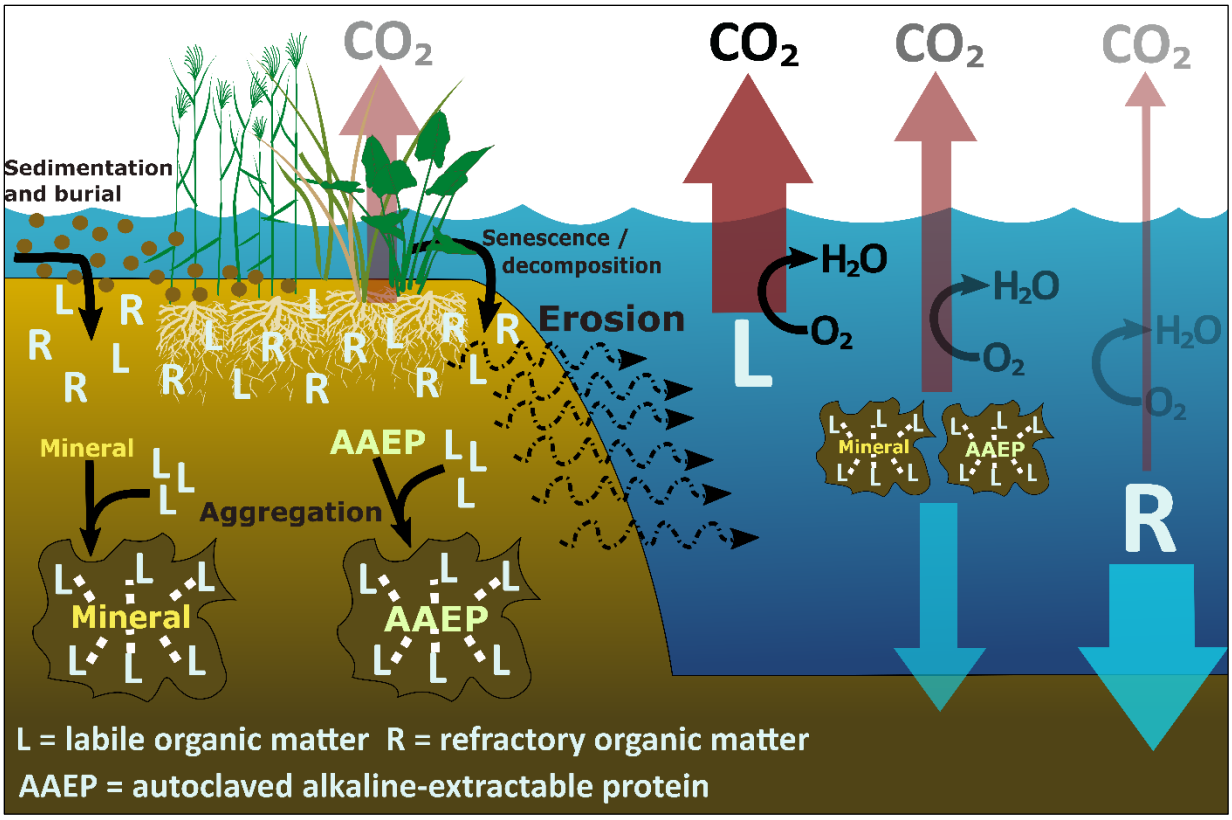

Figure 1.1. Cartoon illustrating the hypothetical processes in which the mineral sediment (Mineral), labile organic matter (L), refractory organic matter (R), and AAE protein (AAEP) fractions may be involved within a coastal marsh, and their potential fates upon marsh erosion. The widths of the red and blue arrows are intended to approximately represent the relative hypothetical ranking of C flux sizes.

Very few studies have investigated AAE protein in coastal wetland soils; yet a couple of these studies (Balachandran and Mishra, 2012; Wang et al., 2018b) have reported AAE protein concentrations in the soil that were comparable to the upper range of those that have been reported for upland soils. Based on similar methods of analysis, I have likewise found that this protein fraction was present in relatively high concentrations along a salinity gradient of marshes in the Liaohe Delta of northeastern China (unpublished data). In this region, typical AAE protein densities in the upper 30 cm of soil among three marsh types ranged as high as ~3 $mg \cdot cm^{-3}$ (Fig. A.1). Based on total organic C data from these sites (Olsson et al., 2015), and assuming the protein to be 53% C (Rouwenhorst et al., 1991), these data suggested that typical soil C contributions of AAE protein in these marshes fell in the range 3–16%. Importantly, however, there is an issue with how these values, and values reported in the literature, were estimated. Because of limitations associated with the methods currently used to measure AAE protein, the amount of actual proteinaceous material that it is present in AAE protein extracts may often be overestimated (Whiffen et al., 2007; Roberts and Jones, 2008; Gillespie et al., 2011). As such, it is hitherto unclear the extent to which AAE protein contributes to C and N in any soil, and whether it is truly correlated with the preservation of labile SOM (Fig. 1.1). Thus,

another aim of this dissertation research was to use alternative methods for estimating the AAE protein concentration in soils, and to then apply this approach to make more realistic estimates of AAE protein C and N contributions, and further, to determine the extent to which it is associated with the preservation of labile SOM.

In an effort to mitigate the loss and deterioration of coastal wetlands, proposed marsh restoration projects in Louisiana have essentially taken either of two approaches—1) diversion of sediment and/or freshwater from the Mississippi River or 2) bulk deposition of dredge-spoil sediments from navigation channels to areas of open water or deteriorating marshes (CPRA, 2017). In view of the growing need for such marsh restoration projects in coastal Louisiana, as well as in other coastal regions, evaluation of the development of restored marshes is critical for informing future restoration efforts. Although many ecosystem functions may be realized in restored marshes within relatively short timeframes, overall soil development and C stocks may take much longer to be regained, if ever (Craft et al., 2003; Edwards and Proffitt, 2003; Abbott et al., 2019). Thus, a focus on what happens to these wetlands following their creation needs to be an important component of such restoration projects.

Chronosequences of restored wetlands can serve as valuable models on which evaluations of the development of new marshes can be made, wherein a close spatial proximity of marshes of different ages facilitates a space-for-time substitution, therefore allowing the study of soil properties over a pseudo-temporal scale. Hence, the study of chronosequences of restored marshes can facilitate investigation of the dynamics of various soil properties without requiring decades of monitoring. The studies described in this dissertation were based on two chronosequences of coastal marsh soils that represent the two principal approaches to coastal wetland restoration in Louisiana. The marshes within each of these two chronosequences were regarded to represent different stages in the development of restored marshes within their respective regions. By *marsh development*, I am referring to the overall change of a marsh ecosystem with time—e.g., changes in vegetation community/density, soil biota, elevation—particularly during the time before a steady-state, or ecological climax, is reached. In this respect, time is represented by the age of a marsh, and throughout this dissertation, I refer to the term *marsh age* to indicate the approximate time since a particular marsh was originally established from open water. Although this research focuses on the soil characteristics of these marshes, I do not address *soil age*, a term that designates the time since a particular soil layer was formed (or deposited), and that is distinct from *marsh age*. Whereas soil age generally increases with soil depth, marsh age is a single value for a given marsh and represents the upper limit of the time since deposition of any sediments contained therein. Hence, the difference between soil age and marsh age is an important distinction to acknowledge when interpreting the findings presented in this dissertation. Another important point is that the characteristics of the soil can vary as functions of both the soil age and marsh age. This is because the composition of the soil is not exclusively affected by the amount of time since the sediment was deposited—it can also be influenced by other factors that may change interactively over time as a result of ecological succession (above- and below-ground) and changes in elevation. It is the combined influence that all of these factors may have on the soil characteristics that is central to the research presented here.

1.2. Overview of chapters

In the following chapters, I describe a series of experiments that focused on refractory SOM and AAE protein in two chronosequences of coastal wetland soils representing distinct models of wetland restoration. The overall aims of these studies were to compare how these two fractions of SOM accumulate between these two distinct systems, and to determine the relative contributions that AAE protein and refractory SOM make to the overall SOM. In the process of investigating the AAE protein fraction, it became apparent that current methods for quantifying this protein fraction are problematic in that they are not specific to proteinaceous material in the extracts and are susceptible to interference from co-extracted compounds. Thus, in Chapter 2, I describe my attempt to develop a more specific and less-interference prone method for estimating the quantity of AAE protein in soils through the combined use of amino acid analysis and elemental analysis. Additionally, I compare this method with the most commonly used approach and demonstrate the potential for divergence between the two. In Chapter 3, I apply this method for estimating AAE protein to determine the pattern with which the protein accumulates along the two chronosequences, its relative contribution to the overall soil C and N, the extent to which it may be bound with labile SOM, and whether it exhibits any correlation with the vegetation and the presence of AMF. Further, I use the results of the amino acid analysis to determine whether systematic differences exist between the amino acid profile of the AAE protein from these two wetland systems, with the expectation that this could provide insight into the dominant sources of this protein fraction. In Chapter 4, I move to address the question of how refractory and labile SOM may differentially accumulate in these two models of coastal wetland restoration given their differences in salinity, vegetation, and mineral sediment input. I also address the question of whether the AAE protein fraction appears to be involved in the preferential preservation of labile SOM in these wetland systems by determining whether the two are positively correlated. Finally, in Chapter 5, I summarize my overall findings and suggest how they can be used to inform further research in the realms of coastal wetland development and SOM stability.

1.3. Study sites and initial sampling

All of the experiments described in the subsequent chapters made use of subsets of the same soil core sections collected from the same marsh plots. Therefore, in the interest of efficiency and ease of reference, the description of the study sites, the initial collection and processing of the soil samples, and the basic characteristics of the soil samples are described only once in this dissertation and can be found below.

1.3.1 Description of study sites

Two chronosequences of coastal wetland soils representing distinct models of wetland restoration were selected for soil sampling. One of the chronosequences, located in Sabine National Wildlife Refuge (Sabine; Fig. 1.2), is a series of dredge-sediment–created brackish marshes on the Chenier Plain of the western Louisiana coast (Edwards and Proffitt, 2003; Abbott et al., 2019). Marshes in this area have suffered from reduced sediment input and

increased seawater intrusion since 1871, when dredging of the adjacent Calcasieu ship channel commenced (DeLaune et al., 1983). That dredging resulted in a shift from freshwater to brackish vegetation and conversion of marsh area to open water (DeLaune et al., 1983; Abbott et al., 2019). Beginning in 1983, the US Army Corps of Engineers deposited dredge spoil from this channel to areas of open water within the refuge at discrete and documented times. Those deposits are the basis of the chronosequence. Marshes in this area accrete primarily by autochthonous organic matter accumulation and receive little allochthonous sediment input. The marsh waters are generally polyhaline, and the dominant vegetation species in the naturally colonized marshes are *Spartina patens* and *Distichlis spicata*. The selected marshes ranged in age at the time of sampling from 1 to 33 years since dredge spoil deposit. Additionally, naturally established reference sites adjacent to the chronosequence sites were sampled for comparison. The locations and elevations of the sampling sites within Sabine are shown in Table 1.1. The locations of the plots were chosen to match (within 10 m) those of Abbott et al. (2019), who selected them randomly. More precise coordinates of each marsh plot are listed in Table A.1 of Appendix A. The specific soil characteristics of each marsh of the chronosequence, including bulk density, loss on ignition, total organic C (TOC), and total N (TN), are summarized in Table 1.2.

The other chronosequence is a series of tidal freshwater marshes within the currently prograding Wax Lake Delta (WLD; Fig. 1.2), which began forming in 1973 as a result of a diversion from the Atchafalaya River to the Gulf of Mexico three decades earlier by the US Army Corps of Engineers (Allen et al., 2012). Marshes within this delta have formed rapidly as a result of the exceptionally large amount of sediment (22.5 $Mt \cdot yr^{-1}$) delivered from the diverted flow, which is currently about 45% of the Atchafalaya River flow—which is, in turn, 30% of the Mississippi River flow (Roberts et al., 2003; Allison et al., 2012)—meaning that the WLD receives approximately 14% of the total normal flow of the Mississippi River north of the Old River Control Structure. The WLD has formed rapidly in recent years, and the fact that it has been possible to track its growth by aerial and satellite imagery (Wellner et al., 2005) has been the basis of the chronosequence used here. This chronosequence was previously established by Henry and Twilley (2014), and the same sampling locations (haphazardly within 10 m) were used for the present study. The delta is highly river-dominated, and the water is typically fresh to oligohaline throughout (Henry and Twilley, 2014). Tides are diurnal and micro-tidal. The approximate ages of the marshes at the time of sampling were 16, 29, and 41 years since subaerial establishment of the sediment surface. A reference marsh area that was adjacent to but outside of the WLD was selected to represent a local climax of marsh development. This reference site was estimated to be >60 years and selected based on historical aerial imagery (Wellner et al., 2005). Table 1.1 shows the approximate coordinates and elevations of the sampling sites. The elevations shown were estimated based on 1-m spatial resolution digital elevation model data obtained from the 2012 USGS National Elevation Dataset (https://www.usgs.gov/core-science-systems/ngp/tnm-delivery/). General trends in elevation with respect to the overall dominant plant species in WLD have been described by Carle et al. (2015). Table 1.2 also provides information on the soil characteristics of this chronosequence.

All vegetation within these two chronosequences colonized these areas naturally and was within areas of restricted anthropogenic activity; thus, these chronosequences were assumed to represent the natural trajectory of marsh development within these two regions.

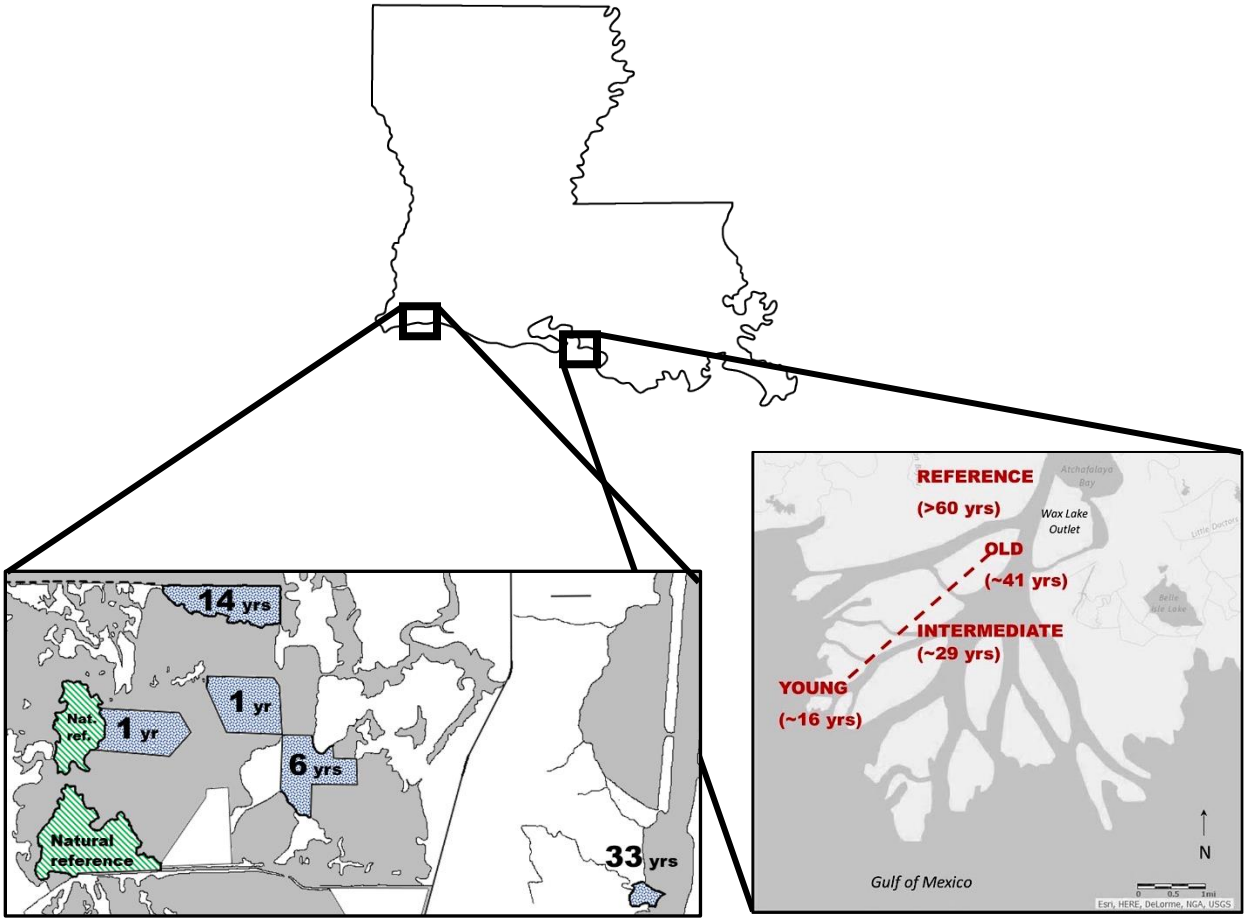

Figure 1.2. Map of Louisiana, USA (top), showing general locations of the studied chronosequences; maps of the Sabine chronosequence marshes (bottom left) and WLD chronosequence marshes (bottom right).

Table 1.1. Location, elevation, and dominant vegetation species of each marsh sampled

	Marsh age	Coordinates[†]	Average elevation[‡] (NAVD88)	Dominant vegetation
Sabine				
	1 year	29°56'48"N, 93°24'39"W	24 ± 3 cm	*Spartina alterniflora*
	6 years	29°56'16"N, 93°24'3"W	10 ± 3 cm	*S. alterniflora*
	14 years	29°57'42"N, 93°24'47"W	10 ± 3 cm	*Distichlis spicata*
	33 years	29°55'8"N, 93°20'48"W	32 ± 3 cm	*Spartina patens*
	Reference A	29°55'37"N, 93°26'17"W	13 ± 1 cm	*S. patens*
	Reference B	29°56'39"N, 93°26'21"W	7 ± 2 cm	*D. spicata*
WLD				
	16 years	29°30'4"N, 91°28'51"W	−32 cm	*Nelumbo lutea*
	29 years	29°30'45"N, 91°27'56"W	55 cm	*Colocasia esculenta*
	41 years	29°31'56"N, 91°26'10"W	53 cm	*Polygonum punctatum*
	Reference	29°33'15"N, 91°25'42"W	50 cm	*P. punctatum, Salix nigra*

[†] Coordinates of the Sabine marsh plots were selected to match a subset of those sampled by Abbott et al. (2019), which were randomly selected (see Table A.1 for specific coordinates of each plot); coordinates of the WLD marsh plots other than the reference were based on Henry and Twilley (2014)—triplicate samples were collected haphazardly within 10 m of these coordinates. [‡] Elevations of the Sabine marsh plots were determined in 2015 by Abbott (2017) based on in situ real-time kinematic positioning measurements (errors are standard error of triplicate plots); approximate elevations of the WLD plots are based on digital elevation model data (1-m resolution) obtained from the 2012 USGS National Elevation Dataset (https://viewer.nationalmap.gov/basic/?basemap=b1&category=ned,nedsrc&title=3DEP%20View; see Fig. A.2 for map of elevation model data). Photos of each marsh at the time of sampling are shown in Figs. A.3–A.12.

1.3.2 Initial soil sample collection and processing

Soil sampling was conducted during the spring and summer of 2016. Triplicate 30-cm-deep cores (i.d. 62 mm) were collected at least 10 m apart in each marsh within patches of representative vegetation. Exceptions were the cores that were collected from the 1-year-old Sabine marsh, which did not extend beyond a soil depth of 20–25 cm. Whole cores were sealed at both ends and immediately placed on ice until transfer to 4°C for storage. Cores were processed within 5 days of collection. Cores were sectioned in 5-cm increments, weighed, and then homogenized. Large (>3 mm) debris, including shell, leaf, and root fragments, were removed. A subset of the homogenized soil was weighed and then dried at 60°C to a constant weight. The bulk density and moisture content were determined from these weights. The dry soil was then ground to a fine powder with a mortar and pestle. Total organic matter of each section was estimated based on the mass lost on ignition of approximately 1 g of dry soil at

550°C for 4 hrs. TOC and TN of each dry soil sample were determined on a Costech 4010 elemental combustion system (Costech Analytical) after fumigation with concentrated HCl for 24 hrs and subsequent drying for 3 hrs at 60°C. To ensure that the sample signals were well above those of the three lowest standards, the quantity of sample used for elemental analysis was controlled so as to achieve a signal of >200 µg C and >15 µg N per sample. The basic soil characteristics are summarized in Table 1.2.

Table 1.2. Soil sample characteristics

	Marsh age	Depth range	Average (SD), n = 9 soil core sections[†]			
			Bulk density ($g \cdot cm^{-3}$)	Loss on ignition ($mg \cdot g^{-1}$)	TOC ($mg \cdot g^{-1}$)	TN ($mg \cdot g^{-1}$)
Sabine						
	1 year	0–15 cm	0.83 (0.14)	57 (4)	16 (1)	1.46 (0.08)
		15–25 cm	0.66 (0.08)[a]	65 (3)[a]	16 (1)[a]	1.53 (0.12)[a]
	6 years	0–15 cm	0.9 (0.3)	60 (19)	16 (5)	1.4 (0.5)
		15–30 cm	1.03 (0.14)[b]	52 (13)[b]	14 (5)[b]	1.2 (0.3)[b]
	14 years	0–15 cm	0.6 (0.3)	110 (60)	44 (26)	3.0 (1.8)
		15–30 cm	0.84 (0.07)	56 (9)	15 (1)	1.28 (0.08)
	33 years	0–15 cm	1.0 (0.2)	60 (30)	21 (9)	1.2 (0.7)
		15–30 cm	0.8 (0.2)	90 (40)	28 (12)	1.7 (0.9)
	Reference A	0–15 cm	0.4 (0.4)	270 (140)	120 (60)	8 (4)
		15–30 cm	0.8 (0.4)	150 (140)	70 (70)	5 (5)
	Reference B	0–15 cm	0.20 (0.12)	360 (140)	140 (50)	9 (4)
		15–30 cm	0.28 (0.11)	410 (90)	190 (40)	12 (2)
WLD						
	16 years	0–15 cm	1.16 (0.13)	34 (6)	8 (2)	0.54 (0.12)
		15–30 cm	1.39 (0.12)	25 (5)	7 (2)	0.41 (0.12)
	29 years	0–15 cm	0.47 (0.09)	121 (16)	39 (7)	2.7 (0.4)
		15–30 cm	0.7 (0.3)	80 (13)	27 (4)	1.7 (0.4)
	41 years	0–15 cm	0.46 (0.19)	170 (70)	60 (30)	4 (3)
		15–30 cm	0.80 (0.10)	78 (9)	22 (3)	1.6 (0.3)
	Reference	0–15 cm	0.23 (0.08)	310 (120)	130 (50)	9 (3)
		15–30 cm	0.41 (0.08)	160 (40)	61 (19)	4.2 (1.4)

Quantities for each individual core section are listed in Appendix E (Table E.1).
[†] n=9 except where noted: [a]n=5; [b]n=8

Chapter 2.
An Alternative Approach for Estimating the Contribution of Autoclaved Alkaline-Extractable Protein to Soil Organic Carbon and Nitrogen

2.1. Introduction

Whereas the overall C fraction of SOM has received much attention, the component of SOM that is associated with N has been less well studied, despite its potential significance in soil C stabilization and storage through a variety of mechanisms (Rillig et al., 2007; Knicker, 2011). The vast majority of soil N (~95%) is in organic form, and there is evidence suggesting that the majority of this organic N (>50%) is attributable to proteinaceous components (e.g., proteins, amino sugars, free/bound amino acids) (Preston, 1996; Martens and Loeffelmann, 2003; Nannipieri and Eldor, 2009). Autoclaved alkaline-extractable (AAE) protein (a.k.a. glomalin-related soil protein) is an operationally defined proteinaceous fraction of SOM that has been given substantial attention, in part, because it is thought to contribute to the stability of SOM, including organic C (Rillig et al., 2001a; Rillig et al., 2007; López-Merino et al., 2015; Zhang et al., 2017). Unfortunately, however, making quantitative assessments of the AAE protein fraction—and its contribution to soil C and N—has not been straightforward. The distinction between the proteinaceous and non-proteinaceous components has been particularly problematic. Thus, critical questions still remain: does the *protein* have anything to do with organic matter preservation and soil aggregation? Or is it simply "along for the ride" with the conglomerate of lignocelluloses, lipids, waxes, metals, and many other compounds that apparently comprise the humic acids fraction? Therefore, the distinction between what is protein and what is not within AAE protein extracts is essential if the role this protein pool may play in the C and N cycles is to be better understood.

Attempts to further our understanding of this proteinaceous fraction have been confounded by the fact that a substantial amount of the material extracted by the AAE protein method resembles humic substances; protein or amino acids comprise a minor proportion (Schindler et al., 2007; Gillespie et al., 2011; Walley et al., 2014). The lack of specificity of the extraction is problematic because it is now well established that the Bradford protein assay exhibits interference from compounds similar to those co-extracted in the AAE protein method, including humic acids (HA) and tannic acid (Mayer et al., 1986; Whiffen et al., 2007; Roberts and Jones, 2008; Redmile-Gordon et al., 2013). This apparent interference, however, is not unique to the Bradford assay nor to AAE protein. In a thorough examination of the susceptibility of several commonly used protein quantification assays to interference from HA in soil solutions, Roberts and Jones (2008) have concluded that all spectrophotometric and fluorescence-based assays they tested exhibited interference to various degrees, depending on the concentration of both protein and HA addition. This interference appears variable and can have effects ranging from overestimation to underestimation of the protein concentration. Concordantly, Whiffen et al. (2007) have shown that addition of HA to AAE protein extracts substantially increases the Bradford signal for some soils, whereas other soils are minimally affected. As evident from the results of such studies of HA-mediated interference in the Bradford assay, the technique of standard addition cannot correct for HA interference in the Bradford assay. This

technique is valid when there is an effect *only* on the slope of the standard curve and no effect on its elevation. Whereas, in the case of HA-Bradford interference, both of these effects are apparent, in addition to nonlinearity at high concentrations. Redmile-Gordon et al. (2013) have suggested the use of a modified Lowry assay that they observed to be less perturbed by HA addition than the Bradford assay. However, they still observed significant interference, despite the relatively low HA concentrations tested. Whereas numerous methods have been successfully applied to purify the protein component of extracts from soil and plant litter (Ceccanti et al., 1978; Criquet et al., 2002; Wang et al., 2006; Benndorf et al., 2007; Masciandaro et al., 2008; Bastida et al., 2009), including AAE protein extracts (Chen et al., 2009; Gillespie et al., 2011), these methods typically do not yield quantitative recovery of the total protein present. This limitation is problematic in estimations of total soil protein fractions because any internal standards added to the starting material may not behave similarly to the endogenous proteins or may become sequestered by humic substances (Kemp and Mudrochova, 1973; Ladd and Butler, 1975; Tan et al., 2008; Wang et al., 2008). Indeed, based on tracing ^{14}C-labeled protein additions to AAE protein extracts, I had little success in recovering a consistently high proportion of the labeled protein from the extracts by various purification methods—including phenol extraction, HA-precipitation with $CaCl_2$ or $MnCl_2$, and HA-binding with polyvinylpolypyrrolidone (unpublished data)—results consistent with the work of others (Aoyama, 2006; Benndorf et al., 2007; Taylor and Williams, 2010). Perhaps the most rigorous workaround employed to distinguish between protein and other organic matter in solutions containing HA when using the Bradford assay was by Mayer et al. (1986), in which enzymatic digestion of protein was used. However, in their case, the goal was to quantify enzymatically hydrolysable protein only—not including protein that may have been bound within the humic matter milieu to the extent that it was protected from enzymatic hydrolysis (Kemp and Mudrochova, 1973; Zang et al., 2000). Yet, from a soil C storage perspective, the protein that is not readily degraded by enzymes is of equal interest.

Despite these shortcomings, assays for AAE protein continue to be used to infer C storage potential and soil health on the basis of the correlative links mentioned in Chapter 1 (for instance, Xie et al., 2015; Zhang et al., 2015; Singh et al., 2017; Sui et al., 2017; Halvorson et al., 2018; Wang et al., 2018a; Wang et al., 2018b; Xiao et al., 2019). However, given the difficulty in distinguishing proteinaceous material from other closely related organic compounds, it seems that this method, as it now stands, cannot provide much insight into AAE protein dynamics and any controls it may have on soil C. Although it is likely that the co-extracted, non-proteinaceous compounds play an important role, measuring a partial and variable combination of these along with protein, all as a single entity, may create confusion and hamper efforts to elucidate the mechanisms that underlie AAE protein dynamics. An example of this problem is the estimation of the contribution of AAE protein to the C and N in soils. A common practice is to estimate the C and N composition of the Bradford-reactive component by assuming that it is equal to that of the total extracted solids, which I will refer to as AAE solids (AAES). There have been several estimates of the C and N composition of AAE protein, nearly all of which have been based on the total extracted solids (for instance, Rillig et al., 2001a; Lovelock et al., 2004; Schindler et al., 2007; Wang et al., 2018a). The estimates typically fall in the range of 10–42% C and 1–5% N. Given the fact that none of the standard proteinogenic amino acids has a N composition <8% (average: 16.9%), these figures are

indicative of a material that must have a substantial non-amide component, consistent with characterization studies of AAE protein extracts (Schindler et al., 2007; Gillespie et al., 2011). By assuming the C and N composition of AAE protein and total extracted solids to be identical, researchers have mixed two definitions of AAE protein—namely, that of the protein and that of the total extract. This confusion has potentially led to grossly inaccurate estimates of the C and N contribution of AAE protein to SOM, particularly in soils of greatest interest with respect to soil C—those with high organic matter and therefore high HA content. Given that AAE protein, as its name suggests, was defined as a collection of proteins, it seems more reasonable to determine the C and N contributed solely by protein, or at least proteinaceous material (including peptides and bound amino acids), and to assign the remaining C to the HA fraction. Although accomplishing this goal is not straightforward, Roberts and Jones (2008) have recommended the use of acid hydrolysis and amino acid analysis (AAA) of the extracts to provide a more accurate estimate of protein content, which would also provide estimates of C and N composition. Despite this recommendation, I found no published studies that have attempted to use this method for whole AAE protein extracts (though Nichols and Wright (2004) purport to have done so). One of the drawbacks of this method, however, is that it is time-consuming and expensive. Routine measurements of hundreds of samples may therefore be impractical. Hence there does not appear to be a satisfactory way to quantify total proteinaceous material in soil extracts on a routine basis. A method suitable for routine estimation that at least gives accurate upper and lower bounds is needed.

Although it has been suggested that published estimates of the contribution of AAE protein to organic C and N in soils may be too high (Gillespie et al., 2011; Walley et al., 2014), I am aware of no studies that have assessed this potential inaccuracy by employing alternative methods of quantification of the total proteinaceous material in AAE protein extracts (i.e., without reliance upon a spectrophotometric assay). Thus, in the present study, and as part of an investigation of soil C and N accumulation within two chronosequences of newly established coastal wetlands, I sought a relatively inexpensive and quick method of estimating the quantity of the proteinaceous component of AAE protein extracts (hereon referred to simply as AAE protein) and its contribution to the total organic carbon (TOC) and total nitrogen (TN) in these soils based on a combination of elemental analysis and pooled-sample AAA. My approach gives upper and lower bounds to these estimates. The method exploits previous observations that the hydrolysable amino acid contribution to total soil organic N varies relatively little between soils and between HA extracts (Schnitzer and Ivarson, 1982; Christensen and Bech-Andersen, 1989; Schulten and Schnitzer, 1998; Friedel and Scheller, 2002). I therefore pooled AAE protein extracts within each chronosequence site to reduce cost and time requirements. The total amino acid content and its C and N composition yielded by the AAA was then paired with the C and N composition of each individual extract determined by carbon-hydrogen-nitrogen (CHN) elemental analysis. Assuming all N in the extracts to be contributed by protein led to a maximum estimate of the protein (Max-AAE protein) content, and an upper bound on the contribution of AAE protein to soil TOC and TN could then be established. Similarly, a minimum estimate (Min-AAE protein) was established by assuming the fraction of extracted N detected as amino acids to be conserved within the upper 0–15 cm or 15–30 cm of soil within a given chronosequence site. For comparison, I also measured the protein concentration in the same extracts using the traditional Bradford assay-based approach, which I will refer to as Bradford-

reactive AAE protein (BR-AAE protein). Being chronosequences of inundated soils, my study sites encompassed an exceptionally broad range of SOM concentration (2–58% loss on ignition) within relatively small areas and thus provided an excellent opportunity to test how these methods of estimation compared across a range of *in situ* SOM concentrations and abundances of humic matter.

Specifically, my goals were to 1) determine minimum and maximum estimates of the contribution of AAE protein to TOC and TN at my study sites without reliance upon a spectrophotometric or fluorometric assay, 2) compare the relationship between AAE protein and TOC among the Min-, Max-, and BR-AAE protein methods, and 3) compare my minimum and maximum AAE protein estimates to Bradford-based AAE protein estimates to determine the extent to which the traditional BR-AAE protein method may be inaccurate. Additionally, I sought to compare these estimates as a function of HA concentration and dilution factor to results of previous studies of HA interference in the Bradford assay. Analyses of overall trends in AAE protein with respect to chronosequence age, soil depth, vegetation, AMF, and refractory organic matter are beyond the scope of this chapter and will be presented in the subsequent chapters.

2.2. Materials and methods

2.2.1 Study sites and initial soil sample processing

The study sites were located in the Sabine National Wildlife Refuge (Sabine) and the Wax Lake Delta (WLD). Information regarding these study sites, the initial soil sampling and processing, and the basic soil characteristics were provided in Section 1.3 (Chapter 1).

2.2.2 AAE protein extraction

Total AAE protein was extracted from the soil of each depth section as per Wright et al. (2006) with minor modifications. Approximately 0.5–1.0 g of dry homogenized soil was weighed into 50-mL polypropylene tubes and sequentially extracted in 8 mL of 100-mM sodium pyrophosphate buffer (pH 9.0) for 60 min at 121°C in an autoclave (liquids setting). Each extraction cycle was followed by centrifugation at 3500×*g* for 20 min, the supernatant extract decanted to a separate tube (stored at 4°C), and a fresh 8 mL of buffer added to the soil pellet. Pellets were thoroughly resuspended in the fresh buffer by vortex mixing before the next autoclave cycle. This cycle was repeated until supernatants appeared pale yellow to colorless—typically 6–9 cycles. The extracts from all cycles of a given sample were pooled, each combined extract was centrifuged at 3500×*g* for 20 min to pellet residual fine soil particles, and the supernatant was transferred to a clean tube. To remove most of the extraction buffer, carbonates, salts, and oligopeptides, the extracts were precipitated with concentrated HCl at 4°C to achieve a pH of 2–2.5 and incubated at 4°C for 1 hr before centrifugation at 3500×*g* for 15 min. Immediately afterward, supernatants were discarded, and pellets were fully re-dissolved in an amount of 0.1 M NaOH approximately commensurate with the amount of solid, then vigorously swirled to mix and stored at −20°C. Total extract volumes were calculated

based on weight and density on a per sample basis at approximately 4°C—the approximate temperature at which samples were aliquoted for downstream analyses.

2.2.3 Quantification by the Bradford assay (BR-AAE protein)

BR-AAE protein was determined using the Coomassie Plus protein assay kit (#23236; Pierce Biotechnology) as per the manufacturer's instructions for the standard microplate protocol, except for the inclusion of additional standard curve concentrations within the linear region. This assay reagent is essentially equivalent to that described by Bradford (1976), except for minor modifications to increase the linear range of response as stated by the manufacturer. Quantification was made on a SpectraMax M2 plate reader (Molecular Devices) based on triplicate standard curves of a bovine serum albumin (BSA) standard solution (Fisher), prepared with 0.1 M NaOH as the diluent. Triplicate aliquots of each extract were combined with the Coomassie reagent in a reagent:sample ratio of 30 (v/v), followed by shaking on a plate shaker for 1 min, and incubation at room temperature for 8 min prior to measurement of absorbance at 595 nm. Samples that were beyond the linear range of the standard curve were diluted accordingly and rerun. Immediately following the readings, the wells were inspected visually to confirm that no material precipitated. To correct for absorbance by the extracts alone (due to co-extracted HA), the process was repeated with deionized water (DI H_2O) substituted for the Coomassie reagent. The average absorbance of each extract was subtracted from the assay absorbance prior to application of the standard curve regression.

2.2.4 Humic acids estimation

The HA concentration in each extract was estimated by absorbance at 465 nm based on triplicate standard curves of Sigma HA mixture (#H16752; Sigma-Aldrich) dissolved in 0.1 M NaOH. Measurements were made in triplicate on a NanoDrop 2000c spectrophotometer (Thermo Fisher). Because the Sigma HA contained a small amount of insoluble material, the standard stock solution was centrifuged in pre-weighed tubes, and the pellet dried and weighed. The insoluble material was cream-colored and was equivalent to approximately 12% of the weight of the initial dry HA. This weight was used to correct the standard curve concentrations accordingly.

2.2.5 Amino acid and elemental analysis of AAE protein extracts (Min-AAE protein and Max-AAE protein)

Prior to elemental and amino acid analyses, a measured volume of each AAE protein extract (Section 2.2.2) was dialyzed against DI H_2O in batches at room temperature with gentle stirring for 60 hrs. The bulk water was changed every 12 hrs. The dialysis tubing (Spectra/Por RC 2; Spectrum Labs) was 16 mm i.d. with a molecular weight cutoff of 12–14 kDa. After dialysis, the contents of each dialysis tube were quantitatively transferred to a clean, pre-combusted and pre-weighed glass vial by rinsing the tube with DI H_2O within the vial. Vials of dialyzed extracts were evaporated to dryness at 60°C and weighed to determine total residue

(AAES) per original extract volume. A subset of each residue was analyzed for %C and %N on an Exeter CE440 elemental analyzer (Exeter Analytical).

The remainder of each residue was suspended in a minimal volume of DI H_2O, and samples from the same site within the 0–15 cm or 15–30 cm depth range were pooled into one vial. This procedure yielded a total of 20 pooled samples. A portion of each pooled sample was dried and analyzed for %C and %N as above. Additionally, for AAA, duplicate aliquots of each pooled sample were carefully pipetted into cleaned, pre-weighed glass hydrolysis tubes, evaporated to dryness at 60°C, and weighed to determine the mass of material for AAA. Each tube contained approximately 7–13 mg of solid. Liquid-phase hydrolysis and AAA were conducted by the Protein Chemistry Lab at Texas A&M University (College Station, TX). Two internal standards (Norvaline and Sarcosine) were combined with each duplicate residue and hydrolyzed in 6 M HCl at 100°C for 22 hrs followed by centrifugation, drying of the supernatant in a vacuum concentrator, and redissolution in 0.4 M borate buffer. The liberated amino acids were derivatized with o-phthalaldehyde and 9-fluoromethyl-chloroformate and quantified on an Agilent 1260 liquid chromatograph (Agilent Technologies) equipped with a reverse-phase column and fluorescence detector. Because of the limitations of the assay, asparagine and glutamine were not distinguished from their respective acid forms, whereas cysteine and tryptophan were not measured. The total amount of amino acids detected in each sample ranged from approximately 200 to 900 µg. A representative chromatogram is included in Appendix C (Fig. C.1). Because not all of the solid material dissolved during the hydrolysis step, the amount of non-hydrolyzed N was determined for the post-hydrolysis residue of each pool. The non-hydrolyzed residue in each pre-weighed tube was rinsed with 6 M HCl at room temperature and centrifuged. After a total of five rinses, each residue was then dried at 60°C. The dry residues were weighed and analyzed for %C and %N as described above.

2.2.6 Assessment of interference from humic acids in the Bradford assay

Although the HA interference pattern of the Bradford assay has been shown previously (particularly by Roberts and Jones, 2008), the pattern may exhibit small differences depending on the reagent:sample ratio, HA concentration, and particular formulation of the Bradford reagent. Thus, I opted to measure this pattern for the specific Coomassie reagent and method used in the present study. The HA standard curve prepared as described above was measured with the Bradford assay without added BSA. The absorbances were translated to protein equivalents based on a BSA standard curve with and without adjusting for potential protein content of the HA standard based on its N content (measured as described for soil TN). Additionally, four BSA standard curve sets differing in HA concentration (0, 220, 440, 880 $\mu g \cdot mL^{-1}$) were prepared in order to determine interactive effects with protein.

2.2.7 Effect of sample dilution on Bradford-based estimates

To test whether the degree of dilution could have affected the relative discrepancy between the methods, I conducted a dilution experiment similar to that described by Reyna and Wall (2014). A portion of each dry, pooled extract was reconstituted in an amount of 0.1 M NaOH to achieve an AAES concentration of approximately 2 $mg \cdot mL^{-1}$, and each serially diluted

2- and 4-fold. Each dilution was analyzed by the Bradford assay as above, and the resulting BR-AAE protein content was normalized to %N of the pools assuming the BR-AAE protein component to have the same %N composition as that of the amino acids liberated during the AAA. The HA concentration of each sample was determined as described above.

2.2.8 Estimations of protein concentration in the AAES and its contribution to TOC and TN in soil

Whereas it is clear that the ability to measure total protein in AAE protein extracts would allow for straightforward calculations, this ability is presently not realized in a practical way. Simple accounting of the N present in the AAES can be expressed as the sum of the N contributed by protein and that contributed by all non-protein within the AAES, as shown by Eq. 2.1,

$$\%\mathrm{N}_{\mathrm{AAES}}(\mathrm{m}_{\mathrm{AAES}}) = \%\mathrm{N}_{\mathrm{P}}(\mathrm{m}_{\mathrm{p}}) + \%\mathrm{N}_{\mathrm{R}}(\mathrm{m}_{\mathrm{R}}) \tag{2.1}$$

in which $\mathrm{m}_{\mathrm{AAES}}$, m_{P}, and m_{R} represent the mass of AAES, protein, and non-protein, respectively. The %N composition of each of these entities is represented by $\%\mathrm{N}$. It is clear that by assuming $\%\mathrm{N}_{\mathrm{R}}$ to be zero (i.e., assuming that R contains no N), Eq. 2.1 reduces to Eq. 2.2,

$$\mathrm{m}_{\mathrm{P}} = \left(\frac{\%\mathrm{N}_{\mathrm{AAES}}}{\%\mathrm{N}_{\mathrm{P}}}\right) \times \mathrm{m}_{\mathrm{AAES}} \tag{2.2}$$

and hence Eq. 2.2 yields an upper bound to the mass of protein in the AAES. By measuring the %N and total weight of the AAES, and by assuming the %N of the protein ($\%\mathrm{N}_{\mathrm{P}}$) to equal that of the amino acids detected by AAA in a corresponding pooled sample ($\%\mathrm{N}'_{\mathrm{AA}}$), a maximum estimate of the protein in the AAES (Max-AAE protein) can be established. From this point, a maximum contribution of AAE protein to TOC and TN can be calculated per Eq. 2.3,

$$\begin{aligned}\%\text{ Max-AAE protein-X of total soil X } &= \left(\frac{\mathrm{m}_{\mathrm{P}}}{\mathrm{m}_{\mathrm{soil}}}\right) \times \left(\frac{\%\mathrm{X}_{\mathrm{AA}}}{\%\mathrm{X}_{\mathrm{soil}}}\right) \times \frac{100\ \%}{1000\ \mathrm{mg/g}} \\ &= \left(\frac{\%\mathrm{N}_{\mathrm{AAES}}}{\%\mathrm{N}'_{\mathrm{AA}}}\right) \times \left(\frac{\mathrm{m}_{\mathrm{AAES}}}{\mathrm{m}_{\mathrm{soil}}}\right) \times \left(\frac{\%\mathrm{X}_{\mathrm{AA}}}{\%\mathrm{X}_{\mathrm{soil}}}\right) \times \frac{100\ \%}{1000\ \mathrm{mg/g}}\end{aligned} \tag{2.3}$$

in which $\%\mathrm{X}$ represents the elemental composition (%OC or %N), depending on which elemental contribution is being estimated, and m represents the dry mass in mg of AAES or g of soil. The subscripts denote the material being measured—AAES, total autoclaved alkaline-extractable solids; AA, amino acids (in pooled sample); soil, total dry soil.

To establish a lower bound to the mass of the proteinaceous component in the AAES, a different approach was needed. Previous observations that the fraction of total soil organic N (SON) that is accounted for by hydrolysable amino acids varies little between soils of differing amounts of TN (Schnitzer and Ivarson, 1982; Christensen and Bech-Andersen, 1989; Schulten and Schnitzer, 1998; Friedel and Scheller, 2002) led me to pool samples for AAA in order to reduce time and cost requirements. Samples within soil depth intervals of 0–15 cm or 15–30

cm and within a given chronosequence site were pooled together prior to AAA. Specifically, the assumption that allows this pooling is represented by Eq. 2.4,

$$\frac{\%N'_{AA}(m'_{AA})}{\%N'_{AAES}(m'_{AAES})} = \frac{\%N_{AA}(m_{AA})}{\%N_{AAES}(m_{AAES})} \quad (2.4)$$

in which the primes represent the values for a given pooled sample, and m_{AA} and $\%N_{AA}$ represent the overall mass and N composition of the detected amino acids, respectively. Assuming that the N composition of the hydrolyzed amino acids is equal to that of the total amino acids (Eq. 2.5), and that all amino acids detected are from protein, Eq. 2.4 can then be reduced to Eq. 2.6.

$$\%N'_{AA} = \%N_{AA} = \%N_P \quad (2.5)$$

$$m_P = m_{AA} = (m_{AAES}) \times \left(\frac{\%N_{AAES} \times m'_{AA}}{\%N'_{AAES} \times m'_{AAES}}\right) \quad (2.6)$$

A minimum AAE protein-C and -N contribution estimate was obtained in a similar manner to that presented in Eq. 2.3, except that the m_P of Eq. 2.6 was used in place of the m_P from Eq. 2.2. Thus, a minimum estimate of the contribution of AAE protein to TOC and TN could be calculated using Eq. 2.7,

$$\%\text{ Min-AAE protein-X of total soil X} = \left(\frac{\%N_{AAES} \times m'_{AA}}{\%N'_{AAES} \times m'_{AAES}}\right) \times \left(\frac{m_{AAES}}{m_{soil}}\right) \times \left(\frac{\%X_{AA}}{\%X_{soil}}\right) \times \frac{100\ \%}{1000\ mg/g} \quad (2.7)$$

which is equivalent to scaling Eq. 2.3 by the ratio of amino acid N to total N in the pooled samples. Because samples for AAA were pooled by site and depth, this estimate assumes that the protein-N contribution to AAES-N is conserved between replicate cores within depths of 0–15 cm and 15–30 cm. Additionally, this estimate relies on the assumption that all protein amino acids were liberated during hydrolysis and that cysteine and tryptophan constitute a negligible proportion of the protein. Thus, I take this as a minimum estimate of proteinaceous content of the extracts.

For comparison, I also estimated the AAE protein-C and -N contribution based on protein concentrations measured using the Bradford assay and the elemental composition of the total extracted solids (AAES), as is often done in studies that include contribution estimates. This estimate is simply calculated using Eq. 2.8,

$$\%\text{ BR-AAE protein-X of total soil X} = \left(\frac{C_{BR} \times V_{extract}}{m_{soil}}\right) \times \left(\frac{\%X_{AAES}}{\%X_{soil}}\right) \times \frac{100\ \%}{1000\ mg/g} \quad (2.8)$$

in which C_{BR} and $V_{extract}$ represent the Bradford assay-based protein concentration ($mg \cdot mL^{-1}$) and the total volume (mL), respectively, of the extracts. A critical assumption in this method of estimation, besides reliance upon the Bradford-based protein concentrations, is that the

elemental composition of the proteinaceous component is equivalent to that of the total AAES after precipitation and dialysis. The elemental composition of the AAES, however, could vary substantially depending on the concentration of co-extracted compounds. This assumption was made here to facilitate comparison with published estimates of AAE protein-C and -N contributions to soil. For comparison of the three estimates in terms of protein concentration in the extracts, these equations can easily be converted by omitting the mass of soil and %X before normalizing to total extract volume.

2.2.9 Data analysis

All statistical analyses were made using MATLAB version R2016b (Mathworks). All chronosequence data included the values from the reference sites. For comparison of extract concentration estimates, uncertainty in the Max-AAE protein concentrations was estimated by propagation of the uncertainty estimates of each measurement on which the Max-AAE protein calculation relied, using a Monte Carlo technique to generate 95% confidence intervals for each calculation based on 1000 sets of normally distributed pseudorandom numbers (n = 175) per calculation (Appendix B, Script 1). The average proportion of AAES-N that was detected as amino acid N was compared between Sabine and WLD, and between the 0–15 cm and 15–30 cm depth increments by one-way analyses of variance (ANOVA). Comparisons of the correlations between the three sets of AAE protein estimates (as based on the three methods described in Section 2.2.8) with TOC were made by one-way analyses of covariance (ANCOVA). The corresponding *p*-values were based on Tukey-Kramer honestly significant differences post hoc tests yielded by the multcompare() function of MATLAB. The contribution of AAE protein to TOC and TN, as estimated by the three methods described above, were plotted against the loss on ignition of the soil. These plots were fit by piecewise linear regressions using a custom MATLAB function (Appendix B, Script 2). The breakpoints of these fits were automatically selected by the function such that the sum of squares of the errors in the dependent variable were minimized. The initial slopes and plateaus of these fits were compared by ANCOVA and ANOVA, respectively. To compare Bradford-based concentration estimates with those of the interference trends in solutions of HA and BSA, a surface was fit to the concentrations of the HA+BSA solution series using the curve fitting toolbox of MATLAB, adding and removing terms to maximize the goodness of fit while omitting non-significant ($p > 0.05$) terms. The discrepancy between BR-AAE and Max-AAE protein estimates of the pooled samples were compared at multiple sample dilution factors using ANOVA.

2.3. Results

2.3.1 BR-AAE protein, Max-AAE protein, and Min-AAE protein concentration estimates in the extracts

The Bradford assay yielded AAE protein concentrations in the extracts (Fig. 2.1) that were in almost all cases greater than the maximum protein estimates and 2–12 times the minimum estimates. The WLD samples exhibited a relatively clear trend of overestimation compared to the Sabine samples, which were more scattered at concentrations above 100

$\mu g \cdot mL^{-1}$. Despite being overestimates of total protein concentration, the BR-AAE protein concentrations were generally correlated with the Min- and Max-AAE protein estimates. The Max-AAE protein concentration estimates suggest that protein never comprised more than approximately 20% of the extracted solids by weight (data not shown), which is about two-thirds that suggested by Nichols and Wright (2004). Because of the way the Min-AAE protein concentrations were estimated, they were directly related to the Max-AAE protein estimates through the proportion of AAES-N accounted for by amino-acid N in the pooled extracts. Thus, the strong correlations among these Min-AAE protein relationships illustrate the consistency of the amino acid yield between the pooled extracts.

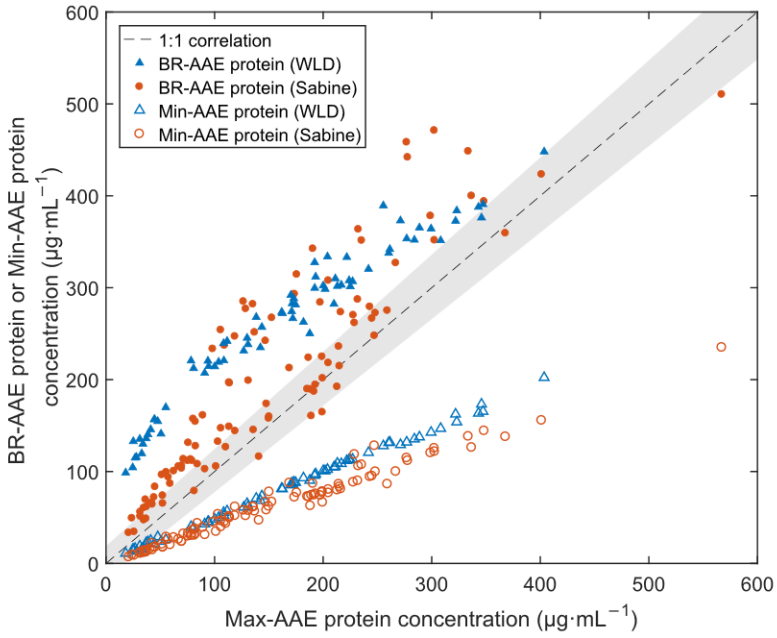

Figure 2.1. Correlation plot of measured BR-AAE protein concentration in the extracts (solid markers) and Min-AAE protein concentration estimates (open markers) versus calculated Max-AAE protein concentration in the same extracts. Dashed line marks the theoretical 1:1 correlation, and the shaded region represents the 95% confidence estimate of the Max-AAE protein concentration estimates based on a Monte Carlo simulated propagation of the error in each measurement that contributed to the estimate.

Table 2.1. Allocation of total N in AAES based on hydrolysis and amino acid analysis.

Chrono-sequence	Age (years)	Depth range	Mean AAES-N of total soil N	% of total extracted N (AAES-N)		
				Hydrolysable amino acid N	Non-hydrolysable N	Balance[†] (hydrolysable unknown N)
Sabine						
	1	0–15 cm	21%	39%	45%	16%
		15–30 cm	17%	45%	59%	(−4%)
	6	0–15 cm	19%	52%	53%	(−5%)
		15–30 cm	17%	39%	61%	0%
	14	0–15 cm	29%	40%	47%	13%
		15–30 cm	18%	34%	52%	14%
	33	0–15 cm	33%	46%	53%	1%
		15–30 cm	29%	44%	53%	4%
	(Ref. A)	0–15 cm	42%	37%	44%	18%
		15–30 cm	26%	33%	54%	13%
	(Ref. B)	0–15 cm	41%	41%	39%	19%
		15–30 cm	42%	39%	43%	19%
			Average ± SD	**41 ± 5%**	**50 ± 7%**	**12 ± 7%**
WLD						
	16	0–15 cm	16%	47%	57%	(−4%)
		15–30 cm	13%	61%	71%	(−31%)
	29	0–15 cm	38%	50%	36%	14%
		15–30 cm	34%	51%	37%	11%
	41	0–15 cm	35%	50%	32%	18%
		15–30 cm	28%	48%	43%	8%
	(Ref.)	0–15 cm	44%	48%	33%	20%
		15–30 cm	38%	50%	35%	15%
			Average ± SD	**51 ± 4%**	**43 ± 14%**	**14 ± 4%**

[†] Based on the difference between the initial N and the N detected as amino acids and in the post-hydrolysis residue; averages exclude negative values.

The Min-AAE protein estimates of protein concentrations in the extracts were substantially less than the estimated maximum. The proportion of the extracted N associated with amino acids was relatively consistent across sites within each chronosequence (Table 2.1), despite the tendency of the proportion of total soil N extracted in the AAE protein fraction to increase with chronosequence age by approximately two-fold or greater. Significant differences were not observed between the two pooled depth increments in the percentage of AAES-N detected as amino acids in either chronosequence (ANOVA, $p = 0.2$). However, a significant difference was observed in this percentage between the two chronosequences ($p < 0.05$). The percentages averaged 41 ± 5% and 51 ± 4% of the extracted N for Sabine and WLD, respectively. I observed that much of the N not detected as amino acids remained in solid form after hydrolysis as opposed to being liberated during hydrolysis. This observation is consistent with hydrolysis-based studies of SON, in which the non-hydrolysable N constitutes a sizable

proportion of the total N (Schulten and Schnitzer, 1998; Stevenson and Cole, 1999). The fraction of N hydrolyzed but not accounted for by the amino acids assayed (the hydrolysable unknown fraction; HUN) was estimated by difference and subject to considerable uncertainty. The uncertainty arose principally from the estimation of post-hydrolysis residue N, which would be artifactually high if the post-hydrolysis residues were not sufficiently rinsed prior to elemental analysis. This source of error likely contributed to some of the HUN values being negative. However, if the negative values were excluded, the estimated HUN fractions suggested that the majority (~78%) of the N liberated during hydrolysis was accounted for by the amino acids assayed.

2.3.2 Trends of estimated protein concentrations in the soil versus soil TOC

Across all three methods and both chronosequences, I observed a remarkably linear relationship and positive correlation between TOC and soil concentrations of AAE protein (Fig. 2.2). The squares of the Pearson correlation coefficients were 0.96–0.98 ($p < 0.001$). Both the Max-AAE protein and BR-AAE protein estimates yielded correlations that were no different between sites (ANCOVA, $p = 0.73$ and $p = 0.052$, respectively)—however, the slopes of the two methods differed ($p < 0.001$) based on an ANCOVA. The slope of the BR-AAE protein regression (0.196 mg·mgC^{-1}) was more positive than the slope of the Max-AAE protein regression (0.173 mg·mgC^{-1}; Fig. 2.2a). In contrast, the Min-AAE protein regression lines did differ significantly ($p < 0.05$) between sites (Fig. 2.2b), with slopes of 0.086 and 0.066 mg·mgC^{-1} for WLD and Sabine, respectively. As noted for the concentration estimates in Fig. 2.1, the slopes of the Min-AAE protein estimates reflected the proportion of total AAES-N that was attributable to hydrolysable amino acids and hence were necessarily less than 100% of the Max-AAE protein slope.

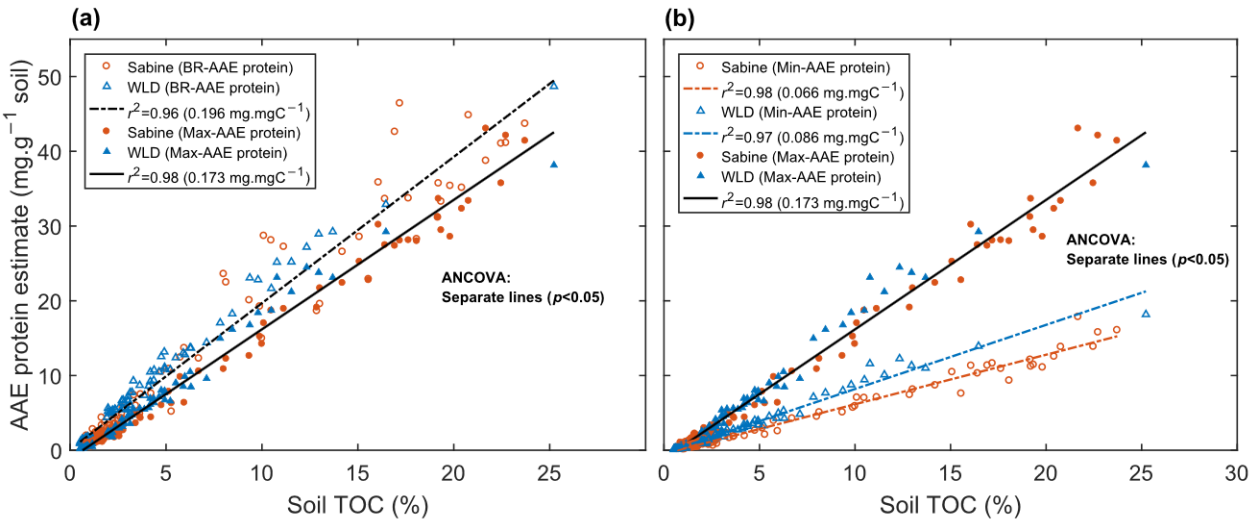

Figure 2.2. Correlation between estimated AAE protein and TOC concentrations in the soil among the different AAE protein estimation methods and ANCOVA results based on Tukey-Kramer HSD pairwise comparison of Model 1 linear regressions; (a) comparison of BR-AAE protein and Max-AAE protein correlations; (b) comparison of Min-AAE protein and Max-AAE protein correlations.

2.3.3 Estimated contribution of AAE protein to soil TOC and TN among the three estimates

Across both chronosequences and all depths, the AAE protein-C contribution to soil TOC as a function of SOM concentration appeared to increase with increasing percentage of SOM up to roughly 15% SOM (Figs. 2.3a and 2.3b). At higher percentages of SOM, the AAE protein-C contribution remained relatively constant. Based on these fits, the range of the estimated minimum to maximum AAE protein-C was 1.6–8.6% of TOC for Sabine and 1.2–9.7% of TOC for WLD. The Max-AAE protein-C estimates between the two chronosequences differed in terms of both initial slope ($p < 0.001$) and plateau ($p = 0.014$), with WLD exhibiting a steeper initial slope and greater plateau. Similarly, the initial slope and plateau of the Min-AAE protein-C estimate in WLD were also steeper ($p < 0.01$) and greater ($p < 0.001$), respectively, compared to Sabine. Overall, AAE protein-C ranged from 1.2–4% of TOC at the lowest percentages of SOM, and to 3.4–9.7% of TOC at SOM percentages above approximately 15%.

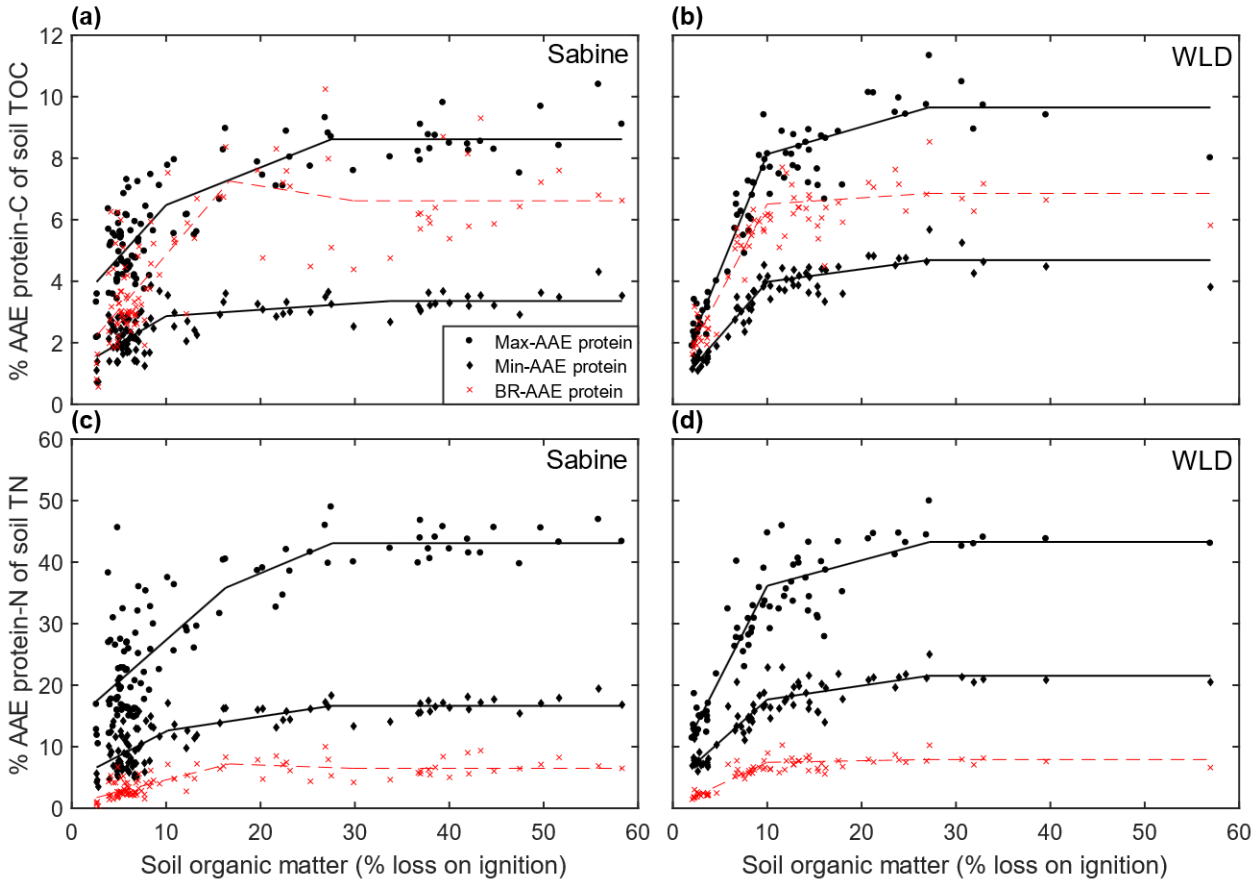

Figure 2.3. Comparison of AAE protein estimates with respect to C and N contribution to total SOM; AAE protein-C in Sabine (a) and WLD (b); AAE protein-N in Sabine (c) and WLD (d). Data were fit piecewise to three linear functions by least-squares regression.

Whereas estimation of Min-AAE protein and Max-AAE protein contributions to TN and TOC were made by assuming the average composition of the total protein to be equal to that of the amino acids liberated during hydrolysis, a different approach was adopted for the BR-AAE protein approach. Because the BR-AAE protein estimates nearly always exceeded the Max-AAE protein concentrations, it is clear that the Bradford method would also tend to overestimate the AAE protein contribution to TOC and TN. However, it has been a common practice to assume that the C and N composition of the protein matches that of the AAES when making BR-AAE protein-C and -N contribution estimates. I therefore took this same approach for the Bradford-based estimates when comparing the methods in terms of AAE protein-C and -N contributions. BR-AAE protein-C estimates were generally more scattered than those of the minimum and maximum estimates. Surprisingly, however, the error associated with protein overestimation in the Bradford assay was roughly balanced by the error associated with the assumption that the percent carbon in the Bradford-reactive protein equaled the percent carbon of the AAES. In other words, the percent carbon of the protein was apparently greater than the percent carbon of the AAES (averaging 52.6% and 25.4%, respectively; Fig. 2.4a). The result was BR-AAE protein-C contribution estimates that frequently fell between the Min-AAE protein-C and Max-AAE protein-C estimates. In all three cases (BR-AAE protein-C, Min-AAE protein-C, and Max-AAE protein-C), the contribution appeared to reach a plateau at high percentages of SOM. This plateau was reached at similar SOM percentages (27–34%) for all three estimates in both chronosequences, but the plateau itself differed between estimation methods in both chronosequences ($p < 0.01$). The estimated range of this plateau contribution was 3.4–8.6% of TOC in Sabine and 4.7–9.7% in WLD, based on the minimum and maximum estimates. Initial slopes of the three estimates did not differ in Sabine ($p = 0.15$) but did differ in WLD ($p < 0.001$) based on ANCOVA.

In contrast to BR-AAE protein-C, the BR-AAE protein-N estimates tended to be well below the Min-AAE protein-N estimates. It seems that, in the case of N, the error of the assumed N composition outweighed the overestimation from the Bradford assay. In other words, the percent nitrogen of the protein was apparently much greater than the percent nitrogen of the AAES (averages were 16.8% and 1.8%, respectively; Fig. 2.4b). The trends for AAE protein-N were similar to those of AAE protein-C. Overall, however, the magnitude of the AAE protein-N contribution to soil TN suggested by the minimum and maximum estimates was substantial—at SOM concentrations exceeding roughly 15%, these estimates suggested that AAE protein-N contributed 17–43% of TN in Sabine and 22–43% of TN in WLD (Figs. 2.3c and 2.3d). Initial slopes of the AAE protein-N contribution estimates all differed within WLD ($p < 0.05$), whereas in Sabine, the Max-AAE protein-N and Min-AAE protein-N slopes differed ($p < 0.001$), yet neither differed from the BR-AAE protein-N slope ($p = 0.36$). As with AAE protein-C, the plateau AAE protein-N contribution differed significantly between the three methods for both chronosequences ($p < 0.001$).

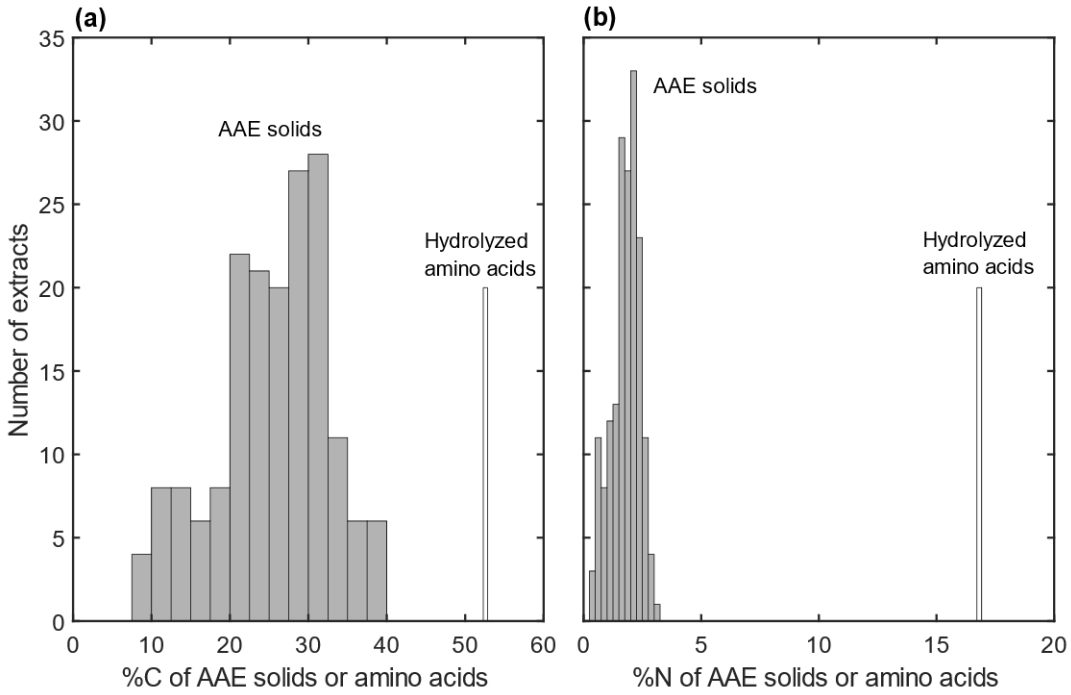

Figure 2.4. Histograms showing the distribution of %C (a) and %N (b) of the individual AAES samples (gray bars), along with those of the total hydrolysable amino acids (open bars) of the pooled AAES samples.

2.3.4 Interference in the Bradford assay

To determine whether a trend between HA concentration and BR-AAE protein overestimation existed in my samples, the relative discrepancy between the maximum protein and BR-AAE protein estimates was plotted against the HA concentration of each extract (Fig. 2.5a). I observed that relative discrepancies tended to be small when HA concentrations were high, whereas they were high and much more variable when HA concentrations were low, and a difference was apparent between the two chronosequences. Redmile-Gordon et al. (2013) have suggested that, in addition to HA concentration, the HA:protein ratio may also affect the extent of observed interference. I used the C:N ratio of the whole extracts as a proxy of HA:protein ratio (Fig. 2.5b). In this case, it appeared that the ratio explained much of the trend of overestimation in the WLD samples, though not in the Sabine samples. The trend differed significantly (ANCOVA $p < 0.001$) between the two chronosequences.

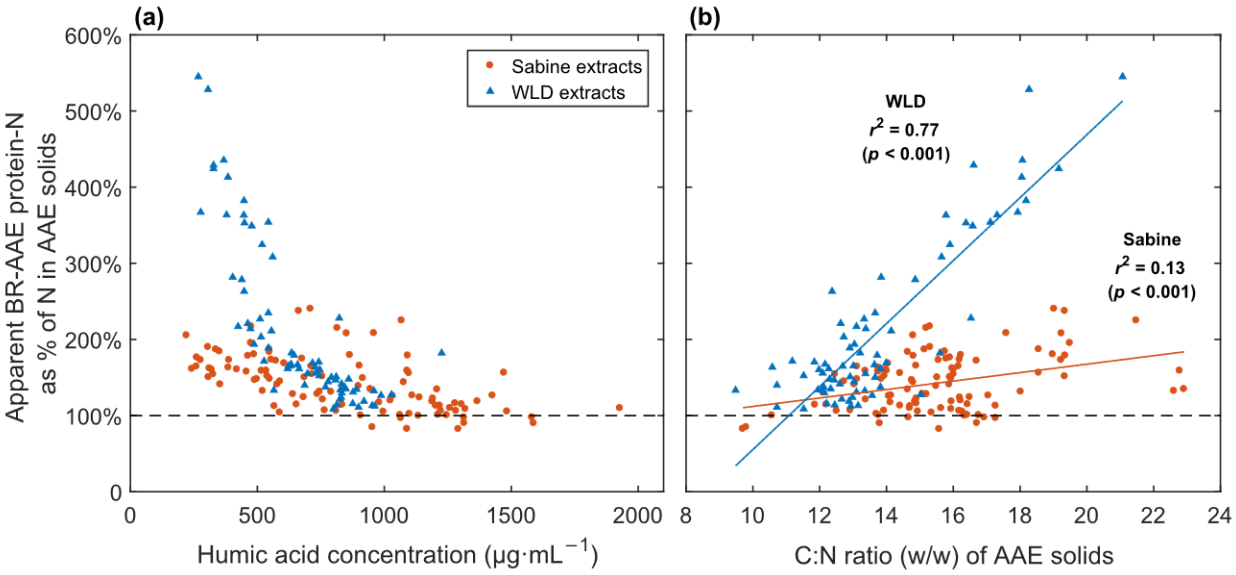

Figure 2.5. BR-AAE protein concentrations normalized to the Max-AAE protein concentrations as a function of HA concentration (a) and AAES C:N mass ratio (b) in each extract. The vertical axis is expressed as the contribution of protein to total N in the extract assuming the N composition of the protein to be equal to that of the amino acids detected after hydrolysis (16.8% N). Dashed line represents equivalence between the BR-AAE protein and Max-AAE protein concentration estimates, i.e., 100% of the N detected as BR-AAE protein.

To determine whether this trend could be explained by the HA addition interferences in the Bradford assay as observed previously (Whiffen et al., 2007; Roberts and Jones, 2008; Redmile-Gordon et al., 2013), I applied the same approach but with the supplies, reagents, and sample:reagent ratio used in the present study. Fig. 2.6a shows the effect of increasing HA concentration on the Bradford signal over a range of BSA standard concentrations, whereas Fig. 2.6b shows the effect of various concentrations of HA alone, in the absence of added protein. The general trends are highly consistent with those observed by Roberts and Jones (2008), in which the overestimation at low protein concentrations progressively diminishes with increasing protein concentration, ultimately yielding underestimates at even greater protein concentrations, though the concentration range of my observations did not extend to the point at which this would be expected. The degree of discrepancy increased with increasing HA concentration. Because a small but non-trivial amount of N (0.80%) was found in the Sigma HA mixture, I checked the extent to which this could explain the signal observed for the HA standard solutions. For this check, I made an adjustment of the observed signal ("total signal") based on the assumption that this N was present as protein with a N composition of 16.8%. This adjustment is demonstrated in Fig. 2.6b, where the adjusted values are termed the "unsupported signal" to denote that this strict interference signal cannot be accounted for by the possibility of protein in the Sigma HA mixture.

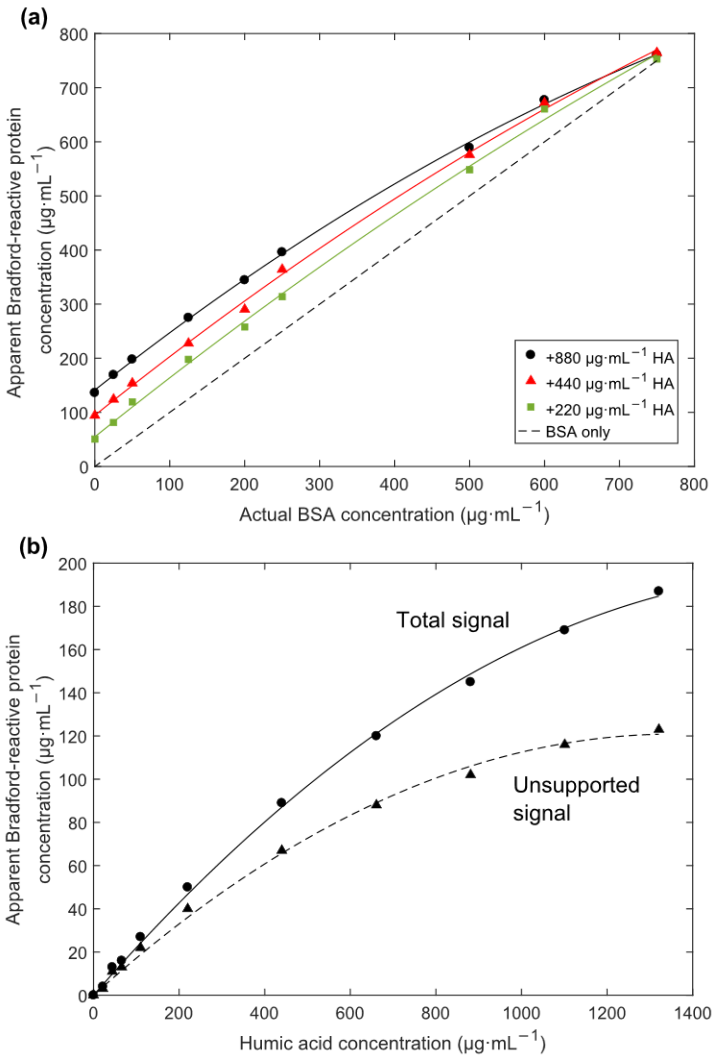

Figure 2.6. (a) Bradford response to the addition of three concentrations of Sigma HA to the BSA standards (solid lines) and the BSA standards with no HA addition (dashed line). (b) Bradford response to a range of HA concentrations without added protein. Dashed line shows the unsupported signal—the proportion of total that cannot be accounted for by the possibility of protein in the HA.

The interference trend observed in the standard addition experiment (Fig. 2.6a) qualitatively resembles the trend of overestimation in the WLD samples (Fig. 2.1) but not that in the Sabine samples. To determine, in a more quantitative manner, whether the standard addition interference trend could account for this overestimation observed in the soil extracts, the data of the standard addition experiment were regressed as a surface with the form of Eq. 2.9, in which the actual protein concentration (C_{corr}) in µg·mL^{-1} is expressed as a function of the apparent Bradford-reactive concentration (C_{BR}) in µg·mL^{-1} and the HA concentration (C_{HA}) in mg·mL^{-1}:

$$C_{corr} = \alpha(C_{HA}) + \beta(C_{BR}) + \gamma(C_{HA})(C_{BR}) + \varepsilon(C_{BR})^2 \quad (2.9)$$

$$\alpha = -0.1464 \text{ μg·mg}^{-1}$$

$$\beta = 0.6718$$

$$\gamma = 1.452 \times 10^{-4} \text{ mL·mg}^{-1}$$

$$\varepsilon = 4.274 \times 10^{-4} \text{ mL·μg}^{-1}$$

Greek letters represent the empirically derived regression coefficients of the surface. This equation was then used to "correct" the BR-AAE protein concentrations of the soil extracts based on the original BR-AAE protein concentration and the measured HA concentration of each extract. The "model-corrected" concentrations for the WLD samples were a substantial improvement with respect to the maximum protein estimates (Fig. 2.7a), whereas those of the Sabine samples were much more scattered and included concentrations that were well below the minimum estimates, including some negative values (Fig. 2.7b).

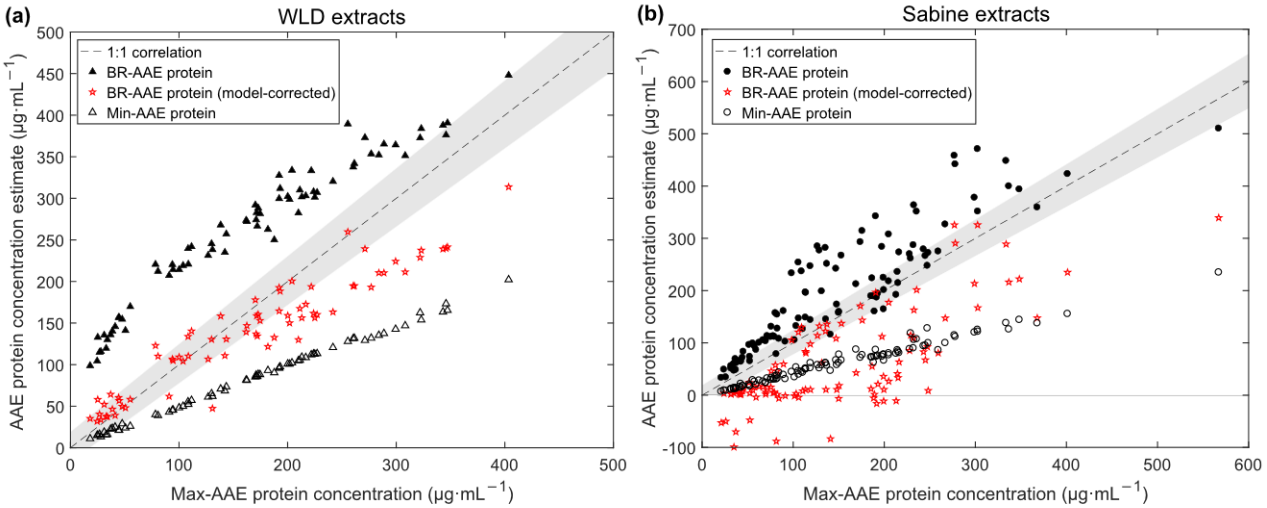

Figure 2.7. Plot of Fig. 2.1 augmented to include the model-corrected BR-AAE protein concentrations (red pentagrams) of (a) WLD soil extracts and (b) Sabine soil extracts.

Reyna and Wall (2014) have observed that apparent BR-AAE protein concentrations are not inversely proportional to volume—diluting the extracts increases the apparent total protein in the extracts—and I observed that the most severe overestimation by the Bradford assay tended to occur when HA concentrations were low (Fig. 2.5a). Thus, I tested the effect of dilution alone on the relative and absolute discrepancies between the Bradford and Max-AAE protein concentration estimates. I asked whether the discrepancies become greater and more variable when the samples are diluted. This assay was conducted on a portion of the pooled extract residues that were initially re-dissolved in a volume such that each solution was of similar AAES concentration ("undiluted" group), and a portion of each was diluted 2-fold and 4-fold. The measured BR-AAE protein concentrations of each dilution were multiplied by the dilution factor and normalized to the corresponding Max-AAE protein concentration estimates (relative discrepancy; Fig. 2.8a). In terms of this relative discrepancy, there was a significant

effect of dilution ($p < 0.05$). The discrepancy increased by a similar proportion with each dilution and was consistent with the general trend that has been observed by Reyna and Wall (2014). In terms of absolute discrepancy, however, it became clear that the proportional increase in relative discrepancy with dilution was primarily due to the normalization, given that the absolute discrepancy increased only subtly with dilution ($p < 0.05$) and ultimately reached a steady value at AAES concentrations of less than 1.1 mg·mL^{-1} ($p = 0.9$), as shown in Fig. 2.8b. Thus, as the extracts were diluted, the relative proportion of the discrepancy, and therefore variability, became increasingly dominant.

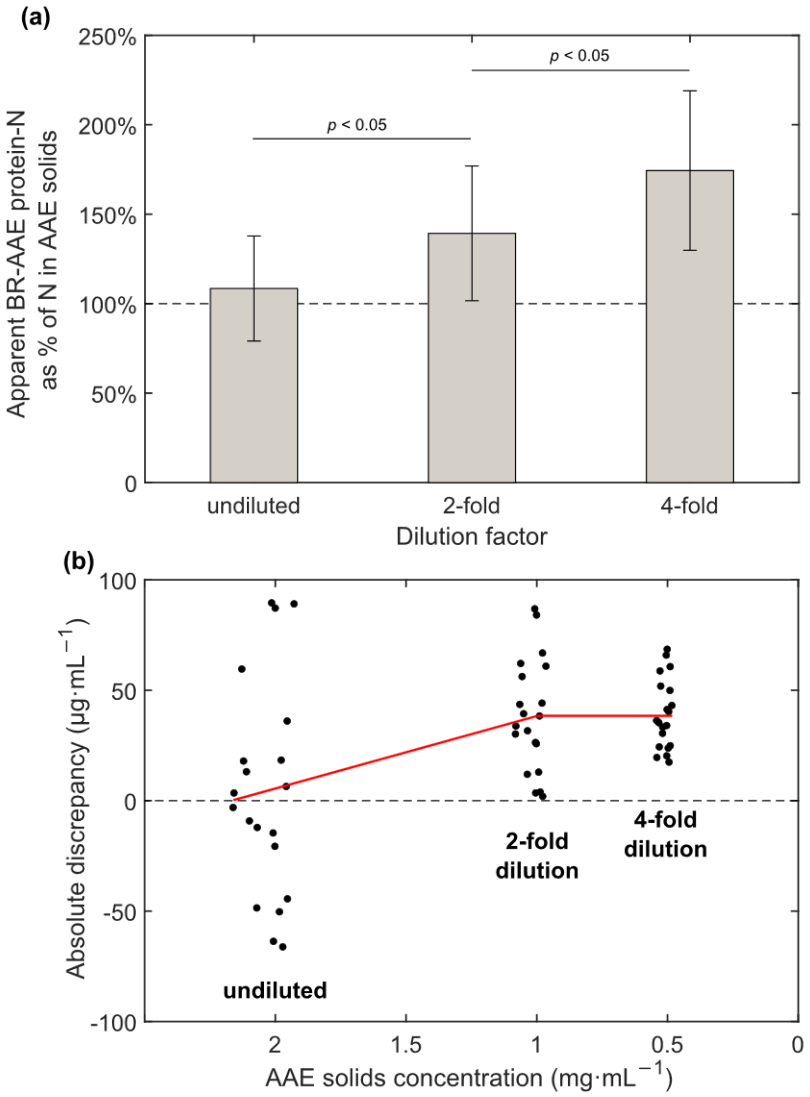

Figure 2.8. Effect of extract dilution on Bradford discrepancy. The relative discrepancy (a) was calculated by normalizing the Bradford concentration to the corresponding Max-AAE protein concentration estimate, whereas the absolute discrepancy (b) is the difference of the Bradford concentration and the Max-AAE protein concentration estimate (accounted for dilution). Error bars are ± SD (n = 20 extracts). Note the reversed abscissa axis in (b).

2.4. Discussion

2.4.1 Correlation with TOC

The strong positive correlation that I observed between TOC and all AAE protein estimates is consistent with numerous previous studies showing similar correlations (Table 2.2). Comparison of the BR-AAE protein slope (0.196 mg·mgC^{-1}) with that of Max-AAE protein (0.173 mg·mgC^{-1}) suggests that previous Bradford-based correlations may overestimate the slope of the relation. A comparison of my slope estimates with those reported in the literature (Table 2.2), however, suggests that these estimates can be quite variable, and the extent to which interference in the Bradford assay may contribute to this variation is unclear.

Table 2.2. Comparison of AAE protein-TOC correlations and AAES compositions among a selection of published studies and the present study

		Total-AAE protein vs TOC			
Reference	System	Slope (mg·mgC^{-1})	Pearson correlation	AAES-C (%)	AAES-N (%)
This study	W(fw), W(s)	0.066–0.173	0.98–0.99	8.3–39.9	0.4–3.2
Rillig et al. (2001a)	Tf	*[0.28]*	0.78–0.89	9.9–22.0	0.8–1.5
Wang et al. (2018a)	W(ds)	*[0.29]*	0.87	10.8–24.3	0.4–1.6
Lovelock et al. (2004)	Tf	N/R	0.60	29–42	3–5
Halvorson and Gonzalez (2006)	Ag, G, Nf	*[0.12]*	0.94	13–34	2.2–8.4
Rillig et al. (2003)	Ag, Nf, Af	N/R	0.87–0.93	27.9–43.1[a]	N/R
Bird et al. (2002)	Sa	*[0.08]*	0.86	30[a]	N/R
Halvorson et al. (2018)	Py	*[0.16]*	*[0.98]*	35[a]	4[a]
Xiao et al. (2019)	Af, G	0.28–1.00	0.60–0.85	N/R	N/R
Kumar et al. (2018)	Rm, Nf	*[0.49]*	*[0.97]*	*[33–36]*	N/R
Xie et al. (2015)	Ag	*[0.10]*	0.66	N/R	N/R
Wang et al. (2018b)	W(mg), W(mf)	*[0.12]*	0.87	19.3	N/R
Wang et al. (2015b)	Ag, Af, Nf	0.30	0.91	N/R	N/R

Square brackets indicate values that were not explicitly stated in the study but were estimated here based on the available published data (including supplementary material). Ag, agricultural; Nf, native forest; Af, afforested; Py, pyroclastic (upland and riparian); G, grassland; Rm, reclaimed mine spoil; Sa, semiarid rangeland; Tf, tropical forest; W, wetland (ds, deltaic shelf; fw, fresh marsh; mf, mudflat; mg, mangrove; s, salt marsh).
N/R = not reported. [a] Value was assumed, not measured, by the referenced authors.

2.4.2 Comparison of AAE protein-C and -N contribution estimates

Calculation of the AAE protein-C contribution to TOC among the three AAE protein estimates revealed that the BR-AAE protein method yielded values between my minimum and maximum estimates. However, this apparent agreement relied on a balance between the

overestimation of protein in the Bradford assay and the underestimation of the %C of the protein. Thus, the agreement I observed may not necessarily be the case in other instances given the variability in both the Bradford assay and the %C of AAES. Moreover, the soils I studied are characteristic of wetland systems and would be expected to differ from those of upland systems, in terms of both AAES-C composition and abundance of co-extracted HA. Nonetheless, the range in AAES-C composition that I observed here (8.3–39.9%) appears to encompass several of the ranges reported elsewhere in both upland and wetland systems (Table 2.2).

In the case of the AAE protein-N contribution to TN, however, the fact that the BR-AAE protein method always yielded an underestimate was directly due to a substantial underestimation of the %N of the proteinaceous component. Given the magnitude of this underestimation, it seems likely that most, if not all, previously reported AAE protein-N contribution estimates (in the few cases that they have been made) are erroneously low. This speculation is supported by the fact that the range of %N of the AAES that I observed here is in line with most previously reported values (Table 2.2). Indeed, the low AAE protein-N contribution estimates of previous studies may be why this contribution is not often reported. Here, I observed that AAE protein-N could account for up to 43% of total soil N in my oldest sites.

I observed trends of AAE protein-C and -N contribution to TOC and TN that were surprisingly similar between the two chronosequences; the main differences were the initial slopes. Furthermore, my data suggest that for a given system, there appears to be a limit on accumulation of AAE protein with respect to TOC, that is, there is some maximum proportion of protein that can constitute the total SOM. This upper bound suggests that the rate of accumulation of AAE protein is strongly linked to the rate of accumulation of the bulk organic matter, which is expected to be primarily of plant origin in my study sites. However, at relatively low SOM concentrations, the fact that AAE protein tends to be disproportionately lower may suggest that there is some priming effect, whereby, perhaps, AAE protein production increases as a response to enhanced primary production, accumulation of total SOM, or refractory forms of SOM. Given that the input of organic matter generally stimulates microbial activity and growth in soils, this pattern may indicate that the AAE protein is principally microbial in origin—not inconsistent with the AMF-source hypothesis. Alternatively, such a disproportionate trend in the younger sites may suggest that the AAE protein represents proteinaceous material that happens to undergo some binding/occlusion mechanism—similar to that proposed by Knicker and Hatcher (1997) or Schulten and Schnitzer (1997)—that may require time to reach a steady state.

2.4.3 Justification and limitations of the Min-AAE protein and Max-AAE protein estimates

Although I identified a reasonable range of protein content within the extracts, there was a substantial divergence between the maximum and minimum estimates. In interpreting this divergence, it is important to acknowledge the fact that both of these sets of estimates relied on certain assumptions. I estimated the maximum possible protein content of each extract based on the N composition of each extract and the amino acids liberated during hydrolysis. The major assumption inherent in this estimate is that all N in the dialyzed extracts

is present as protein; thus, I took it as an upper bound of protein content. It is likely that at least a small proportion of the total N is present as non-protein compounds such as oligopeptides, amino sugars, and N-heterocycles (e.g., plant metabolites, nucleic bases, microbial metabolites), as has been observed for humic substances (Schulten and Schnitzer, 1998); however, given that these extracts were purified by acid precipitation and extensive dialysis, I would expect any such compounds to be either covalently bound to, or tightly coordinated with, large (>12 kDa) molecules or molecular aggregates—in line with contemporary views of HA structures (Sutton and Sposito, 2005). Additionally, it should be noted that this maximum estimate also assumes that the N composition of the amino acids detected in the AAA is representative of all amino acids in the sample. Whereas it would clearly be expected that other, non-assayed amino acids (e.g., cysteine and tryptophan) would contribute, the N composition of proteinogenic amino acids in general does not vary by a substantial amount (17 ± 7%), and therefore I would not expect the inclusion of relatively small quantities of non-assayed amino acids to substantially affect my upper estimate.

My method of estimating the minimum protein in extracts was based on the assumption that, within a 15-cm soil depth range of a given chronosequence site, the proportion of extracted N that is present as hydrolysable amino acids is constant. This assumption is key for allowing individual extracts to be pooled in order to reduce the time and cost associated with the AAA. The small variation in amino acid N contribution that I observed between pools of different sites and depths, even as TN and SOM varied, suggests that this is a reasonable assumption. Furthermore, this assumption is supported by studies of N in soils and HA, in which the hydrolysable amino acids tended to account for a similar proportion of the TN across soils of varying TN concentrations (Schnitzer and Ivarson, 1982; Christensen and Bech-Andersen, 1989; Schulten and Schnitzer, 1998; Friedel and Scheller, 2002). Whereas most of the N liberated during hydrolysis was accounted for by the amino acids assayed, I observed that a minority (approximately 22%) was not. This could have been all or partially comprised by amino sugars and by non-assayed amino acids such as cysteine and tryptophan, as well as some non-protein amino acids such as those that often occur in plants (Seigler, 2012). Cysteine and tryptophan generally exhibit low recoveries under the conditions used for hydrolysis, with tryptophan typically being completely destroyed, and so are typically assayed separately on an additional sample. This was not pursued here because it would have substantially increased the time and cost of the analysis. Looking at studies that include AAA of soils in which these amino acids were assayed, the contributions of these amino acids are relatively small compared to the other amino acids combined (e.g., Martens and Loeffelmann, 2003).

Perhaps the one assumption that most impacted my minimum estimates is the assumption that all amino acids in the extracts were liberated during hydrolysis. Whereas an apparently small proportion of the N liberated during hydrolysis was not detected in the form of the amino acids assayed, I observed that on average around half of the solid material that underwent acid treatment remained in solid form afterwards and that the N composition of the remaining solid did not differ significantly from that of the original pre-hydrolysis material. This led to protein estimates that were much less than expected, prompting the question: do amino acids comprise a larger proportion of the AAES-N than what is suggested by the amino acid analysis? In fact, the question of the extent to which protein contributes to the total organic N in soils and alkaline extracts is long-standing. Early studies of soil organic N often attributed

around 30–45% to amino acids/protein based on acid hydrolysis—leaving around 20–30% of the N in unknown forms (Stevenson, 1994; Stevenson and Cole, 1999). With the advancement of ^{15}N-NMR and other spectroscopic technologies, in concert with improved fractionation methods, more sophisticated analyses of soils and HA have been possible, and estimates based on these refined methods have attributed 70-90% of soil organic N to proteinaceous compounds (Preston, 1996; Martens and Loeffelmann, 2003). Indeed, the idea that HA mixtures are a chemically distinct product of a humification process has fallen out of favor in recent years in light of such studies, including Kelleher and Simpson (2006), whose observations have suggested that the majority of the organic compounds in HA mixtures are consistent with the common biopolymers of cells, including protein. As Burdon (2001) and Lehmann and Kleber (2015) have contended, there is appreciable evidence supporting the hypothesis that HA and other alkaline extracts of soil are principally mixtures of biomolecules in various stages of decomposition. In the present study, the empirical model of humic acids-related interference in the Bradford assay that I derived and applied to the BR-AAE protein concentrations may suggest, at least for the WLD sites, that the majority (roughly 75%) of AAES-N may be present as protein. However, as evident from the application of this model to the Sabine samples, this model was not robust—thus, these model-corrected estimates are far from conclusive and only serve as suggestive evidence for the existence of amino acids in a non-hydrolysable form within my samples. Differences in characteristics between the Sigma HA mixture and the humic materials in the samples may have contributed to the lack of robustness of the model.

If, however, proteinaceous material does comprise a greater proportion of N than is suggested by amino acid analysis, why then would a substantial proportion not be dissolved in the acid during hydrolysis? Preston (1996) has suggested that some of this protein may resist hydrolysis through steric hindrance from other non-hydrolysable compounds, as evidenced by the work of Derenne et al. (1993) and further supported by the observations of Knicker and Hatcher (1997). There is also evidence that the formation of lignin-protein complexes in soils promotes the resistance of protein towards degradation (Lynch and Lynch, 1958). Additionally, it is well established that iron tends to be bound within AAE protein extracts (Wright and Upadhyaya, 1998; Rillig et al., 2001a), and there is growing evidence to suggest that oxides of iron and aluminum may contribute to the apparent partial resistance of soil organic N to acid hydrolysis (Leinweber and Schulten, 2000) and to the preservation of SOM in general (Kaiser and Guggenberger, 2000; Kleber et al., 2015). Indeed, such resistance to hydrolysis may relate to the apparent refractory nature of AAE protein. The work of Lalonde et al. (2012) has suggested that nanoparticulate forms of ferric iron may protect organic matter in marine sediments through both adsorption and co-precipitation mechanisms, a finding that has been supported by observations in WLD soils (Shields et al., 2016).

In my AAA, I opted for HCl hydrolysis on the basis that it is the most commonly used method of hydrolysis, and because I was working with dialyzed soil extracts rather than whole soil. In hindsight, the use of a different method of hydrolysis may have liberated additional amino acids. In light of the aforementioned studies of interaction between iron and organic matter, the application of a dithionite buffer (as used in these studies) to AAE protein extracts would likely be a more efficacious approach than the use of HCl alone. Additionally, Martens and Loeffelmann (2003) have observed that the use of methanesulfonic acid (MSA) for pre-AAA hydrolysis of soils tends to result in greater hydrolysable amino acid yields. The MSA method

has an added advantage in that it leaves tryptophan intact and does not oxidize cysteine. Use of dithionite with HCl, or MSA in place of HCl, may therefore be more appropriate in future analyses. Thus, in the absence of a more accurate yet inexpensive method of estimating AAE protein, the most suitable method for routine analysis may be a modified version of that presented here.

2.4.4 Interference trends in the Bradford assay

I observed that the overestimation of protein concentration in the WLD extracts by the Bradford assay was consistent with the interference observed both in my HA addition experiment and in that of Roberts and Jones (2008). Overestimation was also apparent in the Sabine samples, though generally not as great, and it did not follow the same trend of HA interference. My observations also support the conclusion of Redmile-Gordon et al. (2013) that the ratio of HA to protein is an important factor in determining the extent of the apparent interference. Although I observed that the dilution factor of the extracts also affected the observed interference as reported by Reyna and Wall (2014), it appears that this is directly related to the shape of the HA addition curves (Fig. 2.6a), as evidenced by the fact that the dilution effect is greatly diminished when looking at the absolute overestimation with dilution (Fig. 2.8b). Apparently, whatever mechanism underlies this dilution effect is the same mechanism that contributes to the interference in the first place. As a sample with a given protein and HA concentration is diluted, the relative discrepancy increases dramatically whereas the absolute discrepancy increases only subtly, eventually reaching a maximum once in the linear region of the HA addition curve (Fig. 2.6a). Thus, overestimation is greatest when protein concentration is low and HA concentration is high, meaning that both the HA:protein ratio and the HA concentration are likely to be important factors in determining the Bradford signal. Additionally, this means that interference is expected to be most variable at low protein concentrations, where small differences in HA concentration have the greatest impact. Conversely, at particularly high protein concentrations, the presence of HA may lead to underestimates, as has been established elsewhere (Roberts and Jones, 2008), and is consistent with the observations of Whiffen et al. (2007), who observed differing susceptibility to interference from HA addition among samples of differing organic content. Recently, Moragues-Saitua et al. (2019) have suggested that the Bradford assay may yield more accurate estimates of AAE protein if the extracts are diluted to the point at which the signals from subsequent dilutions are similar. Based on my observations, I would disagree—my data suggest that as the extracts are diluted, the interfering components increasingly dominate the Bradford signals, a phenomenon that often translates to greater levels of overestimation of protein and, in any case, yields estimates that have little to do with the actual protein concentration.

In terms of the estimates of protein concentration in my extracts, the BR-AAE protein estimates were always above the minimum estimate and rarely below the maximum estimate. Such overestimation is consistent with a range of previous studies; however, it is not consistent with the conclusions of Jorge-Araújo et al. (2015). Curiously, these authors took a different approach to evaluation of interference in the Bradford assay. Their standard addition technique involved adding known and differing amounts of a BSA standard to multiple aliquots of each sample. The authors asserted that by extrapolating the Bradford curve of these

standard additions, they could determine an accurate protein concentration. However, based on my observations and those of others (Whiffen et al., 2007; Roberts and Jones, 2008; Redmile-Gordon et al., 2013) that show that protein-free HA strongly interacts with the Coomassie dye (producing a color change in the absence of protein), I do not see how this technique could yield valid estimates. The standard addition method is only intended to account for matrix effects that modify the analyte signal but that do not result in a signal in the absence of analyte. Indeed, I believe this explains why Jorge-Araújo et al. (2015) have incongruently concluded that the presence of HA tends to yield underestimates—because the slope of the curve decreases (and the intercept increases) with increasing HA concentration, the standard addition method would be expected to always yield estimates above that of the raw samples, as observed by Moragues-Saitua et al. (2019). The observation by Jorge-Araújo et al. (2015) that the magnitude of underestimation decreased with increasing HA could also be explained by this mechanism, in that there is some point in the HA+BSA curve at which the overestimation diminishes and the assay appears to yield accurate figures.

A final point in regard to the Bradford assay is that the extracts themselves are not colorless. The fact that they do exhibit some absorption at 595 nm, the Bradford assay wavelength, is consistent with HA spectra. In my analysis, I subtracted this absorbance from each Bradford reading before applying the standard curve in order to account for this non-trivial absorption. Although this seems an intuitive step to take, it is rarely stated in published studies where BR-AAE protein has been measured, as recently pointed out by Moragues-Saitua et al. (2019). Omission of this step would only serve to exacerbate any overestimation already associated with the Bradford assay. In my samples, the extract absorbances alone would have increased the apparent Bradford readings by an average of 25% and up to 43%.

2.4.5 Recommendations for future work

The BR-AAE protein method has received some criticism over the past several years, particularly due to its lack of specificity towards protein in general. Yet, despite calls for new terminology such as Bradford-reactive fraction (Whiffen et al., 2007) and Bradford-reactive substances (Janos et al., 2008) that denote that protein is not specifically being measured, glomalin-related soil protein and related terms still prevail in studies relying on the Bradford assay, perhaps on the basis of consistency with previous literature. Furthermore, all studies that I found quantifying the C and N contribution from AAE protein seem to either 1) assume that all extracted solids are protein, even though the Bradford assay clearly does not measure all organic components in the extracts, or 2) assume that the C and N composition of the proteinaceous component is equivalent to that of the bulk extract. At this point, we must ask what the goal of these analyses is in order to decide whether we define a fraction that is specifically protein, and quantify only its C and N contribution, or we define a fraction that is the total extracted from soil under alkaline conditions and quantify the total C and N in that. The former option should be adopted if we are at all hopeful of elucidating the potential role of AMF and other microbial proteins in enhancing soil C storage. The latter option is essentially the foundation of the century-old humic acids definition. Instead, the mixing of these two by many researchers, perhaps out of convenience, results in various characteristics being wholly attributed to protein despite the fact that the protein is not being analyzed separately. This

further hinders elucidation of any potential role of soil protein in facilitating aggregation, organic matter preservation, and metal sequestration, as well as of any causal link with AMF.

In contrast to the Bradford assay-based method, the alternative approach involving AAA—as presented here—is not only more specific towards proteinaceous material, it also allows some additional information to be gleaned, such as the extent to which non-hydrolysable N contributes to the AAE protein fraction. However, even without the use of AAA, I suggest that the %N of the AAES would be a better metric than the BR-AAE protein method because not only is it unperturbed by HA contaminants, it is also much less prone to inter-study and inter-assay variability. Furthermore, the fact that many previous studies that have quantified BR-AAE protein have also quantified the %N of the extracts potentially allows revised protein estimates to be made from the existing literature.

2.5. Conclusions

By making a few assumptions, I was able to estimate a range for the contribution of AAE protein C and N to the soils of my study sites while minimizing time and cost requirements, and without the use of an interference-prone spectrophotometric assay. This range was wider than expected because a large proportion of N in the AAE protein extracts was unidentified. However, based on current research on the chemical identity of nitrogenous components of soils and HA mixtures, it is likely that this range can be refined. Additionally, improvements with respect to the hydrolysis step, such as the use of a dithionite buffer or MSA, may assist in refining the range further.

Although I observed interference and an associated overestimation of protein concentration when measured by the Bradford assay, consistent with previous findings, my BR-AAE protein-C contribution estimates were within the range of my maximum and minimum estimates. That this seeming contradiction is an apparent result of the method by which Bradford-based contribution estimates are traditionally calculated suggests that previously reported estimates of AAE protein-C contribution to TOC may in fact be reasonably accurate, though this cannot be assured based simply on the results presented here. In contrast, use of this traditional method tended to underestimate the AAE protein-N contribution, most notably at higher SOM concentrations. However, as many others have done, I urge those continuing to opt for the use of the Bradford assay for AAE protein measurement to carefully consider their aims and expectations when doing so, in light of the variable susceptibility to interference.

Overall, in the absence of better analytical procedures for quantification of total proteinaceous material in soils that are both precise and feasible for routine analysis of large numbers of soil samples, the approach based on amino acid analyses as presented here may be a viable alternative to the use of the Bradford or other spectrophotometric assays that are susceptible to interference from bound/co-extracted soil components and that may hamper comparisons between studies and sites. Because elemental analysis of extracts is already common practice in studies of AAE protein, the addition of AAA of pools or subsets of samples would be practical in most cases. Furthermore, this approach yields additional information regarding the samples such as amino acid composition and the relative proportion of refractory constituents in the extracts. This information is certainly of interest within the realm of AAE protein research.

Chapter 3.
The Accumulation and Amino Acid Composition of Autoclaved Alkaline-Extractable Soil Protein in Two Chronosequences of Coastal Wetland Soils

3.1. Introduction

The aggregation of soil particles and the concentration of soil organic matter (SOM) are two factors that play key roles in promoting stability of the soil matrix and its function as a reservoir of organic carbon (C) and nitrogen (N). SOM can interact with the mineral component of soils to form soil aggregates that help resist erosive forces. These aggregates can, in turn, act to preserve organic matter through stabilization or entrapment of otherwise readily decomposable organic compounds (Jastrow et al., 2007), and thus may slow remineralization of soil organic C to CO_2.

Soil aggregation and labile organic matter preservation have been widely linked to autoclaved alkaline-extractable (AAE) soil protein (Wright and Upadhyaya, 1998; Rillig, 2005; Rillig and Mummey, 2006; Bedini et al., 2009; Wilson et al., 2009; Zhang et al., 2017), yet no studies have definitively established the specific source(s) of this protein fraction or the mechanism by which it may enhance soil aggregation. Although AAE protein concentration in soils tends to be correlated with the abundance of arbuscular mycorrhizal fungi (AMF)—which themselves may contribute to soil aggregation (Rillig and Mummey, 2006)—amino acid sequencing of a subset of the protein mixture has failed to reveal the presence of AMF-specific proteins (Gillespie et al., 2011). It has been postulated that AAE protein, through hydrophobic interactions, helps bind organic matter and soil particles, protecting them from water (Wright and Upadhyaya, 1996; Rillig, 2005) and slowing the migration of extracellular hydrolytic enzymes (King, 2011). Correlations between soil aggregation and AAE protein have been observed several times in upland soils (Wright and Upadhyaya, 1998; Rillig et al., 2002; Bedini et al., 2009; Wilson et al., 2009; Spohn and Giani, 2010), and such soil aggregation may further contribute to long-term carbon storage by protecting soil organic matter from oxygen and microbial decomposers (reviewed by Rillig and Mummey, 2006). More recently, AAE protein has been incorporated as one of the metrics in the Comprehensive Assessment of Soil Health protocol for assessing overall soil health in upland soils (Fine et al., 2017). Analyses based on this protocol have further confirmed the correlation between AAE protein and water-stable aggregates (Fine et al., 2017), and Hurisso et al. (2018) have suggested that the AAE protein fraction represents a better indication of the organically bound N pool than total N. Hence, although the link between AAE protein and AMF is tenuous, this fraction of soil protein may still be useful as a relatively rapid metric of assessing the extent of labile SOM preservation and aggregation potential of soils.

However, as discussed in Chapter 2, the methods that are presently used for quantifying this protein fraction involve the use of colorimetric assays that are prone to interference from co-extracted non-proteinaceous materials, and such interference has potentially affected the interpretation of results (Geisseler et al., 2019). Additionally, the extraction process is not selective of any one protein or source of protein (Rosier et al., 2006; Hurisso et al., 2018). It may thus be that the composition of this fraction of soil protein could be a function of microbial

and vegetation communities as well as soil characteristics. It is also unknown whether the extraction method may exhibit some systematic selectivity, perhaps through chemical classes of proteins/peptides or through the extent of their association with the mineral fraction. A few researchers have subjected AAE protein extracts to polyacrylamide gel electrophoresis (PAGE; Wright et al., 1998; Bolliger et al., 2008; Chen et al., 2009; Gillespie et al., 2011). These studies have indicated that there are potentially numerous proteins that survive the extraction procedure intact. Yet there have been few reports in the literature that describe similar attempts to resolve the molecular weight profile of AAE protein, and even fewer that have attempted to sequence these proteins (except see Gillespie et al. (2011) and Gadkar and Rillig, 2006). The paucity of reports that describe attempts at electrophoresis and sequencing of AAE protein likely stems from the fact that such analyses are time-consuming and expensive. Furthermore, as evident from these few studies, the presence of non-protein material in the extracts additionally complicates the process by necessitating further cleanup and extraction procedures. Thus, these approaches are not well-suited for routine analysis of numerous soil samples, and the extent to which the characteristics of the overall protein extracted is a function of the soil environment, versus the extraction procedure itself, remains unclear.

One alternative to electrophoresis and sequencing approaches is amino acid analysis (AAA) of the whole extracts. AAA has previously been applied to whole soils (Sowden et al., 1977; Friedel and Scheller, 2002; Martens and Loeffelmann, 2003), humic acid fractions (Malcolm, 1990; Trubetskaya et al., 1998), and live plants and litter (de la Cruz and Poe, 1975b, a; Hicks et al., 1991). While it is much less informative with respect to specific proteins in the extracts, AAA of the whole extract is faster, less expensive, and may potentially provide an additional source of variation on which soil assessments could be based. Though amino acid compositions of proteins do not vary much overall, some subtle differences have been observed across different environments (Moura et al., 2013), between soils of differing climates, textures, and organic inputs (Sowden et al., 1977), and between different fractions of SOM (Malcolm, 1990). However, to my knowledge there have been no studies of the amino acid composition of the total protein extracted using the AAE protein method (or similar). Yet, there is a need for information regarding what organisms may contribute to this protein fraction, and whether there is any selectivity that may be occurring during this extraction procedure so as to potentially better inform soil management practices that rely on this method of assessment (Hurisso et al., 2018). Additionally, as addressed in Chapter 2, AAA has the added advantage that it can be performed quantitatively, thereby allowing estimates of total protein concentration to be made without the use of interference-prone colorimetric protein assays. Furthermore, the AAA approach involves acid hydrolysis of the extracts, and acid-hydrolysable C has commonly been used as a measure of labile organic matter (Falloon and Smith, 2000; Paul et al., 2006). Hence, this method could also be used to assess the relative amount of labile C that is associated with the protein.

Under the threat of global change, coastal wetlands are among the most vulnerable of all systems. Facing pressure from increased population density, hydrologic manipulation, sea level rise, and intense storm surges, a large extent of coastal wetlands throughout the world has been lost within the past century (Duarte et al., 2013), and more substantial losses are projected within this century (Nicholls, 2004). These systems, however, provide numerous ecosystem services (Barbier et al., 2011), such as water treatment, flood prevention, fisheries

support, CO_2 sequestration, and storm surge buffering. The ability of coastal wetlands to maintain their elevation and areal extent with many of these stressors co-occurring is relatively unknown (Kirwan and Megonigal, 2013). Therefore, assessments of the soils of these systems should incorporate metrics of their capacity to resist erosion and preserve the labile SOM fraction, and AAE protein might be one such metric. Yet, the AAE protein fraction has received relatively little attention in coastal wetland soils, perhaps due to the historically prevailing assumptions that this protein is strictly mycorrhizal in origin and that AMF are generally less abundant in wetland soils (Stevens et al., 2011). However, among the handful of reports of AAE protein in coastal wetland soils, a few authors have reported non-trivial quantities of AAE protein in such soils (Balachandran and Mishra, 2012; Krishnamoorthy et al., 2014; Wang et al., 2018b)—yet, these reports have been based on the interference-prone colorimetric assays mentioned above.

Because AAE protein has often been correlated with AMF colonization in upland soils (typically reported as TG, BRSP, or GRSP; Bedini et al., 2010; Wilson et al., 2009; Rillig, 2004), and despite the paucity of evidence directly linking AAE protein with AMF, some researchers have claimed that AAE protein in coastal wetlands may, nevertheless, originate from AMF (Balachandran and Mishra, 2012; Wang et al., 2018b; Wang et al., 2019). Although AMF are obligate aerobes, there have been numerous cases in which they have been observed in wetland soils (Carvalho et al., 2001; Bohrer et al., 2004; Kandalepas et al., 2010; Burcham et al., 2012), and it has been suggested that AMF may receive oxygen from the plant roots that they colonize (Brown and Bledsoe, 1996). Nevertheless, given the aforementioned problems associated with traditional methods of AAE protein quantification, it is hitherto unclear the extent to which AAE protein may be correlated with AMF colonization in coastal wetlands, beyond its often-observed correlation with total SOM and density of vegetation, and whether such correlation would be similar to those observed in upland soils. Whereas weak to moderate positive correlations ($r^2 \approx 0.36$–0.6) between AAE protein and AMF colonization have been observed in a couple of coastal wetland areas (Balachandran and Mishra, 2012; Krishnamoorthy et al., 2014), a subtle negative correlation was apparent in a mangrove-dominated coastal wetland (Adame et al., 2012). Soils of coastal wetlands can differ from those of uplands in several ways, and it may be that some factors specifically at play in coastal wetlands could differentially affect AMF abundance and AAE protein densities such that the correlation is diminished compared to what has been observed in upland soils. For instance, whereas increased salinity may similarly decrease AMF abundance (Juniper and Abbott, 1993; Adame et al., 2012) and SOM preservation (Craft, 2007), increased flood duration may lessen AMF colonization (Anderson et al., 1984)—yet, the accumulation of protein of bacterial or plant origin would be expected to accumulate to a greater extent with prolonged flooding, as is the case for SOM in general. Additionally, lateral transport and inputs of allochthonous organic matter in coastal wetland soils could also contribute to a mismatch between AMF colonization and AAE protein density if there is a substantial allochthonous source of AAE protein as has been previously observed (Harner et al., 2004; Adame et al., 2012).

In this study, I applied the AAA approach to estimate AAE protein stocks in the Sabine and WLD soils and to compare the extent to which AAE protein contributes to the overall SOM as these marshes develop. I hypothesized that AAE protein stocks would increase with marsh age in both chronosequences and that its contribution to TOC and TN would also increase as a

result of preferential accumulation of the protein in soil aggregates. I also aimed to assess any correlation between AAE protein and AMF colonization in these soils by measuring rates of AMF colonization in the roots of the vegetation within each core sample. To confirm the presence of AMF tissue in the soil, I probed for AMF-specific DNA within each core section. Most of the dominant vegetation species in the Sabine and WLD marshes have been reported to be amenable to association with AMF (Table 3.1)—a notable exception is *Spartina alterniflora*, for which conflicting reports exist. I hypothesized that AMF colonization would increase with vegetation cover, and therefore marsh age, and generally be lower in Sabine—primarily as a result of higher salinity. Further, I hypothesized that AMF colonization would be poorly but positively correlated with AAE protein density, reflecting an impact of factors differentially affecting AMF and AAE protein accumulation. Additionally, I aimed to determine the extent to which the hydrolysable protein was co-purified with other non-proteinaceous hydrolysable organic matter—i.e., is there evidence that the AAE protein is facilitating protection of labile organic matter through some direct binding mechanism? Given its correlation with soil aggregation, and the numerous claims that it has a role SOM preservation, I hypothesized that the non-proteinaceous organic carbon of the AAE protein extracts would be dominated (>50%) by hydrolysable compounds other than protein, reflecting the potential involvement of the protein fraction in labile SOM preservation. Finally, I hypothesized that the amino acid profile of the AAE protein extracts would subtly but significantly differ between the two chronosequences, reflecting the contribution of different microbial communities to the AAE protein fraction.

Table 3.1. Previous observations of AMF colonization in the dominant vegetation species of the Sabine and WLD marshes.

	Dominant vegetation species	Amenable to AMF?	Reference
Sabine			
	Spartina alterniflora	Conflicting	Burcham et al. (2012), Hoefnagels et al. (1993), Pratt-Zossoungbo and Biber (2009)
	Distichlis spicata	Yes	Allen and Cunningham (1983)
	Spartina patens	Yes	Burcham et al. (2012), Cooke et al. (1993)
WLD			
	Nelumbo lutea	?	
	Sagittaria platyphylla	?	
	Colocasia esculenta	Yes	Khade and Rodrigues (2007)
	Alternanthera philoxeroides	Yes	Kandalepas et al. (2010)
	Polygonum punctatum	Yes	Kandalepas et al. (2010)
	Salix nigra	Yes	Lodge (1989)

3.2. Materials and methods

3.2.1 Study sites and initial soil sample processing

The study sites were located in the Sabine National Wildlife Refuge (Sabine) and the Wax Lake Delta (WLD). Information regarding these study sites, the initial soil sampling and processing, and the basic soil characteristics were provided in Section 1.3 (Chapter 1). For the present study, percent vegetation cover at each plot was estimated visually within a 0.25 m^2 quadrat that encompassed the area within which each core was collected. This estimate was based on the approximate area of the soil surface that was displaced by live stems.

3.2.2 Sample preparation for root and DNA analyses

Prior to drying the homogenized soil core sections, a subset of any live root segments observed in each section was immediately placed in 50% ethanol and stored at 4°C for later assessment of AMF colonization. Additionally, a small subset of the homogenized soil was immediately frozen and stored at −20°C for subsequent DNA extraction and PCR analysis.

3.2.3 Assessment of AMF colonization in roots

In an attempt to estimate the extent of any AMF colonization that may have been present within the marshes, the roots collected from each core section were cleared and stained as per Brundrett et al. (1984) and Vierheilig et al. (2005) with modifications. For each core section in which live roots were observed, live root segments of <2 mm in diameter and cumulative length of 10–15 cm were rinsed with DI H_2O to remove soil and debris and then placed into histology cassettes. The roots were cleared by autoclaving in 10% KOH at 121°C for 5 min followed by cooling for 5 min. Afterwards, the roots were soaked in 10% bleach for 5 min, then rinsed first in DI H_2O and then in 1 N HCl. The roots were then stained by autoclaving in 0.03% chlorazol black E dissolved in 1:1:1 lactic acid-glycerol-water at 121°C for 5 min. The roots were then transferred to a 50% glycerol solution and allowed to de-stain for 5 days at room temperature. Following de-staining, roots from each section were cut into segments of <4 cm, and cumulative lengths of approximately 10 cm were placed onto glass slides and observed by microscope under 200–400× magnification. AMF colonization was assessed based on the observation of the arbuscule structures within the root cells, the characteristic morphology of AMF (McGonigle et al., 1990). The same method was applied to roots collected from well-aerated upland soils to serve as a positive control for the assessment.

3.2.4 Assessment of AMF DNA presence in soils by PCR

Total DNA of each soil sample was isolated using the Qiagen PowerLyzer PowerSoil Mini kit per the manufacturer's instructions. Approximately 220–280 mg of field-moist, homogenized soil from each core section was combined with the glass beads in a 2-mL tube and centrifuged at 10000×*g* for 30 seconds to remove excess water. Lysis buffer was then added, and disruption was accomplished on a DisruptorGenie (Scientific Industries) at

maximum speed for 20 min at room temperature. DNA was eluted in a total volume of 100 µL of 10 mM tris. DNA concentrations and purity ratios—the ratios of absorbance at 260 and 280 nm ($A_{260/280}$), and at 260 and 230 nm ($A_{260/230}$)—were measured on a NanoDrop 2000c (Thermo Fisher) spectrophotometer. DNA solutions were stored at −20°C until PCR amplification (<2 months).

PCR amplification of AMF DNA was done based on the nested PCR approach described by Krüger et al. (2009) using Q5 high-fidelity polymerase (New England Biolabs) in a total reaction volume of 50 µL. Each reaction included 1 unit of polymerase, 200 µM of each dNTP, 0.5 µM each of the forward and reverse primer sets, and approximately 200 ng of template DNA (or a minimum of 80 ng for low-concentration samples). The first PCR was carried out using the SSUmAf–LSUmAr degenerate primer set in equimolar concentrations. All PCR cycling was done using an Eppendorf Master Gradient thermocycler preheated to 98°C. Cycling was as follows: 30 s initial denaturation at 98°C; 40 cycles of: denaturation for 6 s at 98°C, annealing for 25 s at 60°C, and elongation for 50 s at 72°C; and a final elongation of 120 s at 72°C. A no-template control was included in every batch of reactions. A positive control was also included, in which DNA from an upland soil containing AMF (based on root colonization) was used as the template. Following the first PCR, 47 µL of each reaction solution was electrophoresed on 1.5% agarose gel in 1× TAE buffer at 3.5 $V \cdot cm^{-1}$ for 2–3 hrs. Gels were visualized on a ChemiDoc MP imager (BioRad) after staining with GelRed (Biotium) per the manufacturer's instructions. Amplification was assessed based on the presence of an approximately 1.8-kb band. For the second (nested) PCR, the SSUmCf–LSUmBr degenerate primer set was used, and the product of the first reaction was used as the template. Nested reaction conditions were the same as for the first reaction except that the annealing temperature was 63°C, the elongation step was for 40 s, and the cycle count was 35. Reaction mixtures for which there was no observable product were used undiluted (2 µL) for the nested PCR. In the reaction mixtures where amplification was observed, the product was diluted 50-, 1000-, or 2500-fold (depending on band intensity), and 2 µL of this dilution was used as the template for the nested reaction. The nested reaction solutions were electrophoresed and visualized in the same manner as the first reactions. The observation of an approximately 1.5-kb band in a nested reaction was regarded as a positive result for the presence of AMF DNA. DNA solutions for which no amplification was observed for both of the two primer sets were subjected to an additional PCR using the NS1–NS4 primer set for amplification of a highly conservative region of fungal ribosomal DNA as described by White et al. (1990). PCR conditions using these primers were the same as for the first PCR reaction (above) except that the annealing temperature was 57°C and the elongation time was 35 s. The observation of an approximately 1.2-kb band in these reactions (in combination with the absence of bands in the other reactions) was regarded as a negative result for the presence of AMF DNA, whereas samples that did not exhibit amplification of the target product size in any of the three reactions were deemed inconclusive.

3.2.5 Extraction, estimation, and amino acid analysis of AAE protein

Extraction and estimation of the hydrolysable AAE protein quantity in each soil section was described in detail in Chapter 2. Briefly, total AAE protein was extracted in 100 mM sodium pyrophosphate (pH 9.0) from 0.5–1 g of dried homogenized soil using established procedures

(Wright et al., 2006). Each extract was partially purified by acid precipitation, redissolution in 0.1 N NaOH, and exhaustive dialysis against DI H_2O. After drying the extracts at 60°C, total extract C and N were measured by elemental analysis. To estimate the AAE protein concentration, some of each of the extracts from the 0–15 cm and 15–30 cm depth intervals were pooled for each marsh (20 pools total), and the pooled extracts were subjected to acid hydrolysis and amino acid analysis. The concentrations of 16 proteinogenic amino acids were determined by liquid chromatography and fluorescence detection of the derivatized hydrolysable amino acids. Glutamine and asparagine were not distinguished from their respective acid forms. Assuming the protein-N to total N ratio in each sample within a given pool to be equivalent, the N concentration of each individual sample led to the estimated amino acid concentration in that sample, which served as the estimate of the hydrolysable AAE protein concentration of each individual extract. This corresponds to the minimum estimate of AAE protein as described in Chapter 2. In the present study, only the minimum estimates were used because these correspond with the actual measurements of hydrolysable amino acids in the extracts.

3.2.6 Acid-hydrolysable components of the AAE protein extracts

In the method of quantifying the amino acids within the AAE protein extracts (Chapter 2), each pooled extract was treated with 6 N HCl at 100°C for 22 hrs. After removal of the supernatant for AAA, the remaining solids were rinsed repeatedly with 6 N HCl as described in Chapter 2 to allow for the analysis of the post-hydrolysis residue. The dried residues were weighed, homogenized, and the %C and %N were determined by elemental analysis (as above) on a subset of each residue. To estimate the size of the inorganic component before and after hydrolysis, the percent loss on ignition (550°C for 4 hrs) was measured for a subset of each pre-hydrolysis residue and for each post-hydrolysis residue. The composition of the post-hydrolysis residues was expressed as a percent of the initial pre-hydrolysis dry weight.

3.2.7 Data analysis and statistics

Soil stocks of AAE protein were calculated for individual cores on a mass per area basis, to a soil depth of 30 cm. Mass per area was determined by integrating the concentrations per gram every 5 cm down to 30 cm based on the bulk density of each core section. In the 1-year-old marsh of Sabine, where the cores did not extend beyond 20–25 cm, the stock of the deepest section sampled from each core was extrapolated to a depth of 30 cm for the purposes of marsh stock comparison. Because the soil in this marsh was almost exclusively homogenized dredge material, the inter-depth variability in these cores was low (Table 1.2 and Fig. D.2a). Contribution ratios of AAE protein to TOC and TN were calculated on a core-wise basis using the stocks of AAE protein, TOC, and TN of each respective soil core. The C and N composition of the AAE protein was assumed to match that of the total amino acids detected in each corresponding pooled extract, which averaged 52.6 ± 0.3 %C and 16.8 ± 0.1 %N, respectively.

All statistical analyses were carried out using MATLAB R2016b (Mathworks) with the statistical package installed. Comparisons among the average AAE protein stocks of each marsh were made within each chronosequence by one-way analyses of variance (ANOVA). Multiple

comparisons and corresponding *p*-values are based on Tukey-Kramer honestly significant difference post hoc tests using the $\mathrm{multcompare}()$ function in MATLAB—letters shown in the figures represent differences at the α = 0.05 level unless otherwise stated. To establish a semiquantitative metric of AMF DNA presence in the soil, a DNA score was calculated for each marsh as the total number of positive PCR results in all core sections of that marsh divided by the total number of sections from that marsh, expressed as a percentage. To determine whether vegetation cover, AMF DNA score, and average AAE protein stock were significantly correlated, the Spearman rank correlation coefficient (ρ) was calculated for each pairwise comparison, and correlations for which $p < 0.05$ were deemed significant. Curvilinear functions of the correlations of AAE protein-C and -N with TOC and TN, respectively, were fitted by stepwise polynomial least-squares regression. The coefficients included in all regressions were significant to $p < 0.01$, and the *p*-value reported for each curvilinear regression is that of the least significant non-intercept coefficient. Data from the reference marshes were included in the regressions against TOC and TN. To determine whether these curvilinear regressions significantly differed between Sabine and WLD, *F*-tests were performed in which the mean sum of squares of the errors were compared for a two-curve model versus a single curve fit to the combined chronosequence data—the null hypothesis that separate curves do not provide a significantly better fit of the data was rejected at the α = 0.05 level. To visualize trends in the overall contribution of AAE protein to TOC and TN as a function of marsh age, the ratios of AAE protein-C (or -N) stock to TOC (or TN) stock that were determined for each soil core were fit by linear regression, excluding those of the reference marshes. The ratios of the reference marshes were compared to those of the chronosequence marshes (separately for Sabine and WLD) based on Tukey-Kramer honestly significant difference post hoc tests following one-way ANOVA.

To determine whether the AAE protein amino acid profiles of Sabine and WLD were significantly different, I took a Bayesian Monte Carlo approach. The amino acid profiles of each sample from Sabine and WLD were assigned to one of two "sets" (set 1 and set 2), and all possible combinations (${}_{20}\mathrm{C}_{12} = {}_{20}\mathrm{C}_{8} = 125970$ possible) of the two-set arrangement were determined. For each possible arrangement, the sum of squares of the relative differences of the average abundance of each amino acid (16 total) between the two sets ($\mathrm{SS}_{\mathrm{Arrangement}}$) was calculated as per Eq. 3.1:

$$\mathrm{SS}_{\mathrm{Arrangement}} = \sum_{\mathrm{AA}=16}^{\mathrm{AA}=1} \left(\frac{\overline{\mathrm{X1}}_{\mathrm{AA}} - \overline{\mathrm{X2}}_{\mathrm{AA}}}{\overline{\overline{\mathrm{X}}}_{\mathrm{AA}}} \right)^2 \tag{3.1}$$

where $\overline{\mathrm{X1}}_{\mathrm{AA}}$ and $\overline{\mathrm{X2}}_{\mathrm{AA}}$ are the mean relative abundances (mole-percent) of a particular amino acid in the samples assigned to set 1 (n=12) and set 2 (n=8), respectively, whereas $\overline{\overline{\mathrm{X}}}_{\mathrm{AA}}$ is the grand mean of that amino acid for all samples. The *p*-value for testing the null hypothesis that there is no difference between the Sabine and WLD amino acid profiles was calculated based on the number of possible arrangements (N_{SS},) for which $\mathrm{SS}_{\mathrm{Arrangement}}$ equaled or exceeded that of the original (observed) arrangement (Eq. 3.2):

$$p = \frac{N_{SS'}}{125970} \tag{3.2}$$

where 125970 is the number of total possible arrangements. This approach was not used to compare with literature-based amino acid profiles of soils and humic acid fractions because it was not computationally feasible.

3.3. Results

3.3.1 Vegetation, AAE protein, and presence of AMF

My sampling sites captured the natural succession of vegetation in both chronosequences. Vegetation in Sabine developed quickly, with the 1-year old marsh already having clonal patches of *Spartina alterniflora*. In the 14-year marsh, average percent cover had reached that of the reference marshes and showed a shift in vegetation community from *S. alterniflora*–dominated to *Distichlis spicata*–dominated (Fig. 3.1a). The 33-year marsh demonstrated a further shift to *Spartina patens*, the late-successional species typical of the natural marshes of the area. I did observe, however, that the randomly selected plots of Ref-B typically had a greater abundance of *D. spicata* than those of Ref-A. In WLD, average percent cover steadily increased along the chronosequence (Fig. 3.1b). *Nelumbo lutea*, dominant in the youngest WLD marsh, gave way to *Colocasia esculenta* in the 29-year old marsh. The oldest marsh of the chronosequence had a composition qualitatively similar to that of the reference marsh, where *Polygonum puntatum* dominated the herbaceous vegetation. While not captured within my quadrats, *Salix nigra* was present in the surrounding areas of the 41-year marsh (as saplings) and the reference marsh (as trees: 20–40 cm diameter at breast height).

Stocks of AAE protein generally appeared to increase with age in both chronosequences and were highest in the reference marshes (Fig. 3.1c and 3.1d). However, no significant differences in stocks were observed among the Sabine created marshes ($p > 0.8$), which ranged from 152 to 279 g·m^{-2} between the 1-year-old and 33-year-old marshes, respectively. The average stock of the Ref-B marsh of Sabine (696 g·m^{-2}) was significantly greater than that of all created marshes ($p < 0.02$), whereas, due to large variation, the Ref-A marsh differed only from the youngest three marshes ($p < 0.05$). In WLD, there was a nearly fivefold difference in AAE protein stock ($p = 0.0008$) between the youngest marsh (16-year-old; 82 g·m^{-2}) and the next-oldest marsh (29-year-old; 398 g·m^{-2}). However, there was no difference in stocks between the 29- and 41-year-old marshes ($p = 0.9$), and stocks of all marshes of the chronosequence were significantly less than that of the reference marsh (608 g·m^{-2}; $p < 0.03$).

I did not observe any unambiguous AMF colonization in any of the live root samples. Most of the roots assessed were from soil depths of 0–20 cm because live roots were generally scarce at depths below 20 cm. Whereas some fungal structures (mostly hyphae) were occasionally apparent, no arbuscules could be confirmed. Preliminary tests of the root staining procedure applied to roots collected from upland soils (positive control), however, did result in a few observable structures that resembled arbuscules (not shown).

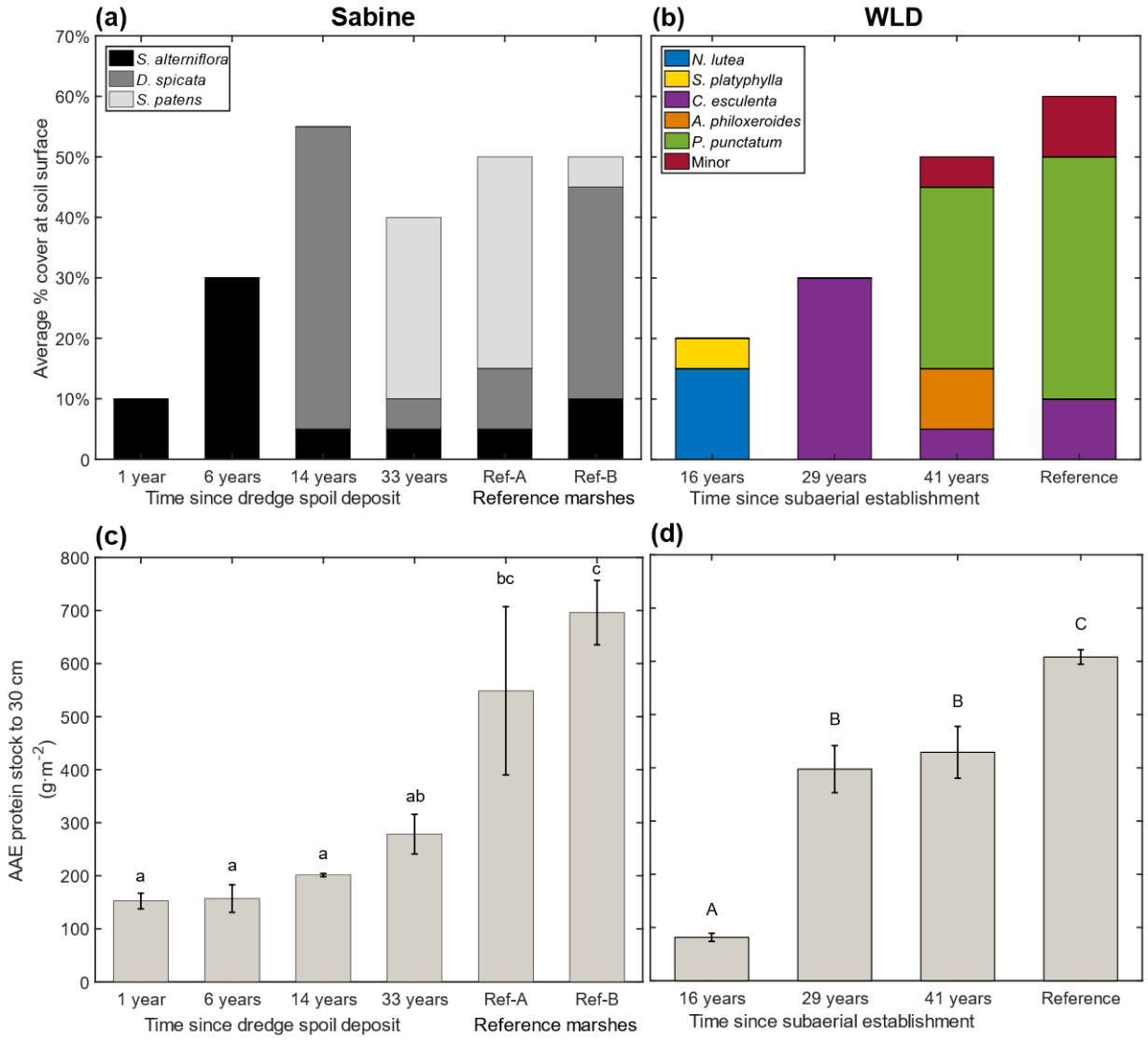

(e)

Depth	1 year	6 years	14 years	33 years	Ref-A	Ref-B
0–5 cm	· · ·	· · +	· + +	· + ·	+ + +	+ + +
5–10 cm	· · ·	− · +	· + +	+ + ·	· + ·	+ + +
10–15 cm	· · ·	− · −	· · +	+ · ·	· + −	+ + +
15–20 cm	· · ·	+ − ·	· − +	+ · ·	· + −	+ + +
20–25 cm	· · ·	− − ·	· · +	+ · ·	· + −	+ + +
25–30 cm	NA	· · ·	· · +	· + ·	· · −	· + +
Score†	0%	18%	44%	39%	39%	94%

(f)

16 years	29 years	41 years	Reference
+ + +	+ + −	+ + +	· + +
+ + +	+ · +	+ + +	+ + +
− − +	· + −	+ + +	+ + +
− − +	+ + +	+ + +	+ + −
− − −	+ + +	+ + +	+ + −
− + +	+ + −	− + −	+ − −
56%	72%	89%	72%

Figure 3.1. Average estimated percent cover of vegetation in 0.25 m^2 quadrats at each core sampling location in Sabine (a) and WLD (b). In (b), miscellaneous low-abundance species are represented by the "minor" group. Average 30-cm stocks of AAE protein for each marsh in Sabine (c) and WLD (d) are shown. Error bars represent ± standard error (n = 3 cores) and letters above the bars indicate significant differences (α = 0.05) based on Tukey-Kramer HSD post-hoc tests. Presence/absence of AMF-specific (caption cont'd)

DNA in soil core sections of Sabine (e) and WLD (f); key: (+), AMF-specific DNA detected; (−), AMF-specific DNA not detected (fungal DNA detected); (·), inconclusive (conserved fungal DNA sequence not detected); shading is a visual aid and corresponds to the number of positive results in each depth increment; NA = not analyzed; †Score is the number of positive results in each marsh divided by 18.

In contrast to the colonization assay results, PCR analysis of the total soil DNA indicated that AMF DNA was likely present in all of the marshes of WLD and in all but the youngest marsh of Sabine (Fig. 3.1e and 3.1f; representative gel images are shown in Fig. C.2 and C.3). Because AMF colonization was not observed, I used the PCR results as a semiquantitative surrogate for relative AMF abundance in the soils of each marsh (AMF DNA score). The number of positive results generally increased with marsh age in both chronosequences, and was similar between the oldest marshes and the reference marshes. However, there were a relatively large number of inconclusive results in the Sabine marshes. Although the $A_{260/280}$ purity ratios of these inconclusive DNA extracts were all ≥ 1.6, these extracts tended to have low DNA quantities and/or exhibit low $A_{260/230}$ ratios (Table E.2), the latter suggesting possible contamination from polyphenolic compounds (e.g., humic materials), which can interfere with PCR amplification (Yeates et al., 1998). Thus, it is uncertain whether a significant trend in AMF presence with age existed in the Sabine marshes.

Although major trends between vegetation cover, AMF DNA, and AAE protein stocks were not readily apparent, Spearman rank correlation analysis did reveal some marginally significant trends in Sabine (Table 3.2). Namely, AMF DNA scores were marginally positively correlated with overall vegetation cover ($\rho = 0.87$, $p = 0.044$), and better correlated with coverage of *D. spicata* ($\rho = 0.91$, $p = 0.022$) across the Sabine marshes. In WLD, however, no significant correlations between these measures were observed ($p > 0.08$). Stocks of AAE protein were not significantly correlated with either AMF DNA score or vegetation coverage within either Sabine or WLD ($p > 0.06$).

Table 3.2. Spearman rank correlation coefficients (ρ) among the measures shown in Fig. 3.1 for the Sabine marshes. All correlations shown were significant ($p < 0.05$).

Sabine marshes	AMF DNA score	AAE protein stock	*D. spicata* cover
Vegetation cover	0.87	*NS*	*(0.97)*
AMF DNA score		*NS*	0.91
AAE protein stock			*NS*

NS = correlation not significant ($p > 0.05$).

3.3.2 AAE protein correlation with TOC and TN

AAE protein concentration in the soil was highly correlated with TOC and TN, more so than with any other soil parameter measured. Significant but distinct relationships ($F_{3,169} = 90$, $p < 0.0001$) were observed between AAE protein-C and TOC among Sabine and WLD (Fig. 3.2a)—a linear relation was apparent for the Sabine samples ($r^2 = 0.98$, $p < 0.0001$), whereas a cubic relation was observed in WLD ($r^2 = 0.987$, $p = 0.0004$). The correlation between AAE protein-N and TN was again distinct between Sabine and WLD (Fig. 3.2b; $F_{3,170} = 101$, $p < 0.0001$)—that of Sabine followed a quadratic relationship ($r^2 = 0.988$, $p = 0.0032$), whereas that of WLD was linear ($r^2 = 0.986$, $p < 0.0001$).

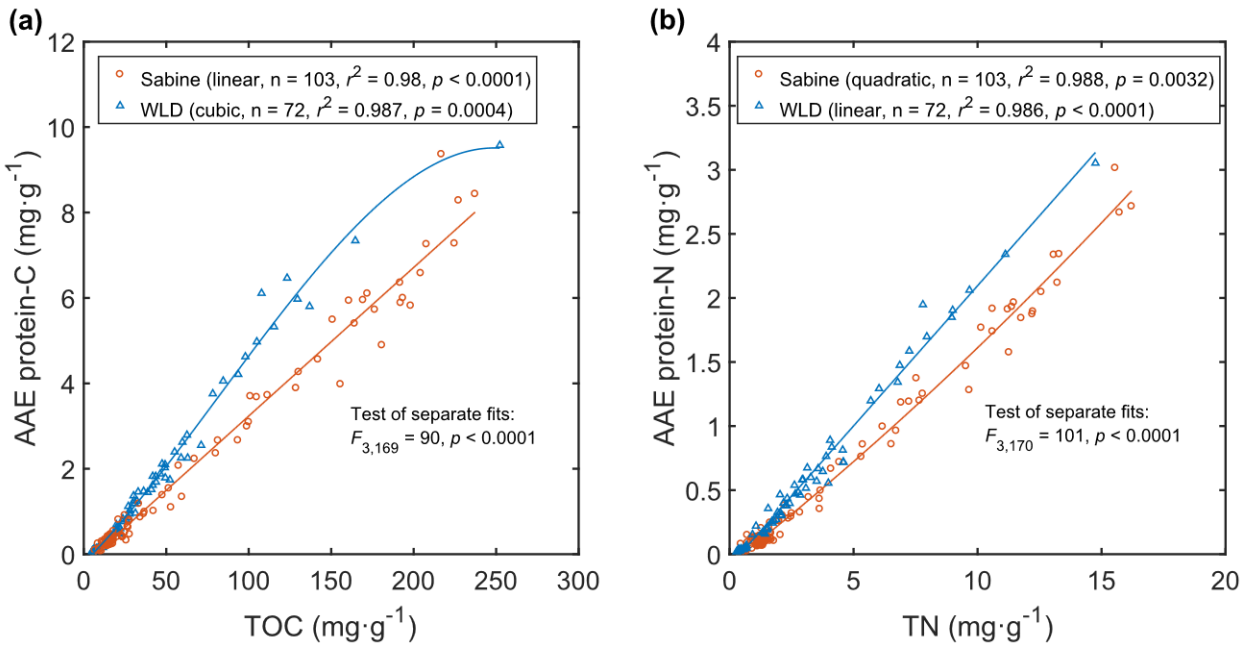

Figure 3.2. Correlations and curvilinear regressions between AAE protein-C and TOC (a) and between AAE protein-N and TN (b) among the individual soil core sections from Sabine (circles) and WLD (triangles).

3.3.3 Contribution of AAE protein to TOC and TN

AAE protein contributions to TOC were small overall (1–5% of TOC). This contrasts with its contribution to TN, which, on average, ranged from around 7% to upwards of 21% of TN (Fig. 3.3). Generally, any significant correlations of AAE protein-C/TOC or AAE protein-N/TN with marsh age were relatively weak to moderate ($r^2 \leq 0.8$) in both chronosequences. In Sabine, the AAE protein-C/TOC ratios were consistent across all created marshes (Fig. 3.3a; $p = 0.26$); the ratios of the oldest created marsh were no different from that of the Ref-A marsh ($p > 0.99$); whereas the ratio was only marginally greater in the Ref-B marsh ($p = 0.046$). A different pattern was observed in WLD, where the ratios in the oldest two marshes were greater than

that of the youngest marsh ($p < 0.0001$) and no different than that of the reference marsh ($p > 0.09$).

Trends in AAE protein-N/TN ratios (Fig. 3.3b) generally followed the same pattern as those of AAE protein-C/TOC, with the exception of the AAE protein-N/TN ratio of the 33-year-old Sabine marsh, which was marginally greater than those of the younger marshes ($p = 0.014$–0.044); this marsh alone contributed to an apparent positive correlation with age ($r^2 = 0.80$, $p < 0.0001$). In both chronosequences, the AAE protein-N/TN ratios of the oldest marshes did not differ from the corresponding reference marshes ($p > 0.05$).

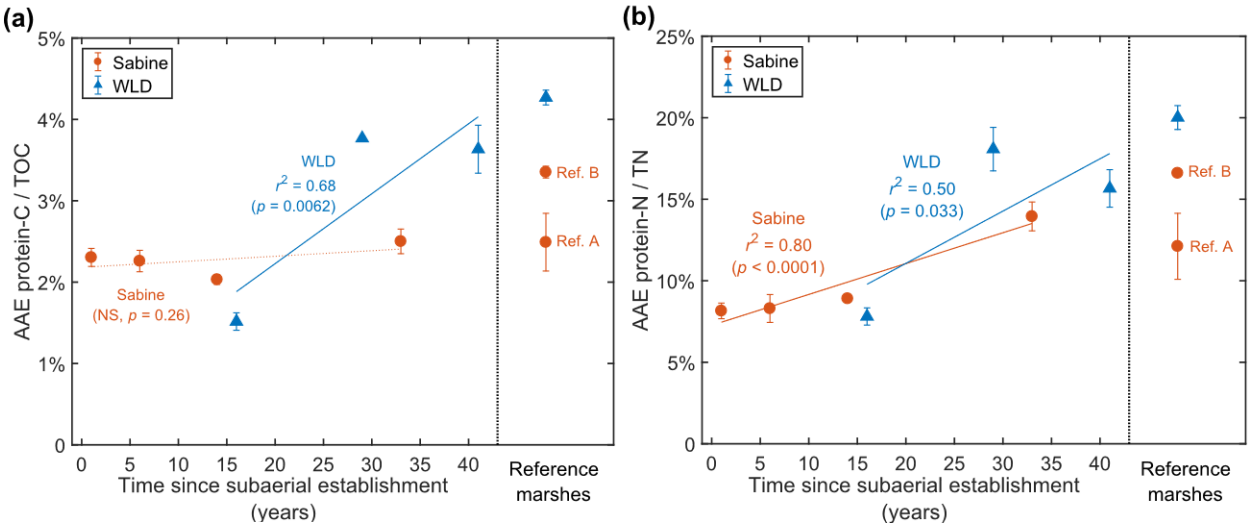

Figure 3.3. Average contributions of AAE protein to TOC (a) and TN (b) as functions of marsh age within the Sabine (circles) and WLD (triangles) chronosequences. Error bars represent ± standard error (n = 3 cores). NS indicates that the correlation was not significant ($p > 0.05$).

3.3.4 Composition of whole AAE protein extracts

Overall, hydrolysable amino acids accounted for 5.5 ± 1.9% by weight of the total solids in the pooled AAE protein extracts and roughly half of the extracted solids were not hydrolysable—a figure that significantly differed between the Sabine (50 ± 4%) and WLD (42 ± 6%) extracts ($p = 0.005$). Yet the fact that the hydrolysis resulted in a near doubling of the %C composition (from an average of 30% C to 57% C) implied that most of the mass lost was inorganic. To confirm this, I performed a loss-on-ignition assay on the post-hydrolysis residues as well as on a subset of the pre-hydrolysis extracts. I attributed any mass not accounted for by C, N, or ash to O and H. An average of 32 ± 4% of the weight of the dialyzed extracts was composed of inorganic (mineral) components, whereas nearly all (average 95 ± 2%) of the remaining post-hydrolysis residue was organic (Fig. 3.4). I observed that the proportion of C that was not hydrolysable did not differ between the Sabine and WLD pooled extracts (92 ± 17% of C; $p = 0.46$), nor did the proportion of N that was non-hydrolysable (47 ± 10% of N; $p = 0.12$). Furthermore, the C and N compositions of the post-hydrolysis residues were remarkably

consistent (57.3 ± 1.5 %C, 1.96 ± 0.19 %N) and very similar to those typical of ash-free humic acid fractions (Reddy and DeLaune, 2008). The estimated amount of O and H in the original pre-hydrolysis extracts was much greater than would be expected for either protein or humic acid. I attributed the excess O and H to structural water of hydration, and possibly, to clay-associated lattice hydroxyl moieties, both of which would be expected to associate primarily with the mineral fraction, an association that is apparent in loss-on-ignition assays of soils (Hoogsteen et al., 2015). This is further supported by my observation that the pre-hydrolysis extracts exhibited a "waxy" consistency after drying, whereas the post-hydrolysis residues did not. Structural water of hydration would likely not be lost during drying at 60°C, but it would be lost with the mineral fraction during the hydrolysis procedure, and it would also be lost during combustion. Hence, this water would appear to be part of the organic fraction, despite being primarily associated with the mineral fraction. While the hydrolysate of all of the extracts exhibited an intense yellow color that suggested the presence of iron, the combustion residue of the post-hydrolysis extracts appeared completely white.

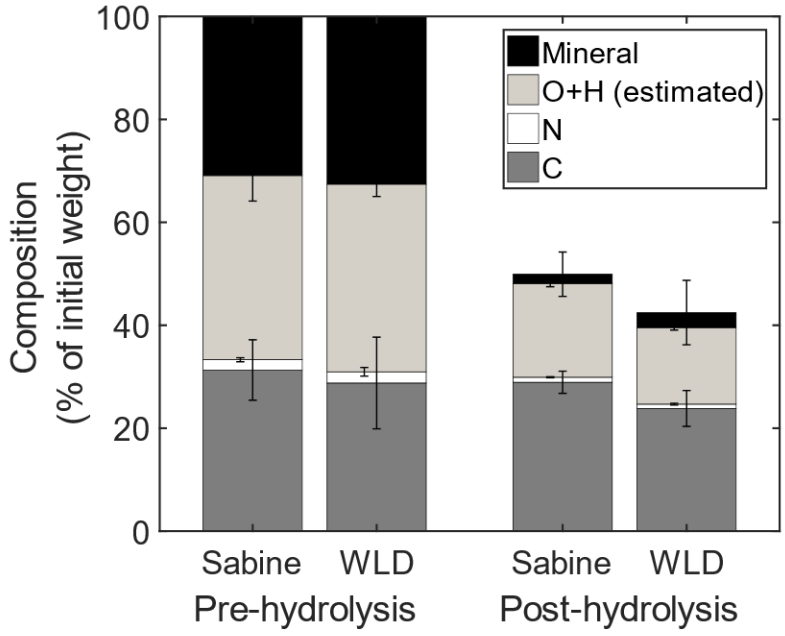

Figure 3.4. Relative composition of pooled dialyzed AAE solids before and after hydrolysis as a percent of the initial (pre-hydrolysis) weight. Error bars represent ± standard deviation (n_{Sabine} = 12, n_{WLD} = 8 pooled extracts). The weight that was not accounted for by C, N, or ash was assumed to be contributed by O and H.

3.3.5 Hydrolysable amino acid composition of the AAE protein extracts

Of the total N in the pooled dialyzed extracts from Sabine, 41 ± 5% was accounted for by the amino acids assayed, whereas this figure was significantly greater (51 ± 4%) in the WLD extracts ($p < 0.05$). Of the extracted C and N that was hydrolyzed, most (an average of ~60% of the hydrolyzed C and ~78% of the hydrolyzed N) was accounted for by amino acids. Moreover, an average of only ~8% of the extracted C could possibly be attributed to non-proteinaceous hydrolysable (labile) organic matter, which was inconsistent with my hypothesis that the protein would be co-purified with a comparatively large amount (>50% by weight) of non-proteinaceous labile organic matter.

The relative amino acid compositions of the pooled extracts were highly consistent and were not significantly different between the 0–15 cm and 15–30 cm depth increments (p = 0.41). Furthermore, and contrary to what I initially hypothesized, the compositions did not significantly differ overall between Sabine and WLD (p = 0.16; Fig. 3.5), as based on the test described in Section 3.2.7.

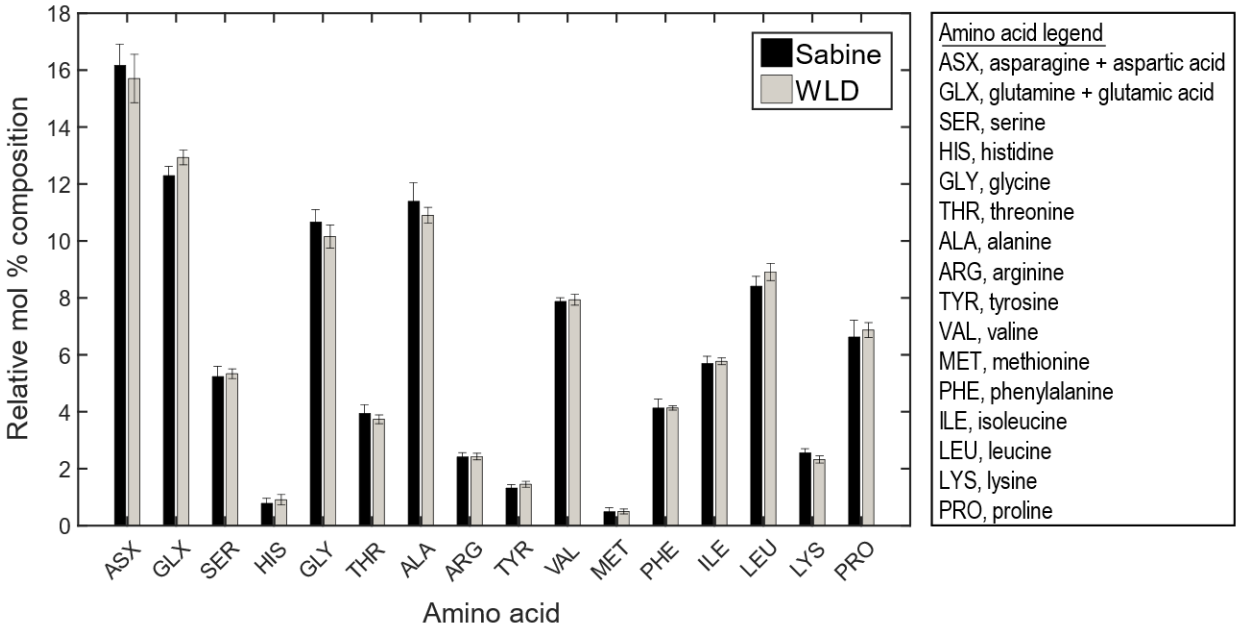

Figure 3.5. Average relative mole-percent amino acid composition of all pooled AAE protein extracts of Sabine (black) and WLD (gray). Error bars are ± standard deviation (n_{Sabine} = 12 pools, n_{WLD} = 8 pools). See Tables C.1 and C.2 for average compositions of each individual marsh.

3.4. Discussion

3.4.1 Trends of AAE protein across the two chronosequences

One of my objectives was to establish whether there were any clear trends in AAE protein abundance as the marshes in these two systems developed. Overall, stocks of AAE protein increased with marsh age as hypothesized, but no significant correlation was apparent between AAE protein stock and vegetation coverage, vegetation composition, or AMF DNA presence for either Sabine or WLD (Table 3.2). Rather, AAE protein was, overall, highly correlated with TOC and TN (Fig. 3.2a and 3.2b), and therefore increased with marsh age. Such correlations are consistent with numerous previous observations (e.g., Rillig et al., 2003; Halvorson and Gonzalez, 2006; Wang et al., 2018a), despite the use of interference-prone colorimetric protein assays in these earlier studies. It is also consistent with the findings of Friedel and Scheller (2002), who observed that the concentration of the total hydrolysable amino acids across several upland soils characterized by distinctly different conditions and land uses were strongly correlated with TOC (r^2 = 0.96) and TN (r^2 = 0.997).

In comparison with studies of AAE protein in upland soils (e.g., Rillig et al., 2001a; Lovelock et al., 2004; Wang et al., 2015b), the concentrations that I observed here are similar. They are also comparable to concentrations reported in two of the few studies of AAE protein in coastal wetland soils (Balachandran and Mishra, 2012; Wang et al., 2018b). However, the overall slope of the relation between AAE protein and TOC that I observed (0.07 mg protein $mg{\cdot}C^{-1}$) is at the low end of a range of other studies of both wetland and upland soils (Chapter 2, Table 2.2). This result is likely due, in part, to overestimation of protein in the soil extracts in these previous studies, as described in Chapter 2.

I did, however, observe significant differences in the slopes of the relations with TOC and TN between Sabine and WLD. Those slopes were themselves apparently not constant because curvilinear regressions provided subtly but significantly better fits to the WLD C data and to the Sabine N data. The marsh-averaged contribution ratios of AAE protein to TOC and TN (Fig. 3.3a and 3.3b) illustrate this variable slope. The contribution of AAE protein to TOC did not vary significantly with marsh age in Sabine, and thus, there did not appear to be preferential accumulation of the protein in these marshes, contrary to my hypothesis. In contrast, the contribution of AAE protein to both TOC and TN increased significantly from the youngest WLD marsh to the older two marshes and reference site, which may suggest preferential accumulation and/or increased production of the protein. This may not have been an effect of age, per se; rather, it may have been more related to the relative influence of the freshwater outlet. As a newly formed river delta, the marshes within the WLD chronosequence not only vary in terms of age, but also in terms of elevation and distance from the river outlet. In the transition from the 16-year-old marsh to the 29-year-old marsh, there is a significant gain in elevation (~0.9 m; Table 1.1) and increase in vegetation density (Fig. 3.1b), which is generally consistent with previous observations (Carle et al., 2015). This would be expected to result in slower flow rates and increased autochthonous litter deposition, which would likely contribute to the overall increase in N input to the soil, and which may in turn promote greater rates of protein production (in both the vegetation and soil microbes) and reduced scavenging of N by plants and microbes.[1] In contrast, the Sabine marshes receive relatively little freshwater input

and so generally experience low input of allochthonous N. Hence, the potentially greater amount of N loading to the older WLD marshes compared to the youngest marsh may have contributed to this divergent pattern of protein:TOC ratios. Additionally, the relatively low contributions of protein at low concentrations of C and N may also suggest that there is some priming effect involved, whereby an initial pool of SOM must accumulate before the microbial community (primarily decomposers) is fully primed.

3.4.2 Presence of AMF within the studied soils

Although I did not observe any unambiguous AMF colonization of the roots collected from my sites, a substantial number of soil samples tested positive for AMF DNA, and the number of which generally appeared to increase with marsh age in both chronosequences (Fig. 3.1e and 3.1f). Although my hypothesis included the assumption that root colonization would be apparent, the observations of AMF DNA are somewhat consistent with the trend of increasing AMF abundance with marsh age and increasing vegetation that I initially hypothesized. In Sabine, the youngest two marshes were colonized solely by *S. alterniflora* at the sampling locations. There have been very few reports of AMF association with this species (Burcham et al., 2012), and some have suggested that *S. alterniflora* may generally be resistant to AMF colonization (Hoefnagels et al., 1993; Pratt-Zossoungbo and Biber, 2009). Thus, the absence of AMF root colonization and paucity of AMF DNA in the youngest two Sabine marshes was expected. Both *D. spicata* and *S. patens*, on the other hand, have been found to exhibit comparatively high rates of AMF colonization in wetland settings (Allen and Cunningham, 1983; Burcham et al., 2012), and these two species dominated my sampling sites in all of the other Sabine marshes. Indeed, the relatively greater number of positive results for AMF DNA that I observed in the soils of these marshes appears to reflect these previously observed associations; however, it is unclear as to why AMF colonization was not apparent in the roots of these soils.[2] In WLD, the species of vegetation that I observed in the 29-year-old, 41-year-old, and reference plots have all been observed to form associations with AMF (Lodge, 1989; Khade and Rodrigues, 2007; Kandalepas et al., 2010). However, I could not confirm the AMF status of the two species of vegetation observed in the youngest WLD plots, *N. lutea* and *S. platyphylla*, and I observed the fewest number of positive AMF DNA results in this marsh. Whereas I observed the lowest rates of DNA amplification in the youngest—and lowest elevation (Table 1.1)—WLD marsh, there was no correlation with vegetation cover. This observation would, to some extent, seem to reflect a tendency for AMF to be less abundant in highly flooded soils as observed previously (Anderson et al., 1984), and thus, some taxa of AMF might exhibit trends of decreasing activity with decreasing redox potential of the soil (Beck-Nielsen and Vindbæk Madsen, 2001). Such a dependency of AMF abundance on elevation appears to have been demonstrated in the Sabine marshes by the observations of Abbott (2017). Abbott (2017) measured the concentration of various microbial fatty acid methyl esters (FAMEs) in the soils of the Sabine created marshes and observed that the AMF-specific FAMEs tended to be associated with high-elevation marshes, primarily the highest-elevation marsh, which was created in 1996 and was not included in the present study. However, given that there have been reports of AMF abundance being equally high across gradients of soil moisture (Cooke et al., 1993; Turner and Friese, 1998), including in roots of submerged aquatic vegetation (Kohout et al., 2012), a

trend with flooding extent may not be a result of anaerobic stress. Rather, such a trend might be related to phosphorous availability, given that phosphate tends to become less bioavailable under aerobic conditions when ferric iron is present (Reddy and DeLaune, 2008). Because the symbiotic relationship between plants and AMF is based on the ability of AMF to efficiently scavenge nutrients (primarily phosphorous) (Smith and Read, 2008), AMF colonization tends to be diminished when phosphorous is readily available to the plants (Cornwell et al., 2001). However, I did not measure phosphorous concentrations in the present study, and hence, it is presently unclear as to whether marsh elevation, per se, contributed to this trend in these marshes.

The seemingly contradictory results between the two methods that I used for assessing AMF should be viewed with the respective methodologies in mind. Theoretically, the PCR method amplifies any AMF DNA in the soil—whether from live, dormant, or dead AMF—and can do so even when the abundance of such DNA is extremely low.[3] In contrast, the root colonization method is only capable of demonstrating active colonization of roots, and the result depends on there being observable arbuscules within the roots (McGonigle et al., 1990; Brundrett, 2004), which would be sparse and heterogeneous if colonization was low. Thus, the PCR method may tend to overestimate active AMF presence whereas the root colonization method may tend to underestimate it. Although the primers that I used for PCR are among the most AMF-specific primers currently known (Xiang et al., 2015), it is possible that there were false positives, and in the future, sequencing of the amplicons could provide more definitive evidence concerning the presence/absence of AMF. It is also conceivable that allochthonous AMF spores, viable or not, could be deposited to these systems through the water (Harner et al., 2011). If this mechanism were a substantial source, however, I would expect comparable amplification rates in the youngest sites, contrary to what I observed. Overall, and given that I was able to observe some arbuscular structures in upland plant roots using the same root preparation method as that used for the chronosequence samples, I suggest that the absence of observable arbuscules in my samples was due to generally low—not absent—AMF colonization at my study sites. Furthermore, whereas AMF abundance has been correlated with AAE protein concentrations in upland soils (Rillig, 2004; Wilson et al., 2009; Bedini et al., 2010), the presence of AMF DNA did not appear to be correlated with AAE protein density in soils studied here. It thus appears, based on my observations, that AMF are not likely to be significant contributors to the AAE protein pool in these marshes.

3.4.3 Hydrolysable non-protein component of the whole AAE protein extracts

Of the total solids extracted in the AAE protein extraction procedure, very little (<10% w/w) resembled protein. This result is qualitatively consistent with molecular characterization studies of AAE protein extracts (Schindler et al., 2007; Gillespie et al., 2011). Based on the previously hypothesized role of AAE protein in facilitating the protection of other forms of SOM through hydrophobic interactions (Rillig and Mummey, 2006), I hypothesized that the AAE protein would be accompanied by comparable amounts or greater of hydrolysable, non-proteinaceous organic material. This hypothesis would be consistent with the protein potentially being directly bound with other labile organic matter. Instead, however, I observed that nearly all of the non-proteinaceous material that was hydrolyzed was inorganic. In fact,

the whole extracts included a substantial amount (~30% w/w) of mineral material, nearly all of which dissolved during the hydrolysis incubation. This observation was somewhat surprising considering that, prior to hydrolysis, the extracts underwent an acid precipitation step and were then re-dissolved and extensively dialyzed against DI water. Although, the presence of such a mineral component does appear to be typical of humic acid fractions (Stevenson, 1994), for which treatment with hydrofluoric acid is needed to obtain an ash-free product. I initially speculated that the large mineral component contributed to the fact that approximately half of the extract N was not hydrolyzed (Chapter 2), under the assumption that the minerals protect these nitrogenous compounds from hydrolysis—as has been proposed previously in the context of whole soils (Loll and Bollag, 1983; Leinweber and Schulten, 2000). However, my observations provide little evidence for this scenario, given how little mineral material remained after hydrolysis. Although the mineral component might still play a role in stabilizing the proteinaceous material in the soil, it did not appear to promote any resistance to acid hydrolysis in my extracts. Yet, whether any association between the protein and mineral material is present in the soil or is formed during extraction cannot be determined from my observations.

In contrast to the hydrolyzed fraction, the post-hydrolysis residue appeared to be almost entirely composed of organic material (~95%), which was very similar to humic acid fractions in terms of elemental composition. This humic acid-like residue accounted for roughly 50% of mass of the initial solids. Given that this organic residue survived 6 N HCl treatment in the apparent absence of mineral material, I suggest that this residue may be primarily composed of lignin-derived compounds, which are generally regarded as the major precursors of humic acid fractions (Reddy and DeLaune, 2008) and exhibit a similar elemental composition (Filip et al., 1988). Thus, my results support previous characterizations of AAE protein extracts (Schindler et al., 2007; Gillespie et al., 2011) that suggest that these extracts are a protein-enriched version of the humic acid fraction. The non-hydrolysable N component may have been partly contributed by additional amino acids that were encapsulated within, or otherwise protected by, the humic acid-like residue—similar to the mechanism proposed by Schulten and Schnitzer (1997) and for which Knicker and Hatcher (1997) and Zang et al. (2000) have provided evidence in organic-rich soils. Small amounts of heterocyclic N may have also contributed (Schulten and Schnitzer, 1998), though likely not to a significant extent (Knicker et al., 1993). Together with the minor insoluble mineral component, the non-hydrolyzed organic residue of my extracts appears to be fully consistent with current models of the overall SOM (Paul, 2016).

3.4.4 Amino acid composition of the AAE protein extracts

In regard to the amino acids liberated upon hydrolysis of the AAE protein extracts, I observed the relative amino acid compositions to be no different between Sabine and WLD, which also did not differ between the two depth intervals (0–15 cm and 15–30 cm), and contrary to my hypothesis. In general, the amino acid profile of SOM does not vary much across soils of different regions (Sowden, 1977; Christensen and Bech-Andersen, 1989; Friedel and Scheller, 2002), and Sowden et al. (1977) have found that the average profile of their wide range of soils most closely resembled that of bacteria. However, the variation observed in whole soils does appear to be greater than what I observed for the AAE protein fraction.

Whereas the profile that I observed for AAE protein was qualitatively similar to those reported for whole soils, a comparison of the amino acid profiles of the AAE protein with those reported for a range of temperate and subtropical soils (Sowden et al., 1977; Friedel and Scheller, 2002; Fig. 3.6a); with those of brackish marsh plant litter, including decayed and detrital material from *D. spicata* and *Spartina* sp. (de la Cruz and Poe, 1975b; Fig. 3.6b); and with the average profiles of a range of aquatic and terrestrial environments (Moura et al., 2013; Fig. 3.6c) revealed that what I observed in the AAE protein fraction tended to fall outside or at the extremes of each of these ranges. For instance, regarding the comparison to the profiles of brackish marsh plant litter, de la Cruz and Poe (1975b) have observed a substantial decline in the relative contribution of glutamic and aspartic acids with increasing decay of the plant material—yet, it was for these two amino acids that I observed the AAE protein profile to be most elevated.

Further, comparison of the AAE protein amino acid profile with these three ranges combined, along with those reported for Arctic and tropical soils, Lake Ontario sediments (Sowden et al., 1977), and humic acid fractions (Malcolm, 1990; Trubetskaya et al., 1998; Fig. 3.6d), showed that this overall range still fails to fully encompass the average profile that I observed for the AAE protein fraction of my samples. Specifically, the profiles of my AAE protein extracts appeared relatively enriched in valine, isoleucine, and leucine; whereas, they were relatively depleted in serine, glycine, and threonine in comparison with the literature values for soils, humic acids, and plant litter. There are a few possible explanations for this consistent discrepancy between the amino acid profiles of the AAE protein in my sites and those typical of whole soils, humic acid fractions, and plant litter: 1) the microbial communities in the soils I studied were very similar between the two depth intervals and the two wetland types, but they differed from those of upland soils; 2) the extraction was selecting for (via chemistry and heat-stability) a relatively narrow and consistent subset of abundant proteins that might have been highly conserved among various microbial taxa; or 3) there was some source of systematic error in my analysis. Without knowing the amino acid profiles of the whole soils in the Sabine and WLD marshes, I cannot rule out any of these possibilities; however, the second possibility seems most likely and is supported by previous observations of distinct and dominant bands when AAE protein extracts are subjected to polyacrylamide gel electrophoresis (Wright et al., 1998; Chen et al., 2009; Gillespie et al., 2011). Furthermore, the impacts that salinity, hydrology, and nutrient inputs can have on soil microbial communities (Reddy and DeLaune, 2008; Dinter et al., 2019) would seem to discount the first possibility—i.e., that these profiles reflect highly similar microbial community compositions among all of the marshes, yet are distinct from those of upland soils. Such a small selection of proteins could be comprised primarily of heat-stable proteins; Gillespie et al. (2011) have provided sequence-based evidence for this possibility. As Gadkar and Rillig (2006) have noted, stress-related proteins tend to be highly conserved, and thus there could still be numerous organisms that are contributing to the AAE protein pool. These authors have provided strong evidence that one of the most abundant proteins that could potentially be extracted intact within the AAE protein fraction is a heat-shock protein from AMF (GiHsp 60), which is similar in sequence to other stress-related proteins from non-mycorrhizal fungi. However, the substantial difference between the amino acid profile of GiHsp 60 and that of the AAE protein in my samples (Fig.

3.6d) suggests that this or other stress-related proteins of similar composition were not dominating the amino acid signal.

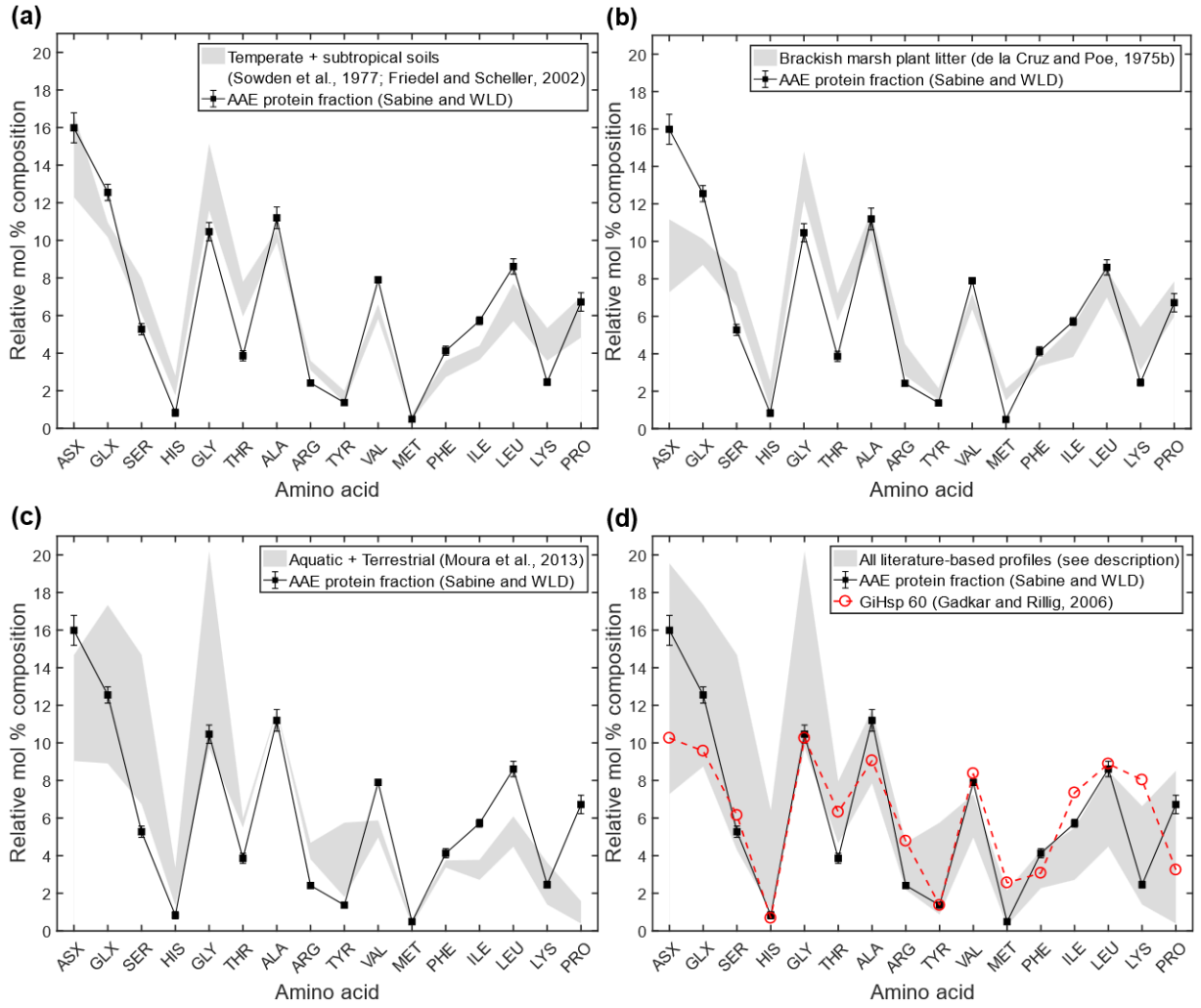

Figure 3.6. Comparison of the hydrolysable amino acid profile of the AAE protein fraction from the present study (solid squares) to the profile ranges (shaded regions) of (a) previously studied soils: cool temperate and subtropical soils (Sowden et al., 1977) and temperate soils (Friedel and Scheller, 2002); (b) brackish marsh plant litter of *D. spicata*, *Spartina cynosuroides*, *Juncus roemarianus*, and *Schoenoplectus americanus* (de la Cruz and Poe, 1975b); (c) literature-based averages of aquatic and terrestrial whole environments (Moura et al., 2013); and (d) the combined ranges of (a)–(c), along with those of Arctic and tropical soils and Lake Ontario sediments (Sowden et al., 1977), Elliot and Ohio soil humic acids (Malcolm, 1990), and Arctic, podzol, forest, chernozem, and Red soil humic acids (Trubetskaya et al., 1998). The dashed line and asterisks in (d) represent the theoretical profile of heat shock protein 60 from Glomus intraradices (GiHsp 60) as calculated based on the sequence reported by Gadkar and Rillig (2006). Error bars are ± standard deviation for all pooled AAE protein extracts from this study (n = 20). See Fig. 3.5 for legend of amino acid abbreviations.

Regarding the possibility of systematic error in my analyses, this would be expected to arise in the sample preparation stage, prior to amino acid analysis, because the analysis itself included a BSA protein standard within the same set of runs as the samples. One possible source could be selective degradation of certain amino acids during the drying steps. However, drying of the soils and extracts was done at 60°C within < 5 days, a temperature at which significant thermal degradation of these amino acids would not be expected based on the observations of Sohn and Ho (1995). These authors observed that only glutamine exhibited non-negligible degradation at 110°C; however, this was explained by deamidation of glutamine to glutamic acid, which is already assumed to occur during the hydrolysis incubation and is accounted for in the amino acid analysis that I performed. Another potential source of error may be in the hydrolysis incubation. It is known that peptide bonds differ in terms of their optimum hydrolysis time; some require longer times to be liberated (Ozols, 1990). Conversely, some amino acids are known to decompose over such longer incubations. Generally, an incubation time of around 24 hours is expected to maximize recovery while minimizing degradation (Ozols, 1990), and 22 hours was the incubation time used in the present study. It is therefore conceivable that the duration of the incubation may have played a major role in determining the composition that I observed. On a relative composition basis, a change in just one or a few amino acid estimates could significantly alter the entire observed profile.

A search of the AAE protein profile using the AACompIdent tool (http://www.expasy.org/tools/aacomp/ ; Gasteiger et al., 2005) for the Swiss-Prot/TrEMBL sequence databases revealed two close matches (similarity score < 30), though both were marginal (scores of 26 and 29). Table 3.3 lists all protein matches with a similarity score < 32. Generally, given the source organisms, molecular weights, and functions of these proteins, all four were somewhat plausible. All were from heterotrophic microbes and, interestingly, three of which were from marine or halophilic organisms. Three of the proteins had extracellular roles in degradation of organic matter—in particular, ureases and β-glucosidases are common hydrolytic enzymes in soils (Tabatabai, 2003)—and Burns et al. (1972) have suggested that ureases may readily become intercalated within humic structures, where they may be protected from proteases and therefore may persist over long time periods. Additionally, Masciandaro et al. (2008) have demonstrated the extraction of humic-bound β-glucosidase from soils using a pyrophosphate buffer similar to that used here; although, the extraction was done at neutral pH and they did not autoclave the extracts. There also appears to be a tendency of these protein candidates to have low isoelectric points (pI)—i.e., they are negatively charged over a large pH range. Among the proteomes of over 4,000 organisms of archaea, viruses, bacteria, and eukaryotes, Kozlowski (2017) has shown that, overall, the majority of proteins have a pI between 5.5 and 7.9. Perhaps the exceptionally low isoelectric points of the candidate proteins indicates some selectivity of the extraction method—although, at the pH of my extractions (9.0), most proteins would have a net negative charge, and the GiHsp 60 protein has a pI of 5.9 (Gadkar and Rillig, 2006).

Table 3.3. Known proteins of greatest similarity to the AAE protein in terms of average amino acid composition.

Protein candidate	Similarity score[†]	pI[‡]	MW (kDa)	Organism	Function
Protein-export protein SecB	26	4.08	18.5	*Sphingopyxis alaskensis*; marine aerobic bacterium	Protein chaperone
Urease accessory protein UreG	29	4.17	22.1	*Haloquadratum walsbyi*; halophilic archaeon	Urea hydrolysis
Probable glucan 1,3-β-glucosidase A	31	4.84	43.3	*Aspergillus clavatus*; non-mycorrhizal fungus	Role in hydrolysis of β-glucosides (e.g. cellulose)
Glycine cleavage system H protein	31	3.72	13.8	*Pseudoalteromonas atlantica*; marine bacterium	Role in degradation of glycine

[†] Measure of similarity with the average amino acid composition of the AAE protein extracts—smaller values indicate greater similarity (Gasteiger et al., 2005). No constraints on isoelectric point (pI), molecular weight, or source taxon were imposed on the search. [‡]Theoretical isoelectric point.

Overall, however, I cannot speculate further regarding the mechanisms of this seemingly unusually consistent amino acid profile without the profile of AAE protein fractions extracted from other soils. As reviewed by Bastida et al. (2009), the currently available methods of protein extraction and purification of soil protein are known to exhibit significant biases in terms of the distribution of proteins obtained. Thus, in my case, it may be that changes in extraction procedure, hydrolysis method, or even laboratory would have a significant effect on the profile, but because it appears that the amino acid profile of AAE protein has not been reported elsewhere, this possibility remains speculation.

3.5. Conclusions

In examining two distinct chronosequences of coastal wetland soils, I observed that the AAE protein fraction monotonically increased with marsh soil development and vegetation succession within both systems and contributed a non-trivial proportion of the overall SOM; however, the rate at which this occurred appeared primarily driven by overall organic matter accumulation and N input. Furthermore, I found that AAE protein was not correlated with the presence of AMF-specific DNA in these soils, nor did it appear correlated with vegetation coverage or community beyond its correlation with TOC and TN. In both systems, the contribution of AAE protein to TOC and TN in the oldest marshes (33- and 41-years old) resembled those of the respective established reference marshes. However, the contribution of AAE protein to TOC and TN significantly increased with age in the WLD chronosequence, whereas in Sabine, there was no change in contribution to TOC with age, and only a marginal increase in contribution to TN at the oldest marsh. I suggested that this discrepancy could be a result of greater N input to the WLD marshes relative to the Sabine marshes. Contrary to what I hypothesized, the fact that the AAE protein did not appear to be bound with appreciable

quantities of other forms of hydrolysable organic matter suggested that it might not have played a direct role in binding SOM or preserving labile organic C in these systems. Examination of the hydrolysable amino acids in the extracts revealed remarkably similar profiles, which did not differ significantly between the 0–15 cm and 15–30 cm soil depth increments, nor did they differ between the two chronosequences. Yet, the average profile did appear to systematically deviate from the ranges reported for whole soils, humic acid fractions, and plant detritus. Overall, these amino acid data suggested that the extraction method may be selecting for a relatively narrow and consistent subset of ubiquitous proteins in the soil, perhaps through a particular association with humic substances and mineral components. Thus, this type of analysis of AAE protein extracts may not offer any additional information with respect to soil health parameters, although similar analyses of extracts from a range of other soils would be needed for comparison before reaching this conclusion.

AAE protein remains a nebulous pool of SOM and, given that my analyses suggest that it is a highly conserved fraction of soil protein that is also highly correlated with TOC and TN, caution is needed when interpreting its significance with respect to soil aggregation and ecological processes.

3.6. Notes

1. Whereas I considered that inorganic N input might have been elevated close to the outlet, the fact that the salinity remained nearly zero throughout the delta would suggest that the flow may be sufficiently high that there would be little proportional uptake of N from the water over the distance of the chronosequence. The implication is that no N gradient would be expected in the overlying water. This conclusion is consistent with previous observations in the WLD (Alexandra Christensen, pers. comm.).

2. My root samples were collected in the middle of spring, and I considered the possibility that any new AMF growth may have been in early log phase (Abbott and Robson, 1991; Bohrer et al., 2004); i.e., that the time of sample collection may have contributed to especially low AMF abundance. However, given that Burcham et al. (2012) observed relatively sustained rates of AMF colonization in Louisiana brackish and salt marshes across seasons, this logic seems an unlikely explanation for my results.

3. I initially considered basing this qualitative assessment on soil RNA under the assumption that the RNA pool would better reflect active versus sporulated AMF. However, because Gamper et al. (2008) have previously shown that AMF spores can contribute substantially to the soil RNA pool—more so than hyphae—and because RNA is prone to rapid degradation upon isolation, I opted to base this analysis on DNA.

Chapter 4.
Refractory Pools of Organic Carbon and Nitrogen Across Two Soil Chronosequences of Restored Coastal Wetlands

4.1. Introduction

Despite the threat to stores of soil organic C in coastal wetlands, few studies have addressed the stability of this C with respect to its relative resistance to decomposition. Such stability has important implications not only for long-term C burial in situ but also for scenarios in which wetland soil structure is compromised and bulk stores of C become exposed to aerobic conditions. Wetland soil C that is relatively resistant to decomposition would be expected to have a greater chance of re-burial upon being transported to open water (Wang et al., 2015a). There are several operationally defined fractions of SOM that have been established and that have served as metrics of slowly decomposing C and nitrogen (N), primarily in upland soils (McLauchlan and Hobbie, 2004). One of these fractions is the non-acid hydrolysable organic C and N, which I will refer to as refractory organic C (ROC) and refractory N (RN), respectively. This is defined as the soil C and N that remains in solid phase after reflux of the soil in 6 N HCl, which is expected to largely consist of macromolecular compounds that are not readily hydrolysable as a result of their structure (e.g., aromatics and fatty acids) and/or possible association with the mineral matrix (Paul et al., 2006; Silveira et al., 2008; Wang et al., 2015a); whereas I will define the C that is lost as the labile organic C (LOC) fraction, which includes both fast- and intermediate-cycling organic C. Using ^{14}C-dating, Leavitt et al. (1996) and others (see Falloon and Smith (2000) and Paul et al. (2006)) have demonstrated that the ROC fraction tends to be significantly older than the total organic C of the bulk soil (TOC)—observations that support the view that the ROC fraction represents a pool of slowly decomposing soil C. One class of compounds that are thought to make substantial contributions to the ROC pool are lignin-derived compounds (Dodla et al., 2012; Bi et al., 2019). These substances can result from microbial degradation of lignocellulosic components of vascular plant tissues, and they may to some degree be relatively resistant to complete re-mineralization (Bi et al., 2019). The associated RN may also be of interest as this pool of N could perhaps be an important sink for excess dissolved inorganic N—similar to the role of denitrification. Although there is debate as to what compounds principally constitute the RN fraction, it is thought to exist in some combination of heterocyclic and proteinaceous forms (Schulten and Schnitzer, 1998), the latter potentially being bound to mineral surfaces (Leinweber and Schulten, 2000) or occluded within ROC structures (Knicker and Hatcher, 1997). Whereas, upon wetland erosion, it is the labile N (LN) that may be readily re-mineralized to ammonium or nitrate and thus potentially contribute to coastal hypoxia by fueling algal growth. The LN fraction includes both hydrolysable organic N and inorganic N, although the latter is generally present in very small proportions (less than a few percent) of the total soil N (TN).

In a review of studies of ROC in various upland soils, Paul et al. (2006) have found that the contribution of ROC to TOC is consistently around 50～60%. The implication is that the concentration of ROC is directly proportional to TOC. Whereas it might be expected that contributions of ROC to TOC would tend to be lower in wetland soils as a result of enhanced

preservation of the LOC pool in anaerobic environments, this may not necessarily be the case as some have observed (Silveira et al., 2008; Ahn et al., 2009). Overall, however, relatively few studies have evaluated ROC in coastal wetlands, and it is therefore unclear whether the combination of anaerobic soil conditions, salinity, and input of allochthonous organic matter and mineral sediment may alter this proportionality. Specifically, rates of mineral sedimentation are thought to affect the relative proportions of LOC through multiple possible mechanisms: 1) high mineral sedimentation can directly cause rapid burial of SOM, thus reducing its exposure to aerobic conditions (Unger et al., 2016); 2) mineral surfaces can bind and stabilize SOM (Kleber et al., 2015); and 3) higher mineral accretion rates can enhance growth of vegetation (DeLaune et al., 1990), which may enhance the production of relatively labile SOM (Elsey-Quirk and Unger, 2018). The first two mechanisms would be expected to increase the relative proportion of LOC by slowing its otherwise rapid decomposition; whereas the third might promote preferential production of LOC. In a study of C accumulation in salt marshes on the mid-Atlantic coast of the USA, Unger et al. (2016) have observed that ROC contribution was disproportionately lower (contribution range: 20∼50%) in the studied marshes that had higher mineral sedimentation rates—an observation that the authors primarily attributed to faster rates of burial, and therefore protection, of the more labile SOM. Such a conclusion might imply that coastal marshes receiving large amounts of sediment input may contain higher proportions of relatively labile C that would be susceptible to degradation upon wetland loss or erosion. In contrast, Dodla et al. (2012) have found the contribution of ROC to be relatively high (contribution range: 51∼84%) among both freshwater and saline marshes in the Mississippi Deltaic Plain, USA. Yet, in soils from nearby marshes, Steinmuller et al. (2019) have recently demonstrated that a large amount of rapidly mineralizable C may persist in deep soil layers, as judged from the fact that this C fueled high rates of microbial respiration upon exposure to aerobic conditions, even more so than the soil C near the surface. Hence, a significant amount of the C stored in these wetlands may be susceptible to rapid re-mineralization if these systems deteriorate or are eroded by climate-driven and anthropogenic forces.

Another operationally defined fraction of SOM—the autoclaved alkaline extractable (AAE) protein fraction (a.k.a. glomalin-related soil protein)—has been correlated with soil aggregation, to which it is hypothesized to directly contribute via hydrophobic interactions with other forms of SOM (Rillig, 2004; Rillig and Mummey, 2006). Specifically, it has been speculated that AAE protein helps protect forms of labile SOM through direct binding or by facilitating the formation of soil aggregates (Wilson et al., 2009; Zhang et al., 2017). It is through this potential to enhance soil aggregation that AAE protein may be involved in the preservation of relatively labile forms of SOM, wherein extracellular enzymes of microbial decomposers may be physically excluded from the interior of these aggregates (Jastrow et al., 2007). Although my previous observation that a trivial amount of labile SOM appeared to be directly bound with the AAE protein suggested that the protein may not have a direct role in binding other forms of labile SOM (Chapter 3), it is unclear whether a correlation might exist between the relative LOC density in the soil and that of the AAE protein, possibly as a result of some other, less direct mechanism.

In this study, I used the same two chronosequences of recently formed coastal wetlands—as in the studies described in the previous chapters—to serve as models of

Louisiana's proposed approaches to wetland restoration (i.e., marsh creation and sediment diversion). I sought to evaluate how soil stocks of ROC and RN in these newly established coastal marshes may change as these marshes develop, as well as the extent to which the refractory and labile fractions of SOM contribute to the overall organic C and N pools. Specifically, I hypothesized that 1) the contribution of ROC to TOC would increase with marsh age as a result of accumulation of lignin-derived compounds in concert with preferential degradation of the more labile organic matter; 2) the relative contribution of ROC to TOC would remain relatively low in the sediment diversion model due to the greater mineral sediment input acting either directly via faster burial and physicochemical stabilization of the LOC and/or indirectly via stimulation of new production; 3) the density of AAE protein in the soil would be positively correlated with LOC/TOC ratios because aggregate formation is expected to enhance preservation of the LOC fraction; and similarly 4) the density of mineral sediment would also be positively correlated with LOC/TOC ratios via the same hypothetical mechanisms mentioned in the second hypothesis.

4.2. Materials and methods

4.2.1 Study sites, field sampling, and initial sample preparation

The study sites were located in the Sabine National Wildlife Refuge (Sabine) and the Wax Lake Delta (WLD). Information regarding these study sites was provided in Section 1.3 (Chapter 1). All analyses conducted in the present study were performed on subsets of the same dried and homogenized soil core sections described in the previous chapters. Results that include AAE protein are based on the AAE protein data presented in Chapter 3.

4.2.2 Quantification of refractory (non-acid-hydrolysable) organic C and N

The refractory organic C (ROC) and refractory N (RN) in each soil sample was taken to be the C and N that is not acid-hydrolysable based on a modified version of the HCl hydrolysis method described by Leavitt et al. (1996). Approximately 1 g of dry ground soil was weighed into 60-mL pyrex tubes, and 30 mL of 6 N HCl was added. The tubes were incubated on a 110°C heat block for 18 hrs. To minimize evaporation, the tubes were covered with glass funnels and beakers during the incubation. After cooling, each soil suspension was transferred to pre-weighed 50-mL polypropylene centrifuge tubes and centrifuged at 3500×*g* for 15 min. The supernatant was discarded. The remaining residue in the glass tubes was then quantitatively transferred to each corresponding centrifuge tube, rinsing the glass tubes thoroughly with ~30 mL of deionized (DI) H_2O. The centrifuge tubes were vortexed to form a slurry, and the centrifugation step was repeated. A final rinse of the soil pellet was done by adding 30 mL of DI H_2O, followed by vortex mixing and an additional centrifugation step. The tubes and hydrolysis residues were dried to a constant weight at 60°C and the final weights recorded. Each dry residue was homogenized by vortex mixing for several minutes, and a subset was weighed and analyzed by CHN elemental analysis (as for whole soils, except without a fumigation step; Section 1.3.2) to determine the concentrations of ROC and RN in each original soil sample ($mg \cdot g^{-1}$) based on Eqs. 4.1 and 4.2:

$$\mathrm{ROC} = \frac{\%\mathrm{OC_{PH}}}{100} \times \frac{\mathrm{m_{PH}}}{\mathrm{m_i}} \tag{4.1}$$

$$\mathrm{RN} = \frac{\%\mathrm{N_{PH}}}{100} \times \frac{\mathrm{m_{PH}}}{\mathrm{m_i}} \tag{4.2}$$

in which $\%\mathrm{OC_{PH}}$ and $\%\mathrm{N_{PH}}$ are the weight % concentrations of OC and N, respectively, in the post-hydrolysis residue, $\mathrm{m_{PH}}$ is the total weight of the post-hydrolysis residue in mg, and $\mathrm{m_i}$ is the total weight of the initial soil sample subjected to hydrolysis in g. The labile organic C (LOC) and labile N (LN) were then defined as the difference between TOC and ROC, and between TN and RN, respectively.

4.2.3 Data analysis and statistics

All statistical analyses were carried out using MATLAB R2016b (Mathworks) with the statistical and curve-fitting packages installed. Carbon and nitrogen stocks were calculated for individual cores on a mass per area basis, integrated every 5 cm down to 30 cm based on the bulk density of each 5-cm core section. In the 1-year-old marsh of Sabine, where the cores did not extend beyond 20–25 cm, the stocks of the deepest section sampled from each core was extrapolated to a depth of 30 cm for the purposes of marsh stock comparison. Because the soil in this marsh was almost exclusively homogenized dredge material, the inter-depth variability within these cores was low (Table 1.2 and Fig. D.2a). Contribution ratios of ROC and RN to TOC and TN, respectively, were calculated as a ratio of stocks for each individual core, and the marsh averages are reported (n = 3 cores per marsh).

The C and N stocks of all marshes were compared across chronosequences by one-way analyses of variance (ANOVA) because nested ANOVAs indicated that there was no significant difference between the two chronosequences ($p > 0.05$). Multiple comparisons and corresponding *p*-values were based on Tukey-Kramer honestly significant difference (HSD) post hoc tests using the $\mathrm{multcompare()}$ function in MATLAB. Alphabet-coded differences shown in the figures represent significant differences at the $\alpha = 0.05$ level.

To estimate the C and N accumulation rates in Sabine and the time expected for the Sabine created marshes to become equivalent to the natural reference marshes in terms of C and N, the stocks of TOC, ROC, TN, and RN were regressed as linear functions of marsh age (assuming the accumulation rates to be constant). The slopes of these functions represented the respective estimates of accumulation rates, whereas the estimated equivalence times were determined by evaluating each function at the corresponding average stock of the reference marsh plots. The 95% confidence interval (CI) of each equivalence time estimate was determined using a Monte Carlo simulation (Appendix B, Script 3), wherein normally distributed pseudorandom numbers (n = 3) were generated based on the observed means and standard deviations of the stocks of each marsh. This simulation was performed for 10,000 iterations, each resulting in an estimate of equivalence time. The bounds of each confidence interval were defined as the 2.5-percentile and 97.5-percentile values of these 10,000 simulated estimates. Because the 30-cm stocks of the WLD marshes did not increase linearly with age, C and N accumulation rates in WLD were estimated as the difference between the corresponding

average stocks of the 29- and 16-year-old marshes, assuming the average accretion rates of these marshes to be < 2.3 cm yr^{-1}, which is consistent with previous estimates along the edges of a WLD island (DeLaune et al., 2016).

To visualize trends in the overall contribution of ROC and RN to TOC and TN, respectively, as functions of marsh age, the ratios of ROC (or RN) stock to TOC (or TN) stock—as determined for each soil core—were fit by linear regression, excluding those of the reference marshes. Analogous regressions were fit to the OC:N ratios of the total soil, refractory, and labile fractions as functions of marsh age.

To assess the relative strengths of the relationships between the soil densities of the C and N fractions, the mineral fraction, AAE protein, and the LOC/TOC ratio, Spearman's rank correlation coefficient (ρ) was calculated for each of the pairwise comparisons, and correlations for which $p < 0.01$ were deemed significant. This coefficient was used, rather than the Pearson coefficient, because the trends between these various soil components were not always linear but were monotonic.

Correlations between ROC and TOC, and between RN and TN, were plotted on a per core section basis and were fit by stepwise polynomial least-squares regression. In each case, the data of Sabine and WLD were fit to either a single model or two separate models, depending on the results of a one-way analysis of covariance (ANCOVA) performed on the log-transformed data at the $\alpha = 0.05$ level. The coefficients included in all regressions were significant to $p < 0.05$. For each curvilinear regression, the *p*-value of an *F*-test against a purely linear fit is reported. The correlations of the LOC/TOC ratio with AAE protein density, and with mineral sediment density, were also plotted on a per core section basis but were fitted by Model 2 least-squares (reduced major axis) regression. Data from the reference marshes were included in all of these regressions.

4.3. Results

4.3.1 Stocks of carbon and nitrogen

Overall, across the two chronosequences, 30-cm stocks of TOC and TN fell in the ranges 2.6–6.8 kg C m^{-2} and 150–490 from g N m^{-2}, respectively. In both chronosequences, the average 30-cm stocks of TOC and ROC increased with marsh age (Fig. 4.1a and 4.1b). Stocks of TOC were similar in magnitude between Sabine and WLD, as were the stocks of ROC (nested ANOVA $p > 0.7$). In Sabine, stocks of TOC and ROC in the created marshes were all significantly less than those of the reference marshes ($p < 0.04$). Whereas in WLD, the TOC stocks of the 29- and 41-year-old marshes did not differ from those of the youngest marsh, the reference marsh, nor the Sabine created marshes; only those of the youngest marsh (2.82 ± 0.18 kg C m^{-2}) and reference marsh (7.5 ± 0.3 kg C m^{-2}) differed ($p = 0.041$).

In Sabine, stocks of TN and RN did not differ significantly across the created marshes ($p > 0.9$; average: 340 ± 50 g N m^{-2} and 80 ± 20 g N m^{-2}, respectively; Fig. 4.1c) and were significantly lower (by approximately 50%) in these marshes versus the reference marshes ($p < 0.02$; average: 700 ± 160 g N m^{-2} and 240 ± 60 g N m^{-2}, respectively). In WLD, stocks of TN increased with marsh age (Fig. 4.1d), though only the TN stock of the reference marsh (510 ± 40 g N m^{-2}) was significantly greater than that of the youngest marsh ($p = 0.011$; 175 ± 19 g N m^{-2}).

Similar to the TOC trend, the TN stocks of the 29- and 41-year old marshes were no different than those of either the 16-year old or reference marshes ($p > 0.05$). RN stocks, however, did not differ among any of the WLD marshes ($p > 0.1$; average: 80 ± 30 g N m^{-2}) and were all similar to those of the Sabine created marshes ($p > 0.3$); they were significantly less than the Sabine reference marshes ($p < 0.0001$).

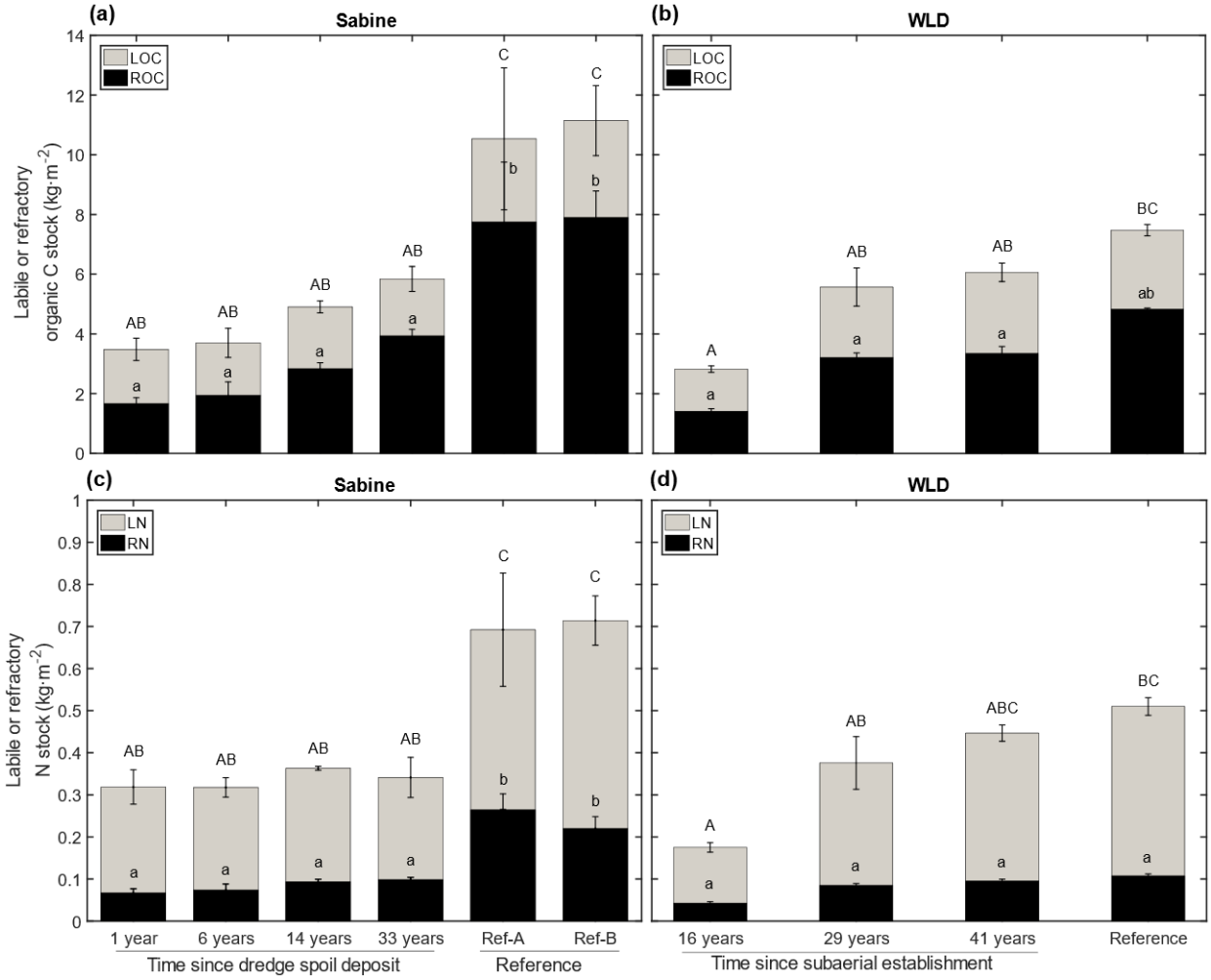

Figure 4.1. Average stocks of LOC and ROC (a and b), and LN and RN (c and d) in the top 30 cm of soil in each marsh of Sabine (left) and WLD (right). Error bars are ± standard error (n = 3 cores). Letters indicate significant differences ($p < 0.05$) based on Tukey-Kramer HSD post-hoc tests after one-way ANOVA, in which all marshes were included. Note that the total height of the bars represents TOC or TN.

In Sabine, stocks of TOC and ROC were linearly correlated with marsh age (r^2 = 0.71 and 0.81, respectively, $p < 0.001$; Table 4.1). Because the stocks of the oldest created marsh in Sabine (33-year-old) were significantly less than those of the references marshes, I applied a linear regression to estimate the approximate time that would be expected for the stocks of these created marshes to reach those of the reference marshes (the equivalence time; Table

4.1), assuming a constant accumulation rate. The equivalence times for TOC (100 yrs; CI: 60–170 yrs) and ROC (90 yrs; CI: 60–130 yrs) were similar, and are consistent with the model of wetland development that has been described by Craft et al. (2003). With respect to TN, however, there was no significant change in stocks with age in Sabine (p = 0.56). Stocks of RN did appear to increase subtly (r^2 = 0.40, p = 0.027), which implied that LN was being converted to RN with an estimated equivalence time of 200 yrs (CI: 100–400 yrs).

Table 4.1. Linear regressions of stocks with marsh age in Sabine, and the corresponding estimates of the time to reach equivalency to those of the reference marshes.

	Sabine				WLD
	TOC	ROC	TN	RN	TOC ROC TN RN
Slope (g m^{-2} yr^{-1})	76 ± 15	72 ± 11	*NS*	1.0 ± 0.4	
Intercept (g m^{-2})	3500 ± 300	1600 ± 200	320 ± 20	70 ± 7	*Oldest (41-yr) marsh did not significantly differ from the reference marsh in terms of C and N stocks (ANOVA, p > 0.05).*
r^2 (p-value)	**0.71 (<0.001)**	**0.81 (<0.0001)**	<0.1 (0.56)	**0.40 (0.027)**	
Reference average (g m^{-2})	10800 ± 1200	7800 ± 980	700 ± 90	240 ± 20	
Equivalence time (95% CI)	100 yrs (60–170)	90 yrs (60–130)	*(>400 yrs)*	200 yrs (100–400)	

Boldface indicates a significant correlation with marsh age (p < 0.05). *NS* = not significant. Errors are ± standard error (n = 3 cores). The equivalence times and corresponding 95% confidence intervals (CI) were estimated based on a Monte Carlo simulation using the means and standard deviations of the stocks of each marsh, and assuming the accumulation rates to be constant (Section 4.2.3).

In WLD, the stocks of the oldest marsh were not significantly different from those of the reference marsh (ANOVA p > 0.05), and the stocks did not follow a linear relationship with age. With respect to the estimation of C accumulation rate in WLD, it would be inappropriate to use an analogous method to that used for Sabine because the high accretion rates that are expected of the WLD marshes (on the order of ~1.5 cm yr^{-1} as estimated on an adjacent WLD island; DeLaune et al., 2016) means that the 16-yr horizon may not always occur within the 30-cm soil depth interval that I sampled. Thus, a curve fit to all three stocks shown here would likely correspond with an underestimate of C accumulation rate. Instead, I assumed the accretion rate to be on the order of 1.5 cm yr^{-1}—hence the intermediate (29-yr) marsh stock would include all of the new accumulation. Therefore, the difference between the stocks of the 16-yr and 29-yr marshes would imply a C accumulation rate of 210 ± 50 g C m^{-2} yr^{-1}, which is consistent with 250 ± 23 g C m^{-2} yr^{-1} as previously estimated for WLD (Shields et al., 2017).

4.3.2 Contributions of ROC and RN to TOC and TN

Generally, the contribution of ROC to TOC (average: 59 ± 12%) was around two-fold that of RN to TN (average: 26 ± 8%). In Sabine, the contribution of ROC to TOC (ROC/TOC; Fig. 4.2a) increased linearly with marsh age (r^2 = 0.72, p < 0.001) as hypothesized, and did not differ between the oldest marsh and the reference marshes (p > 0.8). In contrast, a significant linear trend with age was not observed for ROC/TOC in WLD (p = 0.4), and that of the oldest marsh was no different than that of the youngest marsh (p = 0.75) or that of the reference marsh (p = 0.25).

Despite the fact that TN stocks did not change with marsh age in Sabine, I did observe a subtle but significant linear increase in RN/TN (Fig. 4.2b; r^2 = 0.45, p = 0.016) with marsh age in Sabine. Ultimately, the RN/TN ratio reached that of one of the reference marshes (Ref B; p > 0.99) and did not significantly differ from that of the other (Ref A; p = 0.13). As was the case with ROC/TOC in WLD, I similarly did not observe a significant trend in RN/TN ratios across the same marshes (p = 0.36), and the RN/TN ratio of the oldest (41-year-old) marsh was similar to that of the corresponding reference marsh (p > 0.99).

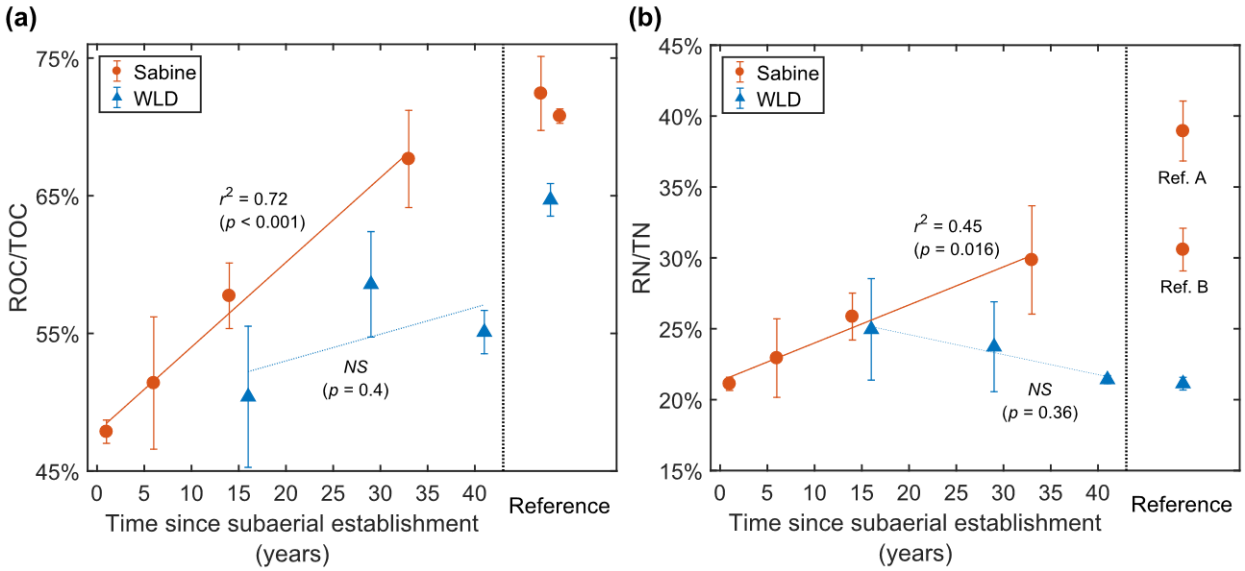

Figure 4.2. Average contributions of ROC to TOC (a) and RN to TN (b) as functions of marsh age within the Sabine and WLD chronosequences. Error bars represent ± standard error (n = 3 cores). *NS* indicates that the correlation was not significant (p > 0.05).

Overall, organic carbon to nitrogen (OC:N) ratios were always much higher (by twofold or more) in the refractory fraction than in the total soil, which is consistent with previous observations in wetland soils (Dodla et al., 2012). In Sabine, OC:N ratios of the total soil and the refractory fraction exhibited linear relationships with age (Fig. 4.3)—both were significantly positively correlated with age (refractory: r^2 = 0.97, p < 0.0001; total: r^2 = 0.77, p < 0.001). The OC:N ratios of the labile fraction, on the other hand, were 3- to 5-fold less than those of the

refractory fraction, and they remained virtually constant across all marshes (r^2 = 0.3, p = 0.054), including the reference marshes, at an average of 7.3 ± 0.4 g·g^{-1}. These trends contrasted with those of WLD, in which subtle but significant negative correlations with age were observed for the total and labile OC:N ratios (total: r^2 = 0.55, p = 0.022; labile: r^2 = 0.74, p = 0.003), whereas no trend was observed for the refractory OC:N ratios (p = 0.3). Additionally, in terms of OC:N ratios, the refractory fraction of WLD was the only instance in which the oldest marsh significantly differed from the reference marsh (ANOVA, p < 0.001).

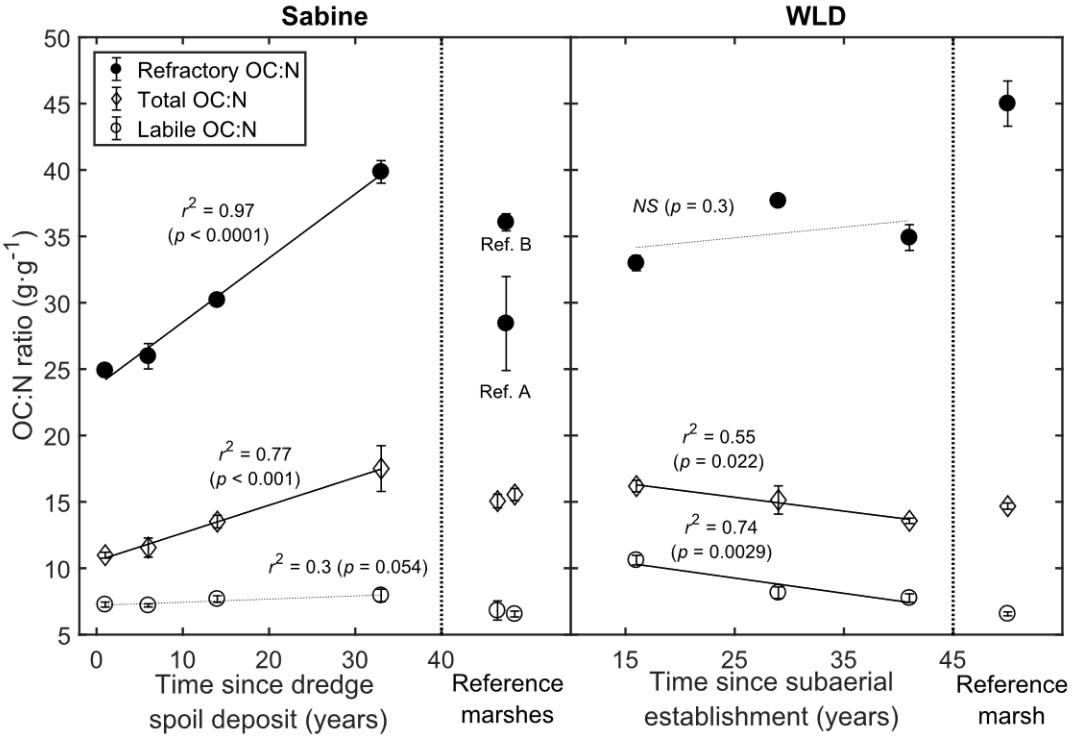

Figure 4.3. Organic C to N ratios of the total soil (diamonds), refractory fraction (closed circles), and labile fraction (open circles) as a function of marsh age in Sabine and WLD. Error bars represent ± standard error (n = 3 cores).

4.3.3 Correlations among mineral density and the fractions of C and N

Overall, all fractions of C and N were highly positively correlated with each other and only moderately negatively correlated with mineral sediment density, based on Spearman rank correlations (Table 4.2; p < 0.01).

As observed with AAE protein (Chapter 3), the ROC and RN fractions appeared to be best correlated with TOC and TN. A remarkably strong quadratic relationship (r^2 = 0.988, p = 0.0092) was observed between ROC and TOC (Fig. 4.4a), and the trends did not differ significantly between the two chronosequences based on an ANCOVA of the log-transformed data (Fig. D.1a; p = 0.16). In contrast with ROC versus TOC, distinct correlations were observed for the two chronosequences (ANCOVA p < 0.0001; Fig. D.1b) with respect to the relationship

between RN and TN (Fig. 4.4b; Sabine: $r^2 = 0.96$, $p < 0.0001$; WLD: $r^2 = 0.988$, $p < 0.0001$), though much of this difference appeared to be driven by the relatively higher RN concentrations of the Sabine reference marshes compared to the created marshes.

Table 4.2. Spearman rank correlation coefficients (ρ) between the densities of various soil components ($mg \cdot cm^{-3}$) and the LOC/TOC ratios in Sabine and WLD. All correlations shown were significant at the $\alpha = 0.001$ level.

				Sabine		
	TN	ROC	RN	AAE protein[†]	LOC/TOC	Mineral
TOC	0.88	0.97	0.95	0.90	−0.78	−0.54
TN		0.80	0.85	0.83	−0.54	−0.62
ROC			0.97	0.88	−0.89	−0.47
RN				0.86	−0.85	−0.47
AAE protein					−0.72	−0.67
LOC/TOC						0.32
				WLD		
	TN	ROC	RN	AAE protein[†]	LOC/TOC	Mineral
TOC	0.98	0.94	0.92	0.95	−0.32	−0.77
TN		0.91	0.92	0.95	*NS*	−0.76
ROC			0.93	0.94	−0.58	−0.81
RN				0.90	−0.46	−0.69
AAE protein					−0.40	−0.85
LOC/TOC						0.52

NS indicates that the correlation was not significant ($p > 0.01$).
[†] Estimation of AAE protein was described in Chapter 3.

The contribution of LOC to TOC was weakly negatively correlated with all C and N fractions (Table 4.2) but slightly positively correlated with mineral sediment density. This included a weak negative correlation between LOC/TOC and AAE protein (Sabine: $\rho = -0.74$, $r^2 = 0.41$; WLD: $\rho = -0.40$, $r^2 = 0.17$; $p < 0.001$; Fig. 4.5a), contrary to my hypothesis. Conversely, I observed a very weak but significant positive correlation between LOC/TOC and mineral sediment density (Sabine: $\rho = 0.32$, $r^2 = 0.12$; WLD: $\rho = 0.52$, $r^2 = 0.19$; $p < 0.001$; Fig. 4.5b)—not inconsistent with my initial hypothesis but not as strong as I expected based on the observations of Unger et al. (2016). Furthermore, this relationship was not significantly different between the two systems (ANCOVA $p > 0.05$), suggesting that mineral sediment input, per se, had little influence on the proportional accumulation of LOC.

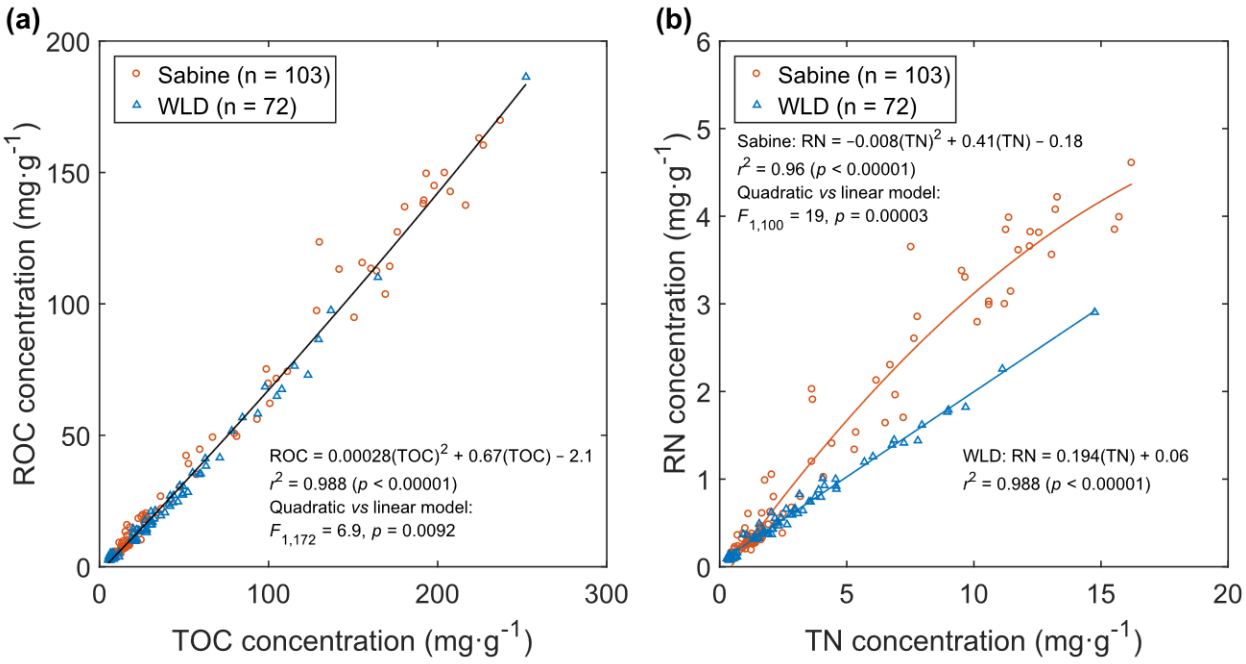

Figure 4.4. Correlations between ROC and TOC (a) and between RN and TN (b) among the Sabine and WLD marshes. Data were fit to either a single model or separate models depending on the results of ANCOVA performed on the log-transformed data (Fig. D.1).

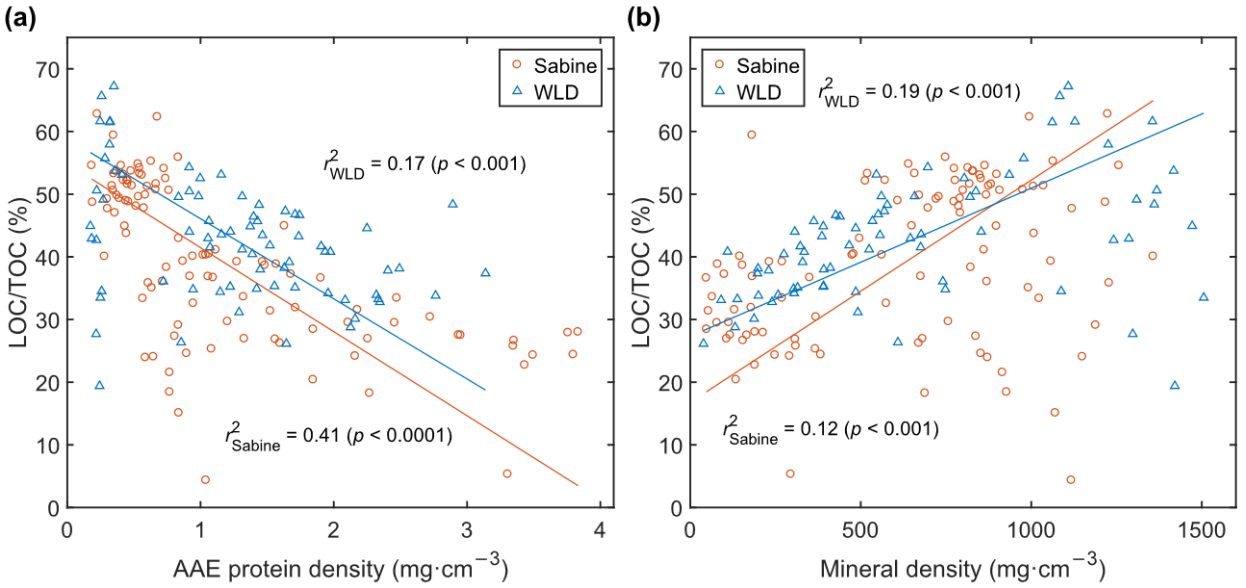

Figure 4.5. Reduced major axis regressions of the proportion of LOC to TOC against AAE protein density (a) and mineral sediment density (b) in Sabine and WLD. Relationships are plotted separately for the two chronosequences; however, the slopes did not significantly differ between the two in either plot (ANCOVA, $p > 0.05$).

4.4. Discussion

4.4.1 ROC and RN across the two chronosequences

While stocks of ROC generally followed the same trends as TOC in both chronosequences, the contribution of ROC to TOC in Sabine significantly increased with age as I hypothesized (r^2 = 0.72; Fig. 4.2a). In fact, the similarity between the ROC accumulation rate and the TOC accumulation rate (72 and 76 g C m^{-2} yr^{-1}, respectively; Table 4.1) would suggest that nearly all of the new C accumulation in the created marshes of Sabine is ROC. Furthermore, the linear increase of the OC:N ratio of the refractory fraction with age (r^2 = 0.97; Fig. 4.3) suggests that the refractory component that is being added to the soil is much more depleted in N than that initially present in the dredge-spoil, corresponding to a significant increase in overall soil OC:N ratios with marsh age (r^2 = 0.77). Indeed, this overall increase appeared to be almost entirely driven by the refractory fraction, given that the OC:N ratios of the labile fraction remained consistently low across all of the Sabine marshes. Such low OC:N ratios may reflect a high contribution of algal and bacterial biomass to the labile fraction, and hence, these trends may demonstrate the relative impact of the marsh vegetation versus algae on SOM quality in this system. Given that the main source of C in this system is expected to be derived from plant litter, these observations are consistent with lignin-derived compounds being primary contributors to ROC[1], as well as with the previously observed high N resorption efficiencies of *S. alterniflora* and *S. patens* (Elsey-Quirk et al., 2011). Overall, the trend of increasing ROC/TOC ratios with age in the Sabine marshes appeared to be primarily driven by the linear accumulation rate of new organic matter, which apparently exhibited much higher ROC/TOC ratios than the dredge-spoil sediment (as judged from the 1-year-old marsh). This increase in ROC contribution with age therefore reflects a consistent quality of the new SOM across the marshes, as opposed to a change in quality with change in vegetation. The relatively high ROC/TOC ratios of this new organic matter are likely related to the slow accretion rates typical of this system. Slow accretion rates—and more specifically, low mineral sedimentation rates—mean that leaf litter and other organic matter on or near the surface is exposed to relatively oxidized conditions for a longer period of time, thereby potentially contributing to re-mineralization of the labile fraction before it is fully incorporated into the soil. The apparently large differences between short-term and longer-term C accumulation rates in these marshes, as previously determined by Abbott et al. (2019), support the idea that much of the C that is initially deposited is not incorporated into these soils. Additionally, the similarity between my estimate of TOC accumulation rate, based on a depth of 30 cm (76 ± 15 g C m^{-2} yr^{-1}), and the average of those reported by Abbott et al. (2019) in the same marshes (60 ± 14 g C m^{-2} yr^{-1}), which were based on the dredge-spoil horizon depth of each marsh, implies that little organic C accumulates in the dredge-spoil layer of these soils (e.g., as a result of the leaching of organic C from the peat layer to the dredge-spoil layer).[2]

My estimate of ROC accumulation rate in Sabine is consistent with estimates made in *S. alterniflora*-dominated salt marshes on the mid-Atlantic US coast (Unger et al., 2016). Unexpectedly, however, my rough estimate of ROC accumulation rate in WLD (139 ± 13 g C m^{-2} yr^{-1}) was higher than in Sabine, and slightly higher than in even the relatively sediment-starved Barnegat Bay marshes of Unger et al. (2016). At least in my sites, it appears that the relative

proportion of ROC to LOC does not vary as much compared to marshes in the mid-Atlantic, therefore leading to comparatively greater rates of ROC accumulation with increases in TOC accumulation. In general, as marsh elevation increases, rates of mineral sediment deposition are expected to decrease, which would imply that there is more time for the labile fraction to decompose, therefore leading me to expect relatively greater ROC/TOC ratios at the higher elevation (older) marshes of WLD. However, whereas the averages of these ratios did appear slightly greater in the higher elevation marshes of WLD (Fig. 4.2a), they were not significantly greater, due in part to an apparently high degree of variability within each marsh. Accordingly, no clear trend with age in these ratios was apparent in the WLD marshes, in contrast to the Sabine marshes. Although ROC/TOC ratios were generally lowest in the youngest WLD marsh, I hypothesized that they would be significantly and substantially lower as a result of the relatively rapid mineral sedimentation rates that would be expected for such a low elevation marsh in this system. Perhaps the ROC/TOC ratio of this marsh was elevated somewhat by the accumulation of allochthonous organic matter, which might have been derived from vegetation with higher lignin content. In salt marshes of the mid-Atlantic, it has been observed that allochthonous organic matter was the major source of refractory C, based on a different operational definition (Leorri et al., 2018). Indeed, my observation that ROC/TOC ratios of WLD tended to be highest in the reference marsh, which included trees and shrubs, might be explained by a combination of greater refractory organic matter input and slower accretion rates at this site.

Trends of RN/TN ratios with age in both chronosequences were qualitatively similar to the respective trends of ROC/TOC ratios. In Sabine, there was a similar linear increase (r^2 = 0.45, p = 0.016) in RN/TN ratios; whereas no significant trend was observed in WLD (r^2 = 0.12, p = 0.36). The observation that RN/TN ratios increased with age in Sabine while stocks of TN did not change, suggests that LN was being converted to RN at a slow but marginally significant rate of 1.0 ± 0.4 g N m^{-2} yr^{-1} (Table 4.1). Because observations have suggested that the majority of nitrogenous compounds in soils may be comprised of intrinsically hydrolysable/soluble compounds, such as proteins, peptides, amino acids, and amino sugars (Preston, 1996; Martens and Loeffelmann, 2003), I speculate that this apparent conversion of LN to RN over time could be due to encapsulation of proteinaceous material within conglomerates of refractory compounds—a speculation that is supported by studies of nitrogenous SOM composition (Knicker and Hatcher, 1997; Knicker et al., 2001). Whether this could be mediated by the vegetation (where N resorption might mean preferential return of RN to the soil) or by post-senescence biogeochemical soil processes is unclear. However, leaf and stem litter of *S. patens* and *S. alterniflora* have been observed to have relatively high amounts of RN as compared to a submerged species and to algae (Buchsbaum et al., 1991), and the authors observed that this RN appeared to be associated with lignin and cell wall remnants. The trends of N in Sabine contrasted with those of WLD, in which the LN fraction appeared to accumulate faster than the RN fraction between the youngest two marshes (Figs. 4.1d and 4.2b). Additionally, this coincided with a significant decrease in OC:N ratio of the labile fraction (r^2 = 0.74), which appeared to drive a subtle decline in OC:N ratio of the total soil (r^2 = 0.55, p = 0.022; Fig. 4.3). It is unclear what might have contributed to this but perhaps the high amount of inorganic N loading in this system is contributing to a disproportionately greater abundance of microbial and algal biomass as SOM concentrations increase. Alternatively, perhaps there is

accumulation of clay-fixed inorganic N (NH_4^+) (Reddy and DeLaune, 2008), which would increase the amount of LN without affecting LOC, and hence, possibly contributing to the slight downward trend in OC:N ratios of the labile fraction.

4.4.2 Relationships of mineral density and AAE protein with LOC contribution

Given the hypothesized role of AAE protein in promoting soil aggregation and the protection of otherwise labile SOM that has been highlighted in the literature (Spohn and Giani, 2010; Dai et al., 2015; Wang et al., 2018b), I hypothesized that AAE protein would be positively correlated with the contribution of such labile compounds to the total SOM, i.e., the LOC/TOC ratio. However, I observed a weak negative correlation between AAE protein density and LOC/TOC ratios for both Sabine (r^2 = 0.41) and WLD (r^2 = 0.17; Fig. 4.5a). This was true even when considering each marsh separately (not shown). This would appear to completely contradict the hypothesis that the AAE protein fraction is directly involved in preservation of the labile C fraction. Rather, these observations are consistent with my findings presented in Chapter 3, in which I reported that the AAE protein fraction of these marshes was not co-liberated with significant amounts of non-proteinaceous labile compounds. Collectively, these results suggest that AAE protein is not playing a role in facilitating the preservation of other forms of soil organic C in these marshes, whether by direct binding mechanisms or by enhancement of soil aggregation. Based on this, an alternative hypothesis could be suggested: the AAE protein accumulates in the soil as a result of its protection via association with the refractory SOM—that is, it is the *protected* rather than the *protector*. Though not testable using the data presented here, this hypothesis is consistent with my overall observations; specifically, that AAE protein density was positively correlated with ROC/TOC ratios, and that the AAE protein was extracted with a comparatively large amount (around tenfold or more) of ROC (Chapter 3).

Based on the hypothetical mechanisms by which mineral sediment could preferentially enhance the accumulation of labile organic matter, as reviewed earlier, I had hypothesized that the high rates of mineral sediment deposition in WLD would drive a trend of increasing LOC/TOC ratios (decreasing ROC/TOC) with mineral sediment density, similar to the trend observed by Unger et al. (2016), and that ROC/TOC ratios would generally be much greater in the Sabine marshes, which are in an area where mineral accretion rates are typically low. Although I did observe a significant positive correlation between LOC/TOC ratios and mineral sediment density in both the Sabine (r^2 = 0.12) and WLD marshes (r^2 = 0.19; Fig. 4.5b), the correlation was much weaker than that observed by Unger et al. (2016) (r^2 = 0.71), and further, the range in ROC/TOC ratios that I observed was more narrow, on average. Thus, the amount of sediment input may not, per se, be driving the trends in LOC/TOC ratios in these systems, which appeared to be subtle overall. Such incongruent observations do not appear to be explainable by differences in accretion rates or TOC accumulation rates, given that rates similar to those of WLD have been reported in the mid-Atlantic marshes (Unger et al., 2016). Elsewhere in coastal Louisiana, bulk density has been correlated with LOC in marsh soils adjacent to the Mississippi River (Dodla et al., 2012); however, plotting these data on a proportional basis, LOC/TOC ratios appeared only moderately correlated with bulk density, similar to what I observed. My results may appear to be generally inconsistent with the

hypotheses of others, who have postulated, based primarily on observations in upland soils, that the mineral component of soils may be having a large influence on SOM preservation (see Kleber et al., 2015). However, my hypothesis that LOC/TOC ratios would be strongly correlated with mineral sedimentation was primarily based on the tendency of organic matter to decompose more slowly under increasingly reduced conditions. Thus, the methods that I applied here were not necessarily intended to elucidate the extent to which the organic matter may be stabilized by molecular interactions with the mineral fraction. A major assumption that I made in defining the LOC fraction is that the C that was stabilized via soil aggregation or association with mineral constituents would necessarily be released upon acid hydrolysis. Although this may be true to some extent (see Chapter 3), evidence has been presented for such mineral associations conferring resistance of SOM to acid hydrolysis (e.g., Leinweber and Schulten, 2000). Hence, my observation of the relatively modest impact that mineral sediment density appeared to have on partitioning of TOC between the labile and refractory fractions does not discount the potential role of organo-mineral associations in C preservation in these systems.

4.4.3 Total carbon and nitrogen stocks across the two chronosequences

Based on the 30-cm C stocks of the Sabine marshes[3], I estimated that these marshes accumulate organic C at a rate of 76 ± 15 g C m^{-2} yr^{-1}, which implies that the total C stocks of created marshes in this area become equivalent to those of the natural reference marshes within 60–170 yrs (Table 4.1). These estimates are consistent with previous estimates of longer-term C accumulation rates in this area (Smith, 2012; Abbott et al., 2019) as well as with equivalence time estimates made in *S. alterniflora*-dominated created marshes on the south Atlantic US (Craft et al., 2003). However, this accumulation rate is at the low end of a range of salt and brackish marshes throughout the US (Chmura et al., 2003) and for Louisiana coastal marshes overall, which appears typical of marshes in the Chenier Plain (Suir et al., 2019).[4]

In contrast to the Sabine marshes, the C stocks that I observed along the WLD chronosequence imply that the marsh soils of WLD are expected to resemble those of the adjacent non-delta marshes within ~50 years after subaerial establishment—i.e., roughly twice as quickly as the created marshes of Sabine.[5] However, my observations in WLD differed from those of DeLaune et al. (2016) on an adjacent island of the delta. Whereas the authors observed much lower C densities (average 13 mg C cm^{-3}) and relatively sparse vegetation at their island sites, I observed C densities in the older WLD marshes that approached those of my inland reference site (~25 mg C cm^{-3}; Fig. D.2b). This discrepancy may illustrate the spatial heterogeneity of these newly forming islands, and it seems likely that the sites studied by DeLaune et al. (2016) were simply at an earlier stage of development—intermediate of my 16-year and 29-year sites.

Whereas stocks of TOC increased with age in both chronosequences, stocks of TN significantly increased only in WLD. In Sabine, stocks of TN were very uniform across all of the created marshes and were generally lower than those of WLD. This is not particularly surprising given how little allochthonous sediment and freshwater these marshes receive, and N accumulation rates of < 2 g N m^{-2} yr^{-1} have been reported in *S. alterniflora*-dominated saltmarshes on the south Atlantic US (Craft et al., 2003; Craft, 2007). Remarkably, the TN stocks

of the natural reference marshes were approximately two-fold higher than those of the created marshes. In combination with the apparently low N accumulation rate within the created marshes, this large difference would seem to suggest that organic N is very efficiently recycled in these marshes, such that a large proportion of the N input stays within the upper 30 cm. Indeed, this would not be inconsistent with the observation that both *S. alterniflora* and *S. patens* can have relatively high N resorption efficiencies (Elsey-Quirk et al., 2011).[6] In WLD, N appeared to accumulate much faster, and making an estimate analogous to that made for C would suggest a N accumulation rate of 15 ± 5 g N m^{-2} yr^{-1}, which is comparable to estimates based on sediment traps in marshes within the Mississippi Delta (DeLaune et al., 1981). This is expected, not only given the large sediment input to the WLD, but also given the high nutrient concentration—particularly nitrate—of the riverine input.

4.4.4 Correlation between ROC and TOC

Because the mineral fraction appeared weakly correlated with LOC/TOC, I took a closer look at the correlation between ROC and TOC. Overall, concentrations of ROC were most strongly and positively correlated with TOC concentrations (Fig. 4.4a). In terms of these correlations, the soils of Sabine and WLD appeared to be no different (ANCOVA, $p = 0.075$). Such strong correlations are typical in studies of ROC in both upland (McLauchlan and Hobbie, 2004; Paul et al., 2006) and wetland (Dodla et al., 2012; Unger et al., 2016) soils. However, the similarities did not end there. In fact, the relationship between concentrations of ROC and TOC that I observed was remarkably similar to those observed in other coastal wetland soils of Louisiana (Dodla et al., 2012; Kelsall, 2019; Fig. 4.6) despite a diverse representation of wetland types, which included a freshwater swamp, freshwater marshes, brackish marshes, and salt marshes. Combined with my data, these observations span much of the length of the Louisiana coast. Moreover, the consistency between the trends of the Chenier Plain marshes (Sabine) and those of the Atchafalaya Basin (WLD) and Mississippi River Plain (Barataria Bay) would seem to suggest that Mississippi River-related factors are not primary contributors to this similarity in correlation. On a related note, this trend also appears very similar to that in bottomland forested wetland soils of inland Georgia, based on the data of Silveira et al. (2008) (slope ~61%; not shown)[7]. Furthermore, this similarity also did not appear to be impacted by minor methodological differences, including a difference in HCl concentration.[8] In contrast to the studies in Louisiana wetland soils, however, the correlation that was observed in mid-Atlantic salt marshes substantially deviated and exhibited more positive curvature (Fig. 4.6; Unger et al., 2016). Specifically, there was a much stronger contribution of LOC (TOC − ROC), which appeared to consistently affect the data from all marshes, as evident from the overall lower elevation of the relation. Comparison with a selection of trends observed in upland soils (Fig. 4.6) suggests that they more closely resemble the observations in coastal Louisiana soils, at least in the range of relatively low TOC concentrations that are characteristic of aerobic soils.[9]

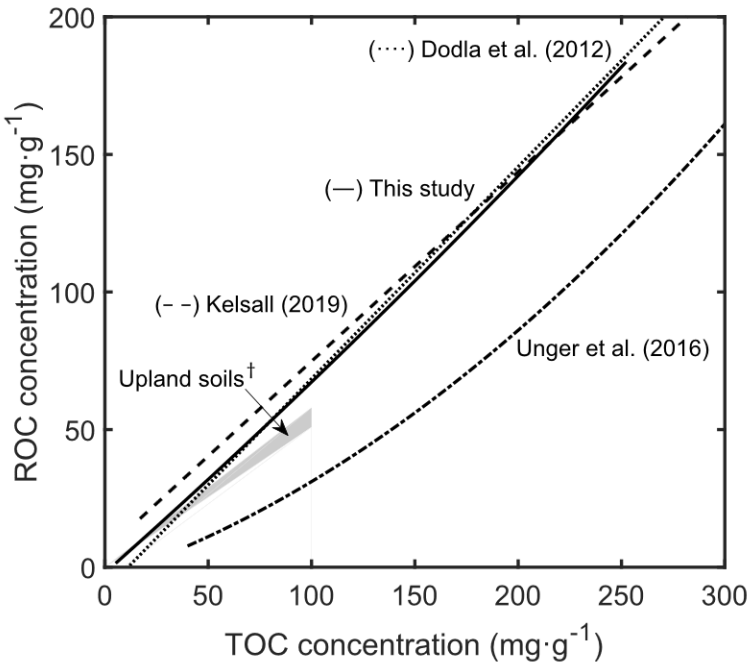

Figure 4.6. Regression of ROC vs TOC of this study (solid curve; Sabine + WLD) and that reported in: (····) Mississippi River deltaic plain marshes (Dodla et al., 2012); (– –) Barataria Bay marshes (Kelsall, 2019); (· – ·) mid-Atlantic salt marshes (Unger et al., 2016); and that based on a range of studies in upland soils as compiled by Paul et al. (2006) (shaded). All studies used similar methodologies for hydrolysis (6 N HCl, 95–116°C, 16–18 hrs), except Unger et al. (2016) and Kelsall (2019), who used 4 N HCl. Regressions were not extrapolated beyond their reported TOC ranges. The *r*-square values of all regressions were >0.90. † Shading represents a range of linear regressions fit to the compiled data depending on minor methodological differences and does not represent the range in observed values.

The obvious question here is: why does this trend differ so substantially between the mid-Atlantic marshes and a wide range of Louisiana marshes? In considering this question, it should be highlighted that the correlations between ROC and TOC are shown here on a concentration basis, rather than a density basis. I opted to focus on this because a correlation based on the densities appeared to differ only by exhibiting slightly more scatter/random error. On a concentration basis, the TOC concentration is essentially a measure of the proportion of solid soil material that is organic versus inorganic (mineral). Therefore, in the case of the Unger et al. (2016) relation, as the proportion of solid material that is mineral increases, the proportion of the TOC that is refractory decreases—consistent with the authors' hypothesis that the mineral fraction would have a role in preferential accumulation of the labile organic matter. Importantly, however, the authors made observations in two areas—Barnegat Bay and Delaware Estuary marshes—that were distinct in terms of, inter alia, mineral sediment input;

yet these observations fell along the same curve (Fig. 4.6). This suggests that there is some common factor or factors that are influencing the partitioning of refractory organic matter across both of these marshes and that do not appear to be present in the Louisiana wetlands. In the coastal Louisiana wetlands, the essentially linear relation suggests that the proportion of soil solids that are inorganic has almost no influence on the proportion of organic matter that is refractory and, further, that little else does either, given that the proportion remains virtually constant, overall, across all of the Louisiana marshes.[10] Although this is not entirely true—it did appear that the dredge-spoil sediment of the Sabine marshes had a slightly lower proportion of ROC—it does seem to apply to the naturally accumulated organic matter of Louisiana's wetlands.

Speculation as to what other factors might be responsible for the apparently different patterns between the Louisiana wetlands and those of the mid-Atlantic is made difficult by the paucity of studies of ROC in coastal wetlands in other regions throughout the US and the world.[11] A difference in contribution of algal biomass to the SOM between the two regions might help to explain the differing trends in ROC; however, the generally higher C:N ratios observed in the mid-Atlantic marsh soils (15∼23 $g \cdot g^{-1}$; Unger et al., 2016) would seem to discount this explanation.[12] One major difference between the two regions, however, is climate. Perhaps the longer and relatively colder winters of the mid-Atlantic region are contributing to enhanced preservation of the soil organic matter by slowing soil microbial respiration, and thereby allowing a greater proportion of LOC to accumulate. This mechanism could act in concert with the influence of mineral accretion but may also help account for the fact that both of the mid-Atlantic marshes were described by a single curve. Indeed, there is evidence that labile forms of SOM make greater contributions to the TOC in wetlands with increasing latitude (Wang et al., 2012), and Meentemeyer (1978) has observed that decomposition of low-lignin plant litter was more sensitive to climatic conditions than plant litter of higher lignin concentrations. Yet, if there is an effect of mineral accretion then why does it appear to be so weak in the Louisiana marshes? One possibility could be that there is a potentiation-type[13] interaction between climate and mineral accretion, whereby in absence of sufficiently cold winters, the rate of mineral accretion has little effect—i.e., the enhanced soil respiration due to warmer soil temperatures offsets the effect of fast burial or mineral surface-mediated stabilization. Support for the hypothesis that SOM preservation can depend on interactive effects of both temperature and physicochemical mechanisms has been presented previously (Davidson and Janssens, 2006). Yet, in the absence of observations based on this method in other coastal wetland regions, the specific impact that climate may have on these trends remains speculation.

4.4.5 Implications for marsh restoration

Although the rapid establishment of new land is of primary interest in proposed marsh restoration projects, development of soil C stocks also needs to be considered if the goal of these projects is also to sequester and store C. It is known that while restored marshes may rapidly reach natural equivalency in terms of the majority of ecological functions (within three decades or less), the time to reach equivalency in terms of soil chemistry is expected to be much longer (Craft et al., 2003). Indeed, I observed that C stocks in the Sabine created marshes

had not yet reached those of the natural reference sites despite the resemblance of the oldest marsh to the reference marshes in terms of both vegetation density and community, which is somewhat consistent with what others have observed in these same marshes (Abbott et al., 2019), in adjacent marshes (Edwards and Proffitt, 2003; Edwards and Mills, 2005), and in created marshes elsewhere (Craft et al., 2003). My average estimate of equivalence time for C stocks in these marshes (100 yrs) was likewise similar to projections in other created marshes (Craft et al., 2003). However, despite this seemingly slow development in terms of C, the fact that the majority of the organic C accumulation in these marshes appeared to be refractory is promising. This would imply that most of this new C is less susceptible to rapid re-mineralization, even if the marshes ultimately deteriorate or are lost completely. In contrast to the Sabine marshes, the relatively rapid accretion of the WLD marshes (as evident from the gain in elevation between the youngest two marshes) appears to greatly enhance the development of C stocks to the point where they might become equivalent to the adjacent non-deltaic marshes within ~50 years. Furthermore, it appears that, despite the WLD marshes exhibiting slightly lower contributions of ROC to TOC compared to the Sabine created marshes, the rapid accretion more than offsets this, such that ROC accumulation rates in WLD may be significantly more than in the created marshes. This means that, unlike what would be implied by observations on the mid-Atlantic coast (Unger et al., 2016), marshes in Louisiana that are formed from sediment diversions may have a substantially greater ability to contribute to the refractory soil C pool, and therefore act as important C sinks despite impacts of sea level rise and storm surges that threaten to export this C to relatively oxidized environments.

Whereas C has primarily been the focus of studies of refractory SOM, soil N is also an important element when considering SOM dynamics (Reddy and DeLaune, 2008; Knicker, 2011). Large amounts of dissolved inorganic N—principally nitrate—in the Mississippi River are being constantly transported to near-shore waters off the Louisiana coast, thereby stimulating algal blooms and the subsequent formation of hypoxic bottom water each spring and summer, which negatively impacts marine life (Rabalais et al., 2002). With respect to RN, I initially speculated that this might constitute an important mechanism for long-term sequestration of some of this excess N that passes through the WLD marshes. However, using denitrification rates as a metric of comparison, my observations suggest that the rate of accumulation of RN between the two youngest WLD marshes (3.3 ± 0.4 g N m^{-2} yr^{-1}; average ~9 mg N m^{-2} day^{-1}) is substantially lower than estimates of denitrification rates in these same marshes (~50 mg N m^{-2} day^{-1}; Henry and Twilley, 2014). Furthermore, rates of denitrification are expected to generally increase as these marshes become more organic-rich (Henry and Twilley, 2014), whereas I might expect RN accumulation rates to be relatively unchanged. Thus, although the accumulation of RN might be acting as a sink of dissolved inorganic N within this system, it appears relatively inconsequential compared to other routes of N removal.

Considering the need to better understand the mechanisms that govern C pools and fluxes in view of global climate change, there has been an ever more increasing emphasis placed on C budgets. Whereas models of wetland C have included categories for fractions of C that have relatively long residence times (Hopkinson et al., 1988; Zhang et al., 2002), there appears to be a deficit of direct measurements of such fractions, particularly in coastal wetland soils. Although the ROC fraction is operationally defined and is not particularly specific, it has been shown to provide some level of indication of the soil C that is less susceptible to

decomposition and that may have a significantly higher mean residence time in the terrestrial C pool (Leavitt et al., 1996; Paul et al., 2006). Given this and the consistent correlation between TOC and ROC that I and others have observed across marshes of coastal Louisiana (Fig. 4.6), it may be worthwhile to exploit this for purposes of rough estimations of ROC stocks and accumulation rates in marshes of this region for which only observations of TOC exist—similar to the way in which regressions have been used for estimating TOC stocks and accumulation rates based on loss-on-ignition and accretion data (Chmura et al., 2003). While relatively imprecise, such a predictive method could have potential to allow broad incorporation of ROC estimates within Louisiana's wetland C budgets and projections, and without the need to carry out the relatively time-consuming measurements associated with the ROC method as applied here.

4.5. Conclusions

The amounts of ROC, LOC, RN, and LN were estimated in two chronosequences of coastal wetland soils, which represented two distinct approaches to wetland restoration. The contribution of ROC to TOC within the upper 30 cm of soil increased with age in the Sabine chronosequence but not significantly in the WLD chronosequence. Overall, ROC/TOC ratios were similar between the two chronosequences, but in Sabine it appeared that the majority of the new C accumulation was accounted for by ROC. Although I observed a significant positive correlation between LOC contribution and mineral density in both chronosequences, the correlations were not as strong as expected and were much weaker than those observed in mid-Atlantic salt marshes (Unger et al., 2016). Based on rough estimates of C accumulation rates, it appeared that the WLD marshes accumulated ROC at a faster rate than the Sabine marshes, and they may resemble the adjacent local climax marshes within a much shorter timeframe than those of Sabine. Unexpectedly, the overall correlation between concentrations of ROC and TOC did not differ between the two chronosequences and were remarkably similar to the correlations that have been previously observed in other coastal wetlands in Louisiana (Dodla et al., 2012; Kelsall, 2019). However, these correlations were clearly distinct from that previously observed in mid-Atlantic salt marshes (Unger et al., 2016). Collectively, these observations suggest that mineral sedimentation may not have a pronounced effect on the relative accumulation of labile SOM in Louisiana coastal marshes, and that the sediment input associated with sediment diversion-facilitated marsh restoration may actually enhance rates of refractory SOM accumulation in the soils of this region. Finally, contrary to what I hypothesized, AAE protein was negatively correlated with LOC contribution in both chronosequences, which, together with my previous findings (Chapter 3), suggests that the AAE protein fraction is not involved in the preservation of the more labile SOM.

4.6. Notes

1. Although lignin itself is readily degradable by aerobic enzyme-mediated processes, the products of which are thought to make important contributions to the refractory SOM (see Paul, 2016).

2. In this study, I made an effort to remove easily discernible plant material from the soil samples prior to analysis, under the reasoning that this material may not readily be redeposited under erosion scenarios as compared to the organic fraction that is finer-sized and/or more closely associated with the mineral fraction. This procedure may have contributed, in part, to the similar accumulation rates that I observed between TOC and ROC in Sabine; however, I feel that this step yields a better representation of the SOM that would be redeposited following erosion of the soil. Moreover, the operational definition of ROC typically includes removal of discernable plant material (Leavitt et al., 1996; Paul et al., 2006; Silveira et al., 2008; Dodla et al., 2012; Cao et al., 2017), which, depending on lignin content, could have potential to variably affect ROC measurements, given that lignin does not readily hydrolyze or dissolve in 6 N HCl. Yet, according to Paul et al. (2006), although inclusion of recently deposited plant material can affect age estimates of the ROC, it is not likely to have major impacts on ROC quantification, at least in the case of upland soils.

3. Stocks of TOC generally appeared to increase with age in both chronosequences. Stocks of the two oldest marshes of WLD approached those of the reference whereas those of even the oldest Sabine marsh did not reach the corresponding reference values (Fig. 4.1a and 4.1b). This difference appears to primarily result from differences in accretion rates between the two chronosequences. For the most part, SOM accumulation arises from the burial of plant material that originates at the soil surface. In Sabine, where accretion is primarily from autochthonous organic matter, accretion rates tend to be lower than in marshes that receive high sediment input, such as the WLD. As a result, a longer time is expected for new accretion to reach a 30-cm depth, which is the depth on which all stocks reported in this study were based. Indeed, I observed a relatively uniform increase in TOC density across the soil depth profiles of the WLD marshes (Figs. D.2a and D.2b), whereas in Sabine, the dredge-sediment horizons were reported to occur at depths < 15 cm in all created marshes as of one year prior to my sampling (Abbott, 2017). Thus, while C densities in the top soil layers in the Sabine marshes were typically no different than those of the reference marsh or those of WLD, the relatively low accretion rates of Sabine corresponded to slower 30-cm stock increases. This implies that, from a C storage perspective, refractory organic matter may be especially important to consider for marshes created in areas of low allochthonous input because the soil C would be expected to exhibit a slower rate of burial and therefore be susceptible to erosion for a longer period of time. Conversely, the deficit in mineral sediment input means that it is expected that, after a sufficient amount of time, the C stocks of the Sabine marshes would ultimately exceed those of WLD, as a result of increased compaction at greater depths in the absence of mineral material, and therefore increased C density. Yet, I observed a particularly large variation in stocks of the Sabine reference marshes and thus, while the TOC stocks of the Sabine reference marshes did appear to be greater than that of the WLD reference marsh, the difference was not significant ($p = 0.4$ and $p = 0.18$ for Ref A and Ref B, respectively). I noticed that some portions of the Sabine reference cores appeared to contain diffuse sandy layers of relatively low SOM concentration, and I speculate that these layers resulted from heterogeneous sediment deposition associated with storm surges from past hurricanes.

4. Although, these estimates diverge considerably from those based on the observations of Bryant and Chabreck (1998), who included in their study impounded and non-impounded natural marshes in the

Sabine NWR. The organic accumulation rates reported by these authors implied that these marshes accumulated C at average rates of 714–1713 g C m^{-2} yr^{-1} since 1963 (Bryant and Chabreck, 1998; Chmura et al., 2003)—around an order of magnitude higher than my estimates and those of others mentioned above. Whereas their reported accretion rates (0.6–0.9 cm yr^{-1}) were similar to those of Abbott et al. (2019), it appears that the primary contributor to this divergence is that the authors apparently observed average SOM contents of 60–68% in the top 20–30 cm soil depths, which are substantially higher than what I observed in my natural reference marshes. Perhaps the closer proximity of their marshes to the coast (~7 km closer) contributed to this.

5. This is not surprising considering the way in which these marshes are expected to accrete sediment and organic matter. In this system, a negative exponential or hyperbolic-like relation between elevation and marsh age would be expected. This is because accretion—principally mineral but also organic—is expected to occur relatively rapidly with age during the initial stages of marsh development. As the elevation of the marsh increases further, however, there is a gradual decrease in average flood duration, depth, and flow rate of the surface water. This corresponds to declining rates of accretion of mineral sediment and allochthonous organic matter, as well as potentially faster rates of organic re-mineralization. Thus, vertical accretion within the marsh becomes more dominated by autochthonous organic input, which tends to occur at a much slower rate (as apparent in the Sabine marshes), and will eventually be countered by enhanced decomposition and compaction as the elevation increases further. In essence, the marsh elevation reaches an equilibrium. This model of marsh development appears entirely consistent with my observations in terms of the patterns in both elevation and 30-cm stocks of C in WLD, although it appears that my WLD chronosequence sites failed to capture the shape of the initial rapid trend in accumulation that would be expected.

6. Additionally, perhaps the greater amounts of N in the natural reference marshes is a relic of greater riverine input in the time before regular dredging of the Calcasieu ship channel commenced (ca. 1937). If organic N is efficiently recycled in these marshes then perhaps much of this N still persists within the upper 30 cm of these natural marshes.

7. In their abstract, Silveira et al. (2008) have mistakenly reported that 24–32% of the total C in the wetland soils was non-hydrolysable (ROC), which has been subsequently misstated by Dodla et al. (2012). In fact, this was the range that was hydrolysable (LOC).

8. The fact that Kelsall (2019) used the same method as Unger et al. (2016) (4 N HCl), yet observed a trend very similar to mine, demonstrates that, within reason, the HCl concentration used for hydrolysis does not appreciably affect the results. Indeed, this is consistent with previous manipulations of the method (Silveira et al., 2008; Xu et al., 1997). This may raise the question as to why a concentration of 6 N was chosen for this operational definition in the first place. In fact, 6 N is not an arbitrary HCl concentration—it is the concentration at which HCl and water form a constant-boiling azeotropic mixture, the boiling point of which is 109°C (Atkins and de Paula, 2006). This means that if a concentration greater than this is boiled, HCl will be disproportionately lost to evaporation until the concentration decreases to 6 N. It also means that the temperature of the sample will never exceed 109°C, regardless of how high the temperature is set on the heat block (assuming the incubation is performed under ambient pressure, which appears typical of this assay). In essence, the use of boiling 6 N HCl ensures that the concentration and temperature remain constant throughout the incubation and that the highest exposure temperature is attained.

9. The slope of the upland soils trend appears slightly more shallow than the Louisiana wetland soils, which implies that these wetlands may have slightly higher ROC/TOC ratios than the upland soils. This is consistent with comparisons made between upland and wetland sites in north Florida (Ahn et al., 2009). Whereas it might be expected that the opposite would be true when considering the relatively slow decomposition in anaerobic soils, it has been suggested that this tendency is driven by the fact that there exist nonhydrolyzable compounds (such as lignin and other phenolic structures) whose decomposition requires oxygen (Reddy and DeLaune, 2008; Ahn et al., 2009). Thus, these compounds may tend to preferentially accumulate under anaerobic conditions.

10. The similarity in trends between coastal Louisiana marshes, as presented in Fig. 4.6, should not be interpreted to mean that the specific compounds and transformations of the SOM are likewise similar. The ROC definition is broad and nonspecific in terms of precise compositions and turnover times. Thus, it may still be—and likely is—that the relative degradability of the SOM across these marshes varies somewhat as a result of the specific hydrology and biogeochemistry of each of these wetland areas, including mineral sediment texture and composition.

11. Whereas the term refractory C has been used to describe observations in several other studies of wetland SOM, the variation in operational definitions among these studies makes it difficult to compare observations across studies and to compare with my observations—differences in chemical fractionation procedure, including differences in the type of acid used for hydrolysis, are known to affect the observations even when applied to the same soils. However, there have been other studies of ROC in wetlands that used compatible methodology but that I did not include in Fig. 4.6. Cao et al. (2017) have applied the same method in coastal wetlands of Laizhou Bay, China. Yet the TOC concentrations in the soils they studied only ranged < 5 $mg \cdot g^{-1}$, and so were not included in the comparison. Ahn et al. (2009) have observed average ROC/TOC ratios in an urban wetland of north Florida that were similar to those that I observed, but the data needed for regression analysis was not provided.

12. I considered that perhaps a greater proportion of the organic matter in the mid-Atlantic marshes is derived from algae, which would be expected if the turbidity of the surface waters was relatively low. Algae do not contain lignin and, under low-light conditions, are typically composed of a large proportion of protein (e.g., Terry et al., 1983). It would therefore be expected that algal biomass would be readily hydrolysable. Without the need for structural C, algae tend to exhibit much lower C:N ratios than vascular plants, and it seems, at least from my data, that the labile organic matter exhibits consistently low C:N ratios. However, average C:N ratios of the soils studied by Unger et al. (2016) ($15 \sim 23\ g \cdot g^{-1}$) were generally greater than those I observed here and appeared to be poorly correlated with ROC/TOC ratios (not shown). Hence, there does not appear to be a significantly larger contribution of algal biomass to the SOM of the mid-Atlantic marshes.

13. Potentiation is a term borrowed from toxicology, where it is used to describe an interaction between two agents in which one agent exhibits no toxicity by itself but enhances the toxicity of the other.

Chapter 5.
Conclusion and Perspective

5.1. Measurement of the AAE protein fraction

In Chapter 2, I presented an alternative approach for estimating the protein concentration in AAE protein extracts and the overall contribution of autoclaved alkaline-extractable (AAE) protein to total organic carbon (TOC) and total nitrogen (TN), based on the use of amino acid analysis (AAA). Essentially, my approach differed from direct measurement of every sample by AAA—my approach exploited the typical consistency with which proteinaceous compounds contribute to the total soil nitrogen within a given soil in order to avoid the need to measure amino acid quantity in every sample. This approach may be suitable for scenarios in which accuracy, time, and cost are more important considerations than precision. Although wetland soil samples were used, I expect the approach to be generally applicable to extracts of all soil types, given that consistent hydrolysable amino acid-N:TN ratios have been observed for a diverse range of soils (Christensen and Bech-Andersen, 1989; Schulten and Schnitzer, 1998; Friedel and Scheller, 2002). Additionally, it is not necessarily limited to only the quantification of AAE protein; the co-extraction of HA is also problematic in other types of soil protein extracts (reviewed in Section 2.1).

In comparing the AAA-based approach to that based on the Bradford assay (Chapter 2), I confirmed that the same qualitative pattern of interference from HA contaminants that has been observed in soil porewater and in non-AAE soil extracts (Roberts and Jones, 2008) appears to be the same for AAE protein extracts. More importantly, however, my observations demonstrate that recently proposed workarounds for overcoming HA-related interference when using the Bradford assay for soil extracts are likely erroneous as a result of the inappropriate application of standard addition (Jorge-Araújo et al., 2015) and standard dilution (Moragues-Saitua et al., 2019) techniques. Whereas application of the standard addition technique would have a tendency to overestimate the protein concentration—more so than the direct standard curve technique—the application of the standard dilution technique may have a tendency to virtually eliminate any protein signal, meaning that the result becomes dominated by the very interfering components whose signal the method is aiming to overcome. Use of these published methods could be particularly problematic in that researchers may incorrectly assume that these methods are more accurate, and they may therefore place more emphasis on the data that result from studies using the standard addition or dilution techniques over those of previous studies. This could further hinder soil protein quantification in general, given that interfering compounds in soils have been problematic not only for AAE protein studies but for any studies seeking to quantify total protein in soil solutions and extracts.

Surprisingly, I found that estimates of the contribution of AAE protein to TOC in the Sabine and WLD soils were quite similar between my approach and the traditional approach. This similarity suggested that overestimation of protein concentration in the Bradford assay and the underestimation of the C composition of the protein may tend to cancel. Although it is unclear whether this cancellation would be typical for all soils, the ranges of C contribution of

the AAE protein in the soils I studied were similar to several of those reported for other soils using the traditional approach (e.g., Rillig et al., 2001a; Lovelock et al., 2004; Wang et al., 2018a). Thus, if the C contribution of the AAE protein is the only metric that is sought, then either approach might be suitable. In contrast, previous estimates of AAE protein contributions to total soil N (Rillig et al., 2001a; Lovelock et al., 2004; Halvorson et al., 2018) may be substantial underestimates. Additionally, I found that the particularly strong correlation between AAE protein concentrations in the soil and concentrations of TOC does not appear to be an artefact of the Bradford assay, given that the AAA-based approach yielded a similarly strong correlation.

5.2. Significance of the AAE protein fraction with respect to soil C storage and preservation

Although it is debated as to whether AMF in soils may help or hinder C preservation under increasing concentrations of atmospheric CO_2 (Cheng et al., 2012; Verbruggen et al., 2013), some have suggested that AMF may contribute to C storage through the production of slowly decomposing compounds, of which glomalin has been thought to be one (Treseder and Allen, 2000; Rillig et al., 2001a; Wang et al., 2018b). AMF might, to some extent, produce compounds that are refractory themselves or otherwise promote the preservation of other compounds; but based on my findings, it seems that AAE protein is not one of them. My observations suggest that AMF are not a major contributor to the AAE protein pool in the marshes I studied (Chapter 3), judging from the paucity of observable AMF colonization in roots from soils with abundant AAE protein (densities of which were similar to those observed in upland soils) and from the discrepancy between the amino acid composition of the AAE protein and that of the putative glomalin gene product GiHsp 60 (Gadkar and Rillig, 2006). Overall, it seems that the recalcitrant status that has been suggested of glomalin and the AAE protein pool has resulted more from confusion over terminology and operational definitions than from real considerations of its specific chemistry and molecular identity. The apparently large contribution of non-hydrolysable—and non-proteinaceous—organic matter in the protein extracts may be the reason that this protein pool has received such interest in the first place. From my observations, it appears that AAE protein may not be involved in the preservation of labile soil organic matter (SOM). Rather, my observation that the AAE protein was negatively correlated with relative proportions of labile organic C, and that it accumulated in concert with a comparatively large amount of refractory SOM with which it was closely associated, might suggest that the AAE protein is being preserved by the refractory SOM—that the density of AAE protein in the soil may primarily be controlled by the amount of this refractory SOM. Hence, the survival of this protein through the harsh extraction procedure that defines this protein pool could be a result of its association with lignin-derived compounds, especially given that its distribution in marine environments tends to correlate with terrestrial inputs (Adame et al., 2012; López-Merino et al., 2015). Support for this hypothesis includes various previous observations that suggest that soil protein can be bound, encapsulated, or otherwise stabilized by the HA fraction (Ladd and Butler, 1975; Knicker and Hatcher, 1997; Zang et al., 2000), including the observation that a portion of BSA that was added to soils apparently survived the AAE protein extraction procedure (Rosier et al., 2006). The presence of a large amount of mineral material that appeared to be bound with the organic matter in the AAE protein extracts

of my study might suggest that the protein is also protected by iron and aluminum oxyhydroxides, as has been suggested for protein and other forms of SOM (Kaiser and Guggenberger, 2000; Leinweber and Schulten, 2000; Lalonde et al., 2012); although the mineral material in my extracts did not appear to affect the hydrolysability of the protein. Overall, it may be that the AAE protein fraction represents a subset of soil proteins that are either fast-cycling yet heat-stable and/or proteins that are incidentally preserved over the course of soil pedogenesis—and that are selected for in the AAE protein extraction technique.

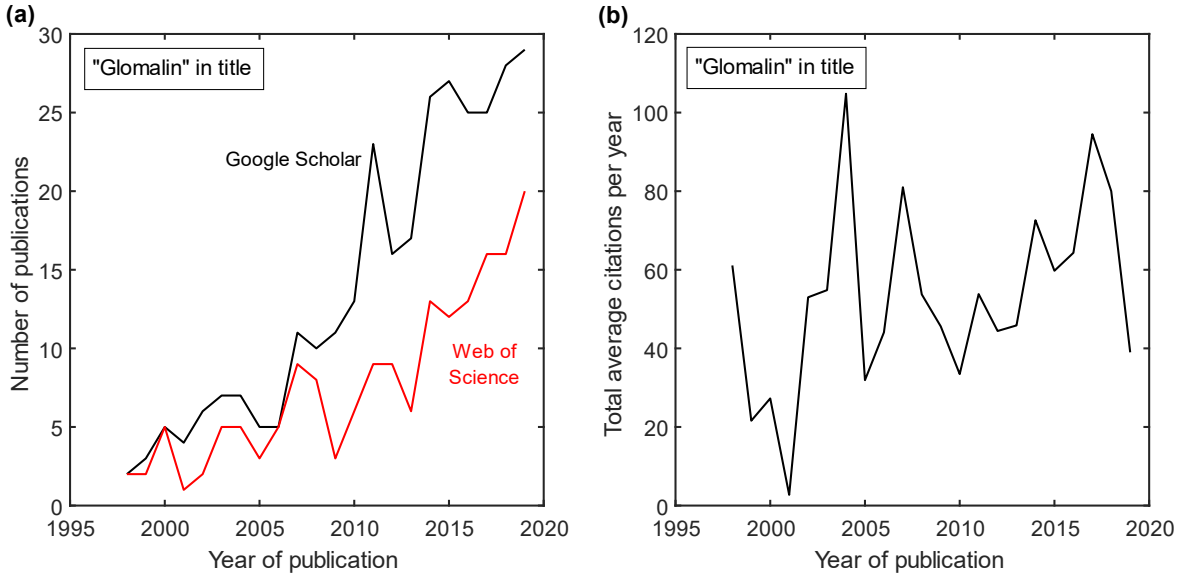

Figure 5.1. Meta-analysis of publications that have included "glomalin" in their title and published between 1998 and 2019. (a), the number of publications from each year as returned from searches of the Google Scholar database (black line) and Web of Science database (red line). (b), the combined average number of citations per year for all publications from each year (as of January 2020) based on Google Scholar indexing—this was calculated using the Publish or Perish software package (Harzing, 2007; Harzing and Alakangas, 2016). Note: the Google Scholar database is generally more comprehensive than Web of Science but it does contain replicate entries and conference proceedings (Martín-Martín et al., 2018). Here, the results from the Google Scholar database were manually filtered to exclude replicate entries and conference proceedings but to include journal articles, book chapters, theses, and dissertations—whereas, the Web of Science search almost exclusively returned journal articles.

As one anonymous reviewer of Chapter 2 has acknowledged, "…some of the concepts around glomalin are folklore and not based on hard data." (pers. comm.). Yet, such "folklore" persists in peer-reviewed scientific journals (e.g., Wang et al., 2017; Yang et al., 2017; Halvorson et al., 2018), and the number of studies of glomalin—and citations thereof—appear to have been increasing, particularly over the last decade (Fig. 5.1). However, the omission of the term glomalin when referring to AAE protein extracts in some of the most recent literature (Fine et al., 2017; Hurisso et al., 2018; Geisseler et al., 2019) may indicate some amount of acceptance

among the soil science community of the fact that these extracts can contain a range of non-mycorrhizal—and non-fungal—proteins and proteinaceous material along with co-extracted organic material (Rosier et al., 2006; Schindler et al., 2007; Gillespie et al., 2011; Hurisso et al., 2018), and it is anticipated that the work that I have presented here will provide further clarity as to the apparently limited significance of this proteinaceous fraction of SOM, at least in the case of coastal wetlands.

5.3. Refractory C and N in models of coastal wetland restoration

In Chapter 4, I showed that soil stocks of refractory organic carbon (ROC) increased with age in both the Sabine and WLD chronosequences. Although nearly all of the new C accumulation in Sabine appeared to be ROC—more so than in WLD—the relatively fast accretion rates of WLD apparently resulted in greater rates of ROC accumulation in WLD than in Sabine. These results appear to further illustrate the potentially positive influence that sediment diversions could have in terms of C accumulation and preservation in lost or deteriorated coastal marshes of Louisiana, and is in addition to previously observed positive effects (DeLaune et al., 2016).

I also observed that the relation between ROC and TOC concentrations in the soil did not differ between the two chronosequences. Furthermore, it generally appeared that mineral sediment density in both systems was poorly correlated with the partitioning of the SOM between labile and refractory fractions. This poor correlation is in contrast to what has been observed in marshes of the mid-Atlantic coast (Unger et al., 2016). Moreover, the strong and nearly linear correlation between ROC and TOC concentrations in the soils was remarkably similar to those observed elsewhere in marshes of coastal Louisiana (Dodla et al., 2012; Kelsall, 2019). This suggests that the relative accumulation of ROC and LOC may, for the most part, be insensitive to differences in coastal restoration approach within Louisiana. With respect to this, I speculated that climate, rather than vegetation or mineral sediment characteristics, may have a larger influence on the proportioning of SOM between refractory and labile fractions in coastal wetlands inasmuch as it might explain the similarity between the Louisiana marshes and their apparent divergence from the mid-Atlantic marshes. However, direct observations to support or discount this hypothesis are lacking. Yet the possibly pronounced role that climate is playing would have important implications for the preservation of SOM under a warming climate, especially in coastal regions of higher latitude. Hence, this is a topic that deserves further research—specifically, the determination of whether SOM partitioning changes systematically across a latitudinal gradient.

In terms of refractory N (RN), it seems that its proportion of TN may be somewhat more sensitive to differences in local environmental factors such as the amount of N loading, as is the case between Sabine and WLD. However, rates of accumulation of RN observed here appeared small overall compared to traditionally considered routes of N removal in wetlands (e.g., denitrification). Nonetheless, RN does appear to form a sizable pool of N in these systems, and it may behoove future studies of ROC in coastal wetlands to include analysis of the RN fraction, especially given that N concentration data are already incorporated in most elemental analyses.

Appendix A.
Supplementary Figures and Tables of Chapter 1

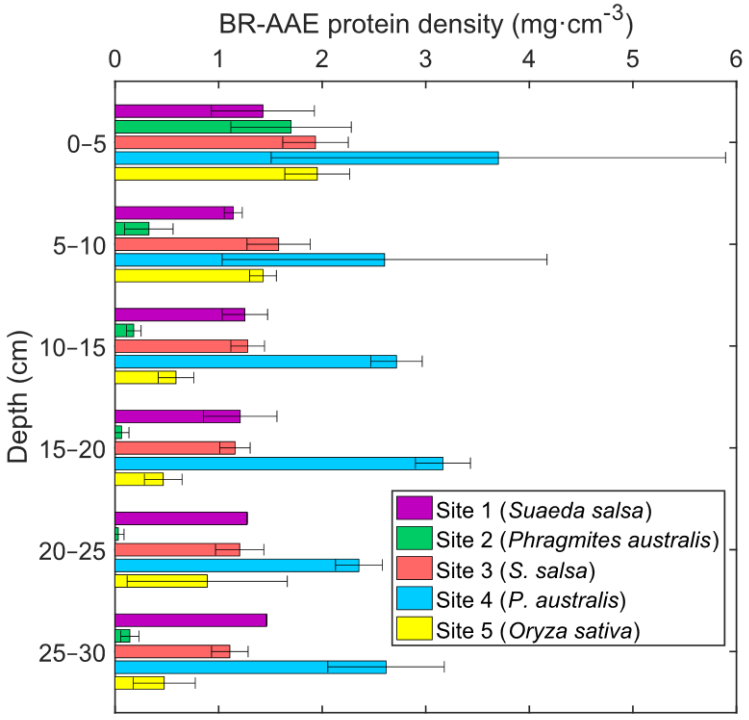

Figure A.1. Density of Bradford-reactive AAE protein in the upper 30 cm of soil in Liaohe Delta marshes. Protein concentrations in the soil extracts were estimated using traditional methods (Bradford assay). The sites correspond to differences in vegetation and salinity—*Oryza:* freshwater rice paddy; *Phragmites:* mesohaline reed stands; *Suaeda:* polyhaline seablite flats. These sites correspond to those that have been described by Olsson et al. (2015). Error bars represent ± standard deviation (n = 3 cores).

Table A.1. Precise locations of each sampling plot in the Sabine marshes.

Chronosequence	Marsh age	Coordinates[†]
Sabine		
	1 year	29°56'59.98"N, 93°24'45.28"W
		29°56'56.58"N, 93°24'27.69"W
		29°56'42.03"N, 93°25'48.82"W
	6 years	29°56'28.71"N, 93°24'11.42"W
		29°56'11.48"N, 93°23'42.58"W
		29°56'5.82"N, 93°24'8.33"W
	14 years	29°57'46.81"N, 93°24'37.36"W
		29°57'44.21"N, 93°24'57.00"W
		29°57'35.68"N, 93°24'40.69"W
	33 years	29°55'5.68"N, 93°20'45.44"W
		29°55'5.86"N, 93°20'45.92"W
		29°55'6.19"N, 93°20'49.64"W
	Reference A	29°56'0.54"N, 93°26'24.28"W
		29°55'46.38"N, 93°25'58.14"W
		29°55'40.87"N, 93°26'30.45"W
	Reference B	29°56'41.70"N, 93°26'13.70"W
		29°56'49.69"N, 93°26'19.56"W
		29°56'26.05"N, 93°26'28.63"W

[†] Coordinates were selected to match a subset of those sampled by Abbott et al. (2019), which were randomly selected.

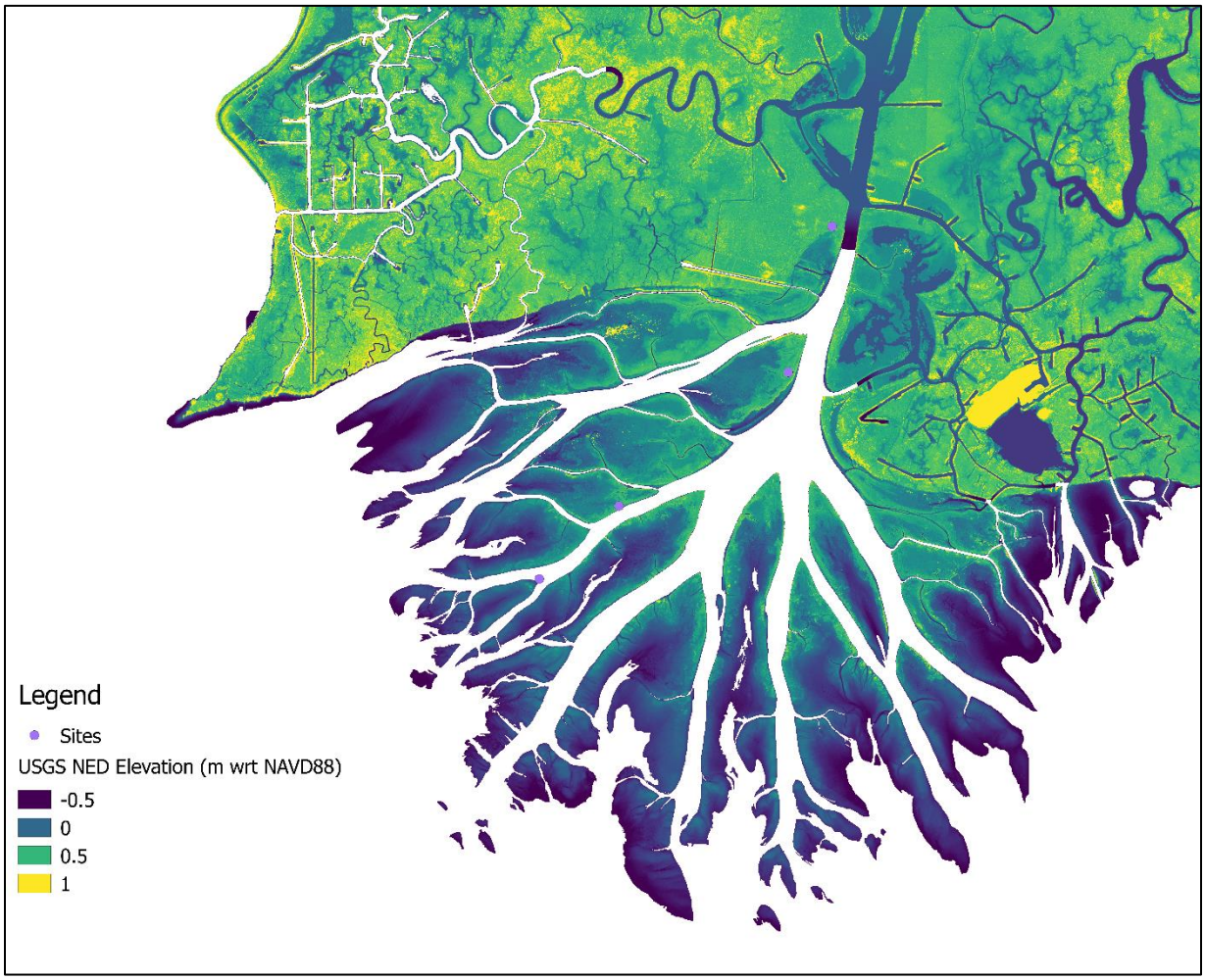

Figure A.2. Elevation map of WLD based on digital elevation model data (1-m resolution) obtained from the 2012 USGS National Elevation Dataset (https://viewer.nationalmap.gov/basic/?basemap=b1&category=ned,nedsrc&title=3DEP%20View).

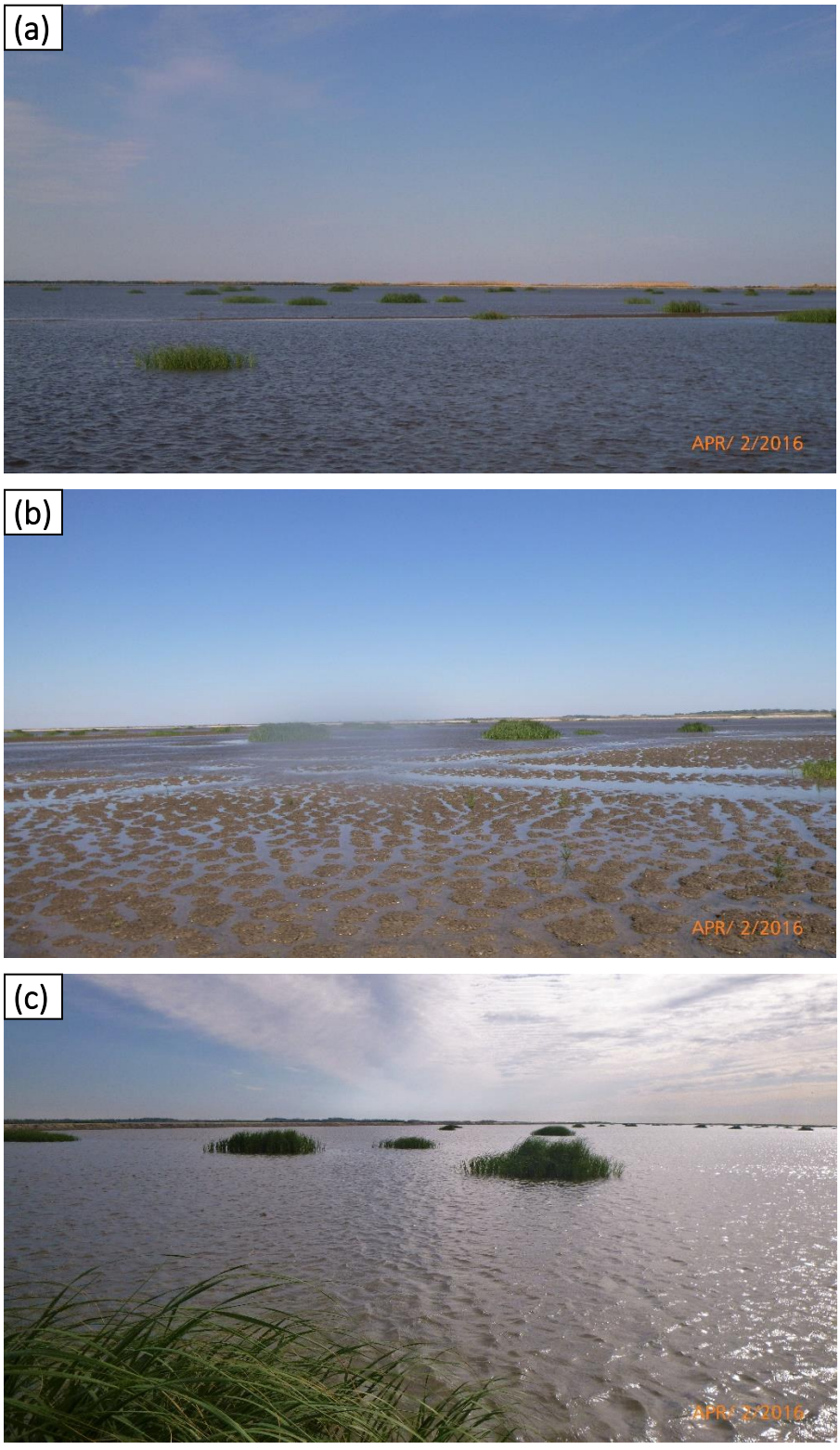

Figure A.3. Sabine 1-year-old marshes, (a)–(c).

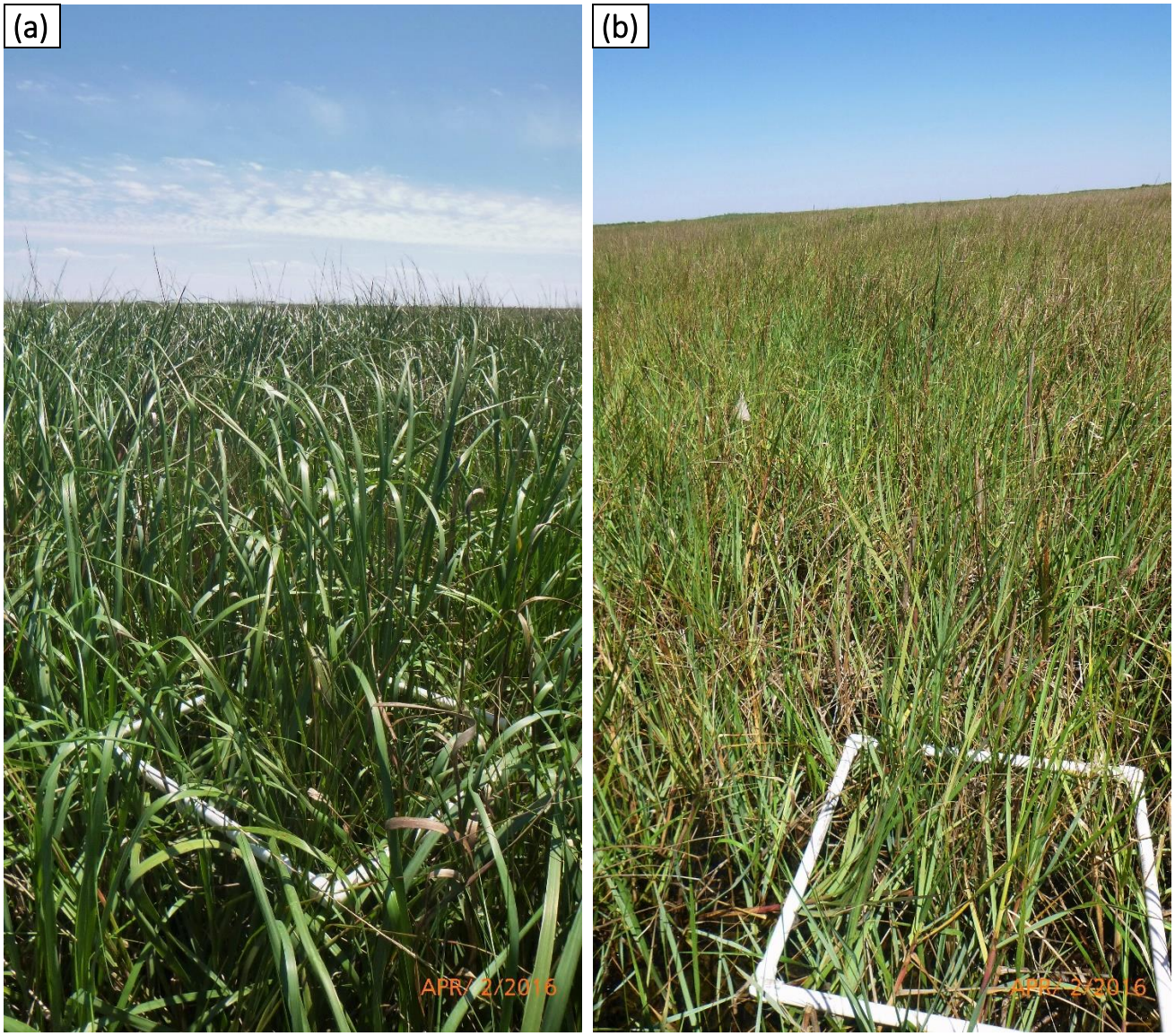

Figure A.4. Sabine 6-year-old marsh (a) and (b).

Figure A.5. Sabine 14-year-old marsh.

Figure A.6. Sabine 33-year-old marsh.

Figure A.7. Sabine natural reference marsh A (Ref. A).

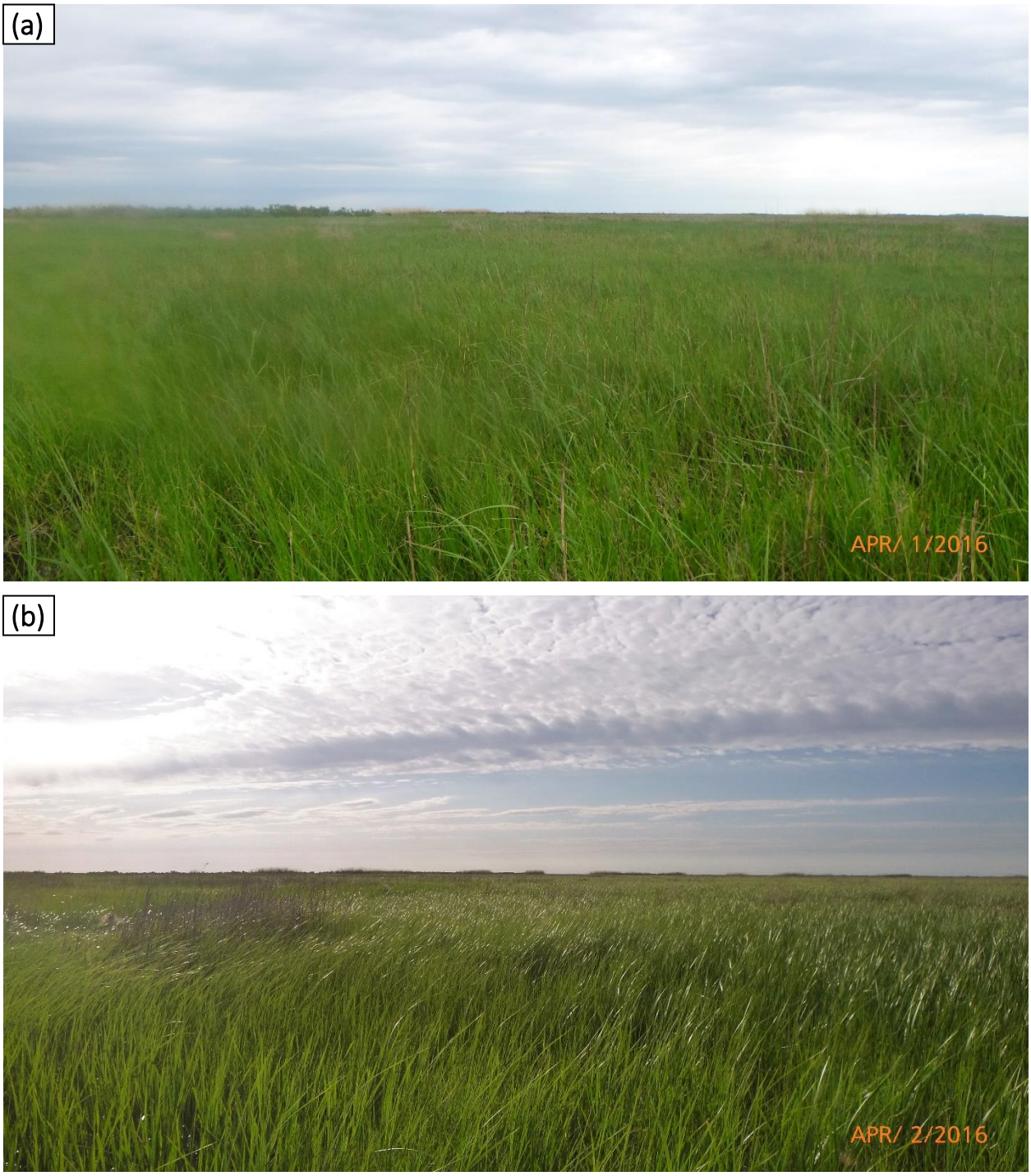

Figure A.8. Sabine natural reference marsh B (Ref. B), (a) and (b).

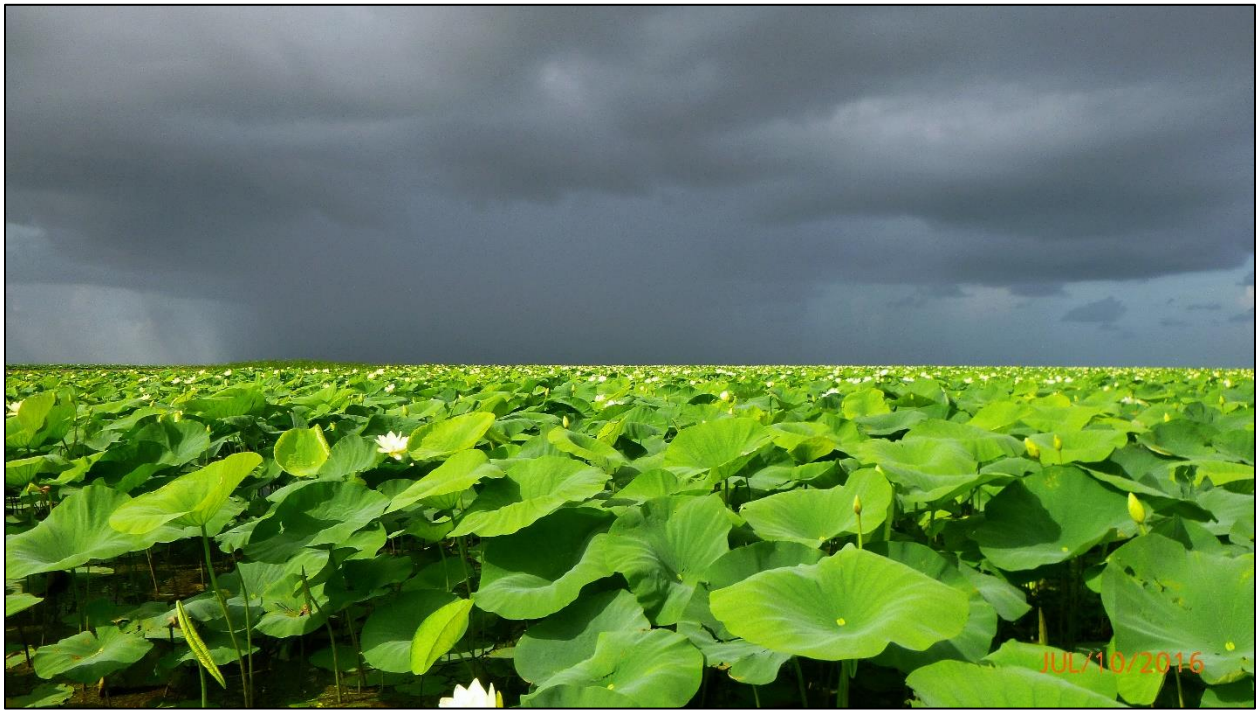

Figure A.9. WLD 16-year-old marsh.

Figure A.10. WLD 29-year-old marsh.

Figure A.11. WLD 41-year-old marsh.

Figure A.12. WLD reference marsh.

Appendix B.
MATLAB Scripts

Script 1. Monte Carlo estimation of the 95% confidence intervals of the Max-AAE protein concentration estimates of the extracts (Chapter 2).

```
%Monte Carlo estimation of CHN concentration error

%errors
%NGRS 2 ug (vector of SDs in workspace)
%NAA 0.10% SD
%Vextract 0.1 mL SD
%Mextract 0.5 mg SD
%measurements is columns %N-grs, %N-AA, M-grs (mg), Vol (mL)

load('montecarloCHN.mat');
clf;
Naa=0.1;
M=0.5;
V=0.1;

conc=zeros(175,1000);
for i=1:1000
    error=
      [normrnd(zeros(175,1),Ngrs) normrnd(0,Naa,175,1) normrnd(0,M,175,1)...
       normrnd(0,V,175,1)];
    valerror=measurements+error;
    conc(:,i)=
      ((valerror(:,1)./valerror(:,2)).*valerror(:,3)./valerror(:,4))*1000;
end;

sorted=sort(conc,2);
realconc=
((measurements(:,1)./measurements(:,2)).*measurements(:,3)./measurements(:,4))...
      *1000;

upper=sorted(:,975);
lower=sorted(:,25);

table(lower,realconc,upper)

U=fitlm(realconc,upper);  plot(U);
hold on
L=fitlm(realconc,lower);  plot(L);
plot(realconc,realconc,'k-');

upperBR=upper+BRsd;
lowerBR=lower-BRsd;

U2=fitlm(realconc,upperBR);  plot(U2);
hold on
L2=fitlm(realconc,lowerBR);  plot(L2);

%%%%END OF SCRIPT
```

Script 2. Three-line piecewise-linear fit of AAE protein contribution to TOC and TN as a function of loss on ignition in Sabine and WLD (Chapter 2).

```
function [plotdata]=piecewise3(x,y)
% Three-line Piecewise-linear Fit
%
% Output is 7x2 matrix with data for plotting the lines
% Form is:
% plotdata=[[min(x) X1];
% polyval(p,xx1);
% [X1 X2];
% [polyval(p,X1) yhat3];
% [X2 max(x)];
% [yhat3 yhat3];
% bestx1 bestx2];

clear;
 load('CNcontribution.mat');
 load('conc-mgpg.mat');

% for graph=1:4
%     if graph==1
%
% x=wldTOC;
% y=wldNmax;
% %y=wldCmax;
% x=sabTOC;
% y=sabNmax;
%y=sabCmax;

%LOI
x2mat=25:0.1:35;
x1mat=10:0.1:20;
%TOC
% x2mat=15:0.1:30;
% x1mat=3:0.1:10;

SS=1000;
for k=1:length(x2mat)
    for j=1:length(x1mat)
        X2=x2mat(k);
        X1=x1mat(j);
        I=find(x<=X1);
        J=find(x>=X2);
        x1=x(I);
        y1=y(I);
        x3=x(J);
        y3=y(J);
        K=find(x>X1 & x<X2);
        x2=x(K);
        y2=y(K);
        p=polyfit(x1,y1,1);
        yhat1=polyval(p,x1);
        yhatb1=polyval(p,X1);
```

(script cont'd)

(Script 2 cont'd)

```
        yhat3=mean(y3);
        yhat2=(yhat3-yhatb1)/(X2-X1)*(x2-X1)+yhatb1;
        ss=sum((y1-yhat1).^2)+sum((y2-yhat2).^2)+sum((y3-yhat3).^2);
        if ss<SS
            SS=ss;
            bestx1=X1;
            bestx2=X2;
        end;
    end;
end;

X2=bestx2;
X1=bestx1;
I=find(x<=X1);
J=find(x>=X2);
x1=x(I);
y1=y(I);
x3=x(J);
y3=y(J);
K=find(x>X1 & x<X2);
x2=x(K);
y2=y(K);
p=polyfit(x1,y1,1);
yhat1=polyval(p,x1);
yhatb1=polyval(p,X1);
yhat3=mean(y3);
yhat2=(yhat3-yhatb1)/(X2-X1)*(x2-X1)+yhatb1;
sse=sum((y1-yhat1).^2)+sum((y2-yhat2).^2)+sum((y3-yhat3).^2);

% hold on;
% plot(x,y,'^k');
% hold on;
xx1=[min(x) X1];
yy1=polyval(p,xx1);

% plot(xx1,yy1,'r');
% plot([X1 X2],[polyval(p,X1) yhat3],'r');
% plot([X2 max(x)],[yhat3 yhat3],'r');

disp([sse bestx1 bestx2]);

plotdata=[xx1; yy1; [X1 X2]; [polyval(p,X1) yhat3]; [X2 max(x)]
            [yhat3 yhat3]; bestx1 bestx2];

end

%%%%END OF SCRIPT
```

Script 3. Monte Carlo estimation of the 95% confidence intervals of the equivalence time estimates for the Sabine chronosequence marshes (Chapter 4).

```
% Monte Carlo estimation of 95% confidence intervals for equivalence
% time estimates for the Sabine chronosequence marshes

clear;

dataset=1; %soil fraction
n=10000; %number of iterations

if dataset==1 %TOC stocks
    sabvals=
   [3.2312  3.5115      4.7624      6.5786      9.6430      9.1837
    4.2168  2.9620      4.6544      5.1360      15.0221     10.9987
    2.9994  4.6264      5.2999      5.8098      6.9392      13.2414]*1000;
      %g/m2
    avgref=10800; %TOC
    semref=1200;  %TOC
elseif dataset==2 %ROC stocks
    sabvals=
   [1.4919  1.7267      2.5231      4.0243      7.0575      6.4246
    2.0591  1.3153      2.7845      3.5198      11.5166     7.7707
    1.4567  2.8037      3.2005      4.2594      4.6799      9.4998]*1000;
      %g/m2
    avgref=7800; %ROC
    semref=980;  %ROC
elseif dataset==3 %RN stocks
    sabvals=
   [0.0587  0.0671      0.0838      0.1051      0.2739      0.1721
    0.0860  0.0538      0.0937      0.0878      0.3249      0.2182
    0.0575  0.1011      0.1040      0.1034      0.1942      0.2696]*1000;
      %g/m2
    avgref=240; %RN
    semref=20;  %RN
end;

avgstocks=mean(sabvals); %means of observed values
stdstocks=std(sabvals);  %stds of observed values

x=[1 6 14 33]; %marsh ages for sabine (yrs)
x=[x;x;x];

rng('shuffle');
estx=zeros(n,1);

for i=1:n
      %pick 3 stocks for each marsh based on obs means and stds
      stocks=
      [normrnd([avgstocks(1) avgstocks(1) avgstocks(1)]',stdstocks(1))...
       normrnd([avgstocks(2) avgstocks(2) avgstocks(2)]',stdstocks(2))...
       normrnd([avgstocks(3) avgstocks(3) avgstocks(3)]',stdstocks(3))...
        normrnd([avgstocks(4) avgstocks(4) avgstocks(4)]',stdstocks(4))];
```

(script cont'd)

(Script 3 cont'd)

```
      p=polyfit(x,stocks,1); %fit stocks as function of age

      refval=normrnd(avgref,semref); % reference marsh estimate

      estx(i)=(refval-p(2))/p(1); %estimated equivalence time for each n

end;

sorted=sort(estx);
lower=sorted(0.025*n);
avg=mean(sorted);
upper=sorted(0.975*n);
stdev=std(sorted);

fprintf('Mean Eq. time = %1.0f years\n95%% CI: %1.0f ~ %1.0f years\nSD =...
      %1.0f years\n',[avg lower upper stdev]);

histogram(estx);

% Minusbound=lower-avg
% Plusbound=upper-avg

%%%%END OF SCRIPT
```

Appendix C.
Supplementary Figures and Tables of Chapters 2 and 3

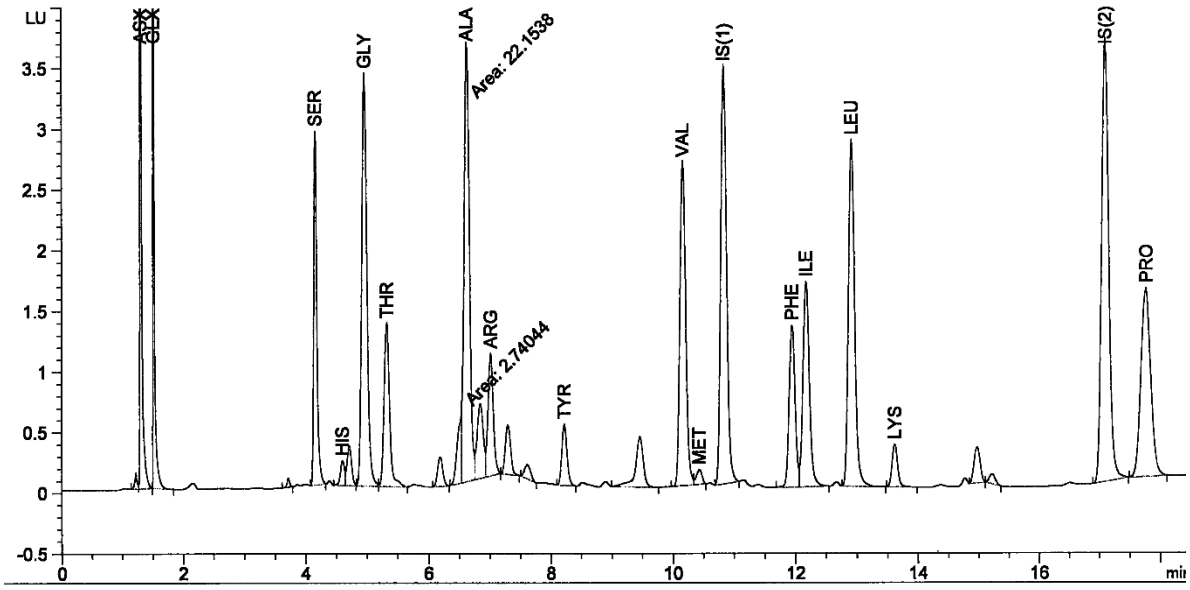

Figure C.1. Representative chromatogram from amino acid analysis. The abscissa is the elution time in minutes and the ordinate is the relative concentration in luminescence units. IS(1) and IS(2) represent the internal standards (Norvaline and Sarcosine). See Fig. 3.5 for legend of amino acid abbreviations.

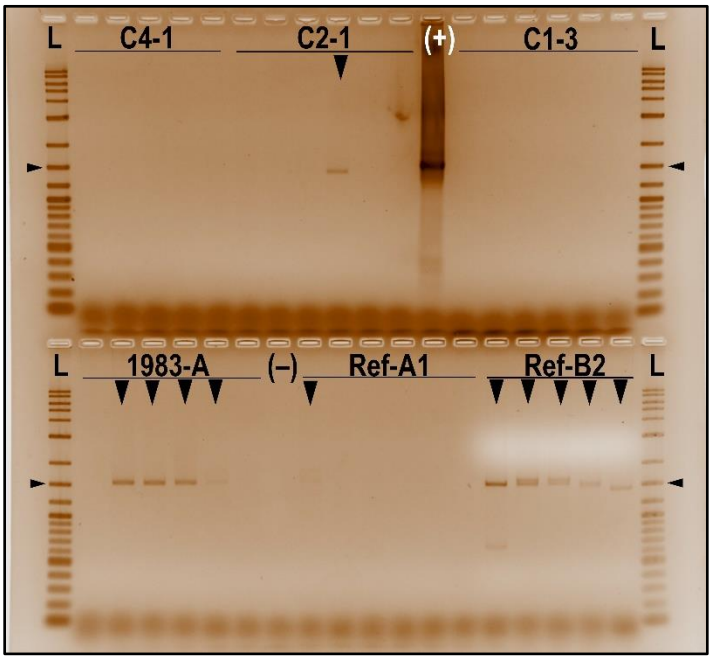

Figure C.2. Representative gel image of PCR products from SSUmCf–LSUmBr (nested) amplification of some Sabine marsh samples. Samples are ordered in increasing soil depth from left to right for each replicate core. "L" marks lanes with a 2-log DNA ladder for which an arrowhead marks the 1.5 kb band. Key: C4-1, 1-year; C2-1, 6-year; (+), positive control; C1-3, 14-year; 1983-A, 33-year; (−), no-template control; Ref-A1, Ref. A; Ref-B2, Ref. B. Downward pointing arrowheads mark samples for which a positive result was observed.

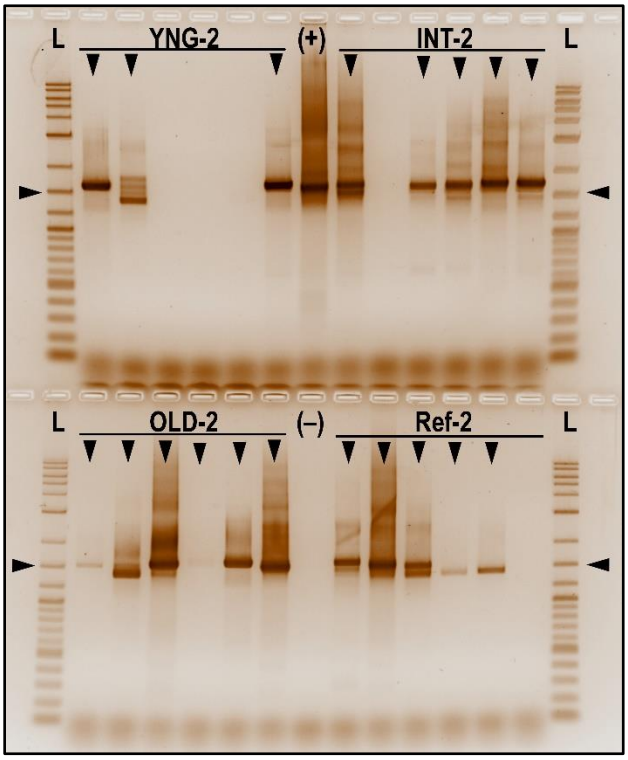

Figure C.3. Representative gel image of PCR products from SSUmCf–LSUmBr (nested) amplification of some WLD marsh samples. Samples are ordered in increasing soil depth from left to right for each replicate core. "L" marks lanes with a 2-log DNA ladder for which an arrowhead marks the 1.5 kb band. Key: YNG-2, 16-year; (+), positive control; INT-2, 29-year; OLD-2, 41-year; (−), no-template control; Ref-2, Reference. Downward pointing arrowheads mark samples for which a positive result was observed.

Table C.1. Relative mole-percent amino acid composition of hydrolyzed AAE protein extracts from the Sabine marshes.

Amino acid[†]	Marsh age (depth interval)								Reference marshes			
	1 yr (0–15 cm)	1 yr (15–25 cm)	6 yrs (0–15 cm)	6 yrs (15–30 cm)	14 yrs (0–15 cm)	14 yrs (15–30 cm)	33 yrs (0–15 cm)	33 yrs (15–30 cm)	Ref. A (0–15 cm)	Ref. A (15–30 cm)	Ref. B (0–15 cm)	Ref. B (15–30 cm)
ASX	16.7%	16.9%	16.2%	16.9%	15.3%	17.2%	15.1%	15.4%	15.6%	16.9%	15.6%	16.3%
GLX	12.6%	12.2%	12.9%	12.4%	12.3%	12.7%	12.1%	12.3%	11.9%	12.2%	11.9%	12.0%
SER	4.8%	4.9%	4.8%	5.0%	5.3%	5.0%	5.2%	5.1%	5.8%	5.6%	5.6%	5.7%
HIS	0.8%	0.7%	0.8%	0.6%	1.0%	0.6%	1.0%	1.0%	0.8%	0.5%	1.0%	0.7%
GLY	10.5%	10.0%	10.0%	10.8%	11.0%	10.6%	11.2%	10.2%	11.1%	11.2%	10.8%	10.7%
THR	3.6%	3.8%	3.7%	3.7%	3.9%	3.6%	3.9%	3.9%	4.4%	4.4%	4.2%	4.4%
ALA	10.6%	10.2%	10.8%	10.8%	12.0%	11.0%	11.8%	11.7%	11.8%	11.6%	12.2%	12.0%
ARG	2.5%	2.6%	2.5%	2.3%	2.3%	2.3%	2.2%	2.2%	2.6%	2.5%	2.4%	2.6%
TYR	1.5%	1.5%	1.5%	1.3%	1.3%	1.4%	1.2%	1.3%	1.3%	1.2%	1.2%	1.2%
VAL	7.9%	8.0%	7.8%	7.9%	7.8%	7.7%	7.8%	7.9%	7.9%	8.1%	7.7%	8.0%
MET	0.6%	0.8%	0.6%	0.6%	0.4%	0.5%	0.5%	0.3%	0.4%	0.5%	0.3%	0.4%
PHE	4.4%	4.5%	4.6%	4.3%	4.1%	4.3%	4.1%	4.2%	3.8%	3.6%	3.9%	3.7%
ILE	5.9%	6.1%	5.9%	5.9%	5.5%	5.9%	5.6%	5.7%	5.4%	5.5%	5.3%	5.5%
LEU	8.5%	8.7%	8.9%	8.6%	8.4%	8.6%	8.6%	8.6%	8.1%	7.7%	8.3%	7.9%
LYS	2.7%	2.8%	2.5%	2.7%	2.4%	2.6%	2.3%	2.5%	2.5%	2.7%	2.3%	2.6%
PRO	6.3%	6.2%	6.5%	6.1%	7.1%	6.0%	7.4%	7.7%	6.5%	5.9%	7.2%	6.4%

[†] See Fig. 3.5 for legend of amino acid abbreviations.

Table C.2. Relative mole-percent amino acid composition of hydrolyzed AAE protein extracts from the WLD marshes.

Amino acid[†]	Marsh age (depth interval)						Reference marsh	
	16 yrs (0–15 cm)	16 yrs (15–25 cm)	29 yrs (0–15 cm)	29 yrs (15–30 cm)	41 yrs (0–15 cm)	41 yrs (15–30 cm)	(0–15 cm)	(15–30 cm)
ASX	17.0%	16.9%	15.3%	15.6%	15.0%	15.9%	14.8%	15.1%
GLX	13.0%	13.2%	13.0%	12.6%	12.8%	12.8%	13.4%	12.7%
SER	5.0%	5.2%	5.3%	5.4%	5.5%	5.3%	5.4%	5.6%
HIS	0.6%	0.7%	0.8%	1.0%	1.1%	0.9%	1.1%	1.1%
GLY	10.7%	10.6%	10.2%	10.0%	10.0%	10.2%	9.4%	10.0%
THR	3.6%	3.5%	3.8%	3.9%	3.9%	3.5%	3.7%	3.9%
ALA	10.8%	10.4%	11.4%	11.0%	11.1%	11.0%	10.6%	10.9%
ARG	2.3%	2.4%	2.6%	2.4%	2.6%	2.4%	2.4%	2.4%
TYR	1.3%	1.4%	1.5%	1.6%	1.6%	1.4%	1.5%	1.5%
VAL	7.8%	7.6%	8.0%	8.0%	7.8%	8.0%	8.1%	8.2%
MET	0.6%	0.5%	0.5%	0.5%	0.5%	0.3%	0.6%	0.4%
PHE	4.1%	4.1%	4.0%	4.2%	4.1%	4.1%	4.2%	4.2%
ILE	5.7%	5.8%	5.6%	5.8%	5.7%	5.7%	6.0%	5.9%
LEU	8.5%	8.6%	8.9%	8.9%	8.9%	8.9%	9.5%	9.2%
LYS	2.5%	2.5%	2.2%	2.3%	2.4%	2.4%	2.2%	2.3%
PRO	6.4%	6.5%	7.0%	7.1%	7.0%	7.1%	7.0%	6.8%

[†] See Fig. 3.5 for legend of amino acid abbreviations.

Appendix D.
Supplementary Figures of Chapter 4

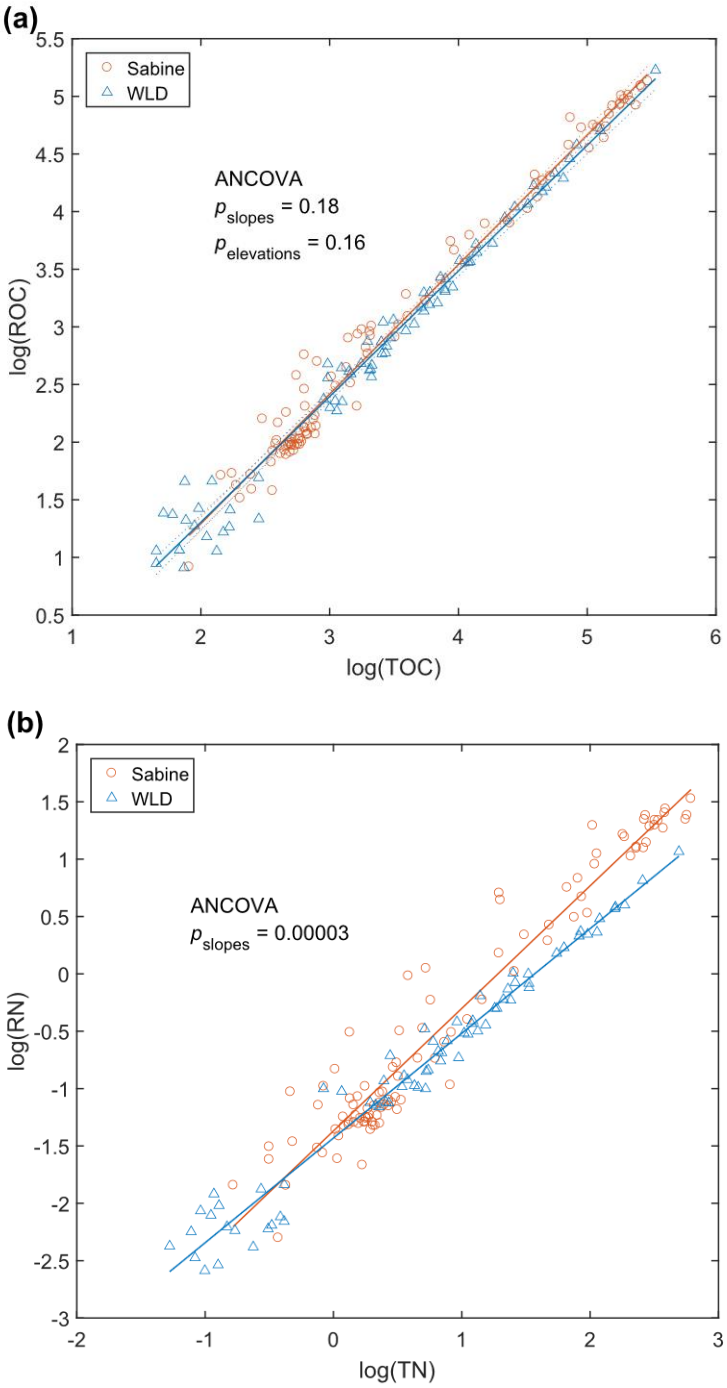

Figure D.1. Log-transformed correlation between TOC and ROC (a) and TN and RN (b), showing separate linear fits and ANCOVA results.

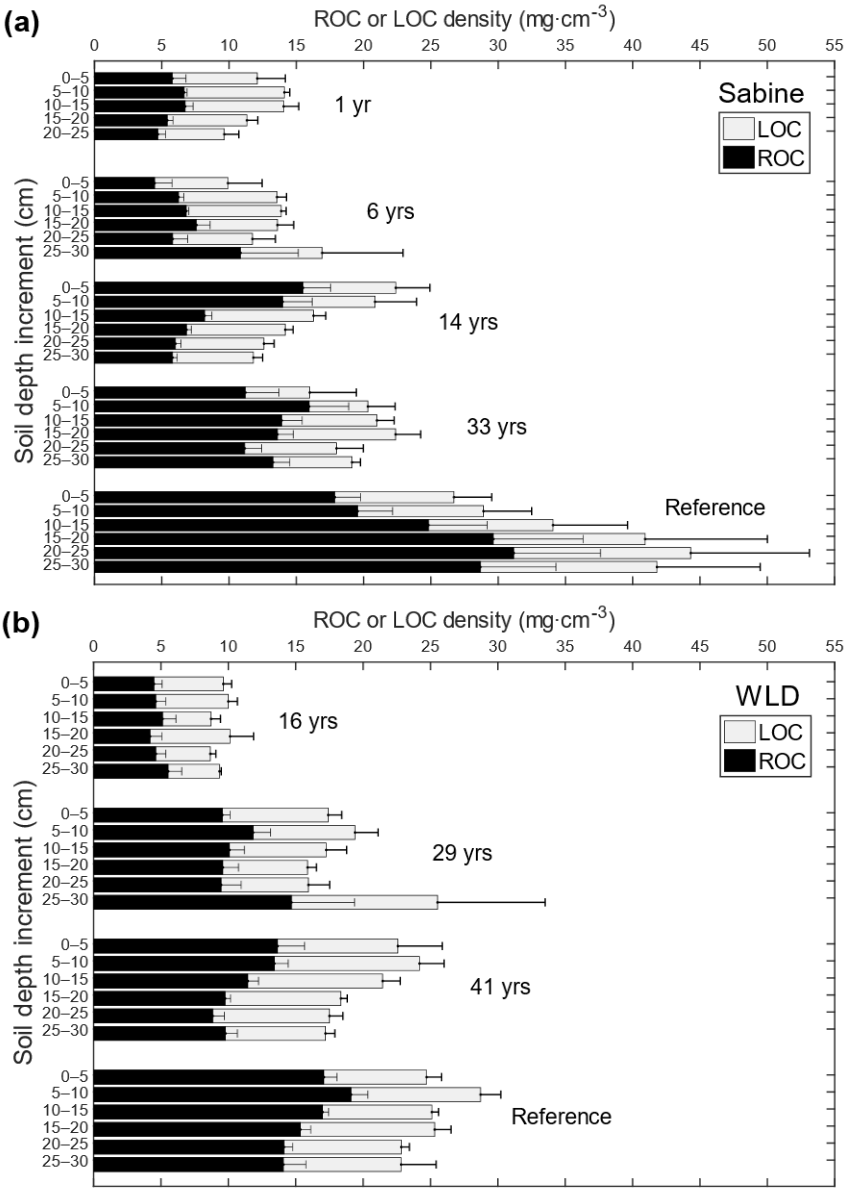

Figure D.2. Depth profiles of average LOC density (light grey) and average ROC density (black) in Sabine (a) and WLD (b). Error bars are ± standard deviation (n = 3, except for Sabine reference: n = 6).

Appendix E.
Data for Each Section of All Soil Cores

Table E.1. Bulk density and compositional data for each soil core section.

Sample vial #	Coded ID[†]	Sample ID	Moisture content (%)	Bulk density ($g \cdot cm^{-3}$)	Loss on ignition ($mg \cdot g^{-1}$)	TOC ($mg \cdot g^{-1}$)	TN ($mg \cdot g^{-1}$)	ROC ($mg \cdot g^{-1}$)	RN ($mg \cdot g^{-1}$)	AAE solids ($mg \cdot g^{-1}$)	AAE humic material[‡] ($mg \cdot g^{-1}$)
1	S01-1-00	C4-1_0-5	39	0.547	60.5	15.8	1.37	7.6	0.32	13.2	11.6
2	S01-1-05	C4-1_5-10	38	0.823	58.5	16.2	1.41	7.4	0.29	14.5	11.3
3	S01-1-10	C4-1_10-15	43	0.869	62.9	14.8	1.36	6.8	0.27	13.4	9.4
4	S01-1-15	C4-1_15-20	45	0.687	67.2	15.2	1.39	6.9	0.27	15.1	9.6
5	S01-1-20	C4-1_20-23	47	0.558	68.1	15.4	1.44	7.2	0.27	11.4	9.6
6	S06-1-00	C2-1_0-5	67	0.200	93.0	24.9	2.49	10.1	0.38	18.9	12.3
7	S06-1-05	C2-1_5-10	49	0.808	73.9	18.0	1.65	7.9	0.31	15.1	10.7
8	S06-1-10	C2-1_10-15	39	0.926	62.4	14.3	1.30	7.2	0.28	14.1	9.4
9	S06-1-15	C2-1_15-20	37	0.938	58.7	14.9	1.28	7.2	0.28	12.1	9.0
10	S06-1-20	C2-1_20-25	39	0.948	53.4	13.2	1.23	7.3	0.28	11.0	8.8
11	S06-1-25	C2-1_25-27	41	0.843	60.8	12.9	1.22	6.9	0.27	11.3	8.5
12	S14-1-00	C1-3_0-5	65	0.185	216.7	93.5	6.53	56.0	1.64	77.2	49.5
13	S14-1-05	C1-3_5-10	61	0.322	163.1	57.5	4.10	35.0	1.02	60.4	36.4
14	S14-1-10	C1-3_10-15	43	0.760	82.6	23.6	1.66	12.3	0.41	19.1	12.3
15	S14-1-15	C1-3_15-20	40	0.926	66.7	16.0	1.34	7.2	0.26	12.9	8.9
16	S14-1-20	C1-3_20-25	42	0.890	69.0	15.7	1.36	7.3	0.27	12.7	9.4
17	S14-1-25	C1-3_25-30	43	0.857	66.3	14.8	1.33	7.3	0.29	12.3	9.2

(table cont'd)

(Table E.1 cont'd)

Sample vial #	Coded ID[†]	Sample ID	Moisture content (%)	Bulk density ($g \cdot cm^{-3}$)	Loss on ignition ($mg \cdot g^{-1}$)	TOC ($mg \cdot g^{-1}$)	TN ($mg \cdot g^{-1}$)	ROC ($mg \cdot g^{-1}$)	RN ($mg \cdot g^{-1}$)	AAE solids ($mg \cdot g^{-1}$)	AAE humic material[‡] ($mg \cdot g^{-1}$)
18	S33-1-00	1983-A'_0-5	48	0.826	83.7	27.4	1.64	19.3	0.46	30.6	14.5
19	S33-1-05	1983-A'_5-10	49	0.724	101.8	33.4	2.21	18.4	0.48	38.6	19.2
20	S33-1-10	1983-A'_10-15	53	0.630	108.5	34.3	2.38	20.5	0.55	31.7	17.5
21	S33-1-15	1983-A'_15-20	59	0.551	130.0	42.3	2.84	25.2	0.67	41.0	22.2
22	S33-1-20	1983-A'_20-25	58	0.541	122.5	36.8	2.51	22.0	0.60	40.2	21.0
23	S33-1-25	1983-A'_25-30	64	0.416	157.0	47.7	3.19	30.2	0.80	51.9	26.6
24	S50-1-00	NR1-1_0-5	81	0.186	393.4	160.8	11.22	113.3	3.00	195.3	122.5
25	S50-1-05	NR1-1_5-10	84	0.156	497.2	227.3	15.73	160.2	3.99	263.2	181.0
26	S50-1-10	NR1-1_10-15	67	0.379	231.3	99.0	6.72	75.0	2.30	121.0	100.3
27	S50-1-15	NR1-1_15-20	48	0.763	121.4	52.9	3.64	39.0	2.02	55.2	57.5
28	S50-1-20	NR1-1_20-25	41	0.907	77.1	27.8	2.06	20.2	1.05	32.5	34.7
29	S50-1-25	NR1-1_25-30	41	0.945	77.3	25.8	1.79	19.6	0.98	28.1	37.5
30	S50-4-00	NR2-1_0-5	83	0.114	433.3	172.0	11.46	114.1	3.14	205.4	91.4
31	S50-4-05	NR2-1_5-10	75	0.235	223.9	80.1	5.32	50.6	1.33	115.1	47.3
32	S50-4-10	NR2-1_10-15	89	0.107	558.2	216.8	15.55	137.4	3.85	264.5	120.6
33	S50-4-15	NR2-1_15-20	87	0.115	583.1	237.2	16.21	169.7	4.61	291.9	153.1
34	S50-4-20	NR2-1_20-25	81	0.203	474.6	198.2	12.21	144.8	3.65	218.1	140.3
35	S50-4-25	NR2-1_25-30	76	0.267	420.7	204.3	13.22	149.8	4.07	259.8	173.9
36	S01-2-00	C4-2_0-5	38	1.028	51.6	15.4	1.43	7.6	0.35	13.3	10.9
37	S01-2-05	C4-2_5-10	41	0.903	55.4	16.0	1.54	7.6	0.32	15.3	11.5
38	S01-2-10	C4-2_10-15	43	0.901	58.0	18.1	1.62	8.5	0.34	17.1	10.4
39	S01-2-15	C4-2_15-20	48	0.779	64.4	16.6	1.70	8.4	0.33	16.4	11.0
40	S01-2-20	C4-2_20-25	49	0.652	66.4	16.5	1.54	8.4	0.33	15.2	10.0

(table cont'd)

(Table E.1 cont'd)

Sample vial #	Coded ID[†]	Sample ID	Moisture content (%)	Bulk density ($g \cdot cm^{-3}$)	Loss on ignition ($mg \cdot g^{-1}$)	TOC ($mg \cdot g^{-1}$)	TN ($mg \cdot g^{-1}$)	ROC ($mg \cdot g^{-1}$)	RN ($mg \cdot g^{-1}$)	AAE solids ($mg \cdot g^{-1}$)	AAE humic material[‡] ($mg \cdot g^{-1}$)
41	S06-2-00	C2-3_0-5	35	1.037	40.8	12.9	1.25	4.9	0.19	12.2	8.0
42	S06-2-05	C2-3_5-10	34	1.111	42.1	11.0	1.03	4.9	0.20	11.1	7.8
43	S06-2-10	C2-3_10-15	35	1.084	44.0	12.8	1.09	6.2	0.27	14.0	7.2
44	S06-2-15	C2-3_15-20	33	1.166	39.9	9.7	0.92	5.1	0.21	11.7	6.2
45	S06-2-20	C2-3_20-25	26	1.258	27.1	6.7	0.65	2.5	0.10	8.3	3.5
46	S14-2-00	C1-4_0-5	64	0.367	160.8	67.2	4.43	49.1	1.41	72.2	44.7
47	S14-2-05	C1-4_5-10	50	0.618	70.3	27.6	2.00	18.6	0.62	29.7	22.3
48	S14-2-10	C1-4_10-15	44	0.827	48.1	17.9	1.47	9.3	0.36	16.7	10.9
49	S14-2-15	C1-4_15-20	45	0.831	48.0	17.8	1.31	9.0	0.31	16.1	9.9
50	S14-2-20	C1-4_20-25	49	0.758	48.9	14.9	1.29	7.6	0.29	16.1	9.5
51	S14-2-25	C1-4_25-30	51	0.709	52.7	14.8	1.31	7.4	0.29	16.3	10.4
52	S33-2-00	1983-D_0-5	32	1.200	41.6	11.9	0.73	9.0	0.23	14.4	8.0
53	S33-2-05	1983-D_5-10	34	1.120	44.2	15.5	0.89	13.2	0.32	19.1	10.4
54	S33-2-10	1983-D_10-15	34	1.116	52.0	16.6	1.04	10.1	0.24	18.7	10.1
55	S33-2-15	1983-D_15-20	39	0.922	56.2	20.4	1.17	13.0	0.32	19.8	9.7
56	S33-2-20	1983-D_20-25	35	1.040	46.5	13.5	0.88	8.7	0.22	15.4	7.1
57	S33-2-25	1983-D_25-30	47	0.740	86.7	26.6	1.59	16.8	0.44	28.5	16.4
58	S50-2-00	NR1-2_0-5	75	0.244	268.7	104.9	6.92	71.4	1.96	129.1	62.6
59	S50-2-05	NR1-2_5-10	79	0.212	385.2	164.2	10.60	112.4	2.99	222.8	122.6
60	S50-2-10	NR1-2_10-15	66	0.407	275.0	130.3	7.54	123.4	3.65	181.5	133.8
61	S50-2-15	NR1-2_15-20	63	0.441	298.6	155.7	9.67	115.5	3.30	217.5	150.5
62	S50-2-20	NR1-2_20-25	69	0.375	337.4	180.8	11.27	136.8	3.84	257.0	169.9
63	S50-2-25	NR1-2_25-30	76	0.263	369.6	192.1	12.24	139.3	3.82	276.9	166.5

(table cont'd)

(Table E.1 cont'd)

Sample vial #	Coded ID[†]	Sample ID	Moisture content (%)	Bulk density ($g \cdot cm^{-3}$)	Loss on ignition ($mg \cdot g^{-1}$)	TOC ($mg \cdot g^{-1}$)	TN ($mg \cdot g^{-1}$)	ROC ($mg \cdot g^{-1}$)	RN ($mg \cdot g^{-1}$)	AAE solids ($mg \cdot g^{-1}$)	AAE humic material[‡] ($mg \cdot g^{-1}$)
64	S50-5-00	NR2-2_0-5	86	0.110	516.4	207.8	13.08	142.6	3.56	234.9	120.8
65	S50-5-05	NR2-2_5-10	77	0.210	271.9	101.0	7.24	62.0	1.70	144.0	59.3
66	S50-5-10	NR2-2_10-15	81	0.160	378.0	150.9	10.15	94.7	2.79	192.0	88.3
67	S50-5-15	NR2-2_15-20	77	0.212	367.2	142.0	9.54	113.0	3.38	183.4	116.9
68	S50-5-20	NR2-2_20-25	71	0.344	379.6	176.5	11.76	127.2	3.61	250.9	154.2
69	S50-5-25	NR2-2_25-30	73	0.316	400.3	191.8	12.57	138.0	3.81	261.1	164.6
70	S01-3-00	C5-1_0-5	44	0.699	57.7	16.9	1.49	7.9	0.32	15.8	11.7
71	S01-3-05	C5-1_5-10	43	0.871	58.9	16.7	1.46	8.1	0.31	16.0	11.6
72	S01-3-10	C5-1_10-15	46	0.817	52.7	15.9	1.43	8.1	0.32	15.4	9.8
73	S01-3-15	C5-1_15-20	52	0.608	60.0	17.5	1.57	8.3	0.33	17.2	10.3
74	S06-3-00	C2-5_0-5	49	0.542	83.9	21.1	1.93	12.0	0.48	20.9	10.8
75	S06-3-05	C2-5_5-10	38	0.958	52.6	14.6	1.13	7.2	0.27	16.5	9.4
76	S06-3-10	C2-5_10-15	35	1.059	49.4	13.7	1.02	6.7	0.26	12.8	8.3
77	S06-3-15	C2-5_15-20	36	1.077	50.1	14.4	1.14	9.6	0.34	19.0	10.5
78	S06-3-20	C2-5_20-25	36	1.066	54.3	13.3	1.08	7.5	0.29	15.2	9.0
79	S06-3-25	C2-5_25-28	42	0.917	70.9	25.0	1.68	18.8	0.61	30.4	21.7
80	S14-3-00	C1-5_0-5	58	0.423	132.7	59.6	3.63	44.5	1.20	55.9	40.2
81	S14-3-05	C1-5_5-10	44	0.740	78.7	36.4	2.13	26.6	0.80	42.2	34.7
82	S14-3-10	C1-5_10-15	39	0.945	48.3	17.0	1.17	7.9	0.27	17.4	8.8
83	S14-3-15	C1-5_15-20	41	0.919	48.4	14.1	1.13	6.9	0.27	14.5	8.9
84	S14-3-20	C1-5_20-25	43	0.873	49.8	14.3	1.19	6.6	0.29	14.6	9.3
85	S14-3-25	C1-5_25-30	46	0.820	51.7	15.0	1.27	7.2	0.27	15.8	9.9

(table cont'd)

(Table E.1 cont'd)

Sample vial #	Coded ID[†]	Sample ID	Moisture content (%)	Bulk density ($g \cdot cm^{-3}$)	Loss on ignition ($mg \cdot g^{-1}$)	TOC ($mg \cdot g^{-1}$)	TN ($mg \cdot g^{-1}$)	ROC ($mg \cdot g^{-1}$)	RN ($mg \cdot g^{-1}$)	AAE solids ($mg \cdot g^{-1}$)	AAE humic material[‡] ($mg \cdot g^{-1}$)
86	S33-3-00	1983-E_0-5	28	1.278	39.0	8.6	0.46	5.5	0.16	17.2	6.9
87	S33-3-05	1983-E_5-10	31	1.175	48.8	16.5	0.72	15.8	0.36	29.7	16.4
88	S33-3-10	1983-E_10-15	37	0.982	68.1	23.2	1.01	18.2	0.44	24.6	12.1
89	S33-3-15	1983-E_15-20	40	0.928	71.3	27.0	1.28	15.9	0.38	31.6	17.1
90	S33-3-20	1983-E_20-25	40	0.874	59.0	22.9	1.21	14.1	0.34	30.2	13.0
91	S33-3-25	1983-E_25-30	36	0.981	54.6	18.2	0.93	14.9	0.38	23.1	12.8
92	S50-3-00	NR1-3_0-5	69	0.349	227.5	111.4	7.66	74.2	2.60	153.3	103.2
93	S50-3-05	NR1-3_5-10	48	0.772	108.9	51.5	3.67	42.1	1.91	82.8	66.4
94	S50-3-10	NR1-3_10-15	29	1.237	39.3	16.5	1.14	11.7	0.60	23.4	23.5
95	S50-3-15	NR1-3_15-20	26	1.394	26.3	9.4	0.61	5.6	0.22	14.7	12.1
96	S50-3-20	NR1-3_20-25	28	1.250	26.4	10.9	0.61	5.6	0.20	14.4	11.6
97	S50-3-25	NR1-3_25-30	28	1.293	28.2	10.0	0.69	4.5	0.16	16.8	11.5
98	S50-6-00	NR2-3_0-5	81	0.138	419.6	169.4	10.61	103.5	3.02	206.2	99.2
99	S50-6-05	NR2-3_5-10	70	0.289	197.0	81.4	5.37	49.5	1.53	110.2	48.9
100	S50-6-10	NR2-3_10-15	57	0.462	202.4	100.0	6.17	69.6	2.13	123.3	94.5
101	S50-6-15	NR2-3_15-20	56	0.512	252.9	128.7	7.79	97.3	2.85	177.3	130.9
102	S50-6-20	NR2-3_20-25	72	0.300	369.3	193.5	11.39	149.5	3.98	260.3	177.9
103	S50-6-25	NR2-3_25-30	78	0.212	447.5	224.8	13.29	162.9	4.22	310.1	191.7
104	W16-1-00	YNG-1_0-5	35	1.171	36.5	9.2	0.62	3.5	0.11	11.7	5.0
105	W16-1-05	YNG-1_5-10	38	0.981	46.4	11.6	0.68	5.4	0.16	14.2	8.3
106	W16-1-10	YNG-1_10-15	33	1.103	37.7	8.8	0.60	3.4	0.11	10.9	5.5
107	W16-1-15	YNG-1_15-20	25	1.399	22.5	5.2	0.34	2.6	0.08	7.2	3.4
108	W16-1-20	YNG-1_20-25	22	1.540	22.1	5.9	0.33	3.9	0.11	8.3	3.5
109	W16-1-25	YNG-1_25-30	22	1.451	23.0	6.3	0.37	2.9	0.08	9.2	3.0

(table cont'd)

(Table E.1 cont'd)

Sample vial #	Coded ID[†]	Sample ID	Moisture content (%)	Bulk density ($g \cdot cm^{-3}$)	Loss on ignition ($mg \cdot g^{-1}$)	TOC ($mg \cdot g^{-1}$)	TN ($mg \cdot g^{-1}$)	ROC ($mg \cdot g^{-1}$)	RN ($mg \cdot g^{-1}$)	AAE solids ($mg \cdot g^{-1}$)	AAE humic material[‡] ($mg \cdot g^{-1}$)
110	W29-1-00	INT-1_0-5	60	0.499	120.3	36.3	2.65	19.4	0.48	40.2	22.7
111	W29-1-05	INT-1_5-10	62	0.488	126.1	46.4	3.28	24.7	0.64	47.4	27.4
112	W29-1-10	INT-1_10-15	54	0.639	96.0	31.0	2.31	16.0	0.47	31.5	19.1
113	W29-1-15	INT-1_15-20	55	0.597	86.4	27.8	2.05	13.0	0.37	27.0	16.2
114	W29-1-20	INT-1_20-25	53	0.610	80.6	27.3	1.88	13.8	0.38	26.0	14.2
115	W29-1-25	INT-1_25-30	54	1.487	85.3	27.9	1.93	14.4	0.37	31.2	14.5
116	W41-1-00	OLD-1_0-5	76	0.271	271.9	107.8	7.80	67.5	1.44	122.7	53.5
117	W41-1-05	OLD-1_5-10	58	0.565	141.2	49.3	3.57	27.3	0.74	50.7	25.2
118	W41-1-10	OLD-1_10-15	54	0.621	112.8	38.7	2.85	20.6	0.59	41.1	20.2
119	W41-1-15	OLD-1_15-20	47	0.736	80.2	23.7	1.78	13.4	0.40	29.1	14.4
120	W41-1-20	OLD-1_20-25	49	0.738	84.4	23.4	1.73	13.7	0.41	28.1	15.1
121	W41-1-25	OLD-1_25-30	41	0.913	65.9	19.2	1.33	10.7	0.33	22.4	11.1
122	W50-1-00	ELD-1_0-5	89	0.090	569.6	252.2	14.75	186.3	2.90	316.8	141.6
123	W50-1-05	ELD-1_5-10	80	0.193	319.0	136.9	8.96	97.5	1.77	177.7	79.0
124	W50-1-10	ELD-1_10-15	77	0.246	239.5	98.0	6.86	68.5	1.45	129.7	53.8
125	W50-1-15	ELD-1_15-20	77	0.264	246.9	104.9	7.25	64.9	1.41	125.6	50.9
126	W50-1-20	ELD-1_20-25	59	0.529	118.6	41.0	2.77	23.8	0.60	47.3	23.1
127	W50-1-25	ELD-1_25-30	68	0.376	162.2	55.1	3.89	35.7	0.88	73.3	33.9
128	W16-2-00	YNG-2_0-5	36	1.015	36.8	9.3	0.66	4.1	0.12	10.8	6.0
129	W16-2-05	YNG-2_5-10	32	1.119	32.2	8.4	0.54	2.9	0.09	10.7	4.9
130	W16-2-10	YNG-2_10-15	32	1.130	37.1	8.0	0.57	5.3	0.15	11.4	5.1
131	W16-2-15	YNG-2_15-20	33	1.150	36.0	11.6	0.68	3.8	0.12	9.6	5.4
132	W16-2-20	YNG-2_20-25	25	1.391	25.5	6.5	0.41	2.5	0.08	8.1	3.6
133	W16-2-25	YNG-2_25-30	26	1.346	27.4	7.0	0.44	3.6	0.11	7.6	3.9

(table cont'd)

(Table E.1 cont'd)

Sample vial #	Coded ID[†]	Sample ID	Moisture content (%)	Bulk density ($g \cdot cm^{-3}$)	Loss on ignition ($mg \cdot g^{-1}$)	TOC ($mg \cdot g^{-1}$)	TN ($mg \cdot g^{-1}$)	ROC ($mg \cdot g^{-1}$)	RN ($mg \cdot g^{-1}$)	AAE solids ($mg \cdot g^{-1}$)	AAE humic material[‡] ($mg \cdot g^{-1}$)
134	W29-2-00	INT-2_0-5	63	0.447	127.8	41.8	3.08	23.0	0.61	49.6	23.7
135	W29-2-05	INT-2_5-10	65	0.448	128.3	41.8	2.96	27.0	0.66	51.2	27.6
136	W29-2-10	INT-2_10-15	58	0.581	97.7	30.0	2.26	17.6	0.51	34.1	19.3
137	W29-2-15	INT-2_15-20	59	0.541	91.9	30.4	2.17	21.0	0.55	35.8	18.2
138	W29-2-20	INT-2_20-25	56	0.583	83.3	31.3	2.09	17.0	0.43	35.1	13.6
139	W29-2-25	INT-2_25-30	51	0.693	68.8	25.6	1.71	14.6	0.37	26.8	10.5
140	W41-2-00	OLD-2_0-5	84	0.158	306.4	123.3	9.67	73.0	1.82	145.6	54.5
141	W41-2-05	OLD-2_5-10	64	0.452	144.8	49.1	3.76	27.8	0.80	58.0	23.7
142	W41-2-10	OLD-2_10-15	55	0.621	103.4	32.3	2.42	18.3	0.56	40.3	17.1
143	W41-2-15	OLD-2_15-20	55	0.630	96.7	30.2	2.32	15.9	0.50	36.4	16.2
144	W41-2-20	OLD-2_20-25	48	0.751	72.5	21.2	1.54	9.7	0.32	25.3	12.0
145	W41-2-25	OLD-2_25-30	45	0.802	67.6	19.8	1.48	12.9	0.39	25.3	11.5
146	W50-2-00	ELD-2_0-5	85	0.150	395.5	164.6	11.12	110.1	2.26	189.5	81.1
147	W50-2-05	ELD-2_5-10	76	0.273	268.9	115.4	7.95	76.4	1.62	145.6	60.4
148	W50-2-10	ELD-2_10-15	73	0.305	212.8	84.5	6.03	56.8	1.26	108.3	44.9
149	W50-2-15	ELD-2_15-20	68	0.397	157.7	59.8	4.12	35.4	0.93	70.7	31.6
150	W50-2-20	ELD-2_20-25	70	0.370	175.5	62.6	4.05	41.2	1.01	77.0	35.2
151	W50-2-25	ELD-2_25-30	63	0.451	132.9	43.8	2.62	27.1	0.66	57.0	28.2
152	W16-3-00	YNG-3_0-5	29	1.321	26.5	6.6	0.39	3.8	0.12	6.6	4.0
153	W16-3-05	YNG-3_5-10	29	1.280	30.0	7.3	0.41	4.2	0.13	10.2	4.8
154	W16-3-10	YNG-3_10-15	27	1.332	25.9	5.5	0.36	4.0	0.13	7.7	4.0
155	W16-3-15	YNG-3_15-20	30	1.261	28.2	7.7	0.46	3.3	0.11	9.8	4.8
156	W16-3-20	YNG-3_20-25	23	1.503	20.6	5.2	0.28	2.9	0.09	8.1	2.8
157	W16-3-25	YNG-3_25-30	25	1.455	23.3	6.5	0.39	5.3	0.15	9.3	3.3

(table cont'd)

(Table E.1 cont'd)

Sample vial #	Coded ID[†]	Sample ID	Moisture content (%)	Bulk density ($g \cdot cm^{-3}$)	Loss on ignition ($mg \cdot g^{-1}$)	TOC ($mg \cdot g^{-1}$)	TN ($mg \cdot g^{-1}$)	ROC ($mg \cdot g^{-1}$)	RN ($mg \cdot g^{-1}$)	AAE solids ($mg \cdot g^{-1}$)	AAE humic material[‡] ($mg \cdot g^{-1}$)
158	W29-3-00	INT-3_0-5	66	0.354	133.8	43.6	2.93	24.4	0.65	48.3	25.9
159	W29-3-05	INT-3_5-10	70	0.354	144.2	47.5	3.13	30.9	0.83	63.5	30.6
160	W29-3-10	INT-3_10-15	65	0.441	115.9	33.0	2.04	21.4	0.62	41.6	21.6
161	W29-3-15	INT-3_15-20	59	0.540	100.5	27.0	1.56	17.7	0.49	33.2	18.1
162	W29-3-20	INT-3_20-25	51	0.653	67.9	19.8	1.07	14.6	0.36	29.3	10.9
163	W29-3-25	INT-3_25-30	46	0.787	58.6	22.0	0.93	14.1	0.37	22.9	9.2
164	W41-3-00	OLD-3_0-5	70	0.324	153.3	59.0	4.59	35.1	0.89	63.0	24.9
165	W41-3-05	OLD-3_5-10	66	0.432	161.0	52.2	3.98	28.4	0.80	53.9	23.6
166	W41-3-10	OLD-3_10-15	49	0.734	103.4	27.6	2.06	13.9	0.43	30.7	14.9
167	W41-3-15	OLD-3_15-20	43	0.888	76.2	21.0	1.43	10.6	0.31	24.6	10.8
168	W41-3-20	OLD-3_20-25	44	0.874	80.9	22.1	1.51	10.5	0.33	25.1	12.8
169	W41-3-25	OLD-3_25-30	43	0.905	75.0	20.1	1.39	10.0	0.32	23.3	12.2
170	W50-3-00	ELD-3_0-5	81	0.206	329.1	129.6	9.00	86.5	1.79	156.3	65.6
171	W50-3-05	ELD-3_5-10	74	0.301	235.7	93.6	6.78	58.2	1.39	109.3	47.5
172	W50-3-10	ELD-3_10-15	72	0.325	207.4	78.2	5.69	51.7	1.20	93.9	39.5
173	W50-3-15	ELD-3_15-20	67	0.390	154.1	63.0	4.58	38.3	0.92	70.2	27.2
174	W50-3-20	ELD-3_20-25	62	0.480	143.9	49.4	3.51	30.5	0.74	56.7	25.6
175	W50-3-25	ELD-3_25-30	68	0.393	180.0	71.1	4.56	41.5	1.00	75.0	34.2
		Column checksum[#]	9176	122.217	24156.6	9339.4	633.14	6165.1	169.25	11357.9	6359.1

All quantities except moisture content and bulk density are expressed on a dry-soil basis. See page vii for definitions of acronyms.

[†] The coded ID represents each soil core section in the form of *Ayy-p-xx*, where *A* is S for Sabine, *A* is W for WLD, *yy* is the marsh age in years, *p* is the plot number, and *xx* is the upper soil depth of the 5-cm section; sections from reference marshes are nominally assigned a 50-year age; Sabine reference marshes A and B are denoted as plot numbers 1–3 and 4–6, respectively.

[‡] AAE humic material is an estimate of the total AAE humic material in the soil based on absorption of the AAE extracts at 465 nm, relative to the Sigma humic acid mixture (Section 2.2.4).

[#] Exact sum of all values in column (to aid in error-checking if data are copied/transcribed).

Table E.2. AAE solids composition, AAE protein estimates, and DNA concentration and purity ratios for each soil core section.

Sample vial #	Coded ID[†]	Sample ID	AAE solids					Soil DNA extracts[¤]		
			%C	%N	BR-AAE protein ($mg \cdot g^{-1}$)	Max-AAE protein ($mg \cdot g^{-1}$)	Min-AAE protein ($mg \cdot g^{-1}$)	DNA concentration ($ng \cdot \mu L^{-1}$)	$A_{260/280}$	$A_{260/230}$
1	S01-1-00	C4-1_0-5	26.16	2.696	1.75	2.11	0.83	6	2.9	12.7
2	S01-1-05	C4-1_5-10	25.54	2.607	1.90	2.25	0.88	7	2.5	2.3
3	S01-1-10	C4-1_10-15	24.30	1.992	1.82	1.59	0.62	7	2.5	0.8
4	S01-1-15	C4-1_15-20	24.53	1.898	1.83	1.71	0.77	7	2.4	3.5
5	S01-1-20	C4-1_20-23	24.64	2.038	1.81	1.38	0.63	8	2.5	1.2
6	S06-1-00	C2-1_0-5	31.24	2.957	3.35	3.35	1.73	14	2.1	1.8
7	S06-1-05	C2-1_5-10	27.62	2.209	2.11	1.99	1.03	6	2.6	3.5
8	S06-1-10	C2-1_10-15	18.09	1.451	1.88	1.22	0.63	6	2.4	1.1
9	S06-1-15	C2-1_15-20	22.28	1.709	1.75	1.24	0.48	6	2.3	1.2
10	S06-1-20	C2-1_20-25	22.73	1.785	1.70	1.17	0.46	5	2.2	1.3
11	S06-1-25	C2-1_25-27	22.42	1.620	1.75	1.09	0.42	6	1.9	1.1
12	S14-1-00	C1-3_0-5	38.68	2.761	20.07	12.62	5.08	10	2.2	2.5
13	S14-1-05	C1-3_5-10	38.81	2.745	12.41	9.81	3.95	12	2.0	2.8
14	S14-1-10	C1-3_10-15	25.25	1.667	3.52	1.88	0.76	9	2.1	1.8
15	S14-1-15	C1-3_15-20	21.75	1.658	2.10	1.28	0.44	8	2.4	3.3
16	S14-1-20	C1-3_20-25	22.27	1.598	1.85	1.21	0.42	9	2.2	2.4
17	S14-1-25	C1-3_25-30	22.09	1.595	1.73	1.17	0.40	9	2.2	1.0
18	S33-1-00	1983-A'_0-5	28.44	1.752	5.73	3.19	1.46	13	2.1	2.6
19	S33-1-05	1983-A'_5-10	34.20	2.145	7.36	4.93	2.25	12	2.1	1.4
20	S33-1-10	1983-A'_10-15	30.97	1.916	5.96	3.62	1.65	12	2.0	2.7
21	S33-1-15	1983-A'_15-20	30.13	1.804	7.58	4.41	1.93	11	2.1	1.6
22	S33-1-20	1983-A'_20-25	29.09	1.797	7.47	4.30	1.88	11	2.2	3.0
23	S33-1-25	1983-A'_25-30	30.68	1.944	10.51	6.01	2.63	9	2.5	4.1

(table cont'd)

(Table E.2 cont'd)

Sample vial #	Coded ID[†]	Sample ID	AAE solids		BR-AAE protein ($mg \cdot g^{-1}$)	Max-AAE protein ($mg \cdot g^{-1}$)	Min-AAE protein ($mg \cdot g^{-1}$)	Soil DNA extracts[¤]		
			%C	%N				DNA concentration ($ng \cdot \mu L^{-1}$)	$A_{260/280}$	$A_{260/230}$
24	S50-1-00	NR1-1_0-5	39.05	2.628	35.84	30.18	11.31	13	2.1	2.3
25	S50-1-05	NR1-1_5-10	39.90	2.722	41.12	42.11	15.78	11	2.3	2.7
26	S50-1-10	NR1-1_10-15	36.46	2.139	19.23	15.21	5.70	9	1.9	1.8
27	S50-1-15	NR1-1_15-20	30.12	1.934	5.17	6.27	2.09	6	2.1	1.3
28	S50-1-20	NR1-1_20-25	23.00	1.395	3.31	2.67	0.89	5	2.4	1.1
29	S50-1-25	NR1-1_25-30	20.25	1.124	2.45	1.86	0.62	4	2.3	2.3
30	S50-4-00	NR2-1_0-5	34.47	2.315	46.41	28.05	11.62	12	2.0	2.2
31	S50-4-05	NR2-1_5-10	24.46	1.599	23.58	10.86	4.50	11	2.0	1.8
32	S50-4-10	NR2-1_10-15	38.07	2.758	38.73	43.04	17.84	12	2.0	2.1
33	S50-4-15	NR2-1_15-20	35.99	2.408	43.69	41.40	16.07	11	2.0	1.6
34	S50-4-20	NR2-1_20-25	36.02	2.223	35.38	28.57	11.09	12	2.1	1.7
35	S50-4-25	NR2-1_25-30	33.66	2.111	35.12	32.31	12.54	10	2.0	1.7
36	S01-2-00	C4-2_0-5	29.31	2.075	1.93	1.64	0.65	12	1.8	1.0
37	S01-2-05	C4-2_5-10	31.44	2.285	2.10	2.08	0.82	9	2.1	1.3
38	S01-2-10	C4-2_10-15	20.46	1.560	2.34	1.58	0.62	11	2.2	1.7
39	S01-2-15	C4-2_15-20	20.76	1.553	2.41	1.52	0.69	14	2.0	1.6
40	S01-2-20	C4-2_20-25	22.56	1.641	2.43	1.49	0.67	11	2.1	1.6
41	S06-2-00	C2-3_0-5	23.17	1.732	1.52	1.26	0.65	14	2.1	1.8
42	S06-2-05	C2-3_5-10	24.82	1.646	1.40	1.09	0.57	11	2.0	1.3
43	S06-2-10	C2-3_10-15	15.33	1.035	1.54	0.86	0.45	12	2.1	1.3
44	S06-2-15	C2-3_15-20	14.08	0.951	1.37	0.67	0.26	12	1.9	0.9
45	S06-2-20	C2-3_20-25	14.81	0.924	0.74	0.46	0.18	8	2.2	1.1

(table cont'd)

(Table E.2 cont'd)

Sample vial #	Coded ID[†]	Sample ID	AAE solids		BR-AAE protein ($mg \cdot g^{-1}$)	Max-AAE protein ($mg \cdot g^{-1}$)	Min-AAE protein ($mg \cdot g^{-1}$)	Soil DNA extracts[¤]		
			%C	%N				DNA concentration ($ng \cdot \mu L^{-1}$)	$A_{260/280}$	$A_{260/230}$
46	S14-2-00	C1-4_0-5	36.85	2.473	12.28	10.57	4.25	12	2.1	2.0
47	S14-2-05	C1-4_5-10	31.80	2.163	4.18	3.80	1.53	11	2.0	1.3
48	S14-2-10	C1-4_10-15	25.03	1.568	2.51	1.55	0.62	9	2.2	1.6
49	S14-2-15	C1-4_15-20	22.75	1.431	2.07	1.37	0.47	8	2.2	1.4
50	S14-2-20	C1-4_20-25	19.03	1.197	2.03	1.15	0.39	9	2.0	1.3
51	S14-2-25	C1-4_25-30	25.08	1.579	2.16	1.54	0.52	7	2.1	1.8
52	S33-2-00	1983-D_0-5	26.63	1.377	2.80	1.18	0.54	10	2.1	1.1
53	S33-2-05	1983-D_5-10	26.72	1.439	2.56	1.64	0.75	10	1.9	1.0
54	S33-2-10	1983-D_10-15	29.91	1.535	3.33	1.71	0.78	8	2.2	1.1
55	S33-2-15	1983-D_15-20	28.45	1.499	3.20	1.77	0.78	7	2.1	1.1
56	S33-2-20	1983-D_20-25	29.26	1.522	2.41	1.39	0.61	8	1.9	0.9
57	S33-2-25	1983-D_25-30	32.33	1.671	4.30	2.84	1.24	6	1.8	1.1
58	S50-2-00	NR1-2_0-5	38.26	2.465	28.09	18.70	7.01	21	2.0	1.9
59	S50-2-05	NR1-2_5-10	31.23	2.096	33.62	27.45	10.29	18	2.0	1.8
60	S50-2-10	NR1-2_10-15	33.95	2.032	19.56	21.68	8.13	13	2.0	1.2
61	S50-2-15	NR1-2_15-20	29.82	1.779	22.89	22.75	7.58	12	2.0	1.7
62	S50-2-20	NR1-2_20-25	30.41	1.852	28.24	27.98	9.32	13	2.1	1.8
63	S50-2-25	NR1-2_25-30	33.44	2.067	35.71	33.64	11.21	11	2.2	1.8
64	S50-5-00	NR2-2_0-5	35.24	2.407	44.83	33.36	13.83	23	2.0	1.9
65	S50-5-05	NR2-2_5-10	28.13	2.001	28.69	17.00	7.05	23	2.0	1.8
66	S50-5-10	NR2-2_10-15	32.10	2.228	28.54	25.24	10.46	23	2.0	1.7
67	S50-5-15	NR2-2_15-20	33.04	2.072	26.55	22.39	8.69	23	1.9	1.7
68	S50-5-20	NR2-2_20-25	30.85	1.901	33.71	28.11	10.91	16	2.0	1.6
69	S50-5-25	NR2-2_25-30	33.16	2.030	31.15	31.21	12.11	12	2.1	1.5

(table cont'd)

(Table E.2 cont'd)

Sample vial #	Coded ID[†]	Sample ID	AAE solids		BR-AAE protein ($mg \cdot g^{-1}$)	Max-AAE protein ($mg \cdot g^{-1}$)	Min-AAE protein ($mg \cdot g^{-1}$)	Soil DNA extracts[¤]		
			%C	%N				DNA concentration ($ng \cdot \mu L^{-1}$)	$A_{260/280}$	$A_{260/230}$
70	S01-3-00	C5-1_0-5	28.87	2.107	2.02	1.98	0.78	15	2.1	1.9
71	S01-3-05	C5-1_5-10	28.60	2.053	2.07	1.95	0.76	12	2.1	1.8
72	S01-3-10	C5-1_10-15	21.45	1.560	2.25	1.43	0.56	14	2.1	1.5
73	S01-3-15	C5-1_15-20	20.95	1.498	2.47	1.53	0.69	13	2.2	1.5
74	S06-3-00	C2-5_0-5	28.32	2.388	3.40	2.98	1.54	31	1.6	0.8
75	S06-3-05	C2-5_5-10	21.86	1.553	1.93	1.54	0.80	8	2.7	1.4
76	S06-3-10	C2-5_10-15	21.70	1.428	1.40	1.09	0.57	14	1.9	0.9
77	S06-3-15	C2-5_15-20	18.86	1.197	2.50	1.35	0.53	8	2.2	1.1
78	S06-3-20	C2-5_20-25	18.01	1.177	2.03	1.07	0.42	9	2.4	1.4
79	S06-3-25	C2-5_25-28	22.16	1.384	3.88	2.51	0.98	9	2.2	1.7
80	S14-3-00	C1-5_0-5	29.15	1.919	13.67	6.36	2.56	39	1.9	1.4
81	S14-3-05	C1-5_5-10	27.90	1.784	4.90	4.46	1.79	12	2.4	1.3
82	S14-3-10	C1-5_10-15	16.67	1.071	1.91	1.11	0.44	18	1.9	1.1
83	S14-3-15	C1-5_15-20	18.32	1.241	1.57	1.07	0.37	10	2.2	1.4
84	S14-3-20	C1-5_20-25	28.23	1.839	1.67	1.60	0.55	17	1.8	0.8
85	S14-3-25	C1-5_25-30	25.01	1.700	1.80	1.60	0.55	8	2.2	1.1
86	S33-3-00	1983-E_0-5	18.90	1.018	1.95	1.04	0.48	27	1.6	0.7
87	S33-3-05	1983-E_5-10	23.61	1.099	4.37	1.94	0.89	8	2.0	0.8
88	S33-3-10	1983-E_10-15	20.60	1.171	3.57	1.71	0.78	20	1.7	0.7
89	S33-3-15	1983-E_15-20	28.23	1.459	4.91	2.74	1.20	11	2.0	1.5
90	S33-3-20	1983-E_20-25	20.52	1.079	4.67	1.94	0.85	11	2.2	1.0
91	S33-3-25	1983-E_25-30	25.02	1.300	3.72	1.79	0.78	10	2.0	0.9

(table cont'd)

(Table E.2 cont'd)

Sample vial #	Coded ID[†]	Sample ID	AAE solids		BR-AAE protein ($mg \cdot g^{-1}$)	Max-AAE protein ($mg \cdot g^{-1}$)	Min-AAE protein ($mg \cdot g^{-1}$)	Soil DNA extracts[¤]		
			%C	%N				DNA concentration ($ng \cdot \mu L^{-1}$)	$A_{260/280}$	$A_{260/230}$
92	S50-3-00	NR1-3_0-5	31.07	2.100	27.22	18.93	7.09	38	1.8	1.4
93	S50-3-05	NR1-3_5-10	24.94	1.610	10.87	7.84	2.94	9	2.4	1.2
94	S50-3-10	NR1-3_10-15	22.52	1.304	1.74	1.80	0.67	30	1.6	0.6
95	S50-3-15	NR1-3_15-20	15.71	0.695	0.80	0.60	0.20	2	10.5	0.3
96	S50-3-20	NR1-3_20-25	12.22	0.536	0.72	0.45	0.15	5	2.0	0.5
97	S50-3-25	NR1-3_25-30	9.87	0.431	0.57	0.42	0.14	23	1.7	0.6
98	S50-6-00	NR2-3_0-5	32.39	2.248	42.60	27.35	11.34	43	1.9	1.1
99	S50-6-05	NR2-3_5-10	27.56	1.882	22.46	12.24	5.07	49	1.8	1.1
100	S50-6-10	NR2-3_10-15	31.82	1.955	14.96	14.22	5.89	37	1.8	0.9
101	S50-6-15	NR2-3_15-20	30.95	1.828	18.64	19.09	7.41	33	1.7	0.8
102	S50-6-20	NR2-3_20-25	33.17	1.921	33.27	29.44	11.43	26	1.8	0.8
103	S50-6-25	NR2-3_25-30	32.13	1.955	41.03	35.72	13.86	25	1.9	0.9
104	W16-1-00	YNG-1_0-5	12.35	0.832	1.61	0.58	0.27	30	1.7	0.6
105	W16-1-05	YNG-1_5-10	16.26	1.042	1.61	0.89	0.42	26	1.7	0.6
106	W16-1-10	YNG-1_10-15	15.54	0.940	1.39	0.61	0.29	27	1.7	0.6
107	W16-1-15	YNG-1_15-20	10.35	0.605	0.92	0.26	0.16	40	1.5	0.6
108	W16-1-20	YNG-1_20-25	10.27	0.536	1.13	0.27	0.16	17	1.8	0.6
109	W16-1-25	YNG-1_25-30	13.33	0.743	1.49	0.41	0.25	32	1.5	0.6
110	W29-1-00	INT-1_0-5	31.39	2.348	8.70	5.61	2.80	49	1.9	1.2
111	W29-1-05	INT-1_5-10	31.56	2.540	10.50	7.15	3.57	48	1.9	1.3
112	W29-1-10	INT-1_10-15	29.09	2.409	6.07	4.51	2.25	34	1.9	1.2
113	W29-1-15	INT-1_15-20	30.50	2.341	5.46	3.78	1.93	30	1.8	0.9
114	W29-1-20	INT-1_20-25	27.84	2.030	5.66	3.16	1.62	27	1.7	0.8
115	W29-1-25	INT-1_25-30	27.86	2.042	6.34	3.80	1.94	25	1.7	0.8

(table cont'd)

(Table E.2 cont'd)

Sample vial #	Coded ID[†]	Sample ID	AAE solids		BR-AAE protein ($mg \cdot g^{-1}$)	Max-AAE protein ($mg \cdot g^{-1}$)	Min-AAE protein ($mg \cdot g^{-1}$)	Soil DNA extracts[¤]		
			%C	%N				DNA concentration ($ng \cdot \mu L^{-1}$)	$A_{260/280}$	$A_{260/230}$
116	W41-1-00	OLD-1_0-5	36.55	3.173	25.17	23.14	11.59	64	1.9	1.7
117	W41-1-05	OLD-1_5-10	28.24	2.635	11.11	7.95	3.98	44	1.7	1.1
118	W41-1-10	OLD-1_10-15	26.86	2.249	7.35	5.49	2.75	30	1.8	1.2
119	W41-1-15	OLD-1_15-20	24.55	1.887	5.40	3.26	1.57	28	1.7	0.8
120	W41-1-20	OLD-1_20-25	23.79	1.801	5.50	3.01	1.45	24	1.7	0.9
121	W41-1-25	OLD-1_25-30	22.07	1.561	4.40	2.08	1.00	25	1.6	0.7
122	W50-1-00	ELD-1_0-5	30.14	2.005	48.68	38.14	18.17	39	1.9	1.5
123	W50-1-05	ELD-1_5-10	29.37	2.165	29.25	23.11	11.01	53	1.8	1.2
124	W50-1-10	ELD-1_10-15	30.70	2.365	22.83	18.42	8.77	41	1.7	1.0
125	W50-1-15	ELD-1_15-20	30.42	2.492	21.66	18.72	9.44	37	1.8	1.0
126	W50-1-20	ELD-1_20-25	26.01	2.016	8.60	5.70	2.87	27	1.7	0.7
127	W50-1-25	ELD-1_25-30	28.43	2.057	12.40	9.01	4.55	28	1.7	0.8
128	W16-2-00	YNG-2_0-5	14.28	0.913	1.82	0.59	0.28	22	1.6	0.7
129	W16-2-05	YNG-2_5-10	12.44	0.760	1.72	0.49	0.23	30	1.6	0.7
130	W16-2-10	YNG-2_10-15	11.75	0.709	1.69	0.48	0.23	27	1.6	0.6
131	W16-2-15	YNG-2_15-20	13.88	0.873	1.62	0.50	0.30	26	1.6	0.6
132	W16-2-20	YNG-2_20-25	9.97	0.600	1.25	0.29	0.18	21	1.6	0.6
133	W16-2-25	YNG-2_25-30	13.21	0.731	1.44	0.33	0.20	17	1.7	0.6
134	W29-2-00	INT-2_0-5	24.71	2.087	10.48	6.15	3.07	46	1.8	1.3
135	W29-2-05	INT-2_5-10	30.46	2.282	9.20	6.95	3.47	44	1.8	1.2
136	W29-2-10	INT-2_10-15	27.49	2.235	6.69	4.52	2.26	40	1.7	0.9
137	W29-2-15	INT-2_15-20	27.40	2.174	6.59	4.66	2.38	28	1.9	1.0
138	W29-2-20	INT-2_20-25	22.22	1.697	7.73	3.56	1.82	26	1.8	1.0
139	W29-2-25	INT-2_25-30	24.29	1.863	5.77	2.98	1.52	19	1.8	0.8

(table cont'd)

(Table E.2 cont'd)

Sample vial #	Coded ID[†]	Sample ID	AAE solids		BR-AAE protein ($mg \cdot g^{-1}$)	Max-AAE protein ($mg \cdot g^{-1}$)	Min-AAE protein ($mg \cdot g^{-1}$)	Soil DNA extracts[¤]		
			%C	%N				DNA concentration ($ng \cdot \mu L^{-1}$)	$A_{260/280}$	$A_{260/230}$
140	W41-2-00	OLD-2_0-5	30.33	2.828	27.19	24.49	12.27	50	1.9	1.8
141	W41-2-05	OLD-2_5-10	24.91	2.228	13.17	7.68	3.85	46	1.8	1.3
142	W41-2-10	OLD-2_10-15	24.95	1.966	7.77	4.71	2.36	29	1.8	1.0
143	W41-2-15	OLD-2_15-20	23.61	2.490	7.19	5.39	2.60	25	1.8	0.9
144	W41-2-20	OLD-2_20-25	21.34	1.678	5.14	2.53	1.22	26	1.7	0.8
145	W41-2-25	OLD-2_25-30	21.69	1.621	5.23	2.44	1.18	24	1.6	0.8
146	W50-2-00	ELD-2_0-5	33.23	2.570	32.91	29.24	13.93	45	1.8	1.3
147	W50-2-05	ELD-2_5-10	31.25	2.427	25.21	21.21	10.11	59	1.7	1.0
148	W50-2-10	ELD-2_10-15	32.66	2.484	18.27	16.16	7.70	39	1.7	0.9
149	W50-2-15	ELD-2_15-20	28.31	2.332	12.80	9.87	4.98	38	1.6	0.8
150	W50-2-20	ELD-2_20-25	29.88	2.280	13.73	10.50	5.29	29	1.7	0.8
151	W50-2-25	ELD-2_25-30	26.10	1.866	10.75	6.36	3.21	14	1.9	0.9
152	W16-3-00	YNG-3_0-5	13.40	0.742	1.20	0.29	0.14	17	1.6	0.6
153	W16-3-05	YNG-3_5-10	10.81	0.595	1.38	0.36	0.17	31	1.5	0.6
154	W16-3-10	YNG-3_10-15	13.00	0.751	1.25	0.34	0.16	45	1.5	0.6
155	W16-3-15	YNG-3_15-20	11.14	0.706	1.50	0.41	0.25	19	1.6	0.6
156	W16-3-20	YNG-3_20-25	8.27	0.392	1.03	0.19	0.11	18	1.6	0.6
157	W16-3-25	YNG-3_25-30	9.00	0.493	1.45	0.27	0.17	29	1.5	0.6
158	W29-3-00	INT-3_0-5	29.77	2.415	9.37	6.93	3.46	55	1.8	1.4
159	W29-3-05	INT-3_5-10	25.79	2.133	12.54	8.04	4.01	61	1.7	1.1
160	W29-3-10	INT-3_10-15	27.33	2.247	9.30	5.55	2.77	33	1.8	1.2
161	W29-3-15	INT-3_15-20	25.08	2.094	6.67	4.16	2.13	33	1.6	0.8
162	W29-3-20	INT-3_20-25	18.42	1.459	5.65	2.56	1.31	22	1.7	0.7
163	W29-3-25	INT-3_25-30	18.14	1.311	5.04	1.79	0.92	31	1.6	0.7

(table cont'd)

(Table E.2 cont'd)

Sample vial #	Coded ID[†]	Sample ID	AAE solids		BR-AAE protein ($mg \cdot g^{-1}$)	Max-AAE protein ($mg \cdot g^{-1}$)	Min-AAE protein ($mg \cdot g^{-1}$)	Soil DNA extracts[¤]		
			%C	%N				DNA concentration ($ng \cdot \mu L^{-1}$)	$A_{260/280}$	$A_{260/230}$
164	W41-3-00	OLD-3_0-5	26.28	2.281	13.02	8.54	4.28	59	1.8	1.3
165	W41-3-05	OLD-3_5-10	21.78	2.059	10.79	6.60	3.30	62	1.8	1.3
166	W41-3-10	OLD-3_10-15	25.25	1.958	6.74	3.57	1.79	25	1.8	1.0
167	W41-3-15	OLD-3_15-20	16.49	1.333	5.14	1.95	0.94	10	2.2	1.9
168	W41-3-20	OLD-3_20-25	21.17	1.589	5.37	2.37	1.14	21	1.8	0.8
169	W41-3-25	OLD-3_25-30	20.67	1.513	4.93	2.10	1.01	8	2.3	1.1
170	W50-3-00	ELD-3_0-5	32.10	2.535	28.95	23.79	11.34	58	1.9	2.0
171	W50-3-05	ELD-3_5-10	30.98	2.556	23.07	16.77	7.99	39	2.0	2.0
172	W50-3-10	ELD-3_10-15	33.05	2.655	17.06	14.97	7.13	24	2.0	1.9
173	W50-3-15	ELD-3_15-20	24.76	2.018	13.69	8.48	4.28	14	2.2	1.6
174	W50-3-20	ELD-3_20-25	27.42	1.984	10.85	6.73	3.40	7	2.4	1.1
175	W50-3-25	ELD-3_25-30	29.22	2.139	14.42	9.60	4.84	9	2.5	1.4
		Column checksum[#]	4444.01	311.442	1847.70	1419.12	605.56	3715	350.8	240.5

Protein quantities are expressed on a dry-soil basis. See page vii for definitions of acronyms.

[†] The coded ID represents each soil core section in the form of *Ayy-p-xx*, where *A* is S for Sabine, *A* is W for WLD, *yy* is the marsh age in years, *p* is the plot number, and *xx* is the upper soil depth of the 5-cm section; sections from reference marshes are nominally assigned a 50-year age; Sabine reference marshes A and B are denoted as plot numbers 1–3 and 4–6, respectively.

[¤] The DNA fraction was eluted in a total of 100 µL of 10 mM tris; $A_{260/280}$ and $A_{260/230}$ are the ratios of absorbance of the DNA solution at 260 and 280 nm, and at 260 and 230 nm, respectively (Section 3.2.4).

[#] Exact sum of all values in column (to aid in error-checking if data are copied/transcribed).

References

Abbott, K.M. (2017). Blue Carbon Accumulation and Microbial Community Composition in a Chronosequence of Created Coastal Marshes in the Chenier Plain, Louisiana. *Louisiana State University*, Thesis. 4509.

Abbott, K.M., T. Elsey-Quirk, R.D. DeLaune (2019). Factors influencing blue carbon accumulation across a 32-year chronosequence of created coastal marshes. *Ecosphere* 10(8), e02828.

Abbott, L.K., A.D. Robson (1991). Factors influencing the occurrence of vesicular-arbuscular mycorrhizas. *Agriculture, Ecosystems & Environment* 35(2), 121-150.

Adame, M.F., S.F. Wright, A. Grinham, K. Lobb, C.E. Reymond, C.E. Lovelock (2012). Terrestrial-marine connectivity: Patterns of terrestrial soil carbon deposition in coastal sediments determined by analysis of glomalin related soil protein. *Limnology and Oceanography* 57(5), 1492-1502.

Ahn, M.-Y., A.R. Zimmerman, N.B. Comerford, J.O. Sickman, S. Grunwald (2009). Carbon mineralization and labile organic carbon pools in the sandy soils of a North Florida watershed. *Ecosystems* 12(4), 672-685.

Allen, E.B., G.L. Cunningham (1983). Effects of vesicular–arbuscular mycorrhizae on Distichlis spicata under three salinity levels. *New Phytologist* 93(2), 227-236.

Allen, Y., B. Couvillion, J. Barras (2012). Using Multitemporal Remote Sensing Imagery and Inundation Measures to Improve Land Change Estimates in Coastal Wetlands. *Estuaries and Coasts* 35(1), 190-200.

Allison, M.A., C.R. Demas, B.A. Ebersole, B.A. Kleiss, C.D. Little, E.A. Meselhe, N.J. Powell, T.C. Pratt, B.M. Vosburg (2012). A water and sediment budget for the lower Mississippi–Atchafalaya River in flood years 2008–2010: Implications for sediment discharge to the oceans and coastal restoration in Louisiana. *Journal of Hydrology* 432, 84-97.

Anderson, R., A. Liberta, L. Dickman (1984). Interaction of vascular plants and vesicular-arbuscular mycorrhizal fungi across a soil moisture-nutrient gradient. *Oecologia* 64(1), 111-117.

Aoyama, M. (2006). Properties of neutral phosphate buffer extractable organic matter in soils revealed using size exclusion chromatography and fractionation with polyvinylpyrrolidone. *Soil Science and Plant Nutrition* 52(3), 378-386.

Atkins, P., J. de Paula (2006). *Physical Chemistry*, 8th ed. Freeman.

Balachandran, S., S. Mishra (2012). Assessment of arbuscular mycorrhizal fungi (AM Fungi) and glomalin in the rhizosphere of heavy metal polluted mangrove forest. *Int. J. Environmental Sciences* 1(4), 392-401.

Barbier, E.B., S.D. Hacker, C. Kennedy, E.W. Koch, A.C. Stier, B.R. Silliman (2011). The value of estuarine and coastal ecosystem services. *Ecological Monographs* 81(2), 169-193.

Barras, J.A., S. Beville, D. Britsch, S. Hartley, S. Hawes, J. Johnston, P. Kemp, Q. Kinler, A. Martucci, J. Porthouse (2003). *Historical and projected coastal Louisiana land changes: 1978-2050*. United States Geological Survey.

Barthès, B., E. Roose (2002). Aggregate stability as an indicator of soil susceptibility to runoff and erosion; validation at several levels. *CATENA* 47(2), 133-149.

Bastida, F., J.L. Moreno, C. Nicolás, T. Hernández, C. García (2009). Soil metaproteomics: a review of an emerging environmental science. Significance, methodology and perspectives. *European Journal of Soil Science* 60(6), 845-859.

Beck-Nielsen, D., T. Vindbæk Madsen (2001). Occurrence of vesicular–arbuscular mycorrhiza in aquatic macrophytes from lakes and streams. *Aquatic Botany* 71(2), 141-148.

Bedini, S., E. Pellegrino, L. Avio, S. Pellegrini, P. Bazzoffi, E. Argese, M. Giovannetti (2009). Changes in soil aggregation and glomalin-related soil protein content as affected by the arbuscular mycorrhizal fungal species Glomus mosseae and Glomus intraradices. *Soil Biology and Biochemistry* 41(7), 1491-1496.

Bedini, S., A. Turrini, C. Rigo, E. Argese, M. Giovannetti (2010). Molecular characterization and glomalin production of arbuscular mycorrhizal fungi colonizing a heavy metal polluted ash disposal island, downtown Venice. *Soil Biology and Biochemistry* 42(5), 758-765.

Benndorf, D., G.U. Balcke, H. Harms, M. von Bergen (2007). Functional metaproteome analysis of protein extracts from contaminated soil and groundwater. *ISME J* 1(3), 224-234.

Bi, W., J.J. Wang, S.K. Dodla, L.A. Gaston, R.D. DeLaune (2019). Lignin chemistry of wetland soil profiles in two contrasting basins of the Louisiana Gulf coast. *Organic Geochemistry* 137, 103902.

Bianchi, T.S., S.F. DiMarco, J.H. Cowan, R.D. Hetland, P. Chapman, J.W. Day, M.A. Allison (2010). The science of hypoxia in the Northern Gulf of Mexico: A review. *Science of The Total Environment* 408(7), 1471-1484.

Bird, S.B., J.E. Herrick, M.M. Wander, S.F. Wright (2002). Spatial heterogeneity of aggregate stability and soil carbon in semi-arid rangeland. *Environmental Pollution* 116(3), 445-455.

Bohrer, K., C. Friese, J. Amon (2004). Seasonal dynamics of arbuscular mycorrhizal fungi in differing wetland habitats. *Mycorrhiza* 14(5), 329-337.

Bolliger, A., A. Nalla, J. Magid, A. de Neergaard, A. Dole Nalla, T.C. Bøg-Hansen (2008). Re-examining the glomalin-purity of glomalin-related soil protein fractions through immunochemical, lectin-affinity and soil labelling experiments. *Soil Biology and Biochemistry* 40(4), 887-893.

Bradford, M.M. (1976). A rapid and sensitive method for the quantitation of microgram quantities of protein utilizing the principle of protein-dye binding. *Analytical Biochemistry* 72(1), 248-254.

Brown, A., C. Bledsoe (1996). Spatial and Temporal Dynamics of Mycorrhizas in Jaumea Carnosa, A Tidal Saltmarsh Halophyte. *Journal of Ecology* 84(5), 703-715.

Brundrett, M. (2004). Diversity and classification of mycorrhizal associations. *Biological Reviews* 79(3), 473-495.

Brundrett, M.C., Y. Piché, R.L. Peterson (1984). A new method for observing the morphology of vesicular–arbuscular mycorrhizae. *Canadian Journal of Botany* 62(10), 2128-2134.

Bryant, J.C., R.H. Chabreck (1998). Effects of impoundment on vertical accretion of coastal marsh. *Estuaries* 21(3), 416-422.

Buchsbaum, R., I. Valiela, T. Swain, M. Dzierzeski, S. Allen (1991). Available and refractory nitrogen in detritus of coastal vascular plants and macroalgae. *Marine Ecology Progress Series* 72(1/2), 131-143.

Burcham, A., J. Merino, T.C. Michot, J.A. Nyman (2012). Arbuscular Mycorrhizae Occur in Common Spartina Species. *Gulf of Mexico Science* 1(2), 14-19.

Burdon, J. (2001). Are the traditional concepts of the structures of humic substances realistic? *Soil Science* 166(11), 752-769.

Burns, R.G., A.H. Pukite, A.D. McLaren (1972). Concerning the Location and Persistence of Soil Urease. *Soil Science Society of America Journal* 36(2), 308-311.

Cao, L., J. Song, Q. Wang, X. Li, H. Yuan, N. Li, L. Duan (2017). Characterization of Labile Organic Carbon in Different Coastal Wetland Soils of Laizhou Bay, Bohai Sea. *Wetlands* 37(1), 163-175.

Carle, M.V., C.E. Sasser, H.H. Roberts (2015). Accretion and Vegetation Community Change in the Wax Lake Delta Following the Historic 2011 Mississippi River Flood. *Journal of Coastal Research* 31(3), 569-587.

Carvalho, L., I. Caçador, M. Martins-Loução (2001). Temporal and spatial variation of arbuscular mycorrhizas in salt marsh plants of the Tagus estuary (Portugal). *Mycorrhiza* 11(6), 303-309.

Ceccanti, B., P. Nannipieri, S. Cervelli, P. Sequi (1978). Fractionation of humus-urease complexes. *Soil Biology and Biochemistry* 10(1), 39-45.

Chen, S., M.C. Rillig, W. Wang (2009). Improving soil protein extraction for metaproteome analysis and glomalin-related soil protein detection. *PROTEOMICS* 9(21), 4970-4973.

Cheng, L., F.L. Booker, C. Tu, K.O. Burkey, L. Zhou, H.D. Shew, T.W. Rufty, S. Hu (2012). Arbuscular mycorrhizal fungi increase organic carbon decomposition under elevated CO2. *Science* 337(6098), 1084-1087.

Chmura, G.L., S.C. Anisfeld, D.R. Cahoon, J.C. Lynch (2003). Global carbon sequestration in tidal, saline wetland soils. *Global Biogeochemical Cycles* 17(4), 1111.

Christensen, B.T., S. Bech-Andersen (1989). Influence of straw disposal on distribution of amino acids in soil particle size fractions. *Soil Biology and Biochemistry* 21(1), 35-40.

Cooke, J.C., R.H. Butler, G. Madole (1993). Some Observations on the Vertical Distribution of Vesicular Arbuscular Mycorrhizae in Roots of Salt Marsh Grasses Growing in Saturated Soils. *Mycologia* 85(4), 547-550.

Cornwell, W.K., B.L. Bedford, C.T. Chapin (2001). Occurrence of arbuscular mycorrhizal fungi in a phosphorus-poor wetland and mycorrhizal response to phosphorus fertilization. *American Journal of Botany* 88(10), 1824-1829.

Couvillion, B.R., H. Beck, D. Schoolmaster, M. Fischer (2017). Land area change in coastal Louisiana (1932 to 2016), *Scientific Investigations Map*. U. S. Geological Survey, Reston, VA. 3381.

CPRA (2017). Louisiana's Comprehensive Master Plan for a Sustainable Coast. Coastal Protection and Restoration Authority of Louisiana, Baton Rouge, LA, p. 171.

Craft, C. (2007). Freshwater input structures soil properties, vertical accretion, and nutrient accumulation of Georgia and U.S tidal marshes. *Limnology and Oceanography* 52(3), 1220-1230.

Craft, C., P. Megonigal, S. Broome, J. Stevenson, R. Freese, J. Cornell, L. Zheng, J. Sacco (2003). The pace of ecosystem development of constructed Spartina alterniflora marshes. *Ecological Applications* 13(5), 1417-1432.

Criquet, S., A. Farnet, E. Ferre (2002). Protein measurement in forest litter. *Biology and Fertility of Soils* 35(5), 307-313.

Dai, J., J. Hu, A. Zhu, J. Bai, J. Wang, X. Lin (2015). No tillage enhances arbuscular mycorrhizal fungal population, glomalin-related soil protein content, and organic carbon accumulation in soil macroaggregates. *Journal of Soils and Sediments* 15(5), 1055-1062.

Davidson, E.A., I.A. Janssens (2006). Temperature sensitivity of soil carbon decomposition and feedbacks to climate change. *Nature* 440(7081), 165-173.

de la Cruz, A.A., W.E. Poe (1975a). Amino acid content of marsh plants. *Estuarine and Coastal Marine Science* 3(2), 243-246.

de la Cruz, A.A., W.E. Poe (1975b). Amino acids in salt marsh detritus. *Limnology and Oceanography* 20(1), 124-127.

DeLaune, R., C. Reddy, W. Patrick (1981). Accumulation of plant nutrients and heavy metals through sedimentation processes and accretion in a Louisiana salt marsh. *Estuaries* 4(4), 328-334.

DeLaune, R., J. White (2012). Will coastal wetlands continue to sequester carbon in response to an increase in global sea level?: a case study of the rapidly subsiding Mississippi river deltaic plain. *Climatic Change* 110(1-2), 297-314.

DeLaune, R.D., R.H. Baumann, J.G. Gosselink (1983). Relationships among vertical accretion, coastal submergence, and erosion in a Louisiana Gulf Coast marsh. *Journal of Sedimentary Research* 53(1), 147-157.

DeLaune, R.D., S.R. Pezeshki, J.H. Pardue, J.H. Whitcomb, J. W. H. Patrick (1990). Some Influences of Sediment Addition to a Deteriorating Salt Marsh in the Mississippi River Deltaic Plain: A Pilot Study. *Journal of Coastal Research* 6(1), 181-188.

DeLaune, R.D., C.E. Sasser, E. Evers-Hebert, J.R. White, H.H. Roberts (2016). Influence of the Wax Lake Delta sediment diversion on aboveground plant productivity and carbon storage in deltaic island and mainland coastal marshes. *Estuarine, Coastal and Shelf Science* 177, 83-89.

Derenne, S., C. Largeau, F. Taulelle (1993). Occurrence of non-hydrolysable amides in the macromolecular constituent of Scenedesmus quadricauda cell wall as revealed by 15N NMR: Origin of n-alkylnitriles in pyrolysates of ultralaminae-containing kerogens. *Geochimica et Cosmochimica Acta* 57(4), 851-857.

Dinter, T., S. Geihser, M. Gube, R. Daniel, Y. Kuzyakov (2019). Impact of sea level change on coastal soil organic matter, priming effects and prokaryotic community assembly. *FEMS Microbiology Ecology* 95(10), fiz129.

Dodla, S.K., J.J. Wang, R.D. DeLaune (2012). Characterization of labile organic carbon in coastal wetland soils of the Mississippi River deltaic plain: Relationships to carbon functionalities. *Science of The Total Environment* 435-436, 151-158.

Duarte, C.M., I.J. Losada, I.E. Hendriks, I. Mazarrasa, N. Marba (2013). The role of coastal plant communities for climate change mitigation and adaptation. *Nature Climate Change* 3(11), 961-968.

Edwards, K.R., K.P. Mills (2005). Aboveground and belowground productivity of Spartina alterniflora (Smooth Cordgrass) in natural and created Louisiana salt marshes. *Estuaries* 28(2), 252-265.

Edwards, K.R., C.E. Proffitt (2003). Comparison of wetland structural characteristics between created and natural salt marshes in southwest Louisiana, USA. *Wetlands* 23(2), 344-356.

Elsey-Quirk, T., D.M. Seliskar, J.L. Gallagher (2011). Nitrogen pools of macrophyte species in a coastal lagoon salt marsh: Implications for seasonal storage and dispersal. *Estuaries and Coasts* 34(3), 470-482.

Elsey-Quirk, T., V. Unger (2018). Geomorphic influences on the contribution of vegetation to soil C accumulation and accretion in Spartina alterniflora marshes. *Biogeosciences* 15(1), 379-397.

Falloon, P., P. Smith (2000). Modelling refractory soil organic matter. *Biology and Fertility of Soils* 30(5-6), 388-398.

Filip, Z., J.J. Alberts, M.V. Cheshire, B.A. Goodman, J.R. Bacon (1988). Comparison of salt marsh humic acid with humic-like substances from the indigenous plant species Spartina alterniflora (Loisel). *Science of The Total Environment* 71(2), 157-172.

Fine, A.K., H.M. van Es, R.R. Schindelbeck (2017). Statistics, Scoring Functions, and Regional Analysis of a Comprehensive Soil Health Database. *Soil Science Society of America Journal* 81(3), 589-601.

Friedel, J.K., E. Scheller (2002). Composition of hydrolysable amino acids in soil organic matter and soil microbial biomass. *Soil Biology and Biochemistry* 34(3), 315-325.

Frost, P.S.D., H.M. van Es, D.G. Rossiter, P.R. Hobbs, P.L. Pingali (2019). Soil health characterization in smallholder agricultural catchments in India. *Applied Soil Ecology* 138, 171-180.

Gadkar, V., M.C. Rillig (2006). The arbuscular mycorrhizal fungal protein glomalin is a putative homolog of heat shock protein 60. *FEMS Microbiology Letters* 263(1), 93-101.

Gamper, H.A., J.P.W. Young, D.L. Jones, A. Hodge (2008). Real-time PCR and microscopy: Are the two methods measuring the same unit of arbuscular mycorrhizal fungal abundance? *Fungal Genetics and Biology* 45(5), 581-596.

Gasteiger, E., C. Hoogland, A. Gattiker, M.R. Wilkins, R.D. Appel, A. Bairoch (2005). Protein identification and analysis tools on the ExPASy server, *The proteomics protocols handbook*. Springer, pp. 571-607.

Geisseler, D., K. Miller, M. Leinfelder-Miles, R. Wilson (2019). Use of Soil Protein Pools as Indicators of Soil Nitrogen Mineralization Potential. *Soil Science Society of America Journal* 83(4), 1236-1243.

Gillespie, A.W., R.E. Farrell, F.L. Walley, A.R.S. Ross, P. Leinweber, K.-U. Eckhardt, T.Z. Regier, R.I.R. Blyth (2011). Glomalin-related soil protein contains non-mycorrhizal-related heat-stable proteins, lipids and humic materials. *Soil Biology and Biochemistry* 43(4), 766-777.

Halvorson, J., J. Gonzalez (2006). Bradford reactive soil protein in Appalachian soils: distribution and response to incubation, extraction reagent and tannins. *Plant and Soil* 286(1-2), 339-356.

Halvorson, J.J., K.A. Nichols, C.M. Crisafulli (2018). Soil Carbon and Nitrogen and Evidence for Formation of Glomalin, a Recalcitrant Pool of Soil Organic Matter, in Developing Mount St. Helens Pyroclastic Substrates, In: Crisafulli, C.M., Dale, V.H. (Eds.), *Ecological Responses at Mount St. Helens: Revisited 35 years after the 1980 Eruption*. Springer New York, New York, NY, pp. 97-112.

Harner, M., N. Opitz, K. Geluso, K. Tockner, M. Rillig (2011). Arbuscular mycorrhizal fungi on developing islands within a dynamic river floodplain: an investigation across successional gradients and soil depth. *Aquatic Sciences* 73(1), 35-42.

Harner, M.J., P.W. Ramsey, M.C. Rillig (2004). Protein accumulation and distribution in floodplain soils and river foam. *Ecology Letters* 7(9), 829-836.

Harzing, A.-W., S. Alakangas (2016). Google Scholar, Scopus and the Web of Science: a longitudinal and cross-disciplinary comparison. *Scientometrics* 106(2), 787-804.

Harzing, A.W. (2007). *Publish or Perish*, v. 7.15.2643 (2019). https://harzing.com/resources/publish-or-perish.

Henry, K.M., R.R. Twilley (2014). Nutrient Biogeochemistry During the Early Stages of Delta Development in the Mississippi River Deltaic Plain. *Ecosystems* 17(2), 327-343.

Hicks, R.E., C. Lee, A.C. Marinucci (1991). Loss and recycling of amino acids and protein from smooth cordgrass (Spartina alterniflora) litter. *Estuaries* 14(4), 430-439.

Hoefnagels, M.H., S.W. Broome, S.R. Shafer (1993). Vesicular-arbuscular mycorrhizae in salt marshes in North Carolina. *Estuaries* 16(4), 851-858.

Hoogsteen, M.J.J., E.A. Lantinga, E.J. Bakker, J.C.J. Groot, P.A. Tittonell (2015). Estimating soil organic carbon through loss on ignition: effects of ignition conditions and structural water loss. *European Journal of Soil Science* 66(2), 320-328.

Hopkinson, C.S., R.L. Wetzel, J.W. Day (1988). 5 - Simulation Models of Coastal Wetland and Estuarine Systems: Realization of Goals, In: Mitsch, W.J., Straškraba, M., Jørgensen, S.E. (Eds.), *Developments in Environmental Modelling*. Elsevier, pp. 67-97.

Hurisso, T.T., D.J. Moebius-Clune, S.W. Culman, B.N. Moebius-Clune, J.E. Thies, H.M. van Es (2018). Soil Protein as a Rapid Soil Health Indicator of Potentially Available Organic Nitrogen. *Agricultural & Environmental Letters* 3(1), 1:180006.

Janos, D.P., S. Garamszegi, B. Beltran (2008). Glomalin extraction and measurement. *Soil Biology and Biochemistry* 40(3), 728-739.

Jastrow, J.D., J.E. Amonette, V.L. Bailey (2007). Mechanisms controlling soil carbon turnover and their potential application for enhancing carbon sequestration. *Climatic Change* 80(1-2), 5-23.

Jorge-Araújo, P., H. Quiquampoix, P.T. Matumoto-Pintro, S. Staunton (2015). Glomalin-related soil protein in French temperate forest soils: interference in the Bradford assay caused by co-extracted humic substances. *European Journal of Soil Science* 66(2), 311-319.

Juniper, S., L. Abbott (1993). Vesicular-arbuscular mycorrhizas and soil salinity. *Mycorrhiza* 4(2), 45-57.

Kaiser, K., G. Guggenberger (2000). The role of DOM sorption to mineral surfaces in the preservation of organic matter in soils. *Organic Geochemistry* 31(7), 711-725.

Kandalepas, D., K. Stevens, G. Shaffer, W. Platt (2010). How Abundant are Root-Colonizing Fungi in Southeastern Louisiana's Degraded Marshes? *Wetlands* 30(2), 189-199.

Kelleher, B.P., A.J. Simpson (2006). Humic Substances in Soils: Are They Really Chemically Distinct? *Environmental Science & Technology* 40(15), 4605-4611.

Kelsall, M.L. (2019). Sources and Chemical Stability of Soil Organic Carbon along a Salinity Gradient and a Chronosequence of Created Brackish Marshes in Coastal Louisiana. *Louisiana State University*, Thesis. 4984.

Kemp, A.L.W., A. Mudrochova (1973). The distribution and nature of amino acids and other nitrogen-containing compounds in Lake Ontario surface sediments. *Geochimica et Cosmochimica Acta* 37(9), 2191-2206.

Khade, S.W., B.F. Rodrigues (2007). Incidence of arbuscular mycorrhizal (AM) fungi in some angiosperms with underground storage organs from western ghat region of Goa. *Tropical Ecology* 48(1), 115-118.

King, G.M. (2011). Enhancing soil carbon storage for carbon remediation: potential contributions and constraints by microbes. *Trends in Microbiology* 19(2), 75-84.

Kirwan, M.L., J.P. Megonigal (2013). Tidal wetland stability in the face of human impacts and sea-level rise. *Nature* 504, 53.

Kleber, M., K. Eusterhues, M. Keiluweit, C. Mikutta, R. Mikutta, P.S. Nico (2015). Mineral–Organic Associations: Formation, Properties, and Relevance in Soil Environments, In: Sparks, D.L. (Ed.), *Advances in Agronomy*. Academic Press, pp. 1-140.

Knicker, H. (2011). Soil organic N - An under-rated player for C sequestration in soils? *Soil Biology and Biochemistry* 43(6), 1118-1129.

Knicker, H., R. Fründ, H.-D. Lüdemann (1993). The chemical nature of nitrogen in native soil organic matter. *Naturwissenschaften* 80(5), 219-221.

Knicker, H., P.G. Hatcher (1997). Survival of protein in an organic-rich sediment: possible protection by encapsulation in organic matter. *Naturwissenschaften* 84(6), 231-234.

Knicker, H., J.C.d. Río, P.G. Hatcher, R.D. Minard (2001). Identification of protein remnants in insoluble geopolymers using TMAH thermochemolysis/GC–MS. *Organic Geochemistry* 32(3), 397-409.

Kohout, P., Z. Sýkorová, M. Čtvrtlíková, J. Rydlová, J. Suda, M. Vohník, R. Sudová (2012). Surprising spectra of root-associated fungi in submerged aquatic plants. *FEMS Microbiology Ecology* 80(1), 216-235.

Kozlowski, L.P. (2017). Proteome-pI: proteome isoelectric point database. *Nucleic Acids Res* 45(D1), D1112-D1116.

Krishnamoorthy, R., K. Kim, C. Kim, T. Sa (2014). Changes of arbuscular mycorrhizal traits and community structure with respect to soil salinity in a coastal reclamation land. *Soil Biology and Biochemistry* 72(0), 1-10.

Krüger, M., H. Stockinger, C. Krüger, A. Schüßler (2009). DNA-based species level detection of Glomeromycota: one PCR primer set for all arbuscular mycorrhizal fungi. *New Phytologist* 183(1), 212-223.

Kumar, S., A.K. Singh, P. Ghosh (2018). Distribution of soil organic carbon and glomalin related soil protein in reclaimed coal mine-land chronosequence under tropical condition. *Science of The Total Environment* 625, 1341-1350.

Ladd, J., J. Butler (1975). Humus-enzyme systems and synthetic, organic polymer-enzyme analogs, In: Paul, E.A., A.D. McLaren (Eds.), *Soil Biochemistry* (vol. 4). Marcel Dekker, New York, NY. pp. 143-194.

Lalonde, K., A. Mucci, A. Ouellet, Y. Gélinas (2012). Preservation of organic matter in sediments promoted by iron. *Nature* 483, 198.

Leavitt, S.W., R.F. Follett, E.A. Paul (1996). Estimation of Slow- and Fast-Cycling Soil Organic Carbon Pools from 6N HCl Hydrolysis. *Radiocarbon* 38(2), 231-239.

Lehmann, J., M. Kleber (2015). The contentious nature of soil organic matter. *Nature* 528(7580), 60-68.

Leinweber, P., H.-R. Schulten (2000). Nonhydrolyzable forms of soil organic nitrogen: Extractability and composition. *Journal of Plant Nutrition and Soil Science* 163(4), 433-439.

Leorri, E., A.R. Zimmerman, S. Mitra, R.R. Christian, F. Fatela, D.J. Mallinson (2018). Refractory organic matter in coastal salt marshes-effect on C sequestration calculations. *Science of The Total Environment* 633, 391-398.

Lodge, D.J. (1989). The influence of soil moisture and flooding on formation of VA-endo- and ectomycorrhizae in Populus and Salix. *Plant and Soil* 117(2), 243-253.

Loll, M.J., J.-M. Bollag (1983). Protein Transformation in Soil, In: Brady, N.C. (Ed.), *Advances in Agronomy*. Academic Press, pp. 351-382.

López-Merino, L., O. Serrano, M.F. Adame, M.Á. Mateo, A. Martínez Cortizas (2015). Glomalin accumulated in seagrass sediments reveals past alterations in soil quality due to land-use change. *Global and Planetary Change* 133, 87-95.

Lovelock, C.E., S.F. Wright, D.A. Clark, R.W. Ruess (2004). Soil stocks of glomalin produced by arbuscular mycorrhizal fungi across a tropical rain forest landscape. *Journal of Ecology* 92(2), 278-287.

Lützow, M.v., I. Kögel-Knabner, K. Ekschmitt, E. Matzner, G. Guggenberger, B. Marschner, H. Flessa (2006). Stabilization of organic matter in temperate soils: mechanisms and their relevance under different soil conditions – a review. *European Journal of Soil Science* 57(4), 426-445.

Lynch, D.L., C.C. Lynch (1958). Resistance of Protein–Lignin Complexes, Lignins and Humic Acids to Microbial Attack. *Nature* 181, 1478.

Malcolm, R.L. (1990). The uniqueness of humic substances in each of soil, stream and marine environments. *Analytica Chimica Acta* 232, 19-30.

Mann, C., D. Lynch, S. Fillmore, A. Mills (2019). Relationships between field management, soil health, and microbial community composition. *Applied Soil Ecology* 144, 12-21.

Martens, D.A., K.L. Loeffelmann (2003). Soil Amino Acid Composition Quantified by Acid Hydrolysis and Anion Chromatography−Pulsed Amperometry. *Journal of Agricultural and Food Chemistry* 51(22), 6521-6529.

Martín-Martín, A., E. Orduna-Malea, M. Thelwall, E. Delgado López-Cózar (2018). Google Scholar, Web of Science, and Scopus: A systematic comparison of citations in 252 subject categories. *Journal of Informetrics* 12(4), 1160-1177.

Masciandaro, G., C. Macci, S. Doni, B.E. Maserti, A.C.-B. Leo, B. Ceccanti, E. Wellington (2008). Comparison of extraction methods for recovery of extracellular β-glucosidase in two different forest soils. *Soil Biology and Biochemistry* 40(9), 2156-2161.

Mayer, L.M., L.L. Schick, F.W. Setchell (1986). Measurement of protein in nearshore marine sediments. *Marine Ecology Progress Series* 30(2/3), 159-165.

McGonigle, T.P., M.H. Miller, D.G. Evans, G.L. Fairchild, J.A. Swan (1990). A new method which gives an objective measure of colonization of roots by vesicular—arbuscular mycorrhizal fungi. *New Phytologist* 115(3), 495-501.

McLauchlan, K.K., S.E. Hobbie (2004). Comparison of Labile Soil Organic Matter Fractionation Techniques. *Soil Science Society of America Journal* 68(5), 1616-1625.

McLeod, E., G.L. Chmura, S. Bouillon, R. Salm, M. Björk, C.M. Duarte, C.E. Lovelock, W.H. Schlesinger, B.R. Silliman (2011). A blueprint for blue carbon: toward an improved understanding of the role of vegetated coastal habitats in sequestering CO2. *Frontiers in Ecology and the Environment* 9(10), 552-560.

Meentemeyer, V. (1978). Macroclimate and Lignin Control of Litter Decomposition Rates. *Ecology* 59(3), 465-472.

Moragues-Saitua, L., L. Merino-Martín, A. Stokes, S. Staunton (2019). Towards meaningful quantification of glomalin-related soil protein (GRSP), taking account of interference with the Coomassie Blue (Bradford) assay. *European Journal of Soil Science* 70, 727-735.

Moura, A., M.A. Savageau, R. Alves (2013). Relative Amino Acid Composition Signatures of Organisms and Environments. *PLoS One* 8(10), e77319.

Nannipieri, P., P. Eldor (2009). The chemical and functional characterization of soil N and its biotic components. *Soil Biology and Biochemistry* 41(12), 2357-2369.

Nicholls, R.J. (2004). Coastal flooding and wetland loss in the 21st century: changes under the SRES climate and socio-economic scenarios. *Global environmental change* 14(1), 69-86.

Nichols, K.A., S.F. Wright (2004). Contributions of Fungi to Soil Organic Matter in Agroecosystems, In: Magdoff, F., Weil, R.R. (Eds.), *Soil Organic Matter in Sustainable Agriculture*. CRC Press. pp. 179-198.

Olsson, L., S. Ye, X. Yu, M. Wei, K.W. Krauss, H. Brix (2015). Factors influencing CO2 and CH4 emissions from coastal wetlands in the Liaohe Delta, Northeast China. *Biogeosciences* 12(16), 4965-4977.

Ozols, J. (1990). Amino acid analysis, In: Deutscher, M.P. (Ed.), *Methods in Enzymology*. Academic Press, pp. 587-601.

Paul, E.A. (2016). The nature and dynamics of soil organic matter: Plant inputs, microbial transformations, and organic matter stabilization. *Soil Biology and Biochemistry* 98, 109-126.

Paul, E.A., S.J. Morris, R.T. Conant, A.F. Plante (2006). Does the Acid Hydrolysis–Incubation Method Measure Meaningful Soil Organic Carbon Pools? *Soil Science Society of America Journal* 70(3), 1023-1035.

Poirier, V., C. Roumet, A.D. Munson (2018). The root of the matter: Linking root traits and soil organic matter stabilization processes. *Soil Biology and Biochemistry* 120, 246-259.

Pratt-Zossoungbo, M., P.D. Biber (2009). Inoculation and Colonization of Four Saltmarsh Species with Vesicular-Arbuscular Mycorrhizal Fungi (Mississippi). *Ecological Restoration* 27(4), 387-389.

Preston, C.M. (1996). Applications of NMR to soil organic matter analysis: history and prospects. *Soil Science* 161(3), 144-166.

Rabalais, N.N., R.E. Turner, W.J.W. Jr. (2002). Gulf of Mexico Hypoxia, A.K.A. "The Dead Zone". *Annual Review of Ecology and Systematics* 33(1), 235-263.

Reddy, K.R., R.D. DeLaune (2008). *Biogeochemistry of wetlands: science and applications*. CRC Press, Boca Raton, FL.

Redmile-Gordon, M.A., E. Armenise, R.P. White, P.R. Hirsch, K.W.T. Goulding (2013). A comparison of two colorimetric assays, based upon Lowry and Bradford techniques, to estimate total protein in soil extracts. *Soil Biology and Biochemistry* 67, 166-173.

Reyna, D.L., L.G. Wall (2014). Revision of two colorimetric methods to quantify glomalin-related compounds in soils subjected to different managements. *Biology and Fertility of Soils* 50(2), 395-400.

Rillig, M., B. Caldwell, H.B. Wösten, P. Sollins (2007). Role of proteins in soil carbon and nitrogen storage: controls on persistence. *Biogeochemistry* 85(1), 25-44.

Rillig, M., P. Ramsey, S. Morris, E. Paul (2003). Glomalin, an arbuscular-mycorrhizal fungal soil protein, responds to land-use change. *Plant and Soil* 253(2), 293-299.

Rillig, M., S. Wright, V. Eviner (2002). The role of arbuscular mycorrhizal fungi and glomalin in soil aggregation: comparing effects of five plant species. *Plant and Soil* 238(2), 325-333.

Rillig, M., S. Wright, K. Nichols, W. Schmidt, M. Torn (2001a). Large contribution of arbuscular mycorrhizal fungi to soil carbon pools in tropical forest soils. *Plant and Soil* 233(2), 167-177.

Rillig, M.C. (2004). Arbuscular mycorrhizae, glomalin, and soil aggregation. *Canadian Journal of Soil Science* 84(4), 355-363.

Rillig, M.C. (2005). A connection between fungal hydrophobins and soil water repellency? *Pedobiologia* 49(5), 395-399.

Rillig, M.C., D.L. Mummey (2006). Mycorrhizas and soil structure. *New Phytologist* 171(1), 41-53.

Rillig, M.C., S.F. Wright, B.A. Kimball, P.J. Pinter, G.W. Wall, M.J. Ottman, S.W. Leavitt (2001b). Elevated carbon dioxide and irrigation effects on water stable aggregates in a Sorghum field: a possible role for arbuscular mycorrhizal fungi. *Global Change Biology* 7(3), 333-337.

Roberts, H., J. Coleman, S. Bentley, N. Walker (2003). An embryonic major delta lobe: A new generation of delta studies in the Atchafalaya-Wax Lake delta system. *Gulf Coast Association of Geological Societies Transactions* 53, 690-703.

Roberts, P., D.L. Jones (2008). Critical evaluation of methods for determining total protein in soil solution. *Soil Biology and Biochemistry* 40(6), 1485-1495.

Rosier, C.L., A.T. Hoye, M.C. Rillig (2006). Glomalin-related soil protein: Assessment of current detection and quantification tools. *Soil Biology and Biochemistry* 38(8), 2205-2211.

Rouwenhorst, R.J., J. Frank Jzn, W.A. Scheffers, J.P. van Dijken (1991). Determination of protein concentration by total organic carbon analysis. *Journal of Biochemical and Biophysical Methods* 22(2), 119-128.

Schindler, F.V., E.J. Mercer, J.A. Rice (2007). Chemical characteristics of glomalin-related soil protein (GRSP) extracted from soils of varying organic matter content. *Soil Biology and Biochemistry* 39(1), 320-329.

Schnitzer, M., K. Ivarson (1982). Different forms of nitrogen in particle size fractions separated from two soils. *Plant and Soil* 69(3), 383-389.

Schulten, H.-R., M. Schnitzer (1997). Chemical Model Structures for Soil Organic Matter and Soils. *Soil Science* 162(2), 115-130.

Schulten, H.-R., M. Schnitzer (1998). The chemistry of soil organic nitrogen: a review. *Biology and Fertility of Soils* 26(1), 1-15.

Sedmak, J.J., S.E. Grossberg (1977). A rapid, sensitive, and versatile assay for protein using Coomassie brilliant blue G250. *Analytical Biochemistry* 79(1), 544-552.

Seigler, D.S. (2012). *Plant secondary metabolism*. Springer Science & Business Media.

Shields, M.R., T.S. Bianchi, Y. Gélinas, M.A. Allison, R.R. Twilley (2016). Enhanced terrestrial carbon preservation promoted by reactive iron in deltaic sediments. *Geophysical Research Letters* 43(3), 1149-1157.

Shields, M.R., T.S. Bianchi, D. Mohrig, J.A. Hutchings, W.F. Kenney, A.S. Kolker, J.H. Curtis (2017). Carbon storage in the Mississippi River delta enhanced by environmental engineering. *Nature Geoscience* 10, 846.

Silveira, M.L., N.B. Comerford, K.R. Reddy, W.T. Cooper, H. El-Rifai (2008). Characterization of soil organic carbon pools by acid hydrolysis. *Geoderma* 144(1), 405-414.

Singh, A.K., A. Rai, V. Pandey, N. Singh (2017). Contribution of glomalin to dissolve organic carbon under different land uses and seasonality in dry tropics. *Journal of Environmental Management* 192, 142-149.

Smith, K.E. (2012). Paleoecological study of coastal marsh in the Chenier Plain, Louisiana: Investigating the diatom composition of hurricane-deposited sediments and a diatom-based quantitative reconstruction of sea-level characteristics. *University of Florida*, Dissertation.

Smith, S.E., D.J. Read (2008). *Mycorrhizal Symbiosis*, 3rd ed. Academic press.

Sohn, M., C.-T. Ho (1995). Ammonia generation during thermal degradation of amino acids. *Journal of Agricultural and Food Chemistry* 43(12), 3001-3003.

Sowden, F.J. (1977). Distribution of nitrogen in representative Canadian soils. *Canadian Journal of Soil Science* 57(4), 445-456.

Sowden, F.J., Y. Chen, M. Schnitzer (1977). The nitrogen distribution in soils formed under widely differing climatic conditions. *Geochimica et Cosmochimica Acta* 41(10), 1524-1526.

Spencer, T., M. Schuerch, R.J. Nicholls, J. Hinkel, D. Lincke, A.T. Vafeidis, R. Reef, L. McFadden, S. Brown (2016). Global coastal wetland change under sea-level rise and related stresses: The DIVA Wetland Change Model. *Global and Planetary Change* 139, 15-30.

Spohn, M., L. Giani (2010). Water-stable aggregates, glomalin-related soil protein, and carbohydrates in a chronosequence of sandy hydromorphic soils. *Soil Biology and Biochemistry* 42(9), 1505-1511.

Steinmuller, H.E., L.G. Chambers (2019). Characterization of coastal wetland soil organic matter: Implications for wetland submergence. *Science of The Total Environment* 677, 648-659.

Steinmuller, H.E., K.M. Dittmer, J.R. White, L.G. Chambers (2019). Understanding the fate of soil organic matter in submerging coastal wetland soils: A microcosm approach. *Geoderma* 337, 1267-1277.

Stevens, K., C. Wall, J. Janssen (2011). Effects of arbuscular mycorrhizal fungi on seedling growth and development of two wetland plants, Bidens frondosa L., and Eclipta prostrata (L.) L., grown under three levels of water availability. *Mycorrhiza* 21(4), 279-288.

Stevenson, F.J. (1994). *Humus chemistry: genesis, composition, reactions*, 2nd ed. John Wiley & Sons.

Stevenson, F.J., M.A. Cole (1999). *Cycles of soil: carbon, nitrogen, phosphorus, sulfur, micronutrients*, 2nd ed. John Wiley & Sons.

Sui, X., Z. Wu, C. Lin, S. Zhou (2017). Terrestrially derived glomalin-related soil protein quality as a potential ecological indicator in a peri-urban watershed. *Environmental Monitoring and Assessment* 189(7), 315.

Suir, G.M., C.E. Sasser, R.D. DeLaune, E.O. Murray (2019). Comparing carbon accumulation in restored and natural wetland soils of coastal Louisiana. *International Journal of Sediment Research* 34(6), 600-607.

Sutton, R., G. Sposito (2005). Molecular Structure in Soil Humic Substances: The New View. *Environmental Science & Technology* 39(23), 9009-9015.

Tabatabai, M.A. (2003). Soil Enzymes, In: Plimmer, J.R., Gammon, D.W., Ragsdale, N.A. (Eds.), *Encyclopedia of Agrochemicals*.

Tan, W.F., L.K. Koopal, L.P. Weng, W.H. van Riemsdijk, W. Norde (2008). Humic acid protein complexation. *Geochimica et Cosmochimica Acta* 72(8), 2090-2099.

Taylor, E.B., M.A. Williams (2010). Microbial protein in soil: influence of extraction method and C amendment on extraction and recovery. *Microbial Ecology* 59(2), 390-399.

Terry, K.L., J. Hirata, E.A. Laws (1983). Light-limited growth of two strains of the marine diatom Phaeodactylum tricornutum Bohlin: Chemical composition, carbon partitioning and the diel periodicity of physiological processes. *Journal of Experimental Marine Biology and Ecology* 68(3), 209-227.

Tisdall, J.M., J.M. Oades (1982). Organic matter and water-stable aggregates in soils. *Journal of Soil Science* 33(2), 141-163.

Treseder, K.K., M.F. Allen (2000). Mycorrhizal fungi have a potential role in soil carbon storage under elevated CO2 and nitrogen deposition. *New Phytologist* 147(1), 189-200.

Treseder, K.K., S.R. Holden (2013). Fungal Carbon Sequestration. *Science* 339(6127), 1528-1529.

Trubetskaya, O.E., O.I. Reznikova, G.V. Afanas'eva, L.F. Markova, T.A. Muranova, O.A. Trubetskoj (1998). Amino acid distribution in soil humic acids fractionated by tandem size exclusion chromatography polyacrylamide gel electrophoresis. *Environment International* 24(5), 573-581.

Turner, S.D., C.F. Friese (1998). Plant-Mycorrhizal Community Dynamics Associated with a Moisture Gradient within a Rehabilitated Prairie Fen. *Restoration Ecology* 6(1), 44-51.

Unger, V., T. Elsey-Quirk, C. Sommerfield, D. Velinsky (2016). Stability of organic carbon accumulating in Spartina alterniflora-dominated salt marshes of the Mid-Atlantic U.S. *Estuarine, Coastal and Shelf Science* 182, 179-189.

Verbruggen, E., S.D. Veresoglou, I.C. Anderson, T. Caruso, E.C. Hammer, J. Kohler, M.C. Rillig (2013). Arbuscular mycorrhizal fungi – short-term liability but long-term benefits for soil carbon storage? *New Phytologist* 197(2), 366-368.

Vierheilig, H., P. Schweiger, M. Brundrett (2005). An overview of methods for the detection and observation of arbuscular mycorrhizal fungi in roots. *Physiologia Plantarum* 125(4), 393-404.

Walley, F.L., A.W. Gillespie, A.B. Adetona, J.J. Germida, R.E. Farrell (2014). Manipulation of rhizosphere organisms to enhance glomalin production and C sequestration: Pitfalls and promises. *Canadian Journal of Plant Science* 94(6), 1025-1032.

Wang, H., Q. Ye, J. Gan, J. Wu (2008). Adsorption of Cry1Ab Protein Isolated from Bt Transgenic Rice on Bentone, Kaolin, Humic Acids, and Soils. *Journal of Agricultural and Food Chemistry* 56(12), 4659-4664.

Wang, J., C. Song, X. Wang, Y. Song (2012). Changes in labile soil organic carbon fractions in wetland ecosystems along a latitudinal gradient in Northeast China. *CATENA* 96, 83-89.

Wang, J.J., S.K. Dodla, R.D. DeLaune (2015a). Characteristics and Functions of Labile Organic Carbon in Coastal Wetland Soils of the Mississippi River Deltaic Plain, In: *Labile Organic Matter—Chemical Compositions, Function, and Significance in Soil and the Environment*. Special publication 62. Soil Science Society of America, Inc., Madison, WI, pp. 315-336.

Wang, Q., J. Li, J. Chen, H. Hong, H. Lu, J. Liu, Y. Dong, C. Yan (2018a). Glomalin-related soil protein deposition and carbon sequestration in the Old Yellow River delta. *Science of The Total Environment* 625, 619-626.

Wang, Q., H. Lu, J. Chen, H. Hong, J. Liu, J. Li, C. Yan (2018b). Spatial distribution of glomalin-related soil protein and its relationship with sediment carbon sequestration across a mangrove forest. *Science of The Total Environment* 613–614, 548-556.

Wang, Q., D. Mei, J. Chen, Y. Lin, J. Liu, H. Lu, C. Yan (2019). Sequestration of heavy metal by glomalin-related soil protein: Implication for water quality improvement in mangrove wetlands. *Water Research* 148, 142-152.

Wang, Q., W. Wang, X. He, W. Zhang, K. Song, S. Han (2015b). Role and Variation of the Amount and Composition of Glomalin in Soil Properties in Farmland and Adjacent Plantations with Reference to a Primary Forest in North-Eastern China. *PLoS One* 10(10), e0139623.

Wang, W., R. Vignani, M. Scali, M. Cresti (2006). A universal and rapid protocol for protein extraction from recalcitrant plant tissues for proteomic analysis. *ELECTROPHORESIS* 27(13), 2782-2786.

Wang, W., Z. Zhong, Q. Wang, H. Wang, Y. Fu, X. He (2017). Glomalin contributed more to carbon, nutrients in deeper soils, and differently associated with climates and soil properties in vertical profiles. *Scientific Reports* 7(1), 13003.

Wellner, R., R. Beaubouef, J. Van Wagoner, H. Roberts, T. Sun (2005). Jet-plume depositional bodies—the primary building blocks of Wax Lake Delta. *Gulf Coast Association of Geological Societies Transactions* 55, 867-909.

Whiffen, L.K., D.J. Midgley, P.A. McGee (2007). Polyphenolic compounds interfere with quantification of protein in soil extracts using the Bradford method. *Soil Biology and Biochemistry* 39(2), 691-694.

White, T.J., T. Bruns, S. Lee, J. Taylor (1990). Amplification and direct sequencing of fungal ribosomal RNA genes for phylogenetics. *PCR protocols: a guide to methods and applications* 18(1), 315-322.

Wilson, C.A., M.A. Allison (2008). An equilibrium profile model for retreating marsh shorelines in southeast Louisiana. *Estuarine, Coastal and Shelf Science* 80(4), 483-494.

Wilson, G.W.T., C.W. Rice, M.C. Rillig, A. Springer, D.C. Hartnett (2009). Soil aggregation and carbon sequestration are tightly correlated with the abundance of arbuscular mycorrhizal fungi: results from long-term field experiments. *Ecology Letters* 12(5), 452-461.

Wright, S., M. Franke-Snyder, J. Morton, A. Upadhyaya (1996). Time-course study and partial characterization of a protein on hyphae of arbuscular mycorrhizal fungi during active colonization of roots. *Plant and Soil* 181(2), 193-203.

Wright, S.F., K.A. Nichols, W.F. Schmidt (2006). Comparison of efficacy of three extractants to solubilize glomalin on hyphae and in soil. *Chemosphere* 64(7), 1219-1224.

Wright, S.F., A. Upadhyaya (1996). Extraction of an abundant and unusual protein from soil and comparison with hyphal protein of arbuscular mycorrhizal fungi. *Soil Science* 161(9), 575-586.

Wright, S.F., A. Upadhyaya (1998). A survey of soils for aggregate stability and glomalin, a glycoprotein produced by hyphae of arbuscular mycorrhizal fungi. *Plant and Soil* 198(1), 97-107.

Wright, S.F., A. Upadhyaya, J.S. Buyer (1998). Comparison of N-linked oligosaccharides of glomalin from arbuscular mycorrhizal fungi and soils by capillary electrophoresis. *Soil Biology and Biochemistry* 30(13), 1853-1857.

Xiang, D., B. Chen, H. Li (2015). Specificity and selectivity of arbuscular mycorrhizal fungal polymerase chain reaction primers in soil samples by clone library analyses. *Acta Agriculturae Scandinavica, Section B — Soil & Plant Science* 66(4), 333-339.

Xiao, L., Y. Zhang, P. Li, G. Xu, P. Shi, Y. Zhang (2019). Effects of freeze-thaw cycles on aggregate-associated organic carbon and glomalin-related soil protein in natural-succession grassland and Chinese pine forest on the Loess Plateau. *Geoderma* 334, 1-8.

Xie, H., J. Li, B. Zhang, L. Wang, J. Wang, H. He, X. Zhang (2015). Long-term manure amendments reduced soil aggregate stability via redistribution of the glomalin-related soil protein in macroaggregates. *Scientific Reports* 5, 14687.

Xu, J.M., H.H. Cheng, W.C. Koskinen, J.A.E. Molina (1997). Characterization of potentially bioreactive soil organic carbon and nitrogen by acid hydrolysis. *Nutrient Cycling in Agroecosystems* 49(1), 267-271.

Yang, Y., C. He, L. Huang, Y. Ban, M. Tang (2017). The effects of arbuscular mycorrhizal fungi on glomalin-related soil protein distribution, aggregate stability and their relationships with soil properties at different soil depths in lead-zinc contaminated area. *PLoS One* 12(8), e0182264.

Yeates, C., M.R. Gillings, A.D. Davison, N. Altavilla, D.A. Veal (1998). Methods for microbial DNA extraction from soil for PCR amplification. *Biological Procedures Online* 1(1), 40-47.

Zang, X., J.D.H. van Heemst, K.J. Dria, P.G. Hatcher (2000). Encapsulation of protein in humic acid from a histosol as an explanation for the occurrence of organic nitrogen in soil and sediment. *Organic Geochemistry* 31(7), 679-695.

Zhang, J., X. Tang, X. He, J. Liu (2015). Glomalin-related soil protein responses to elevated CO2 and nitrogen addition in a subtropical forest: Potential consequences for soil carbon accumulation. *Soil Biology and Biochemistry* 83, 142-149.

Zhang, J., X. Tang, S. Zhong, G. Yin, Y. Gao, X. He (2017). Recalcitrant carbon components in glomalin-related soil protein facilitate soil organic carbon preservation in tropical forests. *Scientific Reports* 7(1), 2391.

Zhang, Y., C. Li, C.C. Trettin, H. Li, G. Sun (2002). An integrated model of soil, hydrology, and vegetation for carbon dynamics in wetland ecosystems. *Global Biogeochemical Cycles* 16(4), 9-1 – 9-17.

Vita

Alex McClellan has worked and studied in a range of fields so as to gain knowledge that is diverse as his interests. He received his baccalaureate in chemistry from the University of Texas at Austin. He has worked—first as a programmer, and then analytical chemist—at Northrop Grumman Space Technology, studied carcinogenesis at MD Anderson Cancer Center and the Dell Pediatric Research Institute, and gained experience in observational astronomy at the McDonald Observatory. Becoming interested in wetlands and environmental processes, he entered the Environmental Sciences doctoral program at Louisiana State University. Upon completion of his doctorate, he hopes to pursue an opportunity in environmental monitoring or a related field.